UNIVERSITY OF SOUTHAMPTON

Faculty of Environmental and Life Sciences
School of Ocean and Earth Science

Investigating the role and interaction of jellyfish blooms and microbes in nutrient cycling and ecosystem productivity

by

Nathan Damien Hubot

MRes Biology

ORCiD: 0000-0001-6917-2255

A thesis for the degree of
Doctor of Philosophy

May 2023

University of Southampton

Abstract

Faculty of Environmental and Life Sciences
School of Ocean and Earth Science

Doctor of Philosophy

Investigating the role and interaction of jellyfish blooms and microbes in nutrient cycling and ecosystem productivity

by Nathan Damien Hubot

Nutrients, particularly nitrogen and phosphorus, play a major role in stimulating primary production, which in turn supports ecosystem productivity by providing organic matter to the marine food chain. While flowing towards higher trophic levels, organic matter is partially remineralised by heterotrophic microbes supplying nutrients back to primary producers. In coastal areas, jellyfish blooms represent a significant but largely overlooked source of organic matter that can impact microbial communities and ecosystem productivity via processes such as the excretion of dissolved inorganic nutrients (ammonium and phosphate) and dissolved organic matter (mucus). The overall objective of this thesis was to investigate the combined role of jellyfish and microbes in nutrient cycling and the consequences for ecosystem productivity, using a combination of incubations experiments and analytical measurements. I show evidence of microbes living in association with jellyfish thriving by oxidizing up to one-third of the ammonia excreted by their host to nitrite and nitrate. The results showed that the jellyfish-associated release of nitrogen can provide more than 100% of the nitrogen required for primary production and revealed a new pathway for pelagic nitrification. I also highlight the macromolecular and elemental similarity between the jellyfish body and mucus compositions and provide biochemical ratios to support the integration of jellyfish into trophic and biogeochemical models. To further investigate the jellyfish mucus, I finally show that jellyfish mucus is a source of organic and inorganic nutrients that is quickly utilised by microbes albeit at a low growth efficiency. These results suggest that jellyfish blooms and their associated microbes can locally support primary production while inducing changes in nutrient stoichiometry and microbial community composition. Overall, this thesis provides data and equations particularly suitable for the integration of jellyfish bloom populations into marine ecosystem models, which is essential to better understand and quantify their effects on the structure and function of coastal ecosystems.

Contents

List of Figures **ix**

List of Tables **xv**

List of Additional Material **xix**

Declaration of Authorship **xxi**

Acknowledgements **xxiii**

Definitions and Abbreviations **xxvii**

1 Introduction **1**
1.1 Background . . . 1
1.2 Jellyfish biology and ecology . . . 4
1.2.1 Population dynamics and life cycle . . . 5
1.2.2 Metabolism and physiology . . . 6
1.2.3 Microbiome . . . 8
1.2.3.1 Composition and diversity . . . 8
1.2.3.2 Role and function . . . 9
1.3 Jellyfish role in large scale processes . . . 11
1.3.1 Role in the marine food chain . . . 12
1.3.2 Role in biogeochemical cycles . . . 14
1.3.2.1 Marine carbon cycle . . . 16
1.3.2.2 Marine Nitrogen and Phosphorous cycles . . . 20
1.4 Jellyfish in models . . . 23
1.5 Thesis overview, aims and objectives . . . 25

2 Evidence of nitrification associated with globally distributed pelagic jellyfish **27**
Hubot Nathan D., Giering Sarah L. C., Fuessel Jessika, Robidart Julie, Birchill Antony, Stinchcombe Mark, Dumousseaud Cynthia, Lucas Cathy H.
2.1 Abstract . . . 28
2.2 Introduction . . . 28
2.3 Materials . . . 31
2.3.1 Sampling sites and species . . . 31
2.3.2 Experimental structure . . . 32
2.3.3 Rate measurements . . . 34
2.3.4 Sample analysis . . . 35

2.3.5 Statistical analysis . . . 35
2.4 Results and Discussion . . . 36
2.4.1 Nutrient excretion and nitrification . . . 36
2.4.2 Evidence of active nitrifying microorganisms in jellyfish . . . 42
2.4.3 Ecological implications . . . 43
2.5 Conclusion . . . 46

3 Similarities between the biochemical composition of jellyfish body and mucus 49
Hubot Nathan D., Giering Sarah L. C., Lucas Cathy H.
3.1 Abstract . . . 50
3.2 Introduction . . . 50
3.3 Materials and methods . . . 51
3.4 Results . . . 53
3.5 Discussion . . . 56
3.5.1 Ecological implications . . . 57
3.6 Conclusion . . . 58

4 Jellyfish mucus as a source of nutrients in marine coastal waters 59
Hubot Nathan D., Giering Sarah L. C., Katja Klun, Gerhard J. Herndl, Lucas Cathy H., Tinkara Tinta
4.1 Abstract . . . 60
4.2 Introduction . . . 60
4.3 Material and methods . . . 62
4.3.1 Sampling . . . 62
4.3.2 Dialysis . . . 63
4.3.3 Leaching experiments . . . 63
4.3.4 Mucus degradation experiment . . . 64
4.3.5 Chemical analyses . . . 66
4.3.5.1 Particulate and Dissolved Organic Carbon and Nitrogen 66
4.3.5.2 Dissolved Inorganic Nutrients . . . 66
4.3.5.3 Dissolved free Amino Acid Analysis . . . 66
4.3.6 Microbial abundance . . . 67
4.3.7 Prokaryotic Heterotrophic Production . . . 67
4.3.8 Microbial metagenomes . . . 67
4.3.9 Statistical analysis . . . 68
4.4 Results . . . 68
4.4.1 Release of nutrients from jellyfish mucus . . . 68
4.4.2 Microbial processing of the mucus DOM pool . . . 69
4.4.3 taxonomic analysis of microbial community . . . 73
4.5 Discussion . . . 73
4.5.1 Comparison between dry- and frozen-mucus . . . 74
4.5.2 Characterisation of the mucus material . . . 75
4.5.3 Microbial utilisation of mucus . . . 76
4.5.4 Microbial community composition . . . 77
4.5.5 Conclusion . . . 78

5 Discussion 81

5.1 Thesis summary . . . 81
5.2 Implications . . . 84
5.2.1 The marine nitrogen cycle . . . 84
5.2.2 The marine carbon cycle and carbon export . . . 85
5.2.3 Marine ecosystem productivity & modelling . . . 86
5.3 Limitations and future directions . . . 87
5.4 Conclusion . . . 89

Appendix A Supplementary Material - Chapter 2 **91**
Appendix A.1 Absolute concentrations of Jellyfish treatment . . . 91
Appendix A.2 Control . . . 94
Appendix A.2.1 Jellyfish-Control . . . 94
Appendix A.2.2 Mucus-Control . . . 95
Appendix A.3 Mucus-Treatment . . . 97
Appendix A.4 ANCOVA . . . 99
Appendix A.5 Allometric scalling . . . 101
Appendix A.6 Lab-on-Chip analyser . . . 101
Appendix A.7 Artificial sea water preparation . . . 105
Appendix A.8 Calibration and limit of detection . . . 105

Appendix B Supplementary Material - Chapter 3 **107**
Appendix B.1 Literature review . . . 108
Appendix B.1.1 References . . . 108
Appendix B.2 Material and Methods . . . 109
Appendix B.2.1 Lipid analyses . . . 109
Appendix B.2.2 Protein analyses . . . 111
Appendix B.2.3 Carbohydrate analyses . . . 112
Appendix B.3 Results . . . 114
Appendix B.3.1 Linear regressions . . . 114

Appendix C Supplementary Material - Chapter 4 **115**
Appendix C.1 Dry-mucus preparation . . . 115
Appendix C.2 Dialysis experiment . . . 115
Appendix C.3 Leaching experiment - Dry-mucus . . . 122
Appendix C.4 Leaching experiment - Frozen-mucus . . . 128
Appendix C.5 Summary tables . . . 135
Appendix C.6 Mucus vs Carcasses . . . 137
Appendix C.7 Mucus degradation experiment . . . 139

List of Figures

1.1 Map of population trends of native and invasive species of jellyfish. Circles represent discrete chronicles with relative sizes reflecting the confidence index (modified from Brotz et al., 2012) 3
1.2 Fishing down marine food webs: the three stages (past, present and future) offer increasingly better conditions for jellyfish (Based on Pauly et al., 2009 and modified by fishingdown.org). 4
1.3 Schematic description of the *Aurelia* spp. life cycle (Drawn by Mike Dawson) 5
1.4 Life cycle strategies of medusae with benthic polyps. Peaks of abundance in the plankton are tuned to food availability. The exploitation of trophic resources leads to sexual reproduction and larval development, followed by the disappearance of adult medusae from the water column and planula metamorphosis into the polyp benthic stage. Polyps have a continuous presence in the benthos producing the next generation of medusae (Boero et al., 2008). 6
1.5 Metabolic budget. Part of the ingested organic matter is digested and the remains are egested mainly as particulate organic matter. The assimilated matter can then be used for growth and respiration or is released back to the environment via the excretion of both dissolved inorganic matter (ammonium and phosphate) and dissolved organic matter (mucus). 7
1.6 Schematic view of the jellyfish metaorganism (*A. aurita* medusa in a cutaway side view) and selected factors that might influence bacterial colonization of the host surfaces (from Weiland-Bräuer et al., 2019). 9
1.7 Map showing the general location of some of the studies and taxa shown to consume jellyfish, namely flying sea birds, penguins, fish including fish larvae, turtles, crabs, rock lobster larvae, and sea cucumber (from Hays et al., 2018). 13
1.8 Conceptual sketch of the main energy flows toward fish production and fisheries in northern Benguela. The sardine was the main link between primary and secondary producers and fish, fisheries, and predators in the early period (A); after the sardine collapse in the early 1970s most of the energy flow (yellow arrows) was diverted away from the pelagos through jellyfish, detritus, benthic recycling, and bearded goby (B; from Roux et al., 2013). 15
1.9 A representation of the biological pump and the biogeochemical processes that remove elements from the surface ocean by sinking biogenic particles (Lebrato et al., 2011). 17

1.10 Visualization of a living jellyfish as sink and source of organic matter (OM) in the ocean (Tinta et al., 2021) 18
1.11 A conceptual diagram of some of the major environmental processes which control the apparent recalcitrance of oceanic DOC. The dots represent DOC molecules and the arrows represent physicochemical and biological processes that impact DOC concentration and molecular composition. In the surface ocean, DOC derived from primary production is rapidly remineralized or transformed through microbial degradation (black arrow), photochemical degradation (yellow arrow), or particle exchange (green arrow). Labile components are removed down the water column and DOC becomes diluted by processes, such as particle exchange (brown arrow), sediment dissolution (grey arrow), and microbial reworking (white arrow), which continue to alter, add, and/or remove molecules from the bulk DOC pool (Wagner et al., 2020) 19
1.12 Major biological processes involved in carbon cycling in the ocean. The biological pump is a process whereby CO_2 in the upper ocean is fixed by primary producers and transported to the deep ocean as sinking biogenic particles (particulate organic matter; POM) or as dissolved organic matter (DOM). The microbial loop is a pathway in the aquatic food web whereby DOM is taken up by bacteria and archaea, which are consumed by protists, which are in turn consumed by metazoans (not shown). The viral shunt reflects virus-mediated lysis of microorganisms, which returns the POM to the DOM pool. The proposed microbial carbon pump is a conceptual framework for understanding the role of microbial processes in the production of recalcitrant DOM (RDOM). Three major pathways have been identified in the microbial carbon pump: direct exudation of microbial cells during production and proliferation (path 1); viral lysis of microbial cells to release microbial cell wall and cell surface macromolecules (path 2); and POM degradation (path 3). The grey shading roughly indicates the total flux of carbon metabolism in the water column (modified from Jiao et al., 2010). 21
1.13 Conceptual models of the contributions of jellyfish to nutrient cycling during the growth of a jellyfish bloom. The width of the arrows represents their relative contributions. The dotted arrows indicate the contribution has not been confirmed. Microbial feedback loops involving bacteria, phytoplankton and zooplankton are not included. POM = particulate organic matter, DOM = dissolved organic matter and DIM = dissolved inorganic matter (modified from Pitt et al., 2009c). 22
1.14 The accumulation of EwE models through time. Light grey represents EwE models with no jellyfish functional group included at all. The dark blue indicates models with jellyfish as part of a wider zooplankton group. The light blue represents models with jellyfish included as their own group (modified from Lamb et al., 2019). 24

2.1 Geographic distribution of the four jellyfish species investigated in this study (*A. aurita, C. hysoscella, C .fulgida*, and *C. pacifica*; based on Dawson et al., 2005 and Morandini et al., 2010) and of the cryptic genus *Aurelia* (based on Dawson et al., 2001). 33

2.2 Experimental setup. Jellyfish were incubated for 1 h in the release treatment. Subsequently, the jellyfish along with half of the volume from the release phase were transferred to the jellyfish treatment; the other half was transferred to the mucus treatment. Controls for both experiments consisted of incubators containing only artificial seawater (ASW). The mucus and control-mucus incubators were spiked with ammonium every hour (Appendix A, Table A.2). 34

2.3 Mean cumulative release of (a) ammonium, (b) phosphate, (c) nitrite, and (d) nitrate by *A. aurita* (blue circle), *C. fulgida* (yellow triangle), *C. hysoscella* (green cross), and *C. pacifica* (red square), normalized to the wet weight (WW) of each specimen. Colored areas indicate uncertainty envelopes (standard deviation) of the mean cumulative release of nutrients. The vertical dotted line corresponds to the time when the jellyfish were removed from the incubators (6 h). 38

2.4 Inorganic nitrogen release rates of different jellyfish species (a) normalized by the wet weight of the specimens, and (b) as a proportion of total inorganic nitrogen release. Wet weight = WW. 42

2.5 Effect of wet weight on the mass-specific release rates of ammonium (a; $p < 0.001$, $R^2 = 0.80$, n = 17) and nitrate (b; $p < 0.001$, $R^2 = 0.55$, n = 15) for the jellyfish *A. aurita* (circle), *C. hysoscella* (cross), *C. pacifica* (square), and *C. fulgida* (triangle) at 16°C. The black line is the linear regression. No significant release of nitrate was observed for *C. fulgida.* 43

2.6 Conceptual diagram of the role and position of jellyfish in the surface marine nitrogen cycle. The flow of organic and inorganic matter is shown by black and white arrows, respectively. Colors indicate ammonium (NH_4^+, orange), nitrite (NO_2^-, yellow), nitrate (NO_3^-, green) and organic matter (OM, gray). Colored arrows represent ammonium-oxidation (orange-to-yellow) and nitrite-oxidation (yellow-to-green). Components linked to small colored circles release/assimilate nutrients of the same color. The average release of nitrogen forms is presented as a percentage ($\pm$ standard deviation) of total dissolved inorganic nitrogen released by jellyfish. The yellow zigzag arrow represents light. The large middle circle zooms in on the jellyfish epithelium. 44

2.7 Heat map of estimated total inorganic nitrogen release associated with the densities of *A. coerula* in the Honjo District sea lake in Japan (a, linear scale: 0–1720 μmol N m^{-2} h^{-1}; map modified from Han et al., 2009b) and of *C. fulgida* along the coast of Namibia (b, exponential scale: 0–1292 μmol N m^{-2} h^{-1}; map modified from Lynam et al., 2006). 46

3.1 Comparison of the macromolecular content (protein, lipid, carbohydrate; A, B and C) and the sum of macromolecules to the ash-free dry weigh (AFDW, D) of mucus and body tissues in jellyfish species (*A. aurita, C. fulgida, C. pacifica, E. inexplicata*, and *R. pulmo*) expressed as percentage of dry wet (%DW) of the samples. The lines represent the linear regressions and the shaded area is the confidence interval (see details in SI, Table S2). The solid lines are the linear regressions on the whole data set with (A) lipid (LD) vs protein (PT; LD = 0.10 $\pm$ 0.01 PT + 0.10 $\pm$ 0.03), (B) carbohydrate (CH) vs lipid (CH = 0.78 $\pm$ 0.10 LP - 0.05 $\pm$ 0.06), (C) carbohydrate vs protein, (CH = 0.10 $\pm$ 0.01 PT - 0.04 $\pm$ 0.05), and (D) sum of macromolecules (SM) vs AFDW (SM = 1.12 $\pm$ 0.03 AFDW - 11.24 $\pm$ 0.16). . . . 54

3.2 Proportion of proteins, lipids and carbohydrates (A) and carbon and nitrogen (B) in the body and mucus of jellyfish species (*A. aurita, C. fulgida, C. pacifica, E. inexplicata*, and *R. pulmo*) expressed as a percentage of the dry weight (DW) of the sample and as the relative proportion of the total proteins, lipids and carbohydrates (C) and carbon and nitrogen (D) content. The dots represent the C:N ratio (D). 55
3.3 Energy content of the body (dark grey) and mucus (light grey) of jellyfish species (*A. aurita, C. fulgida, C. pacifica, E. inexplicata*, and *R. pulmo*) normalised to the dry weight (DW) of the samples (A). Error bars show the standard deviation. Linear regression between the energy content (EC) and the carbon content (CC) of jellyfish body (circles) and mucus (triangles; B). The lines represent the linear regressions and the shaded area is the confidence interval. The solid line is the linear regressions on the whole data set (EC = 35.03 $\pm$ 1.27 CC - 0.05 $\pm$ 0.06; details in Appendix B, Table B.5). 55

4.1 Change in MA (A), PHP (B), DOC (C) and TDN (D) following the addition of mucus-OM (dry-mucus and frozen-mucus) in incubators filled with ASW:FSW (9:1). Lines represent the means with the coloured area being the standard deviation. 70
4.2 Ammonium (A) and phosphate (B) concentrations in treatment incubators (dry-mucus, frozen-mucus and control) in filled with ASW:FSW (9:1). Lines represent the means with the coloured area being the standard deviation. 71
4.3 Results of the Nonmetric multidimensional scaling (NMDS) ordination of amino acid composition of the treatments (dry-mucus, frozen-mucus and control represented by circles, triangles and crosses, respectively) over time (0, 5, 10, 20, 30, 42h represented by the colour gradient from dark to light). The scores for dimensions 1 and 2 are shown in panel A while the contribution of amino acids for dimensions 1 and 2 are shown in panel B, with the length of the arrows indicating the importance of the respective amino acid to the dimension. GLU =glutamic acid, ASP=aspartic acid, SER=serine, HIS=histidine, GLY=glycine, THR=threonine, ARG=arginine, ALA=alanine, TAU=taurine, VAL=valine, MET=methionine, PHE=phenylalanine, ILE=isoleucine, LEU=leucine, LYS=lysine. Glutamine, asparagine and tyrosine are not shown as their contribution to the dimensions were negligible. 72
4.4 (A) Relative abundance of the main microbial orders (>1% of total reads abundance) and (B) nonmetric multidimensional scaling (NMDS) ordination of the normalised number of reads assigned to species for the treatments (dry-mucus, frozen-mucus and control). 73

4.5 Conceptual diagram of the impact of jellyfish mucus and body microbial degradation on coastal marine ecosystems. The central table compares nutrients (organic and inorganic) released by a gram of dry weight (DW). POC= particulate organic carbon. PON= particulate organic nitrogen. DOC=dissolved organic carbon. DON= dissolved organic nitrogen. DIN=dissolved inorganic nitrogen. GLY= glycine. TAU=taurine. DFAA= dissolved free amino acid. TDN= total dissolved nitrogen. LMW= low molecular weight. PGE = prokaryotic growth efficiency. Jellyfish body data is from Tinta et al. (2020). Mucus PGE is from Condon et al. (2011). 79

5.1 Conceptual schematic of the role of jellyfish and their interaction with microbes in nutrient cycles and ecosystem productivity showing: nitrification associated with pelagic jellyfish (Chapter 2), the elemental and macromolecular composition of jellyfish mucus (Chapter 3) and the microbial degradation of jellyfish mucus (Chapter 4). The flows of organic and inorganic matter are shown by grey and white arrows, respectively. Colours indicate ammonium (NH_4^+, orange), nitrite (NO_2^-, yellow), nitrate (NO_3^-, green) and phosphate (PO_4^-, purple). Coloured arrows represent ammonium-oxidation (orange-to-yellow) and nitrite-oxidation (yellow-to-green). Components linked to small coloured circles release inorganic nutrients of the same colour. The large circle zooms in on the jellyfish epithelium. 83

Appendix A.1 Measured concentrations of ammonium (A), phosphate (B), nitrite (C) and nitrate (D) of the Jellyfish treatment incubators for the jellyfish species *A. aurita, C. fulgida, C. hysoscella* and *C. pacifica*. The vertical dashed line corresponds with the time when the jellyfish were removed from the incubators (6 h). 93

Appendix A.2 Ammonium (A), phosphate (B), nitrite (C) and nitrate (D) concentrations of the Jellyfish-Control treatment of *A. aurita* (blue), *C. hysoscella* (green), *C. pacifica* (red) and *C. fulgida* (orange). 94

Appendix A.3 Ammonium (A), phosphate (B), nitrite (C) and nitrate (D) concentrations of the Mucus-Control treatment of *A. aurita* (blue), *C. hysoscella* (green), *C. pacifica* (red) and *C. fulgida* (orange). 96

Appendix A.4 Ammonium (A), phosphate (B), nitrite (C) and nitrate (D) blank corrected concentrations of the Mucus treatment of *A. aurita* (blue), *C. hysoscella* (green), *C. pacifica* (red) and *C. fulgida* (orange). Coloured area = standard deviation of the mean cumulative release of nutrients. . 98

Appendix A.5 Nitrate concentration of an incubator (Volume=4L) with a jellyfish of *A. aurita* measured by a lab-on-chip sensor (left) and nitrate concentrations of the Jellyfish treatment incubator of *A. aurita* measured by gas-segmented continuous flow (QuAAtro, right). The ASW for the Jellyfish treatment incubator was made with reverse osmosis water presenting already high concentrations of nitrate (right). 103

Appendix A.6 Comparing spectrophotometric methods: Gas segmented continuous flow (QuAAtro) vs Lab-on-Chip sensor. Real-time concentrations of nitrate measured by a lab-on-chip sensor and filtered grab samples measured by gas segmented continuous flow 103

Appendix A.7 Relationship between the weight-specific phosphate and ammonium release rates for the jellyfish *A. aurita, C. hysoscella, C. pacifica* and *C. fulgida* at 16°C. The line represents the linear regression. 104
Appendix A.8 Relationship between the weight-specific nitrogen and phosphate release rates for the jellyfish *A. aurita, C. hysoscella, C. pacifica* and *C. fulgida* at 16°C. The continuous line represents the linear regression. The dashed line indicates where N:P ratio is 16:1 (Redfield ratio). 104

Appendix C.1 Cumulative amount of dissolved nutrients (NH_4^+, NO_3^-, NO_2^-, PO_4^{3-}, DIN, TDN, DON, DOC, GLU =glutamic acid, ASP=aspartic acid, ASN=asparagine, SER=serine, GLN=glutamine, HIS=histidine, GLY=glycine, THR=threonine, ARG=arginine, ALA=alanine, TAU=taurine, GABA=gamma-aminobutyric acid, TYR=tyrosine, VAL=valine, MET=methionine, PHE=phenylalanine, ILE=isoleucine, LEU=leucine, LYS=lysine) that leached through a 1kDa Molecular Weight Cut-Off (MWCO) membrane tubing during 24 hours. 122
Appendix C.2 Cumulative amount of dissolved nutrients (NH_4^+, NO_3^-, NO_2^-, PO_4^{3-}, DIN, TDN, DON, DOC, GLU =glutamic acid, ASP=aspartic acid, ASN=asparagine, SER=serine, GLN=glutamine, HIS=histidine, GLY=glycine, THR=threonine, ARG=arginine, ALA=alanine, TAU=taurine, GABA=gamma-aminobutyric acid, TYR=tyrosine, VAL=valine, MET=methionine, PHE=phenylalanine, ILE=isoleucine, LEU=leucine, LYS=lysine) that leached from dry-mucus during 24 hours expressed in µmol per g of DW. 128
Appendix C.3 Cumulative amount of dissolved nutrients (NH_4^+, NO_3^-, NO_2^-, PO_4^{3-}, DIN, TDN, DON, DOC, GLU =glutamic acid, ASP=aspartic acid, ASN=asparagine, SER=serine, GLN=glutamine, HIS=histidine, GLY=glycine, THR=threonine, ARG=arginine, ALA=alanine, TAU=taurine, GABA=gamma-aminobutyric acid, TYR=tyrosine, VAL=valine, MET=methionine, PHE=phenylalanine, ILE=isoleucine, LEU=leucine, LYS=lysine) that leached from frozen-mucus during 24 hours expressed in µmol per g of DW. 134
Appendix C.4 Concentrations of dissolved nutrients (NH_4^+, NO_3^-, NO_2^-, PO_4^{3-}, DIN, TDN, DON, DOC, GLU =glutamic acid, ASP=aspartic acid, ASN=asparagine, SER=serine, GLN=glutamine, HIS=histidine, GLY=glycine, THR=threonine, ARG=arginine, ALA=alanine, TAU=taurine, GABA=gamma-aminobutyric acid, TYR=tyrosine, VAL=valine, MET=methionine, PHE=phenylalanine, ILE=isoleucine, LEU=leucine, LYS=lysine) in treatment incubators (dry-mucus, frozen-mucus and control) during 42 hours expressed in µmol per g of DW. 143

List of Tables

2.1 Jellyfish collection and incubation details. 32
2.2 Release rates and regression statistics for the cumulative nutrient release by the four jellyfish species. The standard deviation of the slope = SD, number of observations = n. Rates at experimental temperatures and adjusted to 16°C are presented, as well as the N : P ratios at 16°C. The rate, SD, R^2, and p are mean values from the replicates individual linear regressions. Levels of statistical significance are indicated by *, **, and *** ($p \leq 0.05$, 0.01, and 0.001, respectively). 41
2.3 Overview of case studies. Surface temperature at sampling time and body characteristics of jellyfish used to estimate inorganic nitrogen release. [a] Calculated from (Han et al., 2009a). [b] Mean annual surface temperature in august from (Junker et al., 2017). [c] Calculated from (Houghton et al., 2007). 45

4.1 Summary of the experimental design. POC: particulate organic carbon, PON: particulate organic nitrogen, DOC: dissolved organic carbon, TDN: total dissolved nitrogen, DFAA: dissolved-free amino acids, IN: inorganic nutrients (ammonium, nitrite, nitrate, phosphate), MA: microbial abundance, PHP: prokaryotic heterotrophic production, ASW: aged seawater, NSW: natural seawater. 65
4.2 Cumulative amount of dissolved nutrients (NH_4^+, NO_3^-, NO_2^-, PO_4^{3-}, DIN, TDN, DON, DOC, DFAA) leached from dry-mucus and frozen-mucus within 24 h. The values are presented as average ± standard deviation (n = 2). 69

Appendix A.1 Summary table of linear regression results from the Jellyfish-Control treatment. The use of *, **, and *** denotes levels of statistical significance (p=0.05, 0.01, and 0.001 respectively). 95
Appendix A.2 Volume of ammonium stock solution (100 mM) and expected increase in concentration of the Mucus and Mucus-Control treatments of *A. aurita*, *C. hysoscella*, *C. pacifica* and *C. fulgida*. 96
Appendix A.3 Summary tables of linear regression results from the Mucus-Control treatment. The use of *, **, and *** denotes levels of statistical significance (p=0.05, 0.01, and 0.001 respectively). 97
Appendix A.4 Summary tables of linear regression results from the Mucus treatment for ammonium (A), phosphate (B), nitrite (C) and nitrate (D). . 99
Appendix A.5 Summary tables of ANCOVA analyses in between species of the Jellyfish treatment for ammonium (A), phosphate (B), nitrite (C) and nitrate (D). The use of *, **, and *** denotes levels .05, .01, and .001 of statistical significance, respectively. NS= non-significative. 100

Appendix A.6 Summary of the linear regressions on the effect of wet-weigh on the mass-specific nutrient releases normalised to 16°C. The use of *, **, and *** denotes levels of statistical significance (p = 0.05, 0.01, and 0.001 respectively). 101
Appendix A.7 Calibration points and limit of detection (LOD) for the different instrument used for the analysis of samples from the experiment of the jellyfish species *A. aurita, C. hysoscella, C. fulgida* and *C. pacifica*. C= concentration (μM) and A= absorbance. 106

Appendix B.1 Review of the biochemical composition (protein, lipid and carbohydrate) of members of marine zooplankton as a percentage of dry body weight, and jellyfish mucus as a relative percentage. 108
Appendix B.2 Table of cholesterol dilutions for calibration 111
Appendix B.3 Table of BSA dilutions for calibration 112
Appendix B.4 Table of glucose dilutions for calibration 113
Appendix B.5 Summary of linear regression ($\sim$) and ANCOVA (:). SM = sum of macromolecules, AFDW = ash-free dry-wet, EC = energy content, CC = carbon content. 114

Appendix C.1 Percentage of dry weight (DW) contained in mucus wet weight (WW) from the jellyfish *A. aurita* after freeze-drying. 116
Appendix C.2 Cumulative amount of dissolved nutrients (NH_4^+, NO_3^-, NO_2^-, PO_4^{3-}, DIN, TDN, DON, DOC, DFAA) that leached through a 1 kDa Molecular Weight Cut-Off (MWCO) membrane tubing within 24 h expressed in µmol per g of dry weight (DW). 117
Appendix C.3 Cumulative amount of dissolved nutrients (NH_4^+, NO_3^-, NO_2^-, PO_4^{3-}, DIN, TDN, DON, DOC, DFAA) that leached from dry-mucus within 24 h expressed in µmol per g of DW. 123
Appendix C.4 Cumulative amount of dissolved nutrients (NH_4^+, NO_3^-, NO_2^-, PO_4^{3-}, DIN, TDN, DON, DOC, DFAA) that leached from frozen-mucus within 24 h expressed in µmol per g of DW. 129
Appendix C.5 Summary of dissolved nutrients (NH_4^+, NO_3^-, NO_2^-, PO_4^{3-}, DIN, TDN, DON, DOC, DFAA) released during the dialysis and leaching experiments (dry-mucus and frozen-mucus). 135
Appendix C.6 Percentages and concentrations of the amino acids (GLU =glutamic acid, ASP=aspartic acid, ASN=asparagine, SER=serine, GLN=glutamine, HIS=histidine, GLY=glycine, THR=threonine, ARG=arginine, ALA=alanine, TAU=taurine, GABA=gamma-aminobutyric acid, TYR=tyrosine, VAL=valine, MET=methionine, PHE=phenylalanine, ILE=isoleucine, LEU=leucine, LYS=lysine) released during the leaching experiment by dry-mucus and frozen-mucus. The last column is the mean of the percentage of both leaching experiments. 136
Appendix C.7 Comparative table of the cumulative amount of DOC, TDN and DON that leached through a 1 kDa Molecular Weight Cut-Off (MWCO) membrane tubing within 24 h and that leached directly from dry-mucus in 24h. The fraction <1 kDa represents low molecular weight compounds (LMW). The amount of high molecular weight compounds (HMW, >1 kDa) is expressed as the percentage of total mucus DW per pool of compounds. 137

Appendix C.8 Cumulative amount of particulate organic matter (POC and PON) released from dry-mucus and frozen-mucus in 1 h, expressed in µmol per g of DW of mucus per hour. 137
Appendix C.9 Comparison between the nutrients (organic and inorganic) released by dry-mucus, frozen-mucus and freeze-dried jellyfish carcasses (Jelly-DM, Tinta et al. 2020) expressed in µmol gDW^{-1} d^{-1}. The two last columns present the ratio between the amount of nutrient released by Jelly-DM against the dry-mucus and frozen-mucus. 138
Appendix C.10 Pairwise beta diversity indices on the relative species abundances from the mucus incubation treatments (dry-mucus, frozen-mucus, control). 143

List of Additional Material

Supplementary Material - Chapter 2

Supplementary Material - Chapter 3

Supplementary Material - Chapter 4

Declaration of Authorship

I declare that this thesis and the work presented in it is my own and has been generated by me as the result of my own original research.

I confirm that:

1. This work was done wholly or mainly while in candidature for a research degree at this University;
2. Where any part of this thesis has previously been submitted for a degree or any other qualification at this University or any other institution, this has been clearly stated;
3. Where I have consulted the published work of others, this is always clearly attributed;
4. Where I have quoted from the work of others, the source is always given. With the exception of such quotations, this thesis is entirely my own work;
5. I have acknowledged all main sources of help;
6. Where the thesis is based on work done by myself jointly with others, I have made clear exactly what was done by others and what I have contributed myself;
7. Parts of this work have been published as:
    - Hubot, N. D., Giering, S. L. C., Füssel, J., Robidart, J., Birchill, A., Stinchcombe, M., Dumousseaud, C., & Lucas, C. H. (2021). Evidence of nitrification associated with globally distributed pelagic jellyfish. *Limnology and Oceanography*, *66*(6), 2159–2173. https://doi.org/10.1002/lno.11736
    - Hubot, N., Giering, S. L. C., & Lucas, C. H. (2022). Similarities between the biochemical composition of jellyfish body and mucus. *Journal of Plankton Research*, *44*(2), 337–344. https://doi.org/10.1093/plankt/fbab091

Signed:..... Date:19/05/2023

Acknowledgements

First and foremost, I am extremely grateful to my supervisors Dr. Sari Giering and Dr. Cathy Lucas for their invaluable support and guidance throughout this journey. Sari, you have been the best mentor I could have dreamed of. All Ph.D. students deserve to have a supervisor like you. Cathy, thank you so much for believing in me and welcoming me to the NOCS in the first place. It has been an honour to work with you all these years. This journey would not have been possible without the support of my additional and unofficial supervisor Dr. Julie Robidart. Julie, you have been essential in guiding me toward my new passion. Thank you all for your patience and trust. What I have learned from your mentorship will remain with me throughout my career.

To my coauthors, J. Fuessel, T. Tinta, A. Birchill, M. Stinchcombe, C. Dumousseaud, K. Klun, G. Herndl. It has been a great pleasure working with you. To all the people that helped me at some point during these 5 years such as M. Gibbons, K. Hanselmann, M. Smith, L. Holman, L. Hirst, S. Evans, R. Pearce, S. Bray, B. Hambach, N. Orel. I extend my gratitude to the captain and crew of the cruise DY090 and of the RV Mirabilis.

To my friends: Pablo, Elena, Stacey, Sandy, Jan, David, Nico, Stefan, Joe, Delphine, Maria, Adeline, Sophie, Ben, Koko and many more. I am so lucky and proud that you are my friends. You are an inspiration and a motivation to do and be better. To the lovely Marika and Giulia for being who they are. All of you are making my life amazing.

To my parents, Bernard & Monica, my sisters, Flora & Zoé and my grandparents, Kiki & Mainene, Ludo & Marion, Ghislaine & Maurice. I am so lucky to have been born and raised in your company. Thank you for making me who I am today.

This thesis was funded by the Graduated School of the National Oceanography Centre Southampton through the Researcher Training Support Grant (RTSG number: 517191102). Additional funding was provided by the UKRI through the COMICS (Controls over Ocean Mesopelagic Interior Carbon Storage; NE/M020835/1) project and by the Newton Fund RCUK-NRF International Ph.D. Partnering Scheme.

To my grandparents, in loving and grateful memory

Definitions and Abbreviations

ANOVA	Analysis of variance
ANCOVA	Analysis of covariance
ASW	Artificial seawater
BGE	Bacterial growth efficiency
BLAST	Basic local alignment search tool
CO_2	Carbon dioxide
DFAA	Dissolved free amino acid
DIC	Dissolved inorganic carbon
DIN	Dissolved inorganic nitrogen
DNA	Deoxyribonucleic acid
DOC	Dissolved organic carbon
DOM	Dissolved organic matter
DON	Dissolved organic nitrogen
DSR	Deep-sea reference
DW	Dry weight
g	Gram
LOD	Limit of detection
m	Milli (10^{-3})
MA	Microbial abundance
MT	Million tonnes
n	Nano (10^{-9})
N	Nitrogen
NH_4^+	Ammonium
NO_3^-	Nitrate
NO_2^-	Nitrite
NSW	Natural seawater
O_2	Oxygen
OM	Organic matter
OPA	Ortho-phthalaldehyde
P	Phosphorus
PCR	Polymerase chain reaction
pH	Potential of hydrogen

PO_3^-	Phosphate
POC	Particulate organic carbon
POM	Particulate organic matter
PON	Particulate organic nitrogen
PGE	Prokaryotic growth efficiency
PHP	Prokaryotic heterotrophic production
qPCR	Quantitative polymerase chain reaction
RNA	Ribonucleic acid
rRNA	Ribosomal ribonucleic acid
T	Tera (10^{12})
TCA	trichloroacetic acid
TDN	Total dissolved nitrogen
UK	United-Kingdom
US	United-States
WW	Wet weight
μ	Micro (10^{-6})

Chapter 1

Introduction

Carbon emissions from human activities are causing ocean warming, acidification and oxygen loss with some evidence of changes in nutrient cycling and primary production. The changing ocean is affecting marine organisms at multiple trophic levels, impacting fisheries with implications for food production and human communities (Intergovernmental Panel on Climate Change (IPCC), 2022). Simultaneously, jellyfish populations are rising in several coastal ecosystems around the world (Brotz et al., 2012). Often considered detrimental to human activities, jellyfish outbreaks represent a significant but largely overlooked source of organic matter to the marine ecosystem (Tinta et al., 2020) capable of having large impacts on biogeochemical cycles and pelagic food webs (e.g. Condon et al., 2011; Pitt et al., 2009c; Tinta et al., 2021). Furthermore, the interaction and association of jellyfish with microorganisms, allow jellyfish blooms to influence the dynamic of marine microbial communities in coastal waters (Condon et al., 2011; Tinta et al., 2020). This thesis aims to evaluate the role that jellyfish and their interaction with marine microbes play in the cycling of nutrients and ultimately on ecosystem productivity. This chapter will introduce the study by first presenting the background and context of the research, identifying the knowledge gaps, deriving the hypothesis and finally describing the objectives of this thesis.

1.1 Background

Jellyfish are part of a larger taxon called “gelatinous zooplankton”, which are defined as soft-bodied animals that live in the water column and cannot propel themselves against currents (Hosia et al., 2017). Gelatinous zooplankton communities include a wide range of organisms belonging to four phyla: the Cnidaria, the Ctenophora, the Chordata and the Chaetognatha (Boero et al., 2008). The term jellyfish broadly refers to the cnidarian medusae and the ctenophores, therefore all the jellyfish are gelatinous

zooplankton but not all the gelatinous zooplankton are jellyfish (Richardson et al., 2009).

Over recent decades, mounting evidence has highlighted an increase in jellyfish outbreaks (i.e. large aggregations of jellyfish, also called "blooms") in several coastal regions around the world (e.g.: Sea of Japan, Black sea, Benguela current, Antarctic; Figure 1.1; Brotz et al., 2012) both in magnitude and frequency (Purcell, 2012). The presence of large jellyfish masses in coastal waters can lead to disturbances to marine ecosystems and human activities, causing severe economic damage, in particular to tourism, energy industries and fisheries (Purcell et al., 2007; Richardson et al., 2009). The tourism industry is impacted by jellyfish outbreaks in swimming areas, as some jellyfish species cause severe injuries, dissuading tourists from going to the beach. For example, an outbreak of *Rhopilema nomadica* on the coast of Israel in summer months has been estimated to reduce the number of visitors by 3 to 10.5%, corresponding to an annual monetary loss of €1.8–6.2 million (Ghermandi et al., 2015). Power plants have been forced to shut down due to jellyfish clogging the cooling towers which causes emergency situations at nuclear power plants, significant power loss and financial harm to cities (Purcell et al., 2007). In 2011, the UK energy company EDF suffered an estimated £10 million loss due to a 7-day shutdown of the Torness nuclear plant in Scotland, due to jellyfish. Lastly, by preying on both zooplankton and ichthyoplankton (eggs and larvae of fish) jellyfish exert a dual bottom-up and top-down control on fish populations, which can negatively impact fisheries (Purcell et al., 2001). For example, the annual direct impact of jellyfish blooms on Korea's fisheries was estimated to range between US$ 68 million and US$ 205 million, which corresponds to a decrease of between 2.1% and 25% of the annual production value, demonstrating that jellyfish cause considerable damage to the fishing industry (Kim et al., 2012).

Despite recent efforts in quantifying jellyfish population abundance and trends (e.g. Brotz et al., 2012; Condon et al., 2012; Lucas et al., 2014b; Luo et al., 2020), a debate remains about the overall global trend of jellyfish populations (Gibbons et al., 2013). These last decades, the high number of reports of jellyfish blooms coupled with media-driven public perception has led to the emergence of a paradigm in which the global ocean ecosystems are becoming dominated by "nuisance" jellyfish (Condon et al., 2012). Still, robust time-series of direct observations of jellyfish abundance are not available for many ecosystems, leaving it difficult to determine changes in jellyfish abundance (Mitchell et al., 2021). The lack of historical data is partly due to jellyfish lacking hard structures that can leave lasting fossil records. In addition, jellyfish are difficult to sample (the fragile bodies of jellyfish are broken by nets). Lastly, jellyfish have been historically dismissed by most researchers conducting regular wide-reaching surveys of abundant economically valuable fish stocks (Mitchell et al., 2021). Better data on the abundance, biomass, and spatiotemporal distributions of jellyfish populations is needed in order to tease apart whether there is a shift in the

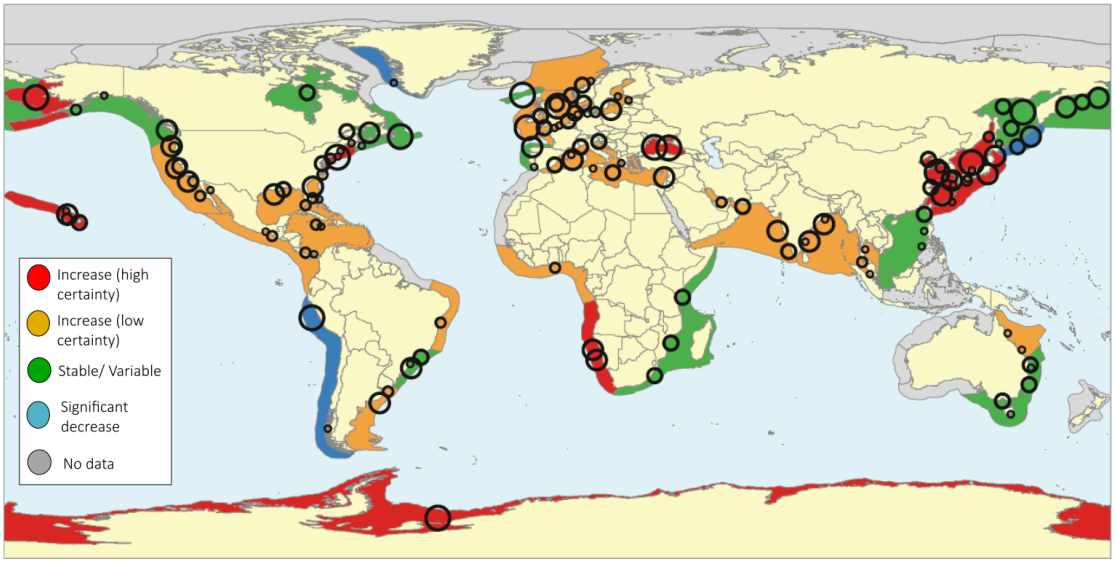

FIGURE 1.1: Map of population trends of native and invasive species of jellyfish. Circles represent discrete chronicles with relative sizes reflecting the confidence index (modified from Brotz et al., 2012)

overall jellyfish abundance baseline or whether the apparent increase is due to a larger oscillation (Condon et al., 2012). Still, regardless of global trends, jellyfish are causing ecological and economic issues in several coastal marine ecosystems (Richardson et al., 2009).

Jellyfish outbreaks have often followed the collapses of formerly dominant local fish (i.e.: Black Sea, Caspian Sea, Benguela upwelling system, Sea of Japan; Richardson et al., 2009). By "fishing down the marine food chain" (Pauly et al., 2005; Figure 1.2), the industry is removing both predators and competitors of jellyfish (Lilley et al., 2011) thus improving the conditions for their population rise (Purcell et al., 2007). In addition to overfishing, several other anthropogenic causes can explain the recent success of some jellyfish populations such as cultural eutrophication, global warming, species translocation and increase in artificial substrates (Richardson et al., 2009). Once established, a jellyfish invasion potentially shunts carbon flows away from higher trophic levels, through their voracious predation on zooplankton, which can lead to a durable ecosystem shift (Condon et al., 2011). For example, in Namibia's coastal waters, the biomass of jellyfish has been estimated to be 12.2 million tonnes (MT), exceeding the biomass of once-abundant fish (3.6 MT; Lynam et al., 2006) by more than three times. Whilst the direct economic impacts of a rise in jellyfish abundance have been increasingly explored, less is known about their indirect effect on the marine ecosystem, such as their impact in biogeochemical cycles and microbial communities. Investigating the role of jellyfish blooms in nutrient cycling is therefore the focus of my thesis.

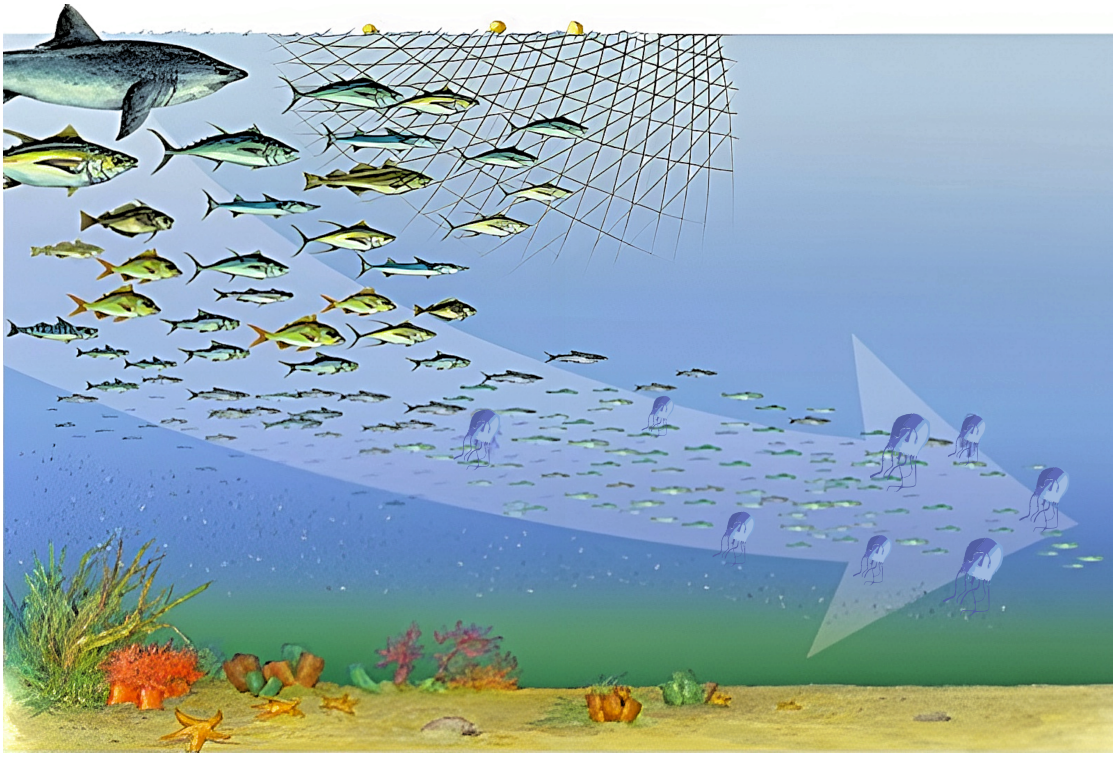

FIGURE 1.2: Fishing down marine food webs: the three stages (past, present and future) offer increasingly better conditions for jellyfish (Based on Pauly et al., 2009 and modified by fishing-down.org).

1.2 Jellyfish biology and ecology

Cnidarian medusae are composed of Hydromedusae and Scyphomedusae (i.e. medusae from hydrozoan and scyphozoan, respectively), together contributing to 92% of the total global biomass of gelatinous zooplankton (Lucas et al., 2014b). Hydromedusae forms a diverse group ($>$ 800 species worldwide), most of which are $<$1 cm in size and transparent whereas Scyphomedusae ($>$ 200 species worldwide) are much larger (up to 80 cm in diameter) and often pigmented (Purcell et al., 2013. Cnidarian medusae blooms are generally due to scyphomedusae, not hydromedusae (Schiariti et al., 2018). Hereafter the term jellyfish will refer specifically to cnidarian medusae. However, the work presented in this thesis has been performed exclusively on bloom-forming large Scyphomedusae.

With the aim of highlighting the specific traits that make jellyfish a unique member of marine zooplanktons, the following sections will describe some of the biological and ecological characteristics of jellyfish such as their life cycle and population dynamic, their metabolism and physiological rates and lastly their associated microbiome.

1.2.1 Population dynamics and life cycle

Jellyfish usually show a metagenetic life cycle composed of a pelagic, short-living lecithotrophic larval stage (planula), an asexual benthic post-larval stage (polyp or scyphistoma) and a sexually reproductive pelagic stage (medusa; Arai, 1996; Figure 1.3). They have a high number of alternate pathways of reproduction (asexual vs sexual, monodisc vs polydisc strobilation, self-fertilization and multiples budding modes; Takeda et al., 2018), survival (podocysts; Arai, 2009) or reverse development and cell trans-differentiation (Piraino et al., 2004). Since many jellyfish are modular organisms, a single event of fertilization does not lead to a single new specimen but rather to a polyp colony (i.e. clone of individual polyps) that will produce a batch of medusae several times over the year. Their complex life cycles allow high rates of reproduction resulting in seasonal development of large blooms when conditions are favourable (Boero et al., 2008).

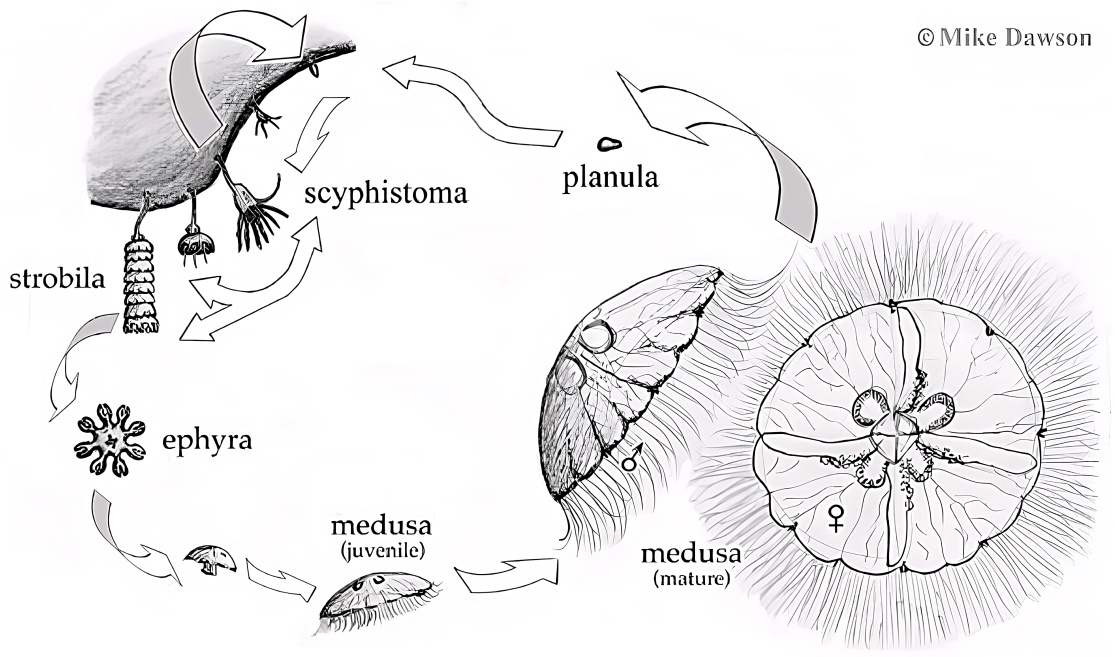

FIGURE 1.3: Schematic description of the *Aurelia* spp. life cycle (Drawn by Mike Dawson)

Jellyfish are usually considered to have boom-and-bust population dynamics, which means that they can opportunistically increase their feeding, growth and reproduction rates upon favourable conditions, leading to a fast increase in the population followed by a sudden collapse (Boero et al., 2008; Pitt et al., 2009b). Their fast and brief appearance is not an anomaly but rather an adaptation allowing them to take advantage of fluctuations in resource availability (Figure 1.4). The episodic bloom events are recognized as an important ecological component of marine ecosystems (Boero, 1994) and their occurrence is attributed to the peculiar life cycle of most jellyfish.

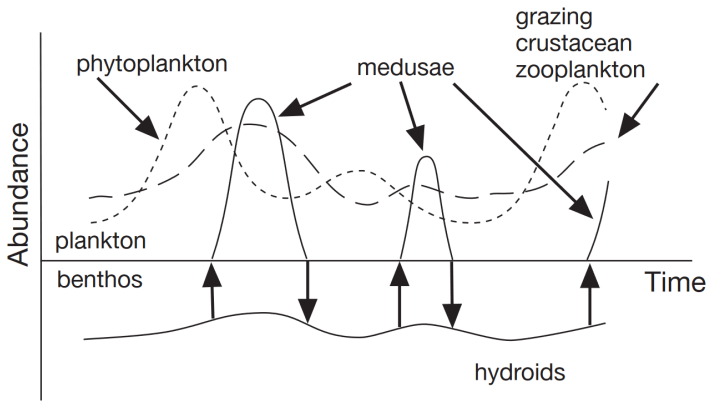

FIGURE 1.4: Life cycle strategies of medusae with benthic polyps. Peaks of abundance in the plankton are tuned to food availability. The exploitation of trophic resources leads to sexual reproduction and larval development, followed by the disappearance of adult medusae from the water column and planula metamorphosis into the polyp benthic stage. Polyps have a continuous presence in the benthos producing the next generation of medusae (Boero et al., 2008).

1.2.2 Metabolism and physiology

Body size and metabolic rate both fundamentally constrain how organisms interact with their environment, and hence ultimately affect their niche (Healy et al., 2013). Metabolic rate, the rate at which organisms take up, transform, and expend energy and materials, is one of the most fundamental biological rates. It determines the demands that organisms place on their environment for all resources, and simultaneously sets powerful constraints on the allocation of resources to all components of fitness (Brown et al., 2004). The way jellyfish affect their environment can thus be investigated through their metabolism and more specifically by looking at their physiological rates such as ingestion, digestion, growth, respiration and excretion (Figure 1.5).

Most jellyfish are considered opportunistic predators preying essentially on zooplankton from a wide range of sizes (i.e.: from microplankton to mesozooplankton; Boero, 2013). They are on average 3.2 times larger than other pelagic animals of equivalent carbon content due to their high-water content (>95%) allowing them to grow much larger and faster than other animals relative to their carbon content (Pitt et al., 2013). For example, *A. aurita* medusae are capable of ingesting more than their body carbon weight per day under excess food concentration (Uye et al., 2005) and most zooplankton are digested within 2-4 h (e.g., Båmstedt et al., 2000; Purcell, 1997). Many jellyfish can exhibit instantaneous growth rates around 0.3 d^{-1} (Pitt et al., 2013) contrasting with the lower rates of other marine invertebrates such as copepods and crustaceans (0.1 and 0.05 d^{-1}, respectively; Hirst et al., 2003). Inversely, when food is limited, jellyfish decrease their swimming pulse and slowly start consuming their biomass, which will induce a reduction of their body size (Lilley et al., 2014). Once

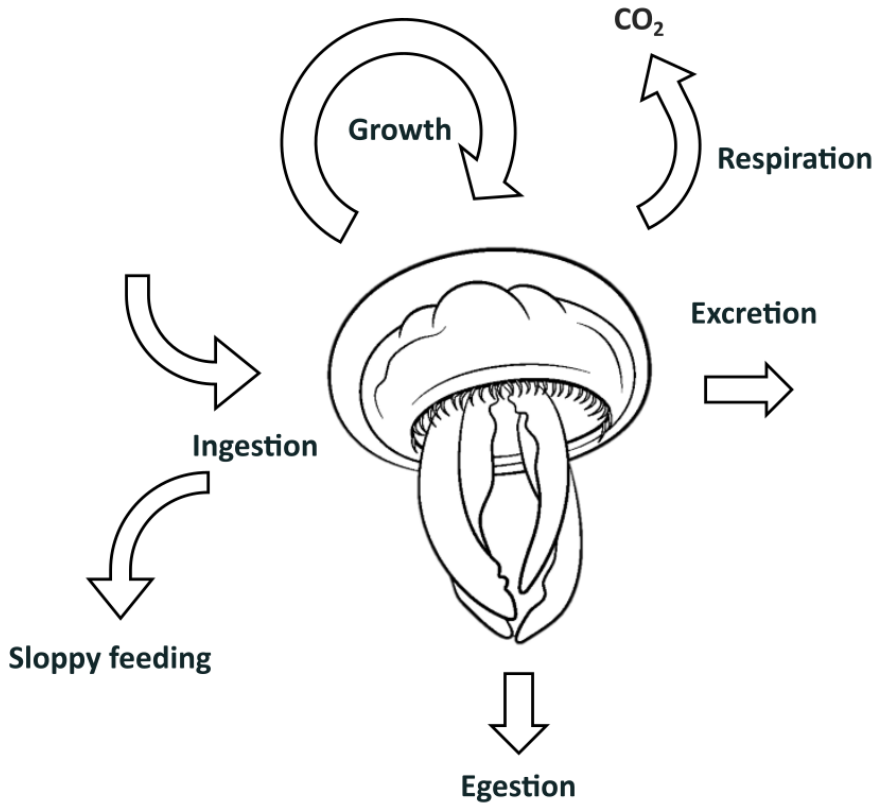

FIGURE 1.5: Metabolic budget. Part of the ingested organic matter is digested and the remains are egested mainly as particulate organic matter. The assimilated matter can then be used for growth and respiration or is released back to the environment via the excretion of both dissolved inorganic matter (ammonium and phosphate) and dissolved organic matter (mucus).

favourable condition returns, they can rapidly resume normal growth (Richardson et al., 2009). This flexibility in growth allows jellyfish to successfully adapt to changes in food availability and to reach important biomass when food is abundant.

Jellyfish have high assimilation efficiencies of both carbon and nitrogen. They assimilate carbon with efficiencies generally over 70% while often exceeding 90%, and have even higher nitrogen efficiencies (>90%; Pitt et al., 2009c). In comparison, the assimilation efficiencies of copepods is 63% and 77% for carbon and nitrogen, respectively (Steinberg et al., 2008). Although most jellyfish do not produce distinctive faeces (Pitt et al., 2009c), they can release particulate organic carbon matter (POM) through egested undigested food. Once assimilated by jellyfish, organic matter is primarily used for respiration (66%), inducing the release of waste products in the form of dissolved inorganic compounds such as carbon dioxide, ammonium and phosphate (Tinta et al., 2021). Biomass production (34% of assimilated food) is dominated by protein synthesis through the production of the mesoglea (protein extracellular matrix) which constitutes the core of the jellyfish body (Tinta et al., 2021). It has been estimated that up to 7% of the carbon assimilated by jellyfish is released in

the environment in the form of mucus (Hansson et al., 1995), which has been suggested to play an important role in carbon cycling (see section 1.3.2.1). However, the release of dissolved organic matter (DOM) by jellyfish has received little attention. To date, the rates of jellyfish DOM release through mucus excretion are poorly estimated. Similarly, the biochemical composition of jellyfish mucus has been analysed for only three species and via different methods of collection and analysis (Condon et al., 2011; Ducklow et al., 1979). Without a clear characterisation of jellyfish mucus composition and release rates, it is to date not possible to have an accurate understanding of the impact of jellyfish blooms on marine nutrient cycling.

In conclusion, while allometric relationships can predict a broad range of functional properties of animals, low carbon and high-water contents alone do not explain the differences in the allometric relationships between jellyfish and other pelagic animals (Pitt et al., 2013). Rather, it is the combination of their large size, simple body plan, and complex life histories that most likely explains the capacity of jellyfish to proliferate and develop spectacular blooms.

1.2.3 Microbiome

Recently, jellyfish have been shown to host a variety of microorganisms, collectively known as the jellyfish microbiome (Kramar et al., 2019; Lee et al., 2018; Weiland-Bräuer et al., 2015). Associated protists, bacteria, archaea, and viruses constitute essential components of the jellyfish microbiome (Weiland-Bräuer et al., 2015) expected to be involved in multiple host functions such as digestion, development and immune defences (Basso et al., 2019; Lee et al., 2018). As a consequence, the host and its associated microbiota form an intimate functional entity, termed the "metaorganism" or "holobiont" (Figure 1.6; Weiland-Bräuer et al., 2015). The holobiont concept represents a recent paradigm shift in the study of complex biological systems and implies that the host and its microbiome since forming a coherent ecological unit need to be studied together to understand their mutual biology, ecology, and evolution (Dittmar et al., 2021).

1.2.3.1 Composition and diversity

While all jellyfish seem to be covered with microorganisms, their microbial communities appear to differ within species and within different body parts of the same individual (e.g. Lee et al., 2018; Peng et al., 2021; Tinta et al., 2021; Weiland-Bräuer et al., 2015). Overall, studies agree on the fact that microbes living on the jellyfish are distinct from the bacterial community of the ambient water. *Gammaproteobacteria, Alphaproteobacteria, Bacteroidetes*, and *Actinobacteria* dominate all jellyfish life stages, with different relative contributions of each bacterial group

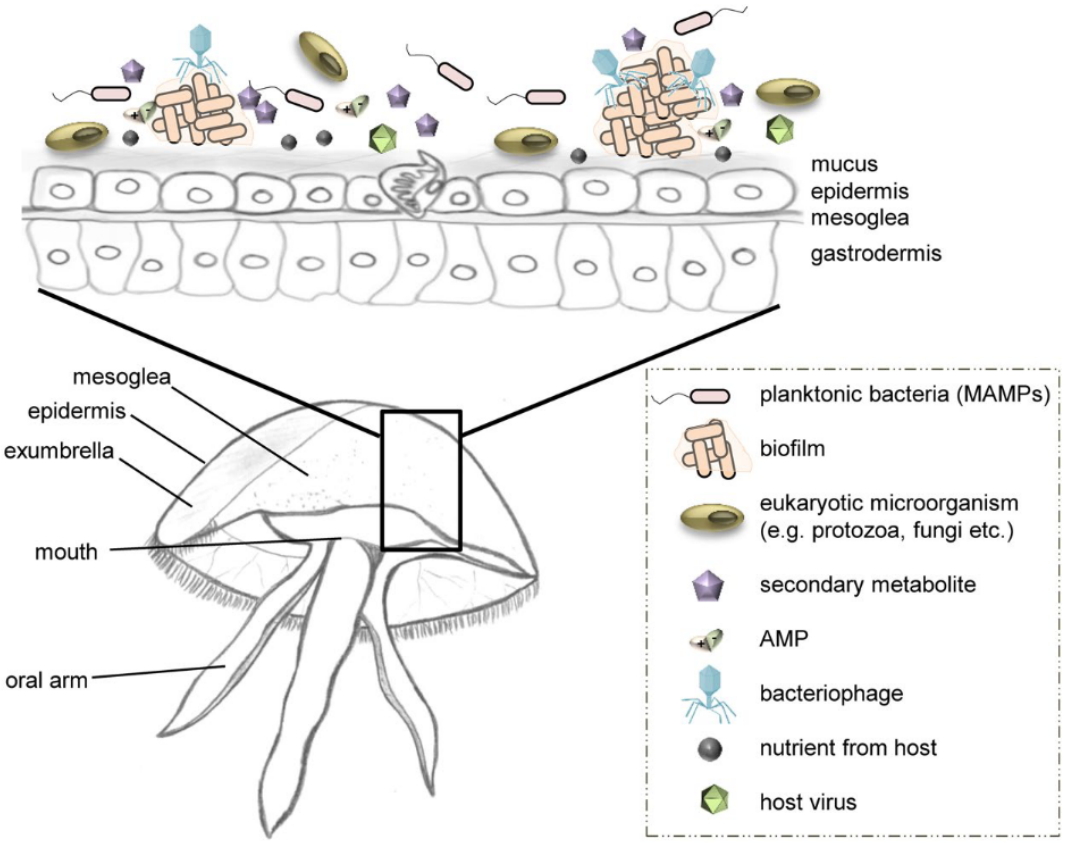

FIGURE 1.6: Schematic view of the jellyfish metaorganism (*A. aurita* medusa in a cut-away side view) and selected factors that might influence bacterial colonization of the host surfaces (from Weiland-Bräuer et al., 2019).

depending on the stage (reviewed by Tinta et al., 2019). The richness of the bacterial community was approximately the same among all examined life stages of *Aurelia aurita* (Weiland-Bräuer et al., 2015) and was closely related to bacteria previously found in association with other host animals, indicating that this relationship is not host-specific (Weiland-Bräuer et al., 2019). Further, it has been suggested that jellyfish harbour a core microbial community that is shared among jellyfish species and life stages (Lee et al., 2018). Still, only a small fraction of the jellyfish microbiomes have so far been investigated and the vast diversity of jellyfish as hosts remains to be explored (Tinta et al., 2019).

1.2.3.2 Role and function

In the ocean, where microorganisms are constantly facing changing environmental conditions on a microscale level, one adaptation/survival strategy consists of seeking a long-term relationship with other organisms (Tinta et al., 2019). The establishment of such symbiosis can be mutually beneficial by having a positive effect on the fitness of

the host while proving a suitable niche for microbes to thrive (Stabili et al., 2018; Tinta et al., 2019).

The jellyfish host can benefit from its microbiome for multiple physiological processes such as immune defence, digestion and development. The microbial community living on the surface of a jellyfish plays a crucial role in its defence against pathogens (Kramar et al., 2019; Tinta et al., 2019). As invertebrates do not have an adaptive immune system like more complex life forms, they rely on their innate immune system for defence. The innate immune system is a nonspecific defence mechanism, present in all multicellular organisms (Smith et al., 2019), allowing them to discriminate pathogens from beneficial microorganisms and to trigger the induction of protective programs (Nyholm et al., 2012). Therefore, a healthy jellyfish host must continuously modulate and control its colonization through a range of measures (e.g. by secreting bioactive compounds) in order to establish and maintain a healthy meta-organismal homeostasis that will protect it from pathogens (Weiland-Bräuer et al., 2019). For example, evidence suggests that *Aurelia aurita* can interfere with the bacterial communication system of its microbiota (i.e. quorum quenching) allowing it to regulate its bacterial population density, preventing unbalanced colonisation (Weiland-Bräuer et al., 2019). Furthermore, the microbiome found within the gastric pouches of jellyfish is involved in the jellyfish's digestive system (Tinta et al., 2019). For example, the gastric cavities of *Chrysaora tuberculata* contained a specific but very low microbial diversity community (4 groups accounting for $>$ 95% of the total bacterial diversity; Cortés-Lara et al., 2015), expected to be highly symbiotic to their host and providing it with carbon and energy sources (Viver et al., 2017). In addition, some bacteria are capable of inducing the settlement and metamorphosis of jellyfish larvae thus impacting the success of the individual and the species distribution (Ohdera et al., 2022). Overall, the jellyfish microbiome plays an important role in the fitness and environmental resilience of its host (Li et al., 2022).

Correspondingly, microorganisms living on the surface of jellyfish can benefit from the association in multiple ways, which are all linked to the jellyfish mucus layer. Jellyfish mucus is considered an attractive niche for marine microorganisms. Its high protein content makes it a high-quality energy source, which is readily utilized by heterotrophic bacteria (Kramar et al., 2018). In addition, jellyfish mucus contains a high proportion of salts including ammonium and phosphate, which can stimulate the growth of primary producers (Tinta et al., 2019). Further, studies have also suggested that jellyfish act as vectors of bacterial pathogens (Kramar et al., 2019; Stabili et al., 2020) transporting pathogens over long distances (Tinta et al., 2019). Overall, the mucus layer provides marine microbes with both a hospitable habitat and a high-quality energy source (Kramar et al., 2019). The microbial community living in the jellyfish mucus is thus relatively rich compared to the surrounding environment and is expected to harbour multiple complex microbial interactions and metabolic

pathways (Lee et al., 2018). Yet, the interactions, metabolic activities and functional traits of the major players within the jellyfish microbial community remain largely unknown.

Recent advances in jellyfish microbiome research have provided what is most likely just a glimpse at the complexity of the microbial communities associated with jellyfish. It has been speculated that the jellyfish microbiome is highly dynamic and complex, but the extent of that complexity is still not clear. Still so little is known about the specific role/function of the most abundant microbes and the mechanisms underlying the jellyfish-microbe relationship (Tinta et al., 2019). For example, though jellyfish do not directly produce nitrate, low rates of nitrate release have been observed in association with pelagic jellyfish ($< 2\%$ of total inorganic nitrogen released; Pitt et al., 2009c) suggesting that the jellyfish microbiome contains nitrifying microorganisms. Yet, to date, no studies have investigated the presence of nitrifiers on large bloom-forming pelagic jellyfish. An association between nitrifiers and jellyfish could have important implications for the nitrogen cycle of coastal marine ecosystems and thus for their productivity. In addition, while there has been some evidence about jellyfish mucus being a rich and labile source of carbon for microbes, its precise biochemical composition and the results of its microbial degradation have not been studied in sufficient detail. In particular, information on the release of nutrients from the microbial degradation of jellyfish mucus is missing. In conclusion, it appears that there are still large knowledge gaps regarding the role of mucus and its microbiome in both organic matter remineralisation and inorganic nutrient release. These aspects will therefore constitute one of the focuses of this thesis.

1.3 Jellyfish role in large scale processes

Jellyfish are ubiquitous and important players in various estuarine, coastal, and open-water ecosystems around the world (Tinta et al., 2021). As members of the marine zooplankton, they play a pivotal role in aquatic ecosystems and global biogeochemical cycles (Keister et al., 2012). However, they differ from other members of the zooplankton taxa in multiple aspects of their biology and ecology (see section 1.2). This section will describe how the previously discussed biology and ecology of jellyfish fit in large-scale processes such as the marine food chain and some aspects of nutrient cycling. The aim of this section is to highlight the relevance of jellyfish blooms for global ocean processes involving energy and nutrient fluxes.

1.3.1 Role in the marine food chain

The trophic ecology of jellyfish is complex and still poorly understood (Stoltenberg et al., 2021). Initially, this lack of understanding was probably due to the challenges in sampling and preservation of jellyfish's fragile bodies, leading to a general underestimation of their trophic and ecological role (Purcell, 2009). Recent methodological advances, e.g. genetic methods such as DNA metabarcoding (McInnes et al., 2017), trophic markers, including stable isotopes and fatty acids (Pitt et al., 2009a) and improved optical observation systems (Heaslip et al., 2012; Thiebot et al., 2017) have led to a renewed scientific focus and a paradigm shift on this topic.

Jellyfish have been identified as predators, prey and competitors of both zooplankton and fish, thus having different trophic roles in the marine food chain (Stoltenberg et al., 2021). Overall, the diet of jellyfish depends on prey availability and on the jellyfish's ability to adapt its prey selectivity (Graham et al., 2001; Purcell, 1997). Jellyfish consume mainly copepods, the dominant member of the zooplankton, but they are also capable of large deviations from that diet (Purcell, 1997). Overall, jellyfish are able to feed on a wide range of organism such as fish larvae (ichthyoplankton), microzooplankton assemblages (e.g. phytoplankton, tintinnids, rotifers and invertebrate larvae; Stoecker et al., 1987) and other members of gelatinous zooplankton (Purcell, 1997). The combination of this dietary flexibility with a unique swimming mechanism allows jellyfish to be efficient predators which partly explains their ecological success (Gemmell et al., 2013).

On the other end, jellyfish have traditionally been considered as trophic dead-ends, shifting away organic matter from higher trophic levels (Condon et al., 2011; Pauly et al., 2009). This paradigm is based on the apparent low abundance of specific predators (both in diversity and abundance) and on the low nutritional content of their biomass making jellyfish a poor prey choice (Hays et al., 2018). Despite their low energy content, recent studies using cutting-edge technologies such as stable isotope analysis (Cardona et al., 2012; Nagata et al., 2015), animal-borne cameras (Thiebot et al., 2017) and molecular techniques (Lamb et al., 2017; Marques et al., 2019) have provided evidence that jellyfish are consumed by many organisms throughout the marine food chain (Figure 1.7; Hays et al., 2018) supporting the notion that jellyfish are integral components of marine food webs.

Besides some specific predators such as the leatherback turtles and the ocean sunfish, jellyfish can be consumed by a wide range of opportunistic carnivores such as fish (Marques et al., 2019), molluscs, arthropods, reptiles and birds, feeding upon jellyfish biomass episodically (Doyle et al., 2014). For example, the jellyfish *Aurelia coerula* was found in the gut contents of 42% of commercially important fish species from the Thau Lagoon (Marques et al., 2019). Further, opportunist scavenging on jellyfish carcasses has been observed in the deep sea thus providing energy to numerous deep-water

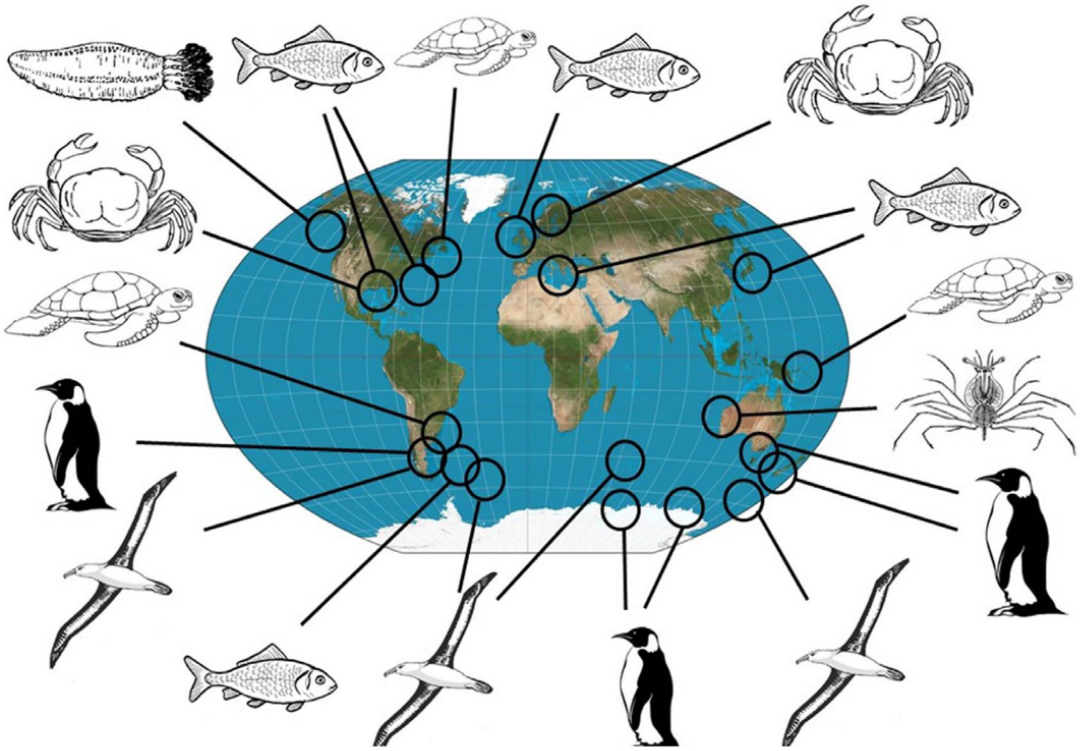

FIGURE 1.7: Map showing the general location of some of the studies and taxa shown to consume jellyfish, namely flying sea birds, penguins, fish including fish larvae, turtles, crabs, rock lobster larvae, and sea cucumber (from Hays et al., 2018).

species (Sweetman et al., 2014). Generally, the high-water content of jellyfish biomass makes it easily and quickly digested (e.g. up to 20 times faster than shrimps) thus counterbalancing their low energy density and reaching comparable rates of energy acquisition for predators feeding on fish or crustaceans (Hays et al., 2018). The consumption of gelatinous biomass can thus represent an alternative food resource when primary prey are not available (Briz et al., 2018) and would be particularly beneficial when energy-rich tissue, such as gonads and arms, are consumed preferentially (Hays et al., 2018). The value of such a diet is further enhanced by the high jellyfish abundance. Finally, jellyfish also provide habitat and space for developing larval and juvenile fish offering protection from predators as well as feeding opportunities (Griffin et al., 2019). Jellyfish blooms thus represent a significant source of food for marine ecosystems and are far from being a trophic dead-end.

The spatio-temporal variability of jellyfish populations makes it challenging to have a systematic and quantitative understanding of their role in the food webs (Stoltenberg et al., 2021). Thus, the importance and trophic role of jellyfish appears to be highly variable in space and time and rather ecosystem dependent. The case of the Benguela Upwelling ecosystem illustrates well the variability of jellyfish as members of the marine trophic chain and the potential importance of jellyfish in marine ecosystem

productivity. Further, this ecosystem will serve as a case study later throughout this thesis.

Case study: The Northern Benguela Upwelling System

The Benguela Current system is one of the world's four major eastern boundary upwelling ecosystems, characterized by wind-driven coastal upwelling resulting in high productivity (Fréon et al., 2009). The northern Benguela region, located on the Namibian shelf, was considered one of the major sardine stocks of the world, with an estimated stock of several million tons (MT) in the early 1960s (Boyer et al., 2001). However, in the late 1960s, heavy and unregulated fishing activities led to the collapse of the sardine stock later followed by increasing reports of the large and conspicuous jellyfish *Chrysaora fulgida* and *Aequorea forskalea* (mean umbrella diameter $\sim$ 27 cm and $\sim$ 13 cm respectively; Brierley et al., 2001). In 2003, a survey estimated jellyfish biomass of Namibian waters to 12.2 MT, exceeding by more than 3 times the biomass of fish (3.6 MT; Lynam et al., 2006), now dominated by the Cape hake and the Horse mackerel (Roux et al., 2013). The almost complete disappearance of sardines has profoundly, and possibly irreversibly, altered the northern Benguela food web from its original state, in which small pelagic fishes constituted the main link between producers and higher trophic levels (Figure 1.8, A; Roux et al., 2013). Nowadays, a large proportion of the energy flow is diverted away from higher-trophic-level production toward detritus through jellyfish (Figure 1.8, B). This shift in the food chain has allowed the bearded goby population to rise and become the predominant prey species for the larger fish, birds, and mammals in the region (Utne-Palm et al., 2010). By using jellyfish as a food source and as a protection from predation, the bearded goby has become the new (but less efficient) main trophic link in the northern Benguela food web ((Figure 1.8, B; Roux et al., 2013). Despite the overall decrease in productivity, Namibia still has one of the most productive fishing grounds in the world (FAO, 2015). While the importance of the bearded goby in the diet of the main predators is still to be clearly quantified, the case of the northern Namibian upwelling system illustrates the potential for jellyfish blooms to cause ecosystem shifts and to support the productivity of higher trophic levels.

1.3.2 Role in biogeochemical cycles

Scyphozoan jellyfish typically live in the epipelagic zone of marine coastal areas, which are among the most productive zones in the ocean. In such rich ecosystems, jellyfish blooms can reach large population sizes and quickly consume considerable amounts of zooplankton thus channeling large quantities of organic matter into gelatinous biomass (Condon et al., 2011). Besides the direct disturbances to the

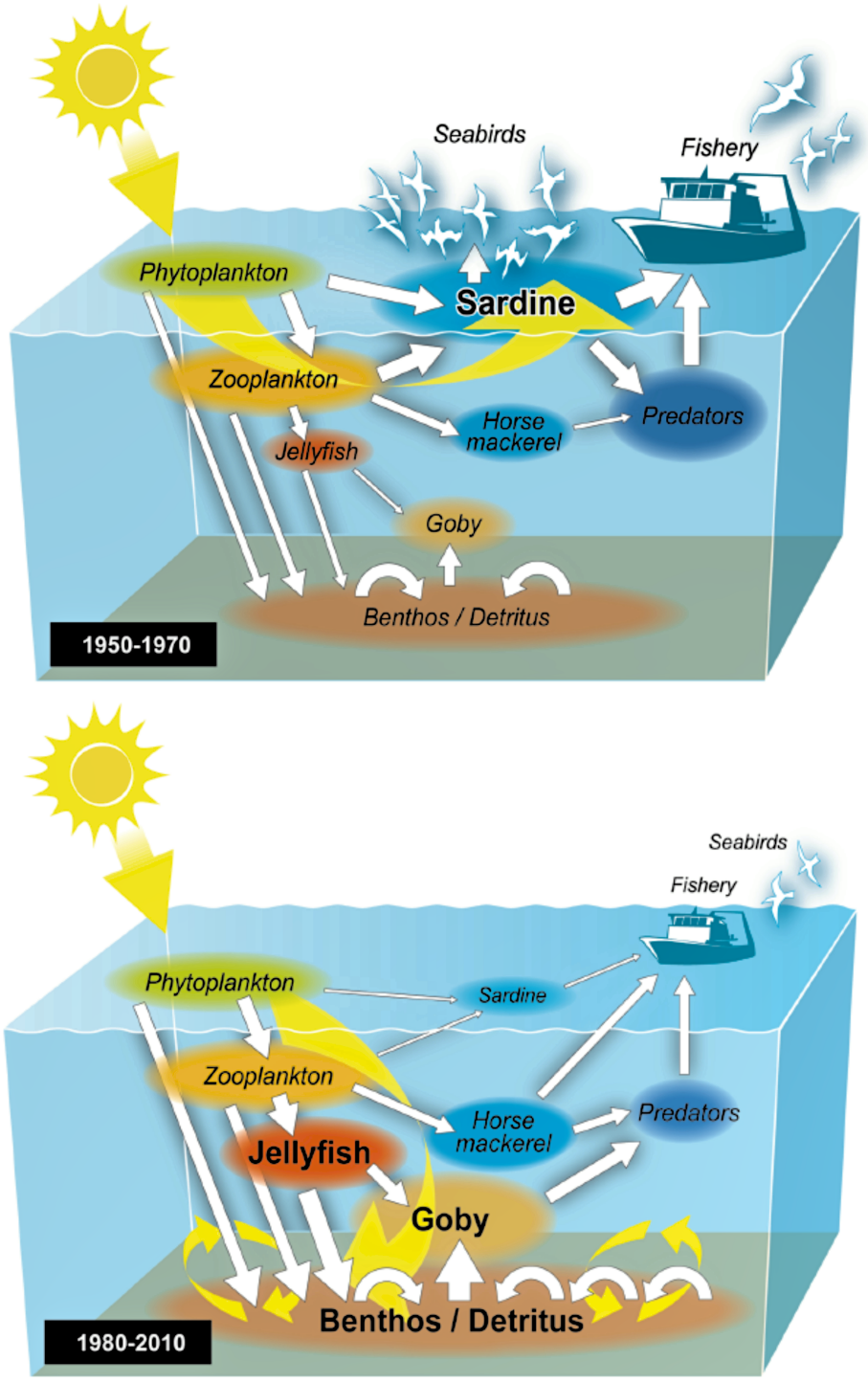

FIGURE 1.8: Conceptual sketch of the main energy flows toward fish production and fisheries in northern Benguela. The sardine was the main link between primary and secondary producers and fish, fisheries, and predators in the early period (A); after the sardine collapse in the early 1970s most of the energy flow (yellow arrows) was diverted away from the pelagos through jellyfish, detritus, benthic recycling, and bearded goby (B; from Roux et al., 2013).

structure and functioning of marine food chains, jellyfish blooms can also impact biogeochemical cycles by affecting element cycling (Condon et al., 2010; Pitt et al.,

2009c; Sweetman et al., 2015; Tinta et al., 2021; West et al., 2009) thus potentially impacting carbon export and ecosystem productivity.

1.3.2.1 Marine carbon cycle

As any member of the marine food web, jellyfish are involved in several carbon cycling processes such as the biological carbon pump, the microbial carbon pump and the microbial loop.

Biological carbon pump

The biological carbon pump is responsible for a vertical carbon flux where dissolved inorganic carbon (DIC; including CO_2, H_2CO_3, HCO_3^-, CO_3^{2-}) is removed from the surface water through photosynthesis and is integrated into POC and DOC by primary producers (Ducklow et al., 2001; Figure 1.9). The efficiency of the biological pump is estimated by the fraction of primary production exported from the euphotic zone, and subsequently by the fraction of that export production that reaches the deep sea. The fraction of fixed carbon that is exported to the deep sea is controlled by numerous, often interrelated, processes, including the aggregation/disaggregation of organic-rich particles, zooplankton grazing and faecal pellet production and microbial activities (De La Rocha et al., 2007). As it sinks, the organic matter is ultimately recycled by heterotrophic organisms resulting in a release of DIC and inorganic nutrients. This remineralisation process is highly efficient and only <1-6% of the POC export production reaches the sea floor where only 0.3% escape benthic degradation to be buried (Ridgwell et al., 2015). Still, the biological carbon pump plays a central role in regulating atmospheric CO_2 (Cavan et al., 2017; Cox et al., 2000).

Jellyfish contribute to the biological carbon pump through two main routes 1) during life mainly through feeding processes, including the release of faecal pellets, mucus and messy-eating debris (Pitt et al., 2009c; Tinta et al., 2021; Figure 1.10), and 2) after death through the sinking of carcasses (Lebrato et al., 2013; Lebrato et al., 2012; Figure 1.9). The high biomass achieved during jellyfish blooms and the rapid sinking of the carcasses might allow such aggregations to significantly export carbon to the deep ocean while providing food for deep-sea scavengers and detritivores (Lebrato et al., 2013; Leu et al., 2020). Still, the magnitude and frequency of jellyfish carcasses reaching the seafloor is poorly known preventing estimation of their impact on carbon export. Similarly, the contribution of a live jellyfish to the biological carbon pump through the release of faecal pellets, mucus and sloppy-feeding debris has been barely studied. In particular, the fate of the mucus and its implications in particle aggregation and/or microbial metabolism is unknown.

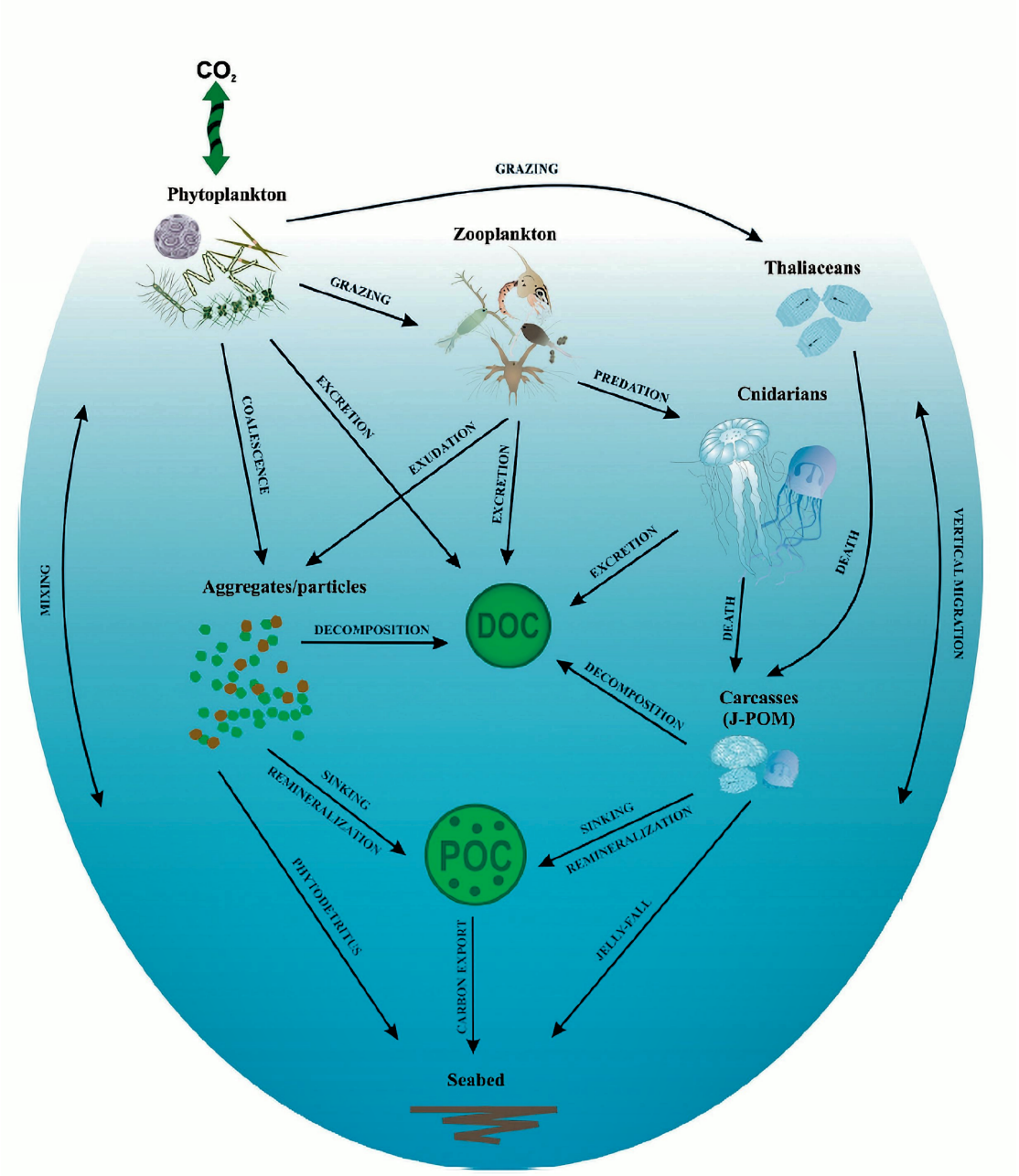

FIGURE 1.9: A representation of the biological pump and the biogeochemical processes that remove elements from the surface ocean by sinking biogenic particles (Lebrato et al., 2011).

Microbial carbon pump

Even though DOC is the main energy source for marine heterotrophic microorganisms, the ocean represents one of the largest pools of reduced carbon on Earth, with ~662 PgC (Hansell et al., 2009). This apparent contradiction is caused by less than 1% of marine DOC being labile, 94% being refractory with the remaining 5% classified as semilabile (Hansell et al., 2009). Marine microbes can produce refractory DOM (lifetime estimated to ~15,000 years; Hansell et al., 2009) from labile DOM via a

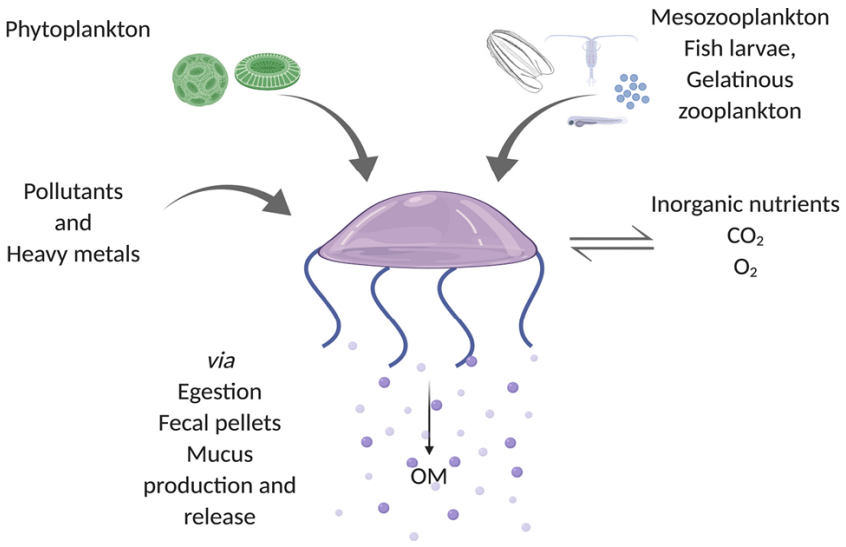

FIGURE 1.10: Visualization of a living jellyfish as sink and source of organic matter (OM) in the ocean (Tinta et al., 2021)

process called the microbial carbon pump (Jiao et al., 2010; Ogawa et al., 2001; Figure 1.11). This process preserves fixed carbon in the ocean thereby participating in long-term carbon storage (Jiao et al., 2014). However, the reason behind this recalcitrance is still unknown (Mentges et al., 2019) and recalcitrance is an emergent property of DOC that is analytically difficult to constrain (Wagner et al., 2020). Therefore, future research will have to improve our understanding of marine organic carbon cycling by revealing predominant biosynthetic and degradation pathways that control DOM production and turnover.

The contribution of jellyfish-derived DOM into the microbial carbon pump has not been investigated so far. Only recently, studies have started to investigated the microbial degradation of jellyfish organic matter. As yet, the microbial processing of jellyfish organic matter has been studied in more detail for jellyfish carcasses (e.g. Blanchet et al., 2015; Tinta et al., 2016; Tinta et al., 2020) than for mucus (Condon et al., 2011). As jellyfish blooms represent a large source of labile DOM for the microbial community (Tinta et al., 2021), it is likely that part of that labile DOM is ultimately transformed into recalcitrant DOM by marine microbes. However, a more in-depth research is needed to fully understand the results of jellyfish OM microbial degradation and major gaps still remain regarding the interaction between jellyfish and microbes. For example, the abundance, the biochemical complexity and the fate of jellyfish organic matter are still to be fully studied (Tinta et al., 2021).

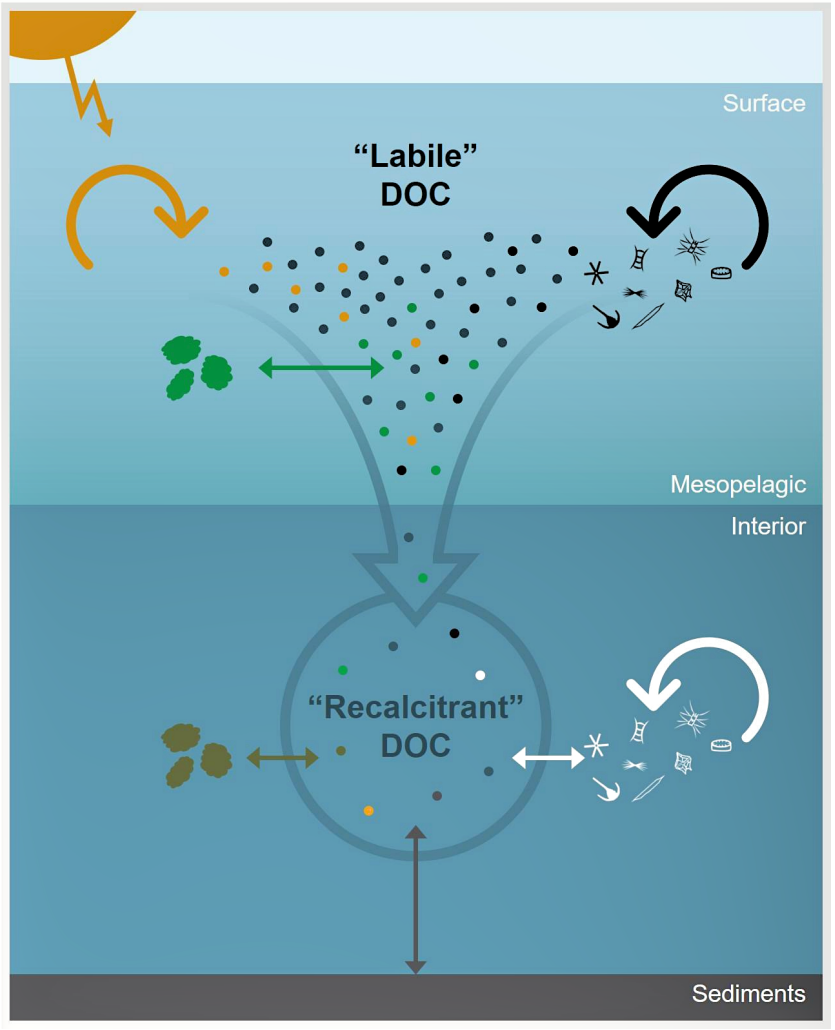

FIGURE 1.11: A conceptual diagram of some of the major environmental processes which control the apparent recalcitrance of oceanic DOC. The dots represent DOC molecules and the arrows represent physicochemical and biological processes that impact DOC concentration and molecular composition. In the surface ocean, DOC derived from primary production is rapidly remineralized or transformed through microbial degradation (black arrow), photochemical degradation (yellow arrow), or particle exchange (green arrow). Labile components are removed down the water column and DOC becomes diluted by processes, such as particle exchange (brown arrow), sediment dissolution (grey arrow), and microbial reworking (white arrow), which continue to alter, add, and/or remove molecules from the bulk DOC pool (Wagner et al., 2020)

Microbial loop

Heterotrophic bacteria form an important link between DOC and higher trophic levels, conceptualised into the "microbial loop" process (Azam et al., 1983). By utilising DOM and incorporating it into microbial biomass, marine microbes supply higher trophic levels with OM otherwise unavailable to other marine organisms (Figure 1.12). The bacterial growth efficiency (BGE), defined as the amount of new bacterial biomass produced per unit of organic carbon substrate assimilated (del Giorgio et al., 1998) represents the efficiency of microbial biomass production,

then available to higher trophic levels. The high BGE of microbial assemblages consuming jellyfish carcasses (65 $\pm$ 27%; Tinta et al., 2021) indicates efficient incorporation of jellyfish carcasses into bacterial biomass. However, a similar experiment induced a BGE $<$ 20% (Blanchet et al., 2015) suggesting that environmental conditions might affect the microbial response to jellyfish organic matter. Regarding the degradation of jellyfish mucus, a study found a BGE of $\approx$30% corresponding to a decrease of 10% to 15% relative to the control treatment (Condon et al., 2011) and suggesting that DOM from jellyfish mucus is shunted towards CO_2 production rather than biomass production, thus away from higher trophic levels. For both mucus and carcasses, more experiments are needed to better understand the fate of jellyfish DOM microbial consumption.

In conclusion, the role of jellyfish in carbon cycling and export appears to be closely connected to the interaction between jellyfish and marine microbes, with many aspects still needing investigation. So far, there are too few studies investigating the role of jellyfish organic matter in carbon cycling and its interaction with marine microbes. While the fate of the jellyfish carcasses (e.g. Lebrato et al., 2011; Tinta et al., 2020) has received more attention than the fate of the mucus (Condon et al., 2011), overall results are too scarce to be conclusive. The marine carbon cycle is a complex and dynamic process intrinsically connected to the other nutrient cycles and where microorganisms play a key role (Figure 1.12). In the context of rising atmospheric CO_2 concentrations and associated climate change, it is crucial to have a clear understanding of the cycling of carbon and other nutrients in marine waters in order to predict future changes in the biological carbon pump (Sen Gupta et al., 2012). Carbon export and storage are intrinsically connected to nutrient cycles as organic matter is only produced if nutrients are not limited. Therefore, carbon export cannot only be related to particle export but also depends on association with remineralised nutrients (Gnanadesikan et al., 2008).

1.3.2.2 Marine Nitrogen and Phosphorous cycles

Jellyfish have also been suggested to play a critical role in nitrogen (N) and phosphorous (P) cycling thus influencing the primary production of marine ecosystems (e.g. Pitt et al., 2009c; West et al., 2009). N and P are key limiting nutrients, required for primary production and thus controlling marine ecosystem productivity (Bristow et al., 2017; Moore et al., 2013). N is essential for protein synthesis, which is the main constituent of the jellyfish body and essential for the synthesis of the mucins, the main constituent of the mucus (Masuda et al., 2007). On the other hand, P is generally required for nucleic acids (DNA and RNA) and energy transfer (Conley et al., 2009). Jellyfish acquire N and P predominantly through predation on zooplankton (Pitt et al., 2009c). The large protein content in jellyfish biomass is

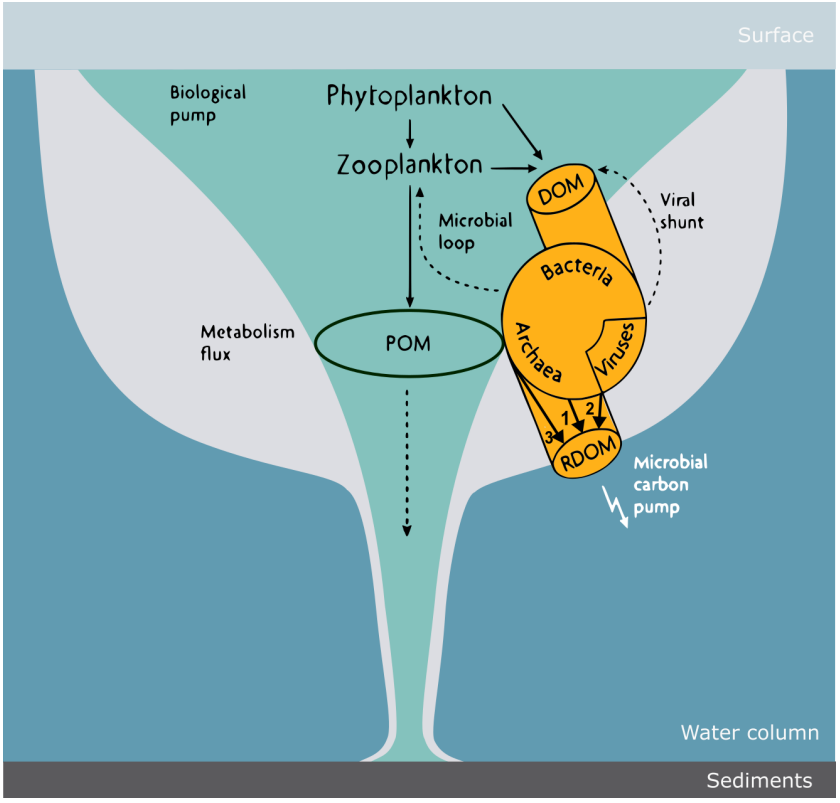

FIGURE 1.12: Major biological processes involved in carbon cycling in the ocean. The biological pump is a process whereby CO_2 in the upper ocean is fixed by primary producers and transported to the deep ocean as sinking biogenic particles (particulate organic matter; POM) or as dissolved organic matter (DOM). The microbial loop is a pathway in the aquatic food web whereby DOM is taken up by bacteria and archaea, which are consumed by protists, which are in turn consumed by metazoans (not shown). The viral shunt reflects virus-mediated lysis of microorganisms, which returns the POM to the DOM pool. The proposed microbial carbon pump is a conceptual framework for understanding the role of microbial processes in the production of recalcitrant DOM (RDOM). Three major pathways have been identified in the microbial carbon pump: direct exudation of microbial cells during production and proliferation (path 1); viral lysis of microbial cells to release microbial cell wall and cell surface macromolecules (path 2); and POM degradation (path 3). The grey shading roughly indicates the total flux of carbon metabolism in the water column (modified from Jiao et al., 2010).

reflected in their low molar C:N (4.4; Lucas Cathy H. et al., 2011) compared to other marine zooplankton organisms (4.8-6.2 for crustacean zooplankton; Pitt et al., 2013).

Jellyfish provide N and P to the environment primarily via excretion of inorganic (predominantly ammonium (NH_4^+) and phosphate (PO_4^{3-}), dissolved organic forms (e.g. dissolved free amino acids, dissolved primary amines and mucus) and particulate organic matter (egested material; Pitt et al., 2009c; Figure 1.13). The excretion of ammonium by populations of jellyfish could theoretically support 8% of the nitrogen requirements for phytoplankton in Lake Illawarra, Australia (Pitt et al., 2005), 11% of the requirements in the Kiel Bight, Western Baltic (Schneider, 1989), and 10% of the requirements in the Inland Sea of Japan (Shimauchi et al., 2007). Similarly, PO_4^{3-} excretion could provide 23% in the Kiel Bight (Schneider, 1989) and 21.6% in the

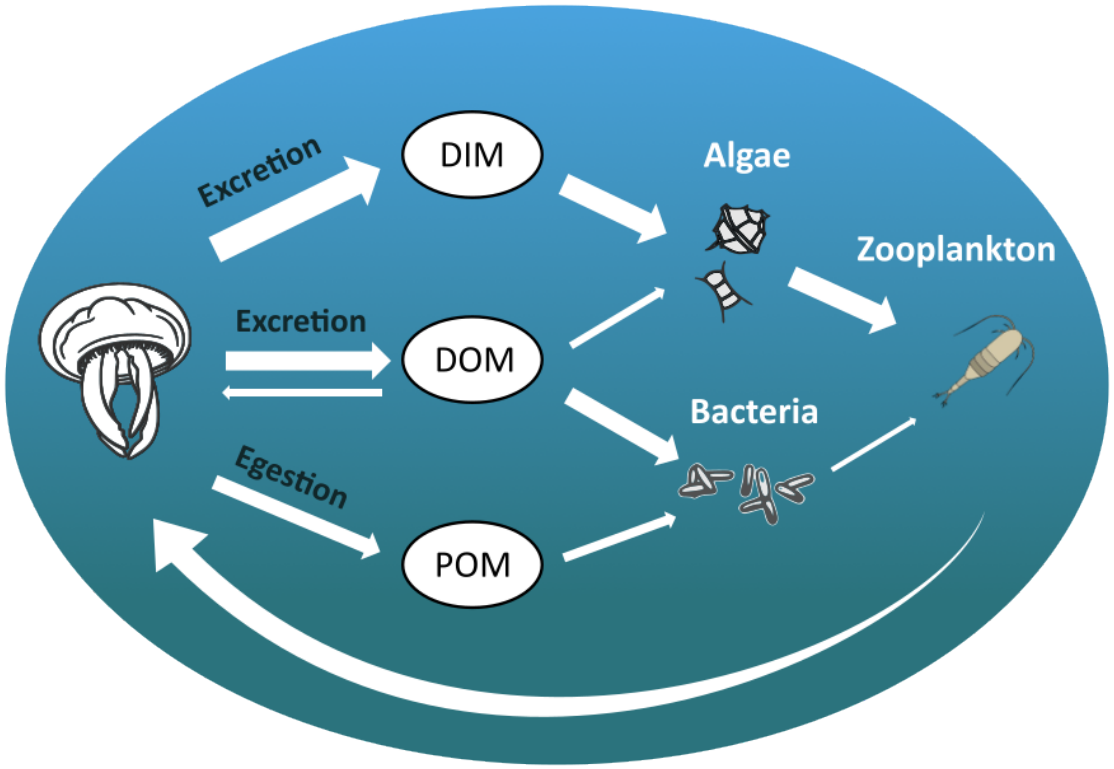

FIGURE 1.13: Conceptual models of the contributions of jellyfish to nutrient cycling during the growth of a jellyfish bloom. The width of the arrows represents their relative contributions. The dotted arrows indicate the contribution has not been confirmed. Microbial feedback loops involving bacteria, phytoplankton and zooplankton are not included. POM = particulate organic matter, DOM = dissolved organic matter and DIM = dissolved inorganic matter (modified from Pitt et al., 2009c).

Inland Sea of Japan (Shimauchi et al., 2007) of the phytoplankton's P requirements. These jellyfish excretions were estimated to be the second most important source of N and P for primary production, after the sediment (Pitt et al., 2005; Schneider, 1989; Shimauchi et al., 2007). Therefore, jellyfish excretion of inorganic P and N should be considered in nutrient budgets and models, particularly when considering nutrient-limited ecosystems such as oligotrophic, N-limited and P-limited ecosystems.

In comparison to the supply of N and P from jellyfish inorganic excretion, the contribution of jellyfish mucus and egested material to the environmental pool of N and P has barely been studied. First, the elemental ratios and biochemical composition of the jellyfish mucus are not currently clear. Until now, the macromolecular (protein/lipid/carbohydrate) composition of jellyfish mucus has been measured only once for the scyphomedusa *Aurelia aurita* in a relatively old study (Ducklow et al., 1979). Secondly, only two studies have so far estimated the rates of mucus release by jellyfish (Condon et al., 2010; Hansson et al., 1995). Therefore, it is not currently possible to estimate the role of jellyfish mucus in biogeochemical cycles.

1.4 Jellyfish in models

Jellyfish are increasingly recognised as important components of marine ecosystems (Wright et al., 2021) having complex roles in biogeochemical cycles and trophic pathways (Tinta et al., 2021) while generating challenges for human societies (Richardson et al., 2009). Yet, their complex role is often poorly defined in ecosystem models, which fail to treat them as a separate component of the zooplankton (Lamb et al., 2019). Models are useful tools to understand the interactions of multiple complex drivers in the environment and provide valuable support for ecosystem-based management (Schuwirth et al., 2019). In the context of the changing ocean and the resulting consequences for humanity, it is paramount to fully understand the impacts of jellyfish blooms in the marine ecosystem and to better manage their presence and impact on coastal activities. Ecological modelling provides the best approach to understanding the role of jellyfish in large fisheries-based ecosystems (Pauly et al., 2009).

Jellyfish play a pivotal role in the processing of energy in fisheries-based ecosystems (Pauly et al., 2009). Yet, in 2019, out of 329 marine ecosystem models (designed using the EwE (Ecopath with Ecosim) software suite), 211 contained no jellyfish groups, 32 included jellyfish as part of a zooplankton group, and 86 models incorporated jellyfish explicitly as their own separate group(s) (Lamb et al., 2019; Figure 1.14). Three reasons might explain this underrepresentation: 1) the jellyfish diversity in size and habitat, their complex physiological and ecological behaviours, and their high spatio-temporal variability make them complex model components; 2) many uncertainties remain regarding their complex interaction with the marine environment (Ramondenc et al., 2020); 3) their trophic and ecological importance is frequently underestimated (Stoltenberg et al., 2021). Even though the inclusion of jellyfish in models has been increasing these last decades (Figure 1.14), efforts are still needed to better integrate them in future models.

To help support the inclusion of jellyfish in ecosystem models, future research should target the uncertainties that remain regarding the role of jellyfish in biogeochemical cycles and trophic food webs. To handle the unique biological/ecological nature of jellyfish ecosystem models need to be properly parameterised. Model parameterisation is commonly performed using either experimental or *in-situ* data. Therefore, more data needs to be collected to support modellers. Subsequently, the results of these models need to be used to support ecosystem-based management decisions. The consequences that jellyfish blooms generate to human activities make them a good example where integrated and adaptive management is required. As illustrated by the northern Benguela case (1.3.1), bad management of coastal regions (i.e. unregulated fishing activities) can generate long-term shifts in ecosystem structure and productivity, which can be detrimental to several sectors such as

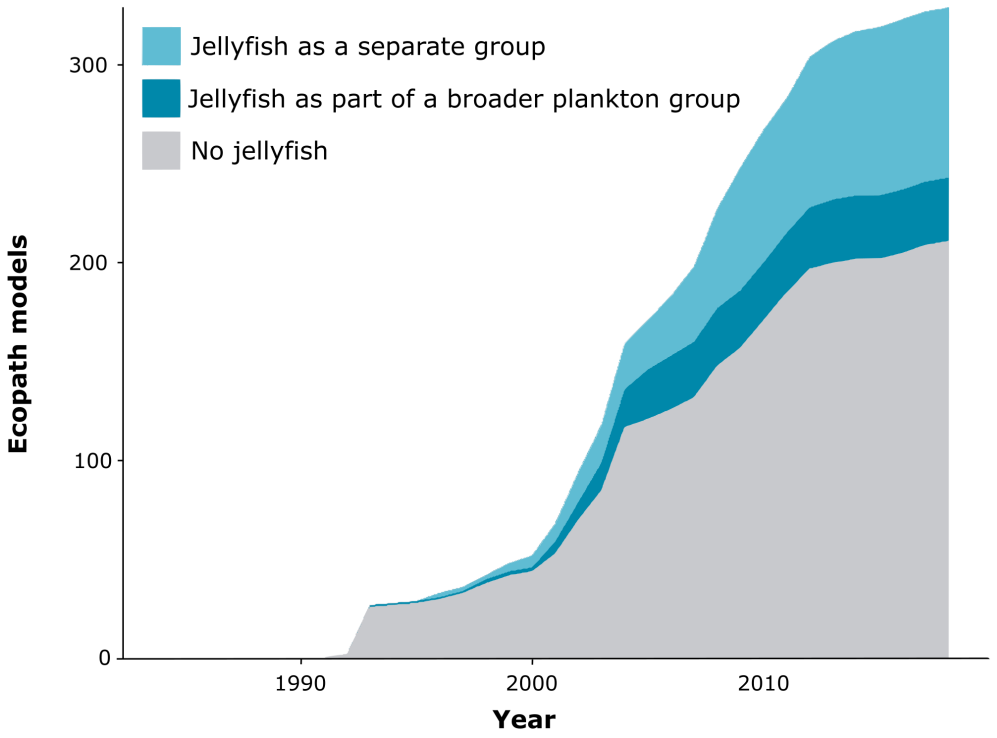

FIGURE 1.14: The accumulation of EwE models through time. Light grey represents EwE models with no jellyfish functional group included at all. The dark blue indicates models with jellyfish as part of a wider zooplankton group. The light blue represents models with jellyfish included as their own group (modified from Lamb et al., 2019).

tourism, energy industries and fisheries (Purcell et al., 2007; Richardson et al., 2009). The combination of accurate ecosystem models with adaptative and integrated ecosystem-based management would ensure sustainable use of coastal areas.

Recent modelling studies have been supporting the important role of jellyfish in marine ecosystems. For example, the introduction of jellyfish in the PlankTOM11 model has a large direct influence on the crustacean macrozooplankton and influences indirectly the rest of the plankton ecosystem through trophic cascades (Wright et al., 2021). Additionally, mean global jellyfish biomass has been estimated to be 290 Tg C with jellyfish carcasses and fecal matter playing an important role in the biological pump (Luo et al., 2020). Models also revealed the 'keystoneness' character of jellyfish with values increasing as the size of the ecosystem decreases suggesting an increasing importance of jellyfish for smaller ecosystems (Pauly et al., 2009). These results illustrate the utility of models both for exploratory- and hypothesis-based studies and to support ecosystem management decisions.

1.5 Thesis overview, aims and objectives

During these last decades, the apparent trend of jellyfish populations increasing in coastal regions around the world (Brotz et al., 2012) has been followed by increased awareness of their importance in marine ecosystems (Wright et al., 2021). Yet, jellyfish as a source of both inorganic nutrients and organic matter is not well characterised. The release of nutrients associated with their presence in the marine environment still presents some gaps. Simultaneously, the research on the interaction between marine microbes and jellyfish is still in its infancy and many questions remain regarding the functional role of the jellyfish microbiome and its impact on biogeochemical cycles. The purpose of this thesis is to investigate the role of jellyfish and their associated marine microbes in marine nutrient cycling to ultimately assess their impact on ecosystem productivity. I will focus on characterising the organic and inorganic nutrients released by jellyfish and the subsequent changes induced by the microbial community surrounding the jellyfish. In particular, I will investigate the different forms of nitrogen released by the jellyfish holobiont, the elemental and biochemical composition of the mucus compared to the body and, finally, the impact of mucus degradation on the nutrients and microbial community of coastal surface waters.

My specific hypothesis and objectives are:

- Hypothesis 1: The jellyfish and its microbiome release various forms of inorganic nitrogen (ammonium, nitrite, nitrate) that can play a significant role in nitrogen cycling and ecosystem productivity
  - Objective: Perform incubation experiments on a range of bloom-forming pelagic jellyfish in order to measure their nitrogen release rates, assess their potential role in marine nitrification and evaluate the potential impact on ecosystem productivity (Chapter 2).
- Hypothesis 2: The biochemical and elemental composition of jellyfish mucus is similar to that of their body and remains comparable across different species.
  - Objective: Collect, analyse and compare the macromolecular and elemental composition of a set of samples of both jellyfish body and mucus from a range of specimens (Chapter 3).
- Hypothesis 3: The mucus excreted by jellyfish blooms in coastal waters is rapidly degraded by a fraction of the pelagic microbial community inducing the release of nutrients and subsequent changes in the microbial community.
  - Objective: Perform incubation experiments using jellyfish mucus and natural coastal seawater to measure the nutrients (organic and inorganic)

and microbial community changes following mucus degradation (Chapter 4).

Chapter 2

Evidence of nitrification associated with globally distributed pelagic jellyfish

Hubot Nathan D.[1,2], Giering Sarah L. C.[1], Fuessel Jessika[2,3], Robidart Julie[1], Birchill Antony[1,4], Stinchcombe Mark[1], Dumousseaud Cynthia[2], Lucas Cathy H.[2]

1 – National Oceanography Centre, University of Southampton Waterfront Campus, Southampton, UK

2 – Ocean and Earth Science, University of Southampton, National Oceanography Centre, University of Southampton Waterfront Campus, Southampton, UK

3 – Department of Medicine, University of Chicago, Chicago, Illinois

4 – School of Geography, Earth and Environmental Sciences, University of Plymouth, Plymouth, UK

This chapter was peer-reviewed and published as:

Hubot, N. D., Giering, S. L. C., Füssel, J., Robidart, J., Birchill, A., Stinchcombe, M., Dumousseaud, C., & Lucas, C. H. (2021). Evidence of nitrification associated with globally distributed pelagic jellyfish. *Limnology and Oceanography*, *66*(6), 2159–2173. https://doi.org/10.1002/lno.11736

2.1 Abstract

Often considered detrimental to the environment and human activities, jellyfish blooms are increasing in several coastal regions worldwide. Yet, the overall effect of these outbreaks on ecosystem productivity and structure is not fully understood. Here we provide evidence for a so far unanticipated role of jellyfish in marine nitrogen cycling. Pelagic jellyfish release nitrogen as a metabolic waste product in form of ammonium. Yet, we observed high rates of nitrification ($NH_4^+ \rightarrow NO_3^-$, 5.7–40.8 nM gWW^{-1} [wet weight] h^{-1}) associated with the scyphomedusae *Aurelia aurita*, *Chrysaora hysoscella*, and *Chrysaora pacifica* and low rates of incomplete nitrification ($NH_4^+ \rightarrow NO_2^-$, 1.0–2.8 nM gWW^{-1} h^{-1}) associated with *Chrysaora fulgida*, *C. hysoscella*, and *C. pacifica*. These observations indicate that microbes living in association with these jellyfish thrive by oxidizing the readily available ammonia to nitrite and nitrate. The four studied species have a large geographic distribution and exhibit frequent population outbreaks. We show that, during such outbreaks, the jellyfish-associated release of nitrogen can provide more than 100% of the nitrogen required for primary production. These findings reveal a so far overlooked pathway when assessing pelagic nitrification rates that might be of particular relevance in nitrogen-depleted surface waters and at high jellyfish population densities.

2.2 Introduction

Jellyfish (here referring to pelagic medusozoan) blooms are increasing in frequency and magnitude in several coastal regions around the world (e.g. Sea of Japan and Benguela current; Brotz et al., 2012). The presence of jellyfish blooms in coastal waters can cause severe damage to economic activities such as fisheries (e.g. 2.1 - 25% decrease in annual Korean fishery production every year; Kim et al., 2012), tourism (e.g. costing the Israeli coastal tourism industry an estimated annual monetary loss of €1.8–6.2 million every year; Ghermandi et al., 2015) and power generation (e.g. the closure costs of Torness nuclear plant in Scotland due to a jellyfish bloom from 28th June to 1st July 2011: approximately £1 million d^{-1}; Kopytko, 2015). Simultaneously, jellyfish outbreaks create ecological disturbances by altering the marine food chain structure (Pitt et al., 2009b). Their voracious predation on zooplankton makes them competitors to planktivorous fish (Condon et al., 2011). The grazing pressure that jellyfish put on zooplankton grazers releases primary producers from predatory control, causing a trophic cascade that can result in phytoplankton blooms (Schnedler-Meyer et al., 2018). By preying on ichthyoplankton (eggs and larvae of fish), jellyfish even exert top-down control on their competitors and predators (Gordoa et al., 2013). Overall, the complex interaction of jellyfish with the food web can have large impacts on ecosystem structure, function and resilience (Baum et al., 2009).

The role of jellyfish as top-down predators has been widely studied (e.g.: Stone et al., 2018), yet their bottom-up influence as a nutrient source on marine ecosystems is less clear. Ammonium excreted by jellyfish has been estimated to support up to 8%, 10% and 11% of the phytoplankton nitrogen requirement in the Lake Illawarra (Australia), the Inland Sea of Japan and the Kiel Bight, respectively (Pitt et al., 2005; Schneider, 1989; Shimauchi et al., 2007). Ammonium and phosphate released by jellyfish more than doubled the phytoplankton biomass in a mesocosm experiment conducted in a saline lake (West et al., 2009). In addition, the release of organic matter in the form of mucus provides an extremely labile source of organic carbon for bacterioplankton (Condon et al., 2011). While there is clear evidence that jellyfish can alter both biogeochemical cycles and food web structure, their role in pelagic nitrogen cycling remains understudied.

Ammonia is an intensely contested compound in most of the world's sunlit oceans, where nitrogen availability limits primary productivity ($\sim$75% of the surface ocean; Bristow et al., 2017; Moore et al., 2013). Additionally, ammonia provides the substrate for ubiquitous chemolithoautotrophic nitrifying bacteria and archaea that generate energy by the stepwise oxidation of ammonia to nitrite and nitrate. The first step is mediated by ammonia-oxidizing bacteria (Kowalchuk et al., 2001) and archaea (Hallam et al., 2006). Ammonia oxidizing archaea can reach high abundances, especially in the dark ocean ($>$ 30% of the microbial community; Karner et al., 2001) and appear to be the main drivers of marine ammonia oxidation (Wuchter et al., 2006). As for the second step, all known nitrite oxidizers belong to the bacterial domain (Spieck et al., 2015) and are characterized by their often remarkable metabolic versatility (Füssel et al., 2017). Both ammonia oxidizers and nitrite oxidizers (collectively called nitrifiers) are ubiquitous in pelagic environments, where they contribute substantially to carbon fixation in absence of light (dark carbon fixation), influencing ocean carbon fluxes (Pachiadaki et al., 2017). Nitrifiers have also been shown to live in association with benthic invertebrates such as sponges (e.g. Subina et al., 2018), corals (e.g. Hoffmann et al., 2009), zoanthids (Sun et al., 2014), bivalves (Welsh et al., 2004), ascidians (Martínez-García et al., 2008) and insect larvae (Stief et al., 2009). As part of invertebrate microbiomes, nitrifiers can provide a source of nutrition for their host when phagocytosed (Martínez-García et al., 2008), preventing the loss of nitrogen into the environment by recycling the excess of ammonium trapped in the mucus (Rädecker et al., 2015). Understanding the role of these associations is important for accurate mapping of marine nitrogen biogeochemistry and may help to improve our ability to predict future change (Pajares et al., 2019).

Jellyfish are densely populated with microorganisms (Kramar et al., 2019; Lee et al., 2018; Weiland-Bräuer et al., 2015), which play a beneficial role in the fitness of the host and contribute to the ecological features of the jellyfish (Stabili et al., 2018; Tinta et al., 2019). The epithelial mucus layer of a jellyfish is an attractive niche for microbes,

providing them with both a habitat and a high-quality energy source (Kramar et al., 2019). By attracting profitable bacteria and preventing colonization by potentially harmful microorganisms (via interferences with bacterial quorum sensing), the host maintains a healthy microbiome providing immune system functions (Weiland-Bräuer et al., 2019). In addition, jellyfish microbiomes are production hotspots of chemical compounds (e.g. exopolysaccharides, vitamins, enzymes, toxins, antibiotics; Tinta et al., 2019) and harbour microbes closely related to known drivers of major elemental cycles (e.g. nitrogen cyclers, chemolithoautotrophs, methylotrophs, methane oxidizers, and polycyclic aromatic hydrocarbon degraders; Lee et al. 2018). In terms of the nitrogen cycle, two species of nitrifiers (the ammonia-oxidizing bacterium *Nitrosospira multiformis* and the nitrite-oxidizing bacterium *Nitrospira moscoviensis*) have been found in association with the jellyfish *Chrysaora plocamia* (Lee et al., 2018) and *A. aurita* (Weiland-Bräuer et al., 2015). This discovery leads to the suggestion that these two nitrifiers are ubiquitous members of the microbiome of these two genera (Lee et al., 2018) and indicates that jellyfish could contribute to marine nitrogen cycling beyond the excretion of ammonia via their microbiome.

Cnidarian jellyfish excrete ammonium, a by-product of their metabolism, by diffusion through their body surface (Lőw et al., 2016). Though they are not known to directly produce nitrite or nitrate, low rates of nitrate release have been observed in association with pelagic jellyfish ($<$ 2% of total inorganic nitrogen released; Pitt et al., 2009c). For benthic jellyfish that live in symbiosis with zooxanthellae (photosynthetic dinoflagellates), experiments have shown nitrite/nitrate release rates equivalent to 21.5% of the total dissolved inorganic nitrogen release, indicating substantial colonization by nitrifying microorganisms (Welsh et al., 2009). While the authors suggested the association with nitrifiers to be specific to zooxanthellate jellyfish, we hypothesize that nitrifying microorganisms that benefit from the excreted ammonium are commonly associated with jellyfish and play a significant role in the nitrogen cycling. To test this hypothesis, we chose four species of non-zooxanthellate scyphozoan jellyfish, *Aurelia aurita, Chrysaora hysoscella, Chrysaora fulgida* and *Chrysaora pacifica* from four contrasting environmental conditions (brackish lake, both North and South Atlantic Ocean coastal waters, and artificial seawater), representing a wide range of environmental conditions (Dawson et al., 2005; Morandini et al., 2010). All of these species exhibit population outbreaks in coastal areas (Abato, 2017; Lucas, 2001; Lynam et al., 2006; Makabe et al., 2015) leading to high population biomass potentially disturbing human activities. We experimentally measured the release rates of ammonium, nitrite, nitrate and phosphate in association with all four jellyfish species in order to assess the global prevalence of an association between nitrifiers and jellyfish as well as its potential role in the marine nitrogen cycle.

2.3 Materials

Adult medusae of *Aurelia aurita* (n = 5), *Chrysaora hysoscella* (n = 5) and *Chrysaora fulgida* (n = 2) were sampled from Horsea lake (UK), the Rame Peninsula (UK), and Walvis Bay (Namibia), respectively (Table 2.1). Medusae were collected carefully from near-surface waters using a 10-L bucket and kept in approximately 5 L of ambient water during transportation to the laboratory. The water temperature was kept as close to *in-situ* conditions as possible (maximum fluctuations: ±2°C from *in-situ* conditions; Table 2.1). Maximum transportation time was four hours. All jellyfish survived transportation and were transferred to the lab in good condition, indicated by regular swimming pulse. Once in the lab, jellyfish were transferred to their respective experimental conditions (Table 2.1). *Chrysaora pacifica* specimen (n = 5) were collected from the London aquarium. The medusae were produced from polyps cultured in artificial conditions (artificial seawater with continuous UV-treatment and filtering system) and had not been in contact with natural seawater.

2.3.1 Sampling sites and species

Horsea Lake (Portsmouth, United Kingdom; 50° 83′ 68.26″ N, 1° 10′ 19.11″ W) is an enclosed, shallow (6-7 m), brackish (salinity: 19-23) lake situated on the south coast of England. The lake is oligotrophic with annual surface temperatures between 5°C and 23°C (Lucas, 1996). It lacks a riverine input and is replenished with seawater 2–3 times a year during high water spring tides (Lucas et al., 1997). The moon jellyfish *A. aurita* is found in Atlantic boreal waters and in the Black Sea (Dawson, 2003; Figure 2.1). The species was previously associated with a cosmopolitan distribution and is now known to be composed of many regional "cryptic" species spread globally (Scorrano et al., 2016, Figure 2.1). The medusae of *A. aurita* can reach bell diameters up to 40 cm (Arai, 1996) and are often found in high densities in coastal and brackish waters such as estuaries and bays (Lucas, 2001). They are present in Horsea Lake throughout the year (Lucas, 1996).

The Rame Peninsula (Cornwall, United Kingdom) is located on the southwest coast of England. Medusae of the species *C. hysoscella* were collected in waters characteristic of the English Channel (50° 19′ 54.5″ N, 4° 11′ 59.2″ W). The mean monthly surface temperature ranges from 9.2°C to 16.5°C and the mean monthly surface salinity ranges from 35.1 to 35.3 (Smyth et al., 2010). Medusae of *C. hysoscella* are of medium sizes (15–25 cm in bell diameter) and are found in the North Sea, the English Channel and the Mediterranean Sea (Morandini et al., 2010; Figure 2.1), where they can form dense populations (Abato, 2017). They appear in the English Channel during the summer months (Pikesley et al., 2014).

Walvis Bay is a large bay located on the coast of Namibia (22° 57′ 22″ S, 14° 30′ 29″ E). The water conditions of the bay are dictated by the Northern Benguela Upwelling System, which is a highly productive eastern boundary ecosystem. The seawater temperature in Walvis Bay varies between 10°C and 22°C and the salinity mainly ranges between 34.5 and 35.5 (Pryor et al., 2009). *C. fulgida* is an exclusively marine species found along the west coast of Africa (Figure 2.1) with medusae of medium size (10–20 cm in diameter). This species has previously been identified as *C. hysoscella* due to their morphological similarities (Morandini et al., 2010). *C. fulgida* medusae are found in Walvis Bay throughout the year and frequently reach significant population densities during the summer months (Skrypzeck, 2019).

Medusae of the species *C. pacifica* are slightly smaller (typically 10–15 cm in diameter) than the two studied species of *Chrysaora* described above, and occur in the Northern Pacific Ocean in the vicinity of Japan (Figure 2.1; Morandini et al., 2010). Since the beginning of the century, the number of *C. pacifica* medusae in the Inland Sea of Japan has been growing, and the population now has recurring annual blooms (Makabe et al., 2015; Takasu et al., 2019).

Species	*A. aurita*	*C. hysoscella*	*C. fulgida*	*C. pacifica*
Origin	Horsea Lake	Rames peninsula	Walvis Bay	London Aquarium
Country	UK	UK	Namibia	UK
Date (DD-MM-YY)	23-10-2018	21-08-2018	21-07-2019	27-02-2019
Bell diameter (cm)	12 – 16	9 – 13	12 – 16	6 – 9
Wet weight (g)	73 – 190	100 – 278	180 – 279	35 – 59
Number of specimens	5	5	2	5
in-situ conditions				
Temperature (°C)	14	18	14	16
Salinity	25	35	35	30
Experimental condition				
Temperature (°C)	15	20	14	16
Salinity	25	35	35	30

TABLE 2.1: Jellyfish collection and incubation details.

2.3.2 Experimental structure

Prior to the experiment, all equipment was acid washed in 10% hydrochloric acid and rinsed three times with ultra-high purity water (MilliQ $\leq$ 18.2 10^6 Ω $cm^{-}1$, Millipore, UK). The incubators consisted of 5-L high-density polyethylene buckets filled with artificial seawater (ASW; ultra-high purity water + Tropic Marin synthetic sea salt;

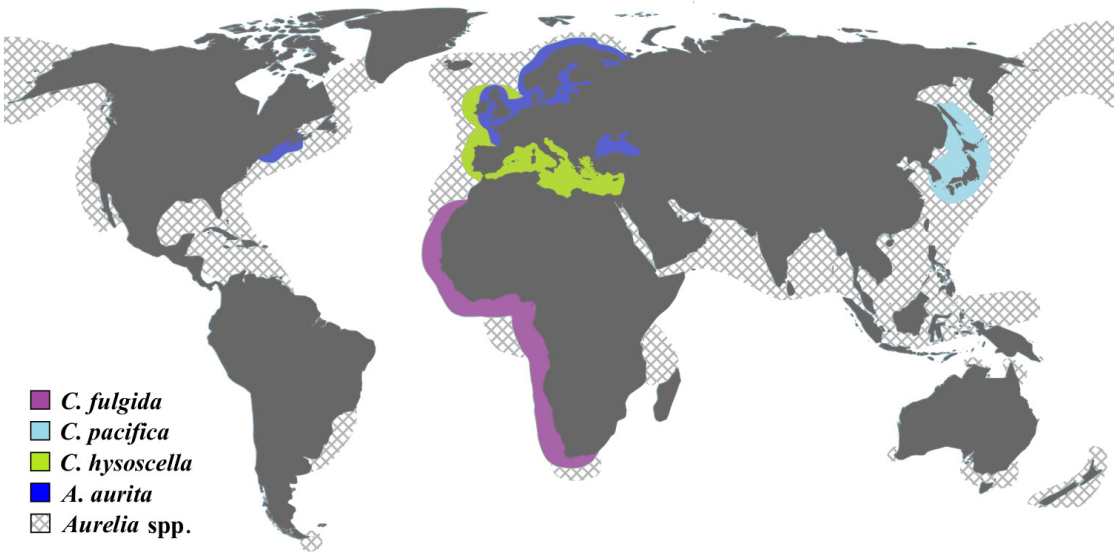

FIGURE 2.1: Geographic distribution of the four jellyfish species investigated in this study (*A. aurita, C. hysoscella, C .fulgida*, and *C. pacifica*; based on Dawson et al., 2005 and Morandini et al., 2010) and of the cryptic genus *Aurelia* (based on Dawson et al., 2001).

detailed preparation is available in Appendix A (section A.7). A maximum number of five healthy and undamaged adult medusae were selected for each experiment. The health of a jellyfish was evaluated based on the swimming rhythm with active swimming behaviour indicating good health. Two hours before the experiment, selected jellyfish were individually transferred to an incubator filled with 4 L of ASW. The purpose of this first 'acclimation/egestion' phase was to allow the medusae to egest any food they might have held in their gastric pouches. The experiment consisted of an initial Release phase, followed by an incubation phase with four incubation treatments: Jellyfish (ASW + jellyfish), Jellyfish-Control (ASW only), Mucus (ASW + mucus + ammonium), and Mucus-Control (ASW + ammonium; Figure 2.1). First, the jellyfish were gently transferred by hand to the Release incubators (2 L of ASW) using sterile vinyl gloves, whilst trying to minimise the amount of water transferred with it. The Release phase allowed mucus and its associated microbes to be released into the water. After 1 hour, the jellyfish along with half of the volume of the water in the Release incubator (1 L) were transferred to the Jellyfish incubators (3 L of ASW; final volume = 4 L). The other half of the water was transferred to the Mucus incubators (3 L of ASW; final volume = 4 L). The controls (Jellyfish-Control and Mucus-Control) consisted of incubators containing only ASW (3 L of ASW).

As ammonia is continuously excreted by jellyfish, the nitrification rates associated with jellyfish in ASW (continuously increasing ammonium concentrations) would not be directly comparable to those associated with mucus in ASW (ammonium concentration of <0.1 µM). To allow direct comparison of nitrification rates in the

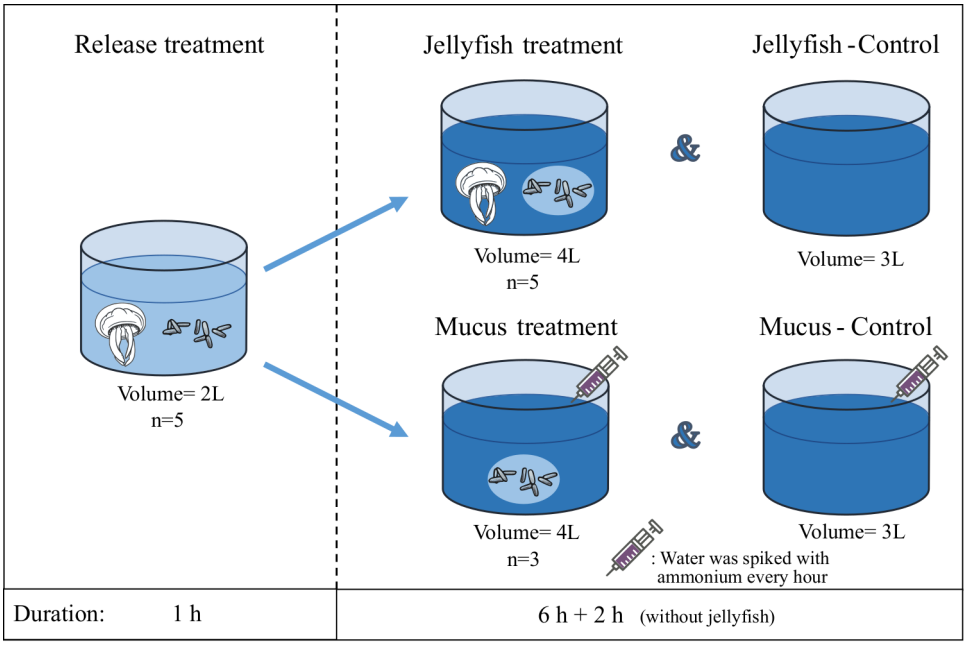

FIGURE 2.2: Experimental setup. Jellyfish were incubated for 1 h in the release treatment. Subsequently, the jellyfish along with half of the volume from the release phase were transferred to the jellyfish treatment; the other half was transferred to the mucus treatment. Controls for both experiments consisted of incubators containing only artificial seawater (ASW). The mucus and control-mucus incubators were spiked with ammonium every hour (Appendix A, Table A.2).

Mucus and Jellyfish treatments, we simulated jellyfish ammonium excretion in both the Mucus and the Mucus-Control treatments by adding ammonium (NH_4Cl, Fisher Scientific, UK) to the incubators after each sample collection. The amount of ammonium added was estimated based on literature (Pitt et al., 2009c) and previous trial experiments. The expected increase in ammonium concentrations ranged from 0.5 to 2.5 µM h^{-1} (Appendix A, Table A.2) depending on species, size of the jellyfish and temperature.

2.3.3 Rate measurements

Water samples for nutrient analysis were collected every hour. Before collecting each sample, the water was stirred gently to homogenise it. Two sets of 15-mL samples (one for nitrate, nitrite and phosphate, and one for ammonium) were collected using a 20 mL polypropylene syringe. The sample was filtered through a 0.22-µm polyethersulfone sterile syringe filter (33-mm diameter, Millipore, UK) with the first 5 mL discarded to wash the filter. The remaining 10 mL were collected in centrifuge tubes (polypropylene conical centrifuge tubes, 15 mL volume, Fisher Scientific, UK). For each treatment, a dedicated syringe was used to avoid cross-contamination. In between sample collection, the incubators were covered with a lid to avoid contamination. Based on initial experiments and findings of a previous study measuring ammonia release in *C. mosaicus* (Pitt et al., 2005), we decided an incubation

volume and duration of 4 L and 6 hours as ideal to measure a significant rate of nutrient release without causing excessive stress to the jellyfish. The jellyfish were then removed from the incubators, and the jellyfish bell diameter and the wet weight (WW) were measured using a ruler and a balance (FireKingdom SF-400, ± 1 g). Water sample collection continued for 2 hours after the removal of the jellyfish, resulting in a total experiment duration of 8 hours.

2.3.4 Sample analysis

The duplicate sample for ammonium was analysed using the o-phthalaldehyde fluorometric method (Taylor et al., 2007). The ammonium measurements were performed the same day using a Turner design Trilogy fluorometer (model 7200, US) with a UV module (7200-047). The duplicate sample for nitrite, nitrate and phosphate was immediately frozen for later analysis. Frozen samples were thawed at room temperature and phosphate, nitrate and nitrite concentrations were measured using standard gas-segmented continuous flow spectrophotometric techniques (QuAAtro, Seal Analytical). The baseline of the auto-analyser was determined using the same ASW as used in the experiment (except for *C. fulgida* samples, for which we used ultra-high purity water as baseline; detailed descriptions of the calibrations and detection limits in Appendix A, Table A.7).

Our hourly sampling regime, which provides a relatively low temporal resolution, was determined by the time it takes to collect the sample and the sample volume removed relative to the incubation volume. To determine the release rates at a higher temporal resolution, for one of the specimen of *A. aurita* incubations, nitrite and nitrate were measured at high-resolution (every 20 minutes) using a microfluidic lab-on-chip analyser (Beaton et al., 2012). This novel application of lab-on-chip microfluidic analysers allowed high-resolution measurements with small sample volumes and avoiding the need for sample storage. The nitrate and nitrite concentrations measured using the "manual" and lab-on-chip method agreed well (Appendix A, Figure A.5), as shown by the linear regression between the two methods (Auto-Analyzer = 1.04 ± 0.06; Lab-on-Chip = 0.15 ± 0.04; $R^2 = 0.98$, $p < 0.001$, n = 8; Appendix A, Figure A.6). For both techniques, gas segmented continuous flow spectrophotometric and lab-on-chip, the combined (random + systematic) analytical uncertainty associated with nitrate + nitrite and phosphate measurements was $<5\%$ (details in Appendix A, section A.6; Birchill et al., 2019).

2.3.5 Statistical analysis

Contamination, wall effects and production/absorption by microorganisms were accounted for by subtracting the changes in concentrations observed in the ASW

controls from the treatments. In order to account for the loss of liquid due to the collection of nutrient samples, the total number of moles of nutrient released at each time point was calculated using the equation:

$$n[t] = n[t-1] + V[t-1] \times (C[t] - C[t-1]) \tag{2.1}$$

where n is the number of moles released at a certain time point (t) since the beginning of the experiment, V is the volume of the incubator, and c is the molar concentration of nutrients (Giering et al., 2012).

The rates of nutrient (ammonium, phosphate, nitrite and nitrate) release per incubator (or per jellyfish for the Jellyfish treatment) were calculated using linear regression for each replicate. The rates were then normalised by the wet weight of the jellyfish and their differences were investigated by an analysis of covariance (ANCOVA; results are presented in Appendix A, section A.4). The rates of nutrient release per species were calculated by averaging the rates of the replicates for each species. Finally, the differences in weight-specific rates of nutrient release caused by the differences in experimental temperatures were standardized using Q10 temperature coefficient factors from the literature. For ammonium and phosphate release, a Q10 of 3.1 was used for *A. aurita* (Møller et al., 2007), and the general Q10 of 2.66 was used for the other jellyfish species (Ikeda, 2014). For nitrite and nitrate release rates, a Q10 of 2.2 was used for all species (Zheng et al., 2017), corresponding to the temperature coefficient factor of nitrifying microorganisms. Rates were adjusted to the median temperature of the experimental conditions (16°C) and N:P ratios were calculated as the sum of ammonium, nitrite and nitrite over phosphate. The temperature-corrected nutrient production rates were plotted against the wet weight of the jellyfish, and a linear regression was fitted to investigate the allometric relationships between body weight and nutrient release rates. Finally, estimates of inorganic nitrogen release by jellyfish blooms were calculated using the allometric equations together with jellyfish densities from two case studies. The uncertainty range of these estimates was determined from the error on the allometric exponents and the temperature. All statistical analyses were carried out using R Statistical Software (R Core Team, 2019).

2.4 Results and Discussion

2.4.1 Nutrient excretion and nitrification

To determine rates of nitrification catalysed by members of the jellyfish microbiome, we performed incubation experiments with four species of non-zooxanthellate scyphozoan jellyfish, *A. aurita*, *C. hysoscella*, *C. fulgida* and *C. pacifica*. We measured

rates of ammonium and phosphate excretion along with partial ($NH_4^+ \rightarrow NO_2^-$) and complete ($NH_4^+ \rightarrow NO_3^-$) nitrification associated with these jellyfish species. Ammonium and phosphate concentrations increased continuously in all incubations with jellyfish, whereas nitrite and nitrate concentrations increased only in the presence of three of the four species (see discussion below). For all nutrients, concentrations stabilised or decreased once the jellyfish were removed (Figure 2.3, Table 2.2; for absolute concentrations see Appendix A, Figure A.1). In the presence of mucus alone, rates of nitrification were negligible for all investigated jellyfish species ($<2.0 \times 10^{-3}$ nmol L^{-1} h^{-1}; Appendix A, Table A.3), strongly suggesting that the observed rates of nutrient release were directly related to jellyfish metabolism and the associated microbiome. Mass-specific release rates of ammonium ranged from 23 to 86 nmol NH_4^+ gWW^{-1} h^{-1} at experimental temperatures (28 - 86 nmol NH_4^+ gWW^{-1} h^{-1} when normalised to 16°C), which falls within the range of previous observations (2 - 111 nmol NH_4^+ gWW^{-1} h^{-1}: Pitt et al., 2013). The observed intraspecies variability of ammonium excretion was relatively low, with *C. hysoscella* showing the highest variation (14%) in release rates across specimens. In contrast, excretion rates between different jellyfish species varied widely (up to 3.7-fold). Mass-specific release rates of phosphate ranged from 3.2 to 12 nmol PO_4^- gWW^{-1} h^{-1} at experimental temperatures (3.7 - 12 nmol PO_4^- gWW^{-1} h^{-1} when normalised to 16°C). Excretion rates of phosphate were linearly correlated with ammonium excretion rates (all species included, not taking into account ammonium conversion; $p < 0.001$, $R^2 = 0.60$; n = 17; Appendix A, Figure A.7). Ammonium:phosphate excretion ratios ranged from 2.7 to 15.2 with an average of 7.4, in accordance with previous reports (8.2 for *A. aurita*, Shimauchi et al., 2007; 8.7 for *C. mosaicus*, Pitt et al., 2005; 7.5 for *P. noctiluca*, Malej, 1991).

Ammonia oxidation is usually considered the rate-limiting step in nitrification (Zhang et al., 2020a): nitrite is immediately oxidized by free-living nitrite-oxidizing bacteria, preventing its accumulation at significant rates. We observed these expected dynamics in the presence of *A. aurita* when nitrite concentrations did not increase whereas nitrate accumulated (5.7±1.3 nmol NO_3^- gWW^{-1} h^{-1}; Table 2.2), indicating a tight coupling of both nitrification steps. However, this paradigm did not apply to nitrification in association with the other three jellyfish species that we investigated. In the presence of *C. hysoscella* and *C. pacifica*, accumulation rates were significant for both nitrite (*C. hysoscella*: 2.8±1.9 nmol NO_2^- gWW^{-1} h^{-1}; *C. pacifica* 2.1±0.4 nmol NO_2^- gWW^{-1} h^{-1}) and nitrate (*C. hysoscella*: 12±6.0 NO_3^- gWW^{-1} h^{-1}; *C. pacifica* 41±3.1 nmol NO_3^- gWW^{-1} h^{-1}; Table 2.2). The decoupling was more pronounced in incubations with *C. hysoscella* (nitrite accumulation rate was 23% of the nitrate accumulation rate), whereas nitrite accumulation in association with *C. pacifica* was lower (5% of nitrate accumulation). During the incubations with *C. fulgida*, ammonia oxidation to nitrite was the only detectable nitrification process (1.0±0.2 nmol NO_2^- gWW^{-1} h^{-1}; Table 2.2).

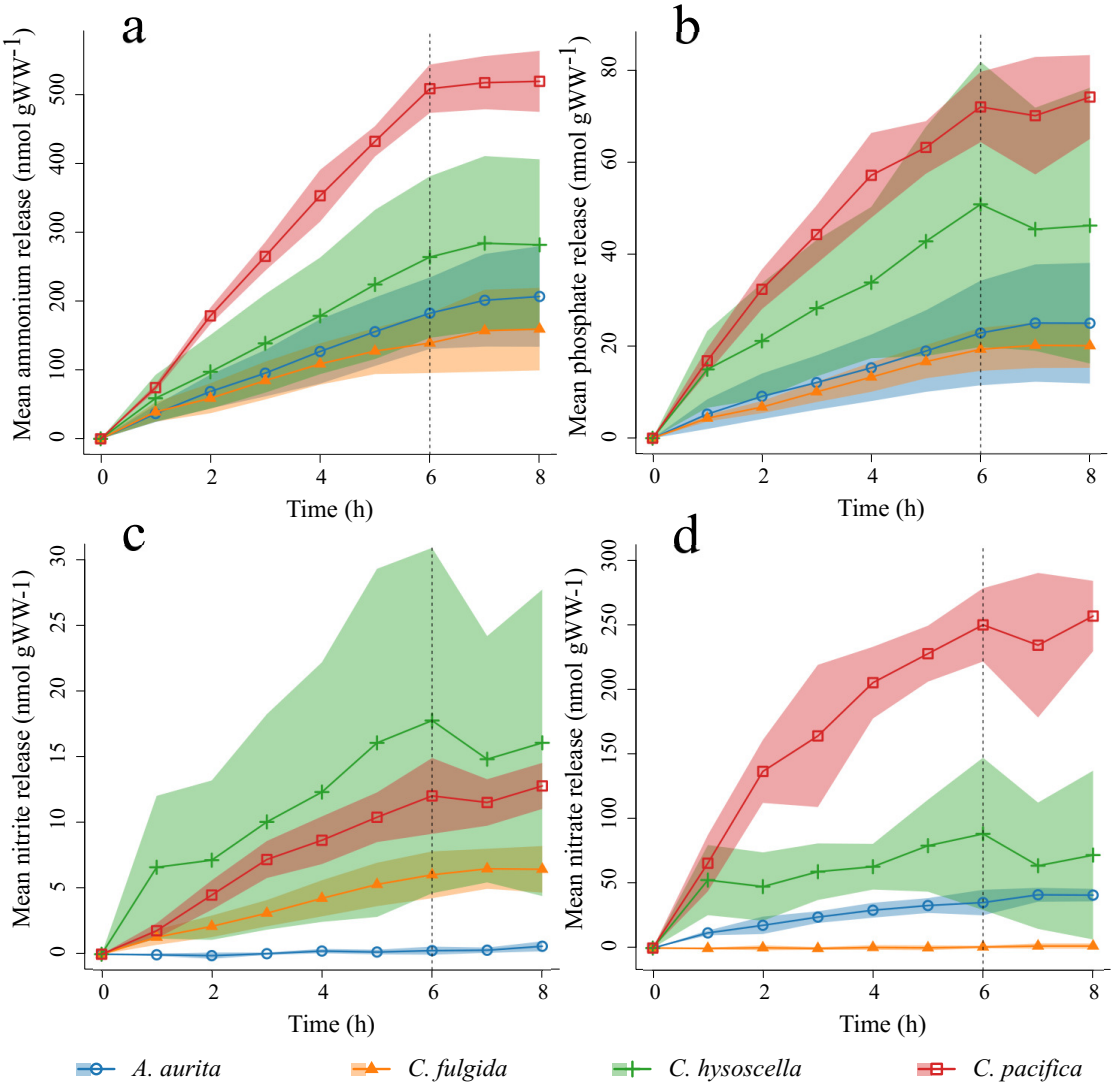

FIGURE 2.3: Mean cumulative release of (a) ammonium, (b) phosphate, (c) nitrite, and (d) nitrate by *A. aurita* (blue circle), *C. fulgida* (yellow triangle), *C. hysoscella* (green cross), and *C. pacifica* (red square), normalized to the wet weight (WW) of each specimen. Colored areas indicate uncertainty envelopes (standard deviation) of the mean cumulative release of nutrients. The vertical dotted line corresponds to the time when the jellyfish were removed from the incubators (6 h).

To our knowledge, two other studies investigated the nitrite + nitrate (NOx, no distinction made) release by non-zooxanthellate scyphomedusae: Pitt et al., 2005 found that *C. mosaicus* released <2% of the released nitrogen in form of NOx, and Shimauchi et al., 2007 did not observe significant release of NOx associated with *A. aurita*. The latter study contrasts with our observation that 16% of the released nitrogen by *A. aurita* was in the form of nitrate. This discrepancy indicates a potential effect of past and present environmental conditions on the jellyfish-associated microbial community composition and, subsequently, on the balance of jellyfish-associated nitrification rates. In contrast to the hypothesis that nitrifiers are specific to zooxanthellate jellyfish (Welsh et al., 2009), our results suggest that jellyfish

are potential hosts for nitrifiers and can thus be a source of nitrite and nitrate to the environment.

Together nitrite and nitrate release rates were 5-50% lower than ammonium excretion rates (Figure 2.4) and contributed 5-33% of the total inorganic nitrogen release. Under saturating substrate levels (ammonia and nitrite), nitrification reactions follow a zero-order kinetic (Chen et al., 2006), meaning that increases in substrate concentration do not increase the reaction rates. As ammonium excretion exceeded that of nitrite and nitrate substantially, we conclude that nitrification rates were not limited by ammonia availability in any of the experiments. Moreover, since the total ammonia concentrations of the incubators were well below toxicity levels for polyps and ephyrae (2 mg L^{-1}, Jian-Long et al., 2018), we are confident that the observed nitrification rates are reflective of *in-situ* processes.

Between species, the rates of nitrification varied more than the excretion rates of ammonium and phosphate. For example, we observed a >6-fold difference between the nitrate release rates of *A. aurita* and *C. pacifica* (Table 2.2, Figure 2.4). Both the inter- and intraspecies variability observed in ammonia and phosphate excretion as well as nitrification rates can partly be explained by allometric scaling of the mass-specific release rates to the wet weight of each individual (ammonium excretion: 80%, phosphate excretion: 73%, nitrification: 55%, Figure 2.5; Appendix A, Table A.6). The allometric relationships for the ammonium, phosphate and nitrate-specific release (ASR, NSR and PSR, respectively; nmol gWW^{-1} h^{-1}) were:

$$ASR = 1.84 \times 10^3 \pm 1.6 WW^{-0.82 \pm 0.10} \qquad (p < 0.001, R^2 = 0.80, n = 17) \tag{2.2}$$

$$PSR = 369 \pm 1.9 WW^{-0.90 \pm 0.13} \qquad (p < 0.001, R^2 = 0.73, n = 17) \tag{2.3}$$

$$NSR = 2.84 \times 10^3 \pm 3.6 WW^{-1.20 \pm 0.28} \qquad (p < 0.001, R^2 = 0.55, n = 15) \tag{2.4}$$

The negative scaling exponents indicate that smaller specimens release more nutrients per gram of mass, and hence follow the expected allometric scaling. The high rates of nutrient excretion and nitrification associated with *C. pacifica* can therefore be partly explained by the small size of these specimens (35 – 59 gWW) compared to the other investigated species. Similarly, the high variability in *C. hysoscella* rates matches the wider range of wet weights per individual (100 – 278 gWW, Table 2.1). All scaling exponents (Equation 2.2, 2.3 and 2.4; Appendix A: Slope, Table A.6) were lower than the -¼ allometric exponent commonly observed for other zooplankton mass-specific physiological processes (Arhonditsis et al., 2019). We suggest that this divergence relates to the jellyfish's high water contents and unique body plans (Pitt et al., 2013). The scaling exponent of the nitrate release allometric equation (-1.20±0.28, Equation 2.3) being lower than the exponent for the ammonium release (-0.82±0.10, Equation 2.2) indicates that when wet weight increases, the nitrate-specific rate

decreases faster than the ammonium-specific rate. This difference in scaling exponent is likely to be related to the changes in the jellyfish surface-to-volume ratio: the release of ammonium is likely more depending on the jellyfish's body volume as it is a metabolic waste product, whereas nitrate is likely more dependent on the jellyfish surface owing to the association with the microbiome living on the jellyfish. Our data show that release rates by jellyfish are highly variable between populations, yet, when normalized to wet weight, we observe strong allometric scaling. This observation highlights the potential for these pathways to be incorporated into models.

Species	Nutrient	Rate (nmol gWW^{-1} h^{-1})	SD	n	R^2	p	n	Rate at 16°C (nmol gWW^{-1} h^{-1})	SD	N:P
A. aurita	Ammonium	30.1	8.1	5	0.99	***	7	33.7	9.1	10.3
	Phosphate	3.6	1.5	5	0.98	***	7	3.9	1.7	
	Nitrite	0.1	0	5	0.31	0.22	7			
	Nitrate	5.7	1.3	5	0.89	**	7	6.2	1.4	
C. fulgida	Ammonium	22.9	4.5	2	0.97	***	7	27.9	5.5	7.89
	Phosphate	3.2	0.5	2	0.99	***	7	3.7	0.6	
	Nitrite	1	0.2	2	0.99	***	7	1.2	0.2	
	Nitrate	0.1	0.1	2	0.16	0.52	7			
C. hysoscella	Ammonium	42.9	17	5	0.99	***	7	29	11.5	6.95
	Phosphate	7.9	4.1	5	0.94	***	7	5.7	2.8	
	Nitrite	2.8	1.9	5	0.87	**	7	1.9	1.4	
	Nitrate	11.9	6	5	0.61	*	7	8.7	4.4	
C. pacifica	Ammonium	86.2	5	5	0.99	***	7	86.1	5	10.8
	Phosphate	11.9	1.2	5	0.96	***	7	11.9	1.2	
	Nitrite	2.1	0.4	5	0.98	***	7	2.1	0.4	
	Nitrate	40.8	3.1	5	0.91	***	7	40.8	3.1	

TABLE 2.2: Release rates and regression statistics for the cumulative nutrient release by the four jellyfish species. The standard deviation of the slope = SD, number of observations = n. Rates at experimental temperatures and adjusted to 16°C are presented, as well as the N : P ratios at 16°C. The rate, SD, R^2, and p are mean values from the replicates individual linear regressions. Levels of statistical significance are indicated by *, **, and *** ($p \leq 0.05$, 0.01, and 0.001, respectively).

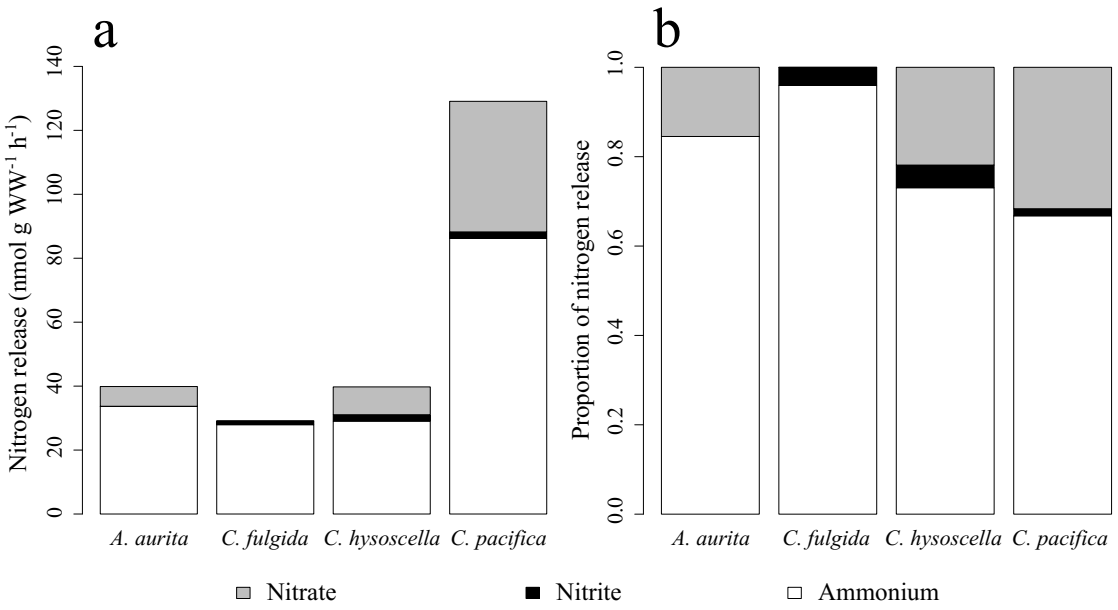

FIGURE 2.4: Inorganic nitrogen release rates of different jellyfish species (a) normalized by the wet weight of the specimens, and (b) as a proportion of total inorganic nitrogen release. Wet weight = WW.

2.4.2 Evidence of active nitrifying microorganisms in jellyfish

Jellyfish host diverse microbial communities on their epithelium as their mucus provides an attractive niche for microorganisms (Kramar et al., 2019; Tinta et al., 2019; Tinta et al., 2012; Weiland-Bräuer et al., 2015). Two species of nitrifiers, the ammonia-oxidizing bacterium *Nitrosospira multiformis* and the nitrite-oxidizing bacterium *Nitrospira moscoviensis*, have been identified as members of the microbiome of jellyfish *C. plocamia* (Lee et al., 2018) and *A. aurita* (Weiland-Bräuer et al., 2015). However, neither of these nitrifiers was highly abundant (<2% of the total operational taxonomic unit; Lee et al., 2018). The high nitrification rates we observed strongly support the presence of either highly active or highly abundant nitrifying microorganisms in the jellyfish microbiome. The low coupling between nitrification rates could be caused by poor diffusional connectivity between nitrifiers (Welsh et al., 2001), i.e., a fraction of the produced nitrite might diffuse directly to the water column rather than to a zone where it can be oxidised to nitrate. The differential production of nitrite and nitrate associated with the four jellyfish populations investigated strongly indicates variable community composition or distribution of the microbiome on the jellyfish depending on jellyfish species or environmental factors. While our findings are representative only of a subset of jellyfish populations, the diverse identity and origin of the investigated specimens strongly support our hypothesis of a widespread association with nitrifying bacteria and archaea. The detailed nature of this association requires further investigations including molecular approaches to determine the identity and distribution of nitrifiers within the jellyfish microbiome.

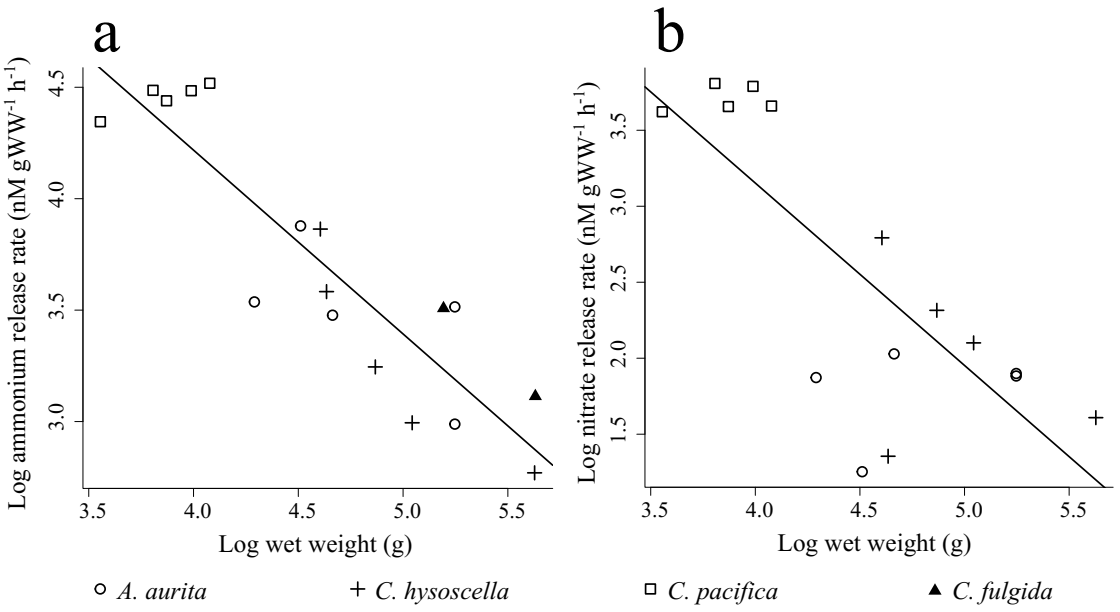

FIGURE 2.5: Effect of wet weight on the mass-specific release rates of ammonium (a; $p < 0.001$, $R^2 = 0.80$, n = 17) and nitrate (b; $p < 0.001$, $R^2 = 0.55$, n = 15) for the jellyfish *A. aurita* (circle), *C. hysoscella* (cross), *C. pacifica* (square), and *C. fulgida* (triangle) at 16°C. The black line is the linear regression. No significant release of nitrate was observed for *C. fulgida.*

2.4.3 Ecological implications

Jellyfish stimulate primary production through the excretion of ammonium and phosphate (Pitt et al., 2005). The average inorganic N:P ratio of the released nutrients (7.3 – 10.9, Table 2.2) lies below the Redfield Ratio (N:P = 16; Redfield, 1963) and substantially below the N:P ratios of their main diet, zooplankton (N:P > 20; Elser et al., 1994). Thus, the gelatinous biomass of these jellyfish appears to retain nitrogen efficiently, which is further supported by their low molar C:N ratio (4.4; Lucas Cathy H. et al., 2011) compared to other marine zooplankton organisms (4.8-6.2 for crustacean zooplankton; Pitt et al., 2013). By storing nitrogen over phosphorus, expanding jellyfish blooms may locally drive the ecosystem toward N-limitation (Sterner, 1990). Whereas under starvation, during which jellyfish consume up to 85% of their own nitrogen-rich tissues (Lilley et al., 2014; Pitt et al., 2014), the N:P ratio of the excreted nutrients would increase. Starvation, a major cause of jellyfish bloom decline (Pitt et al., 2014), could temporarily drive the ecosystem towards P-limitation. A large jellyfish bloom could thus act as a "nitrogen buffer", storing nitrogen over phosphorus when food is abundant and releasing nitrogen over phosphorus during its decay.

Our findings demonstrate that a substantial fraction of the excreted ammonium is shunted through partial or complete nitrification (ammonium: 80±12%, nitrite: 3±2%, nitrate: 17±13%; Figure 2.6), thereby fueling dark carbon fixation in the sunlit surface ocean. An association with jellyfish allows nitrifiers direct access to ammonium in the

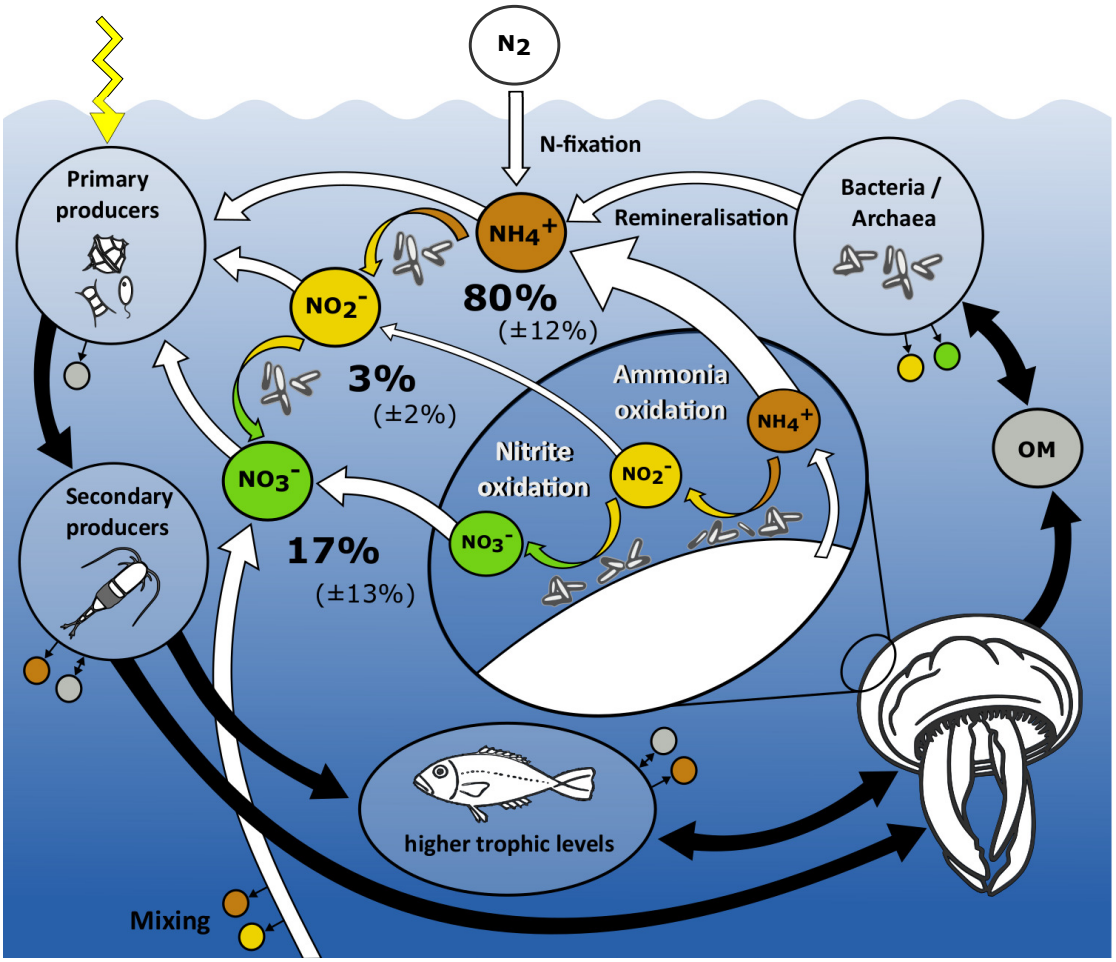

FIGURE 2.6: Conceptual diagram of the role and position of jellyfish in the surface marine nitrogen cycle. The flow of organic and inorganic matter is shown by black and white arrows, respectively. Colors indicate ammonium (NH_4^+, orange), nitrite (NO_2^-, yellow), nitrate (NO_3^-, green) and organic matter (OM, gray). Colored arrows represent ammonium-oxidation (orange-to-yellow) and nitrite-oxidation (yellow-to-green). Components linked to small colored circles release/assimilate nutrients of the same color. The average release of nitrogen forms is presented as a percentage (± standard deviation) of total dissolved inorganic nitrogen released by jellyfish. The yellow zigzag arrow represents light. The large middle circle zooms in on the jellyfish epithelium.

surface ocean, thereby bypassing competition with phytoplankton for this otherwise scarce resource (Zakem et al., 2018). During jellyfish blooms, the release of different forms of bioavailable inorganic (nitrite, nitrate and ammonium) has the potential to locally enhance surface primary production and even influence phytoplankton community composition (Figure 2.6; Shilova et al., 2017). This effect on the community composition, in turn, could impact the quantity and quality of organic matter that sinks to depth (Basu et al., 2018).

To explore the potential relevance of jellyfish blooms on surface nitrogen cycling, we extrapolated our nitrification rate measurements based on two jellyfish blooms, whose whose spatial extent was measured in high resolution (Han et al., 2009a; Lynam et al., 2006). The blooms were observed in (1) the shallow eutrophic and brackish Honjo

lagoon, northwest of Lake Nakaumi, Japan (Han et al., 2009a) and in (2) the coastal area of Namibia representing the Northern Benguela Upwelling System (Lynam et al., 2006). We applied our allometric equations for ammonium and nitrate release (Equation 2.2 and 2.4) to the average body characteristics of the jellyfish (Table 2.3), corrected for temperature (Table 2.3 and as described in methods), and multiplied by abundance.

Location	Species	Surface temperature (C°)	mean WW (g)	mean bell diameter (cm)	References
Honjo District	*A. coerula*	28 - 28.7	92.5[a]	13.1	Han & Uye 2009
Northern Benguela	*C. fulgida*	13[b]	1100[c]	27	Lynam et al. 2006

TABLE 2.3: Overview of case studies. Surface temperature at sampling time and body characteristics of jellyfish used to estimate inorganic nitrogen release. [a] Calculated from (Han et al., 2009a). [b] Mean annual surface temperature in august from (Junker et al., 2017). [c] Calculated from (Houghton et al., 2007).

In the Honjo District Lake, *Aurelia coerula* (a cryptic species to *A. aurita* and until recently named *A. aurita*) is highly abundant (up to 18 medusae m^{-3}) from June to November and are thought to ingest up to 47% of the daily mesozooplankton production (Han et al., 2009a; Han et al., 2009b). During these months, average ammonium and nitrate levels are consistently low ($\leq$0.01 mg L^{-1} for both ammonium and nitrate; Chugoku Regional Development Bureau, 2018). We estimated that the large aggregation of *A. coerula* could have released up to 1.7 mmoles N m^{-2} h^{-1} (uncertainty: 1.0 - 3.2 mmoles N m^{-2} h^{-1}), of which 85% was in the form of ammonium and 15% in the form of nitrate (Figure 2.7, a). On a daily basis, assuming the Redfield ratio (C:N = 106:16; Redfield, 1963), this nitrogen release would be able to support a primary production rate of 3.2 g C m^{-2} d^{-1} (uncertainty: 1.9 -6.1 g C m^{-2} d^{-1}), equivalent to 463% (uncertainty: 275 – 884%) of the mean daily primary production of a typical estuarine-coastal ecosystem (global average: 252 g C m^{-2} y^{-1}; Cloern et al., 2014).

The Benguela Upwelling System is one of the four major coastal upwelling regions presenting the highest primary production of the world oceans (Carr, 2001). Large jellyfish populations occur sporadically throughout the year with the highest abundances observed in June–August (Flynn et al., 2012). The biomass of these blooms can at times exceed the biomass of fish by a factor of three (Lynam et al., 2006). We estimated that the *C. fulgida* blooms in August 2006 (Lynam et al., 2006) could have released up to 1.3 mmoles N m^{-2} h^{-1} (uncertainty range: 0.7 - 2.7 mmoles N m^{-2} h^{-1}; Figure 2.7, b), of which 95% was in the form of ammonium and 5% in the form of nitrite. Assuming the Redfield ratio (C:N = 106:16; Redfield, 1963), this nitrogen

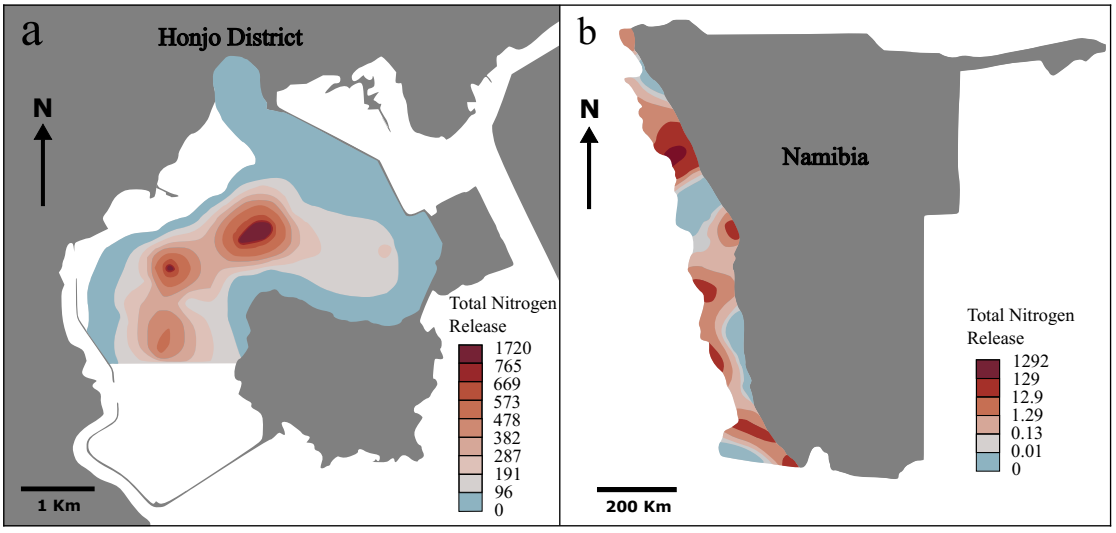

FIGURE 2.7: Heat map of estimated total inorganic nitrogen release associated with the densities of *A. coerula* in the Honjo District sea lake in Japan (a, linear scale: 0–1720 μmol N m^{-2} h^{-1}; map modified from Han et al., 2009b) and of *C. fulgida* along the coast of Namibia (b, exponential scale: 0– 1292 μmol N m^{-2} h^{-1}; map modified from Lynam et al., 2006).

release corresponded to a daily primary production of 2.5 g C m^{-2} d^{-1} (uncertainty: 1.3 – 5.2 g C m^{-2} d^{-1}), which is equivalent to 208% (uncertainty range: 108 – 433) of the average daily primary production of the Northern Benguela ecosystem (1.2 g C m^{-2} d^{-1}; Brown et al., 1991).

The densities observed in the Honjo District lake, although high, are not unusual for coastal habitats (e.g.: 36 $\pm$ 34 *A. aurita* m^{-3} in Limfjorden; Riisgård et al., 2010). Likewise, the jellyfish densities of the Northern Benguela Upwelling System are to our knowledge the highest currently on record, yet such high densities are predicted to become more common in some coastal areas of our changing ocean (Cheung et al., 2019). For areas experiencing increases in jellyfish blooms, the two case studies provide a guide to understanding how jellyfish and their associated microbiomes can impact the nitrogen cycle and supply nutrients for primary production.

2.5 Conclusion

Overall, our results suggest a widespread association between jellyfish and nitrifying microorganisms, which can oxidize up to one-third of the ammonium excreted by jellyfish. While the identity of the nitrifiers and their distribution on the jellyfish remain unknown, it appears that the result of their activity and abundance is constant in a given jellyfish population but likely vary between different environments. The allometric relationships obtained from our observations allow us to estimate the amount of nutrients released by a jellyfish population via extrapolation of the individual mass-specific release rates based on the abundance and size distribution of

a population. This study highlights the importance and complex role of jellyfish blooms in coastal nitrogen cycling, where they can locally support high rates of surface ocean nitrification. Equally, the substantial release of ammonium likely supports phytoplankton growth and may locally impact phytoplankton community composition. Considering the widespread geographic distribution of bloom-forming jellyfish species investigated in this study (Figure 2.1) and the predicted future increase of jellyfish blooms, our findings point toward an increasing relevance of jellyfish on coastal nitrogen and carbon cycling.

Chapter 3

Similarities between the biochemical composition of jellyfish body and mucus

Hubot Nathan D.[1,2], Giering Sarah L. C.[1], Lucas Cathy H.[2]

1 – National Oceanography Centre, University of Southampton Waterfront Campus, Southampton, UK

2 – Ocean and Earth Science, University of Southampton, National Oceanography Centre, University of Southampton Waterfront Campus, Southampton, UK

This chapter was peer-reviewed and published as:

Hubot, N., Giering, S. L. C., & Lucas, C. H. (2022). Similarities between the biochemical composition of jellyfish body and mucus. *Journal of Plankton Research*, *44*(2), 337–344. https://doi.org/10.1093/plankt/fbab091

3.1 Abstract

Recognition of the importance of jellyfish in marine ecosystems is growing. Yet, the biochemical composition of the mucus that jellyfish constantly excrete is poorly characterised. Here we analysed the macromolecular (proteins, lipids and carbohydrates) and elemental (carbon and nitrogen) composition of the body and mucus of five scyphozoan jellyfish species (*Aurelia aurita, Chrysaora fulgida, Chrysaora pacifica, Eupilema inexpectata* and *Rhizostoma pulmo*). We found that the relative contribution of the different macromolecules and elements in the jellyfish body and mucus were similar across all species, with protein being the major component in all samples (81 $\pm$ 4% of macromolecules; 3.6 $\pm$ 3.1% of dry weight, DW) followed by lipids (13 $\pm$ 4% of macromolecules; 0.5 $\pm$ 0.4%DW) and carbohydrates (6 $\pm$ 3% of macromolecules; 0.3 $\pm$ 0.4%DW). The energy content of the jellyfish matter ranged from 0.2 to 3.1 KJ g^{-1} DW. Carbon and nitrogen content was 3.7 $\pm$ 3.0%DW and 1.0 $\pm$ 0.8%DW, respectively. The average ratios of protein:lipid:carbohydrate and carbon:nitrogen for all samples were 14.6:2.3:1 and 3.8:1, respectively. Our study highlights the biochemical similarity between the jellyfish body and mucus and provides convenient and valuable ratios to support the integration of jellyfish into trophic and biogeochemical models.

3.2 Introduction

Jellyfish (cnidarian medusae and ctenophores) can affect the marine food chain and biogeochemical cycles by converting large amounts of organic matter from low trophic levels (e.g. primary producers) into gelatinous biomass at higher trophic levels (Condon et al., 2011). Up to 7% of the carbon assimilated by jellyfish is released in the environment in the form of mucus (Hansson et al., 1995), which has been suggested to play an important role in carbon cycling (Condon et al., 2011; Hansson et al., 1995; Tinta et al., 2021). Yet, jellyfish mucus has received little attention. For example, the rates of mucus excretion, mucus composition and its fate in the ecosystem are not well understood. To date, the biochemical composition of jellyfish mucus has been analysed for only three species (two medusae and one ctenophore) using different methods of collection and analysis (Condon et al., 2011; Ducklow et al., 1979); thus characterisation of jellyfish mucus remains largely unclear (Tinta et al., 2021). In the context of the apparent increase in jellyfish abundance observed in many of the world's coastal ecosystems Brotz et al., 2012, it is increasingly important to include jellyfish in energy flux models and ecosystem studies (Ramondenc et al., 2020). The lack of knowledge of jellyfish mucus composition challenges our ability to understand and model its role in the marine ecosystem.

Cnidarian mucus is predominantly composed of water, approximately 95% of its wet mass, with the remaining 5% composed of glycoproteins (∼3%) and other molecules (∼2%) such as antibodies, peptides, lipids, nucleic acids and inorganic salts such as sodium chloride (Bakshani et al., 2018; Stabili et al., 2015). The glycoproteins dictate the biophysical properties of the mucus, namely its viscosity and elasticity (Bansil et al., 2018), allowing it to lubricate and protect the underlying epithelia as well as to entrap, entrain and transport particles to the digestive pouches (Bakshani et al., 2018). Jellyfish can excrete large amounts of mucus in different situations, including under stress, during digestion, and during reproduction (Patwa et al., 2015). Once released into the environment, jellyfish mucus is quickly metabolised by bacteria, creating major shifts in microbial assemblages and shunting carbon toward bacterial respiration (Condon et al., 2011). The fast remineralisation of jellyfish mucus potentially releases nutrients to the environment with elemental ratios reflecting its composition.

To our knowledge, the macromolecular (protein/lipid/carbohydrate) composition of jellyfish mucus has been measured only once for the scyphomedusa *Aurelia aurita* (proteins = 73%, lipids = 27% and carbohydrates = 5%; Ducklow et al., 1979), which appeared comparable to the macromolecular composition of the species' whole body. Thus, we hypothesise that the consistency in macromolecular composition of the body and the mucus of jellyfish medusae is ubiquitous and can be found in other species of scyphomedusae. In addition, we expect the elemental composition of the mucus to also reflect the elemental composition of the body. To test our hypotheses, we performed macromolecular and elemental analyses on the jellyfish body and mucus of five scyphomedusae species (*Aurelia aurita, Chrysaora fulgida, Chrysaora pacifica, Eupilema inexpectata* and *Rhizostoma pulmo*).

3.3 Materials and methods

Adult medusae of five scyphomedusae species (*A. aurita, C. fulgida, C. pacifica, E. inexpectata* and *R. pulmo*) were collected, following the protocol by (Hubot et al., 2021), from Horsea Lake (UK), Walvis Bay (Namibia), the London Aquarium (UK), Port Elizabeth (South Africa) and the Isle of Portland (UK), respectively. The identity of *R. pulmo*, which is typical of the Mediterranean and adjacent seas (Holst et al., 2007), was confirmed genetically (Ramšak, pers. comm.) Following transfer to the laboratory, specimens were rinsed with filtered seawater (0.7 µm) and the body tissue and mucus samples were collected. Mucus samples were collected for all five species, while body samples were only available for four of the species (*C. pacifica* missing). Mucus was collected by placing the medusae in an empty clean container. The stress caused by the absence of seawater induced the production of mucus and its accumulation in the container. This aggressive approach for mucus collection has the advantage of quickly

obtaining dense mucus material, although we acknowledge that stress-induced mucus might differ slightly compared to mucus produced under 'natural' conditions. When a minimum of 50 mL of mucus was produced (after 1-15 min depending on the size of the jellyfish), the medusae were removed and the mucus was transferred to a 50 mL polypropylene centrifuge tube via a clean glass funnel. For small medusae (*A. aurita*) the whole body was frozen, whereas for large specimens (*C. fulgida, C. pacifica, E. inexpectata* and *R. pulmo*) a pie section of the medusae body (½ for *C. fulgida* and *C. pacifica* and ¼ for *E. inexpectata* and *R. pulmo*) containing all organs and tissue (including umbrella, gonads and arms) in the same proportion as the full body was sliced off and stored at -20°C. Double-bagged frozen samples were carefully crushed using a hammer and lyophilized using a freeze drier. After lyophilization, samples were ground into a fine powder using a clean mortar and pestle and kept at -20°C.

Total lipids were extracted using a single-step extraction method based on the chloroform-methanol solvent system following the protocol by Axelsson et al., 2014 (see details in Appendix B, subsection B.2.1). Total proteins were measured using a modification of the Lowry assay by Gerhardt et al., 1994 (see Appendix B, subsection B.2.2). Total carbohydrates were measured following the protocol by DuBois et al., 1956 (Appendix B, subsection B.2.1)). The carbon and nitrogen content of the samples were measured using a CHNS Elemental Analyzer (Elementar Vario Micro Cube). Ash-free dry weight (AFDW, i.e. the organic portion of the dry weight) was calculated by measuring the ash weight (AW) following combustion at 400°C in a muffle furnace using an ultra-microbalance (Sartorius SE2, readability: 0.1 µg) and subtracting this value from the dry weight (DW; AFDW = DW – AW). All samples were measured in triplicate.

The energy content (EC) of the jellyfish body and mucus samples were calculated based on the macromolecule composition (protein, lipid and carbohydrate) and their mean combustion equivalents (Equation 3.1; Doyle et al., 2007). As significant amounts of bound water (∼10% of DW) remain in medusae after drying (i.e., freeze-drying or drying at 50°C; Larson, 1986), the measurements were corrected for the dilution effect of the bound water by assuming a residual hydration of 11.7% DW (correction factor: 1.13). Hence, EC (kJ g^{-1}) was calculated as:

$$EC = [(\%\ \text{protein} \times a) + (\%\ \text{lipid} \times b) + (\%\ \text{carbohydrate} \times c)] \times d \qquad (3.1)$$

where a, b and c are the gross energy values for protein, lipid and carbohydrate of gelatinous zooplankton (23.9, 39.5 and 17.5 kJ g^{-1}, respectively; Clarke et al., 1992), and d is the water of hydration correction factor of 1.13.

All biochemical measurements were normalised to the DW of the sample. The relationships between the macromolecular content (protein/lipid/carbohydrate) of

the samples were modelled using linear regression and the differences between the linear regressions of mucus and body were investigated by analysis of covariance (ANCOVA). All statistical tests were performed using R Statistical software (version 4.0.3, R Core Team, 2021).

3.4 Results

The total macromolecules (protein + lipid + carbohydrate) content was 7.3 ± 3.6%DW and 1.7 ± 0.9 %DW for the jellyfish body and mucus, respectively. The amount of AFDW (total organic content) was 20.0 ± 3.9%DW and 12.9 ± 1.5%DW for body and mucus, respectively. Protein was the main component of the jellyfish body tissue (82 ± 4% of macromolecules; 6.0 ± 3.0%DW) and of the mucus (80 ± 4% of the macromolecules; 1.4 ± 0.8%DW), followed by lipids (body: 11 ± 3% of the macromolecules, 0.7 ± 0.4%DW; mucus: 14 ± 4% of the macromolecules, 0.2 ± 0.1%DW) and carbohydrates (body: 7 ± 4% of the macromolecules, 0.6 ± 0.4%DW; mucus: 6 ± 3 % of the macromolecules, 0.1 ± 0.1%DW). The jellyfish body tissue contained 6.2 ± 2.4%DW of carbon and 1.7 ± 0.6%DW of nitrogen, resulting in a C:N ratio of 3.6 ± 0.2. The jellyfish mucus contained 1.5 ± 0.6%DW of carbon and 0.4 ± 0.1%DW of nitrogen, producing a C:N ratio of 3.9 ± 0.4.

Protein, lipid and carbohydrate contents were all linearly correlated with each other, with the type of sample (body or mucus) having no effect on the linear regressions as indicated by the absence of significant interaction ($p>0.05$; Appendix B, Table B.5) between the type of tissue and the macromolecule contents (Figure 3.1, A, B and C; Appendix B, Table B.5). The sum of macromolecules was linearly correlated with the AFDW Figure 3.1, D; Appendix B, Table B.5), though there was a consistent offset - with the sum of macromolecules being less than AFDW - as indicated by the negative intercept (slope: 0.8 ± 0.0, intercept = -9.1 ± 0.3; Appendix B, Table B.5). Both tissue types had the same linear regression between the sum of macromolecules and the AFDW (p = 0.20, Figure 3.1, D; Appendix B, Table B.5).

The absolute content of macromolecules (Figure 3.2, A) and carbon and nitrogen (Figure 3.2, B) in body tissue and mucus varied widely between species but were consistent when expressed in relative proportion (Figure 3.2, C and D). Overall, the relative proportions of protein:lipid:carbohydrate and carbon:nitrogen were fairly consistent between the mucus and the body and across the species with an average ratio of 14.6:2.3:1 and 3.7:1, respectively.

The energy content of the jellyfish body and mucus ranged from 0.4 to 3.1 KJ g^{-1} DW for the body tissue (*A. aurita*: 1.3 ± 0.2, *C. fulgida*: 2.4 ± 0.7, *E. inexplicata*: 0.4 ± 0.1 and *R. pulmo*: 3.1 ± 0.3 KJ g^{-1} DW) and from 0.2 to 0.6 KJ g^{-1} DW for the mucus (*A. aurita*: 0.6 ± 0.2, *C. fulgida*: 0.6 ± 0.3, *C. pacifica*: 0.3 ± 0.1, *E. inexplicata*: 0.2 ± 0.01 and *R.*

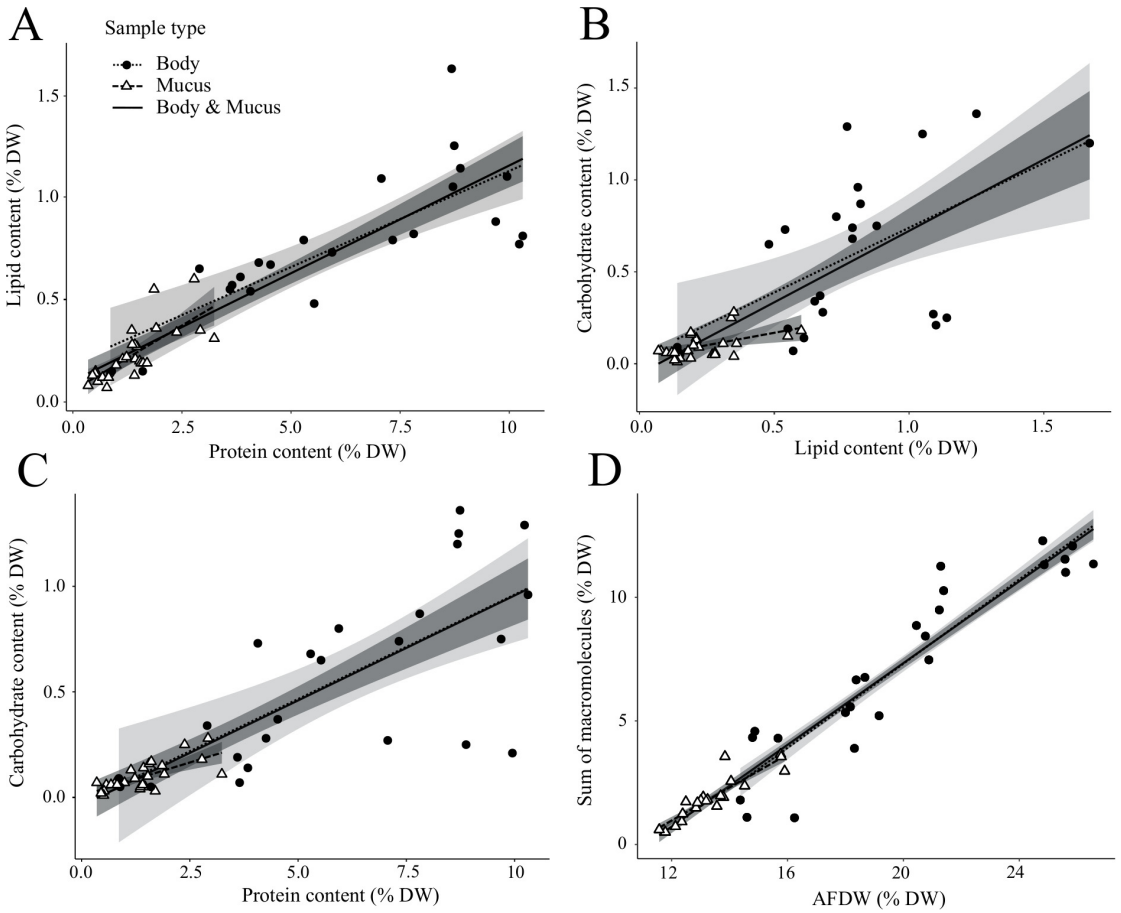

FIGURE 3.1: Comparison of the macromolecular content (protein, lipid, carbohydrate; A, B and C) and the sum of macromolecules to the ash-free dry weigh (AFDW, D) of mucus and body tissues in jellyfish species (*A. aurita, C. fulgida, C. pacifica, E. inexplicata*, and *R. pulmo*) expressed as percentage of dry wet (%DW) of the samples. The lines represent the linear regressions and the shaded area is the confidence interval (see details in SI, Table S2). The solid lines are the linear regressions on the whole data set with (A) lipid (LD) vs protein (PT; LD = 0.10 $\pm$ 0.01 PT + 0.10 $\pm$ 0.03), (B) carbohydrate (CH) vs lipid (CH = 0.78 $\pm$ 0.10 LP - 0.05 $\pm$ 0.06), (C) carbohydrate vs protein, (CH = 0.10 $\pm$ 0.01 PT - 0.04 $\pm$ 0.05), and (D) sum of macromolecules (SM) vs AFDW (SM = 1.12 $\pm$ 0.03 AFDW - 11.24 $\pm$ 0.16).

pulmo: 0.5 $\pm$ 0.1 KJ g^{-1} DW). The mucus was consistently less dense in energy than the body tissues (Figure 3.3, A) with its energy content varying largely with the species (48%, 23%, 87% and 16% of the energy content of body tissue for *A. aurita, C. fulgida, E. inexplicata* and *R. pulmo*, respectively). The energy content of jellyfish biomass (body and mucus) was linearly correlated with its carbon content (Figure 3.3, B), with the type of tissue having no effect on the linear regression (see Appendix B, Table B.5).

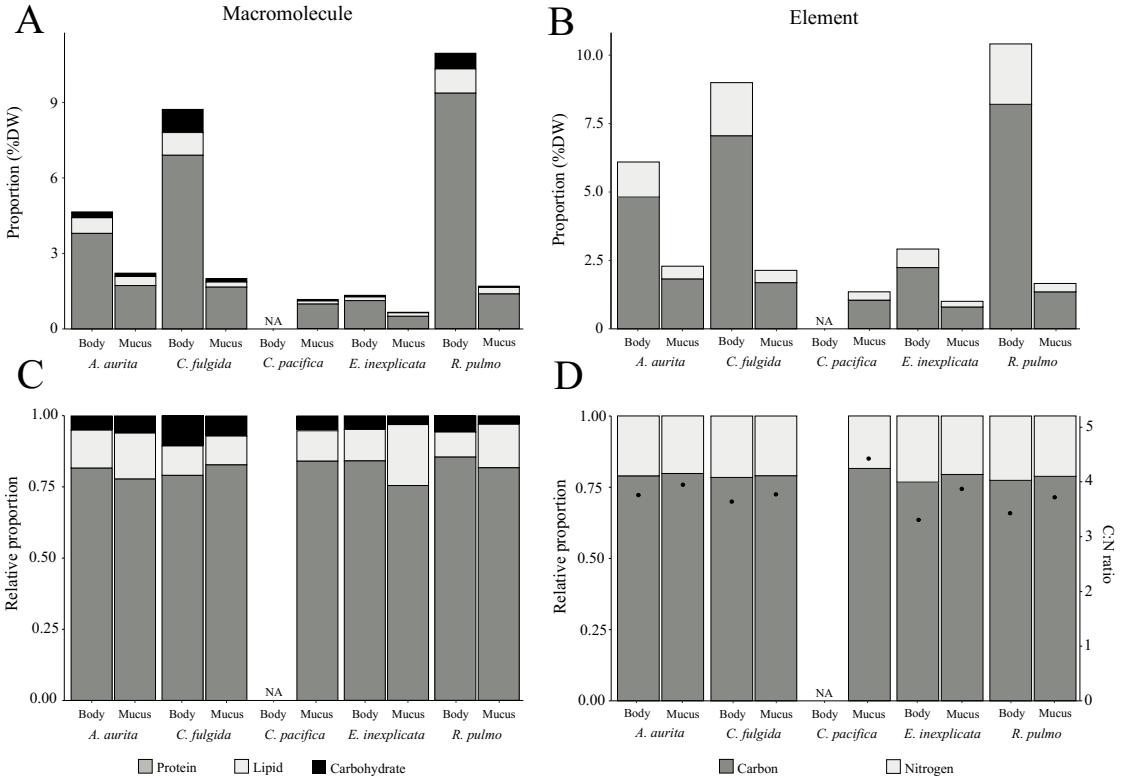

FIGURE 3.2: Proportion of proteins, lipids and carbohydrates (A) and carbon and nitrogen (B) in the body and mucus of jellyfish species (*A. aurita*, *C. fulgida*, *C. pacifica*, *E. inexplicata*, and *R. pulmo*) expressed as a percentage of the dry weight (DW) of the sample and as the relative proportion of the total proteins, lipids and carbohydrates (C) and carbon and nitrogen (D) content. The dots represent the C:N ratio (D).

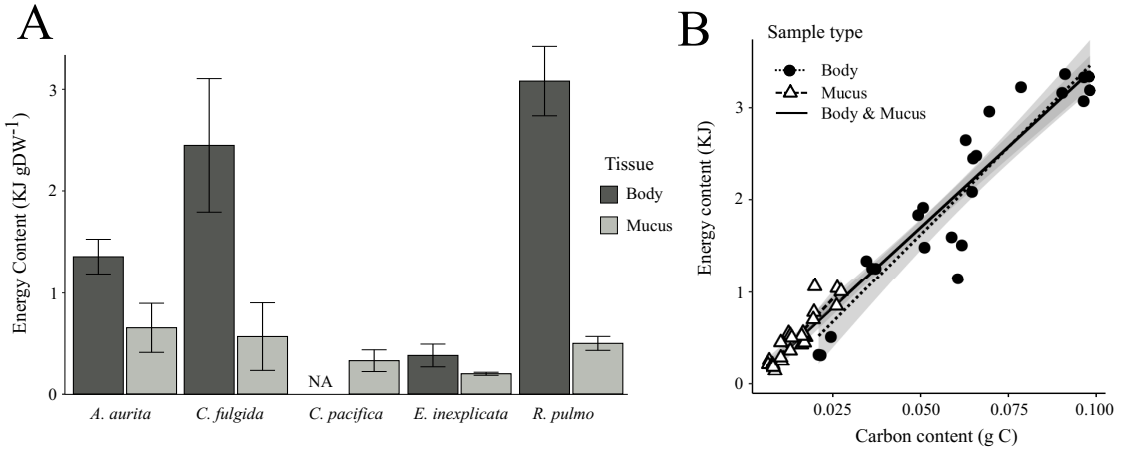

FIGURE 3.3: Energy content of the body (dark grey) and mucus (light grey) of jellyfish species (*A. aurita*, *C. fulgida*, *C. pacifica*, *E. inexplicata*, and *R. pulmo*) normalised to the dry weight (DW) of the samples (A). Error bars show the standard deviation. Linear regression between the energy content (EC) and the carbon content (CC) of jellyfish body (circles) and mucus (triangles; B). The lines represent the linear regressions and the shaded area is the confidence interval. The solid line is the linear regressions on the whole data set (EC = 35.03 $\pm$ 1.27 CC - 0.05 $\pm$ 0.06; details in Appendix B, Table B.5).

3.5 Discussion

Our measurements of the protein and carbohydrate content of the jellyfish body (protein: 6.0 ± 3.0%DW, carbohydrate: 0.6 ± 0.4%DW) are in the range of previous studies (protein: 2.1 - 28.6%DW, carbohydrate: 0.1 - 2.9%DW; Appendix B, Table B.1), whereas our values for the lipid content of the body (0.7 ± 0.4%DW) are slightly lower than previous studies (1.2 – 11.0%DW; Appendix B, Table B.1). The high percentage of inorganic material in jellyfish biomass (body: 80.0 ± 3.9%DW, mucus: 87.1 ± 1.5%DW, body and mucus: 83.8 ± 4.6%DW) is likely due to the fact that jellyfish are osmoconformers, having an internal osmolarity similar to their surrounding environment (Kogovšek et al., 2014). When we consider the water content of jellyfish (∼96% of wet weight; Pitt et al., 2013), 1 kg of jellyfish would contain 40 g of dried matter and 960 g of pure water. In seawater of salinity 35 g/kg, 960 g of pure water would be associated with 33.6 g of salts. Hence, the potential salt content of jellyfish tissue can explain ∼84% of the DW of jellyfish body (33.6 g salt in 40 g DW), which matches our measured values. We suggest that the high inorganic content of the mucus can also be explained by its high salt content, as already suggested for gastropod mucus (Stabili et al., 2015).

We observed a notable discrepancy between the sum of macromolecules and the AFDW for both mucus and body tissue (Figure 3.1, D), which are both representing the organic content of the samples. A possible explanation is that the water bound to jellyfish DW induces an overestimation of the AFDW (Kogovšek et al., 2014). In addition, nucleic acids were not considered in the sum of macromolecules, thus inducing an underestimation of the macromolecular content. Altogether, the bound water found in jellyfish DW and the absence of nucleic acids in our macromolecular calculations likely caused the sum of macromolecules to be significantly smaller than the AFDW.

Our data suggest that the relative content of macromolecules, and of carbon and nitrogen, are conserved between the jellyfish body and mucus across species. The high proportion of protein in jellyfish bodies (82 ± 4% of macromolecules) reflects that most of the jellyfish body tissue is made of proteinous mesoglea (Kogovšek et al., 2014; Lucas, 1994). In contrast, the high protein content of the mucus (80 ± 4% of macromolecules) was unexpected as the glycoproteins found in mucus, which make up most of the dry content of mucus (∼60%; Bakshani et al., 2018), usually have 50 – 80% of their molecular weight comprised of carbohydrates (Bansil et al., 2018). We would hence expect the protein/carbohydrate ratio of the glycoproteins to determine the protein/carbohydrate ratio of the mucus. Our results suggest that the glycoproteins produced by jellyfish are low in carbohydrates. The scarcity of highly soluble hydrocarbon chains in the mucus, as suggested by our data, would decrease

its solubility and rigidity (Davies et al., 1998) allowing it to hold more to the epithelium while retaining viscosity.

The high protein content of the mucus is reflected in the relatively low C:N ratio (3.9 $\pm$ 0.4), which contrasts with the higher but largely variable C:N ratio previously found for the mucus of the scyphomedusa *C. quinquecirrha* (C:N = 8.1 $\pm$ 6.2, Condon et al., 2011). The difference in mucus elemental C:N ratio between (Condon et al., 2011) and our study is most likely caused by a difference in the analysed material. We analysed concentrated mucus directly extracted from stressed jellyfish (including the particulate and dissolved phases) whereas (Condon et al., 2011) studied the dissolved organic phase of the mucus produced by unstressed jellyfish. The two differing results indicate that the dissolved organic phase of the mucus is less rich in nitrogen compounds (e.g. lacking proteins and amino acids) compared to the particulate organic phase. Although it has been suggested that jellyfish mucus produced under different conditions or situations (e.g. reproduction, feeding, stress) might cause differences in biochemical composition (Tinta et al., 2020), there is to date no evidence to confirm this hypothesis.

3.5.1 Ecological implications

The capacity of marine ecosystems to support stocks of living resources can be estimated by calculating energy flux circulating through food webs (Schaafsma et al., 2018). Our calculations of energy density based on the macromolecular composition of jellyfish body biomass (0.4 - 3.1 KJ g^{-1} DW; Figure 3.3) are slightly lower than in a previous study (2.83 - 4.30 KJ g^{-1} DW; Doyle et al., 2007). The energy content of jellyfish bodies is low compared to most marine organisms (e.g. fishes: 14.8 - 39.3 kJ g^{-1} DW, crustaceans: 7.1 - 25.3 kJ g^{-1} DW, squid: 16.2 - 24.0 kJ g^{-1} DW; Schaafsma et al., 2018) owing to their high inorganic content. Despite their low energy content, recent studies have shown that jellyfish are consumed by many organisms throughout the marine food chain (Marques et al., 2019). Their high water content allows jellyfish biomass to be quickly digested (e.g. up to 20 times faster than shrimps) thus counterbalancing their low energy density and reaching comparable rates of energy acquisition for predators feeding on fish or crustaceans (Hays et al., 2018). In addition, the consumption of gelatinous biomass by fishes can represent an alternative food resource when primary prey are not available (Briz et al., 2018) allowing fish to adapt to prey availability. Furthermore, the dietary value of jellyfish is enhanced by their high abundance, their slow movements (no need for active pursuit) and their fast growth rates. Feeding on jellyfish could thus be strategically beneficial, especially when energy-rich tissue, like gonads and arms, are consumed preferentially (Hays et al., 2018).

The lower energy density of jellyfish mucus (0.2 to 0.6 KJ g^{-1} DW; Figure 3.3, A) compared to the body (0.4 - 3.1 KJ g^{-1} DW, Figure 3.3, A) can be explained by its higher water and thus salt content. When compared to carbon content (Figure 3.3, B), the energy content of the mucus and the body remain proportionate due to the similar proportion of macromolecules, providing a convenient relationship to calculate the energy content of jellyfish biomass based on carbon content.

Our jellyfish organic matter (body and mucus) was rich in nitrogen (C:N = 3.7) compared to the global medians (6.6 - 7.4, Martiny et al., 2014) and to other marine zooplankton organisms (4.8 - 6.2 for crustacean zooplankton; Pitt et al., 2013). Jellyfish, particularly in high abundances such as during blooms, represent storage of nitrogen-rich organic matter that can be supplied to the environment through excretion of inorganic nutrients (Hubot et al., 2021) and mucus production (Condon et al., 2011) or reach higher trophic levels through predation (Hays et al., 2018). Subsequently, when a jellyfish dies and starts decaying, its body mass will be available for bacterial degradation. The microbial remineralization of jellyfish organic matter (mucus and carcasses) may have an important impact on nutrient cycles (Condon et al., 2011; Tinta et al., 2021) supplying primary producers with nutrients and ultimately supporting the whole food chain. As nitrogen availability limits primary productivity in most of the surface ocean (∼75%; Bristow et al., 2017), the remineralisation of the labile nitrogen-rich jellyfish organic matter could potentially reduce nitrogen limitation thus enhancing primary production in nitrogen-limited environments. In addition, the sinking of carcasses creates a downward flux of organic nutrients, participating in carbon sequestration and supplying the deep-sea food webs with organic matter thus supporting commercially important invertebrate species (Dunlop et al., 2017). Overall, jellyfish organic matter has the potential to support the marine food web at multiple levels.

3.6 Conclusion

Our study provides a first general characterisation of the biochemical composition of jellyfish mucus across different species and highlights its similarity with the jellyfish body composition. The data suggest that jellyfish organic matter is not species-specific and indicate a much higher homogeneity in jellyfish organic matter than previously expected (Tinta et al., 2021). As jellyfish biomass can largely exceed (up to 3 times) the biomass of fish in highly productive ecosystems (Lynam et al., 2006), it is crucial to investigate its impact on marine ecosystem productivity. Our data facilitate the inclusion of jellyfish in ecosystem studies by providing convenient and valuable biochemical relationships allowing to model the role of jellyfish in marine food webs and biogeochemical cycles and thus to estimate changes in the future ocean.

Chapter 4

Jellyfish mucus as a source of nutrients in marine coastal waters

Hubot Nathan D.[1,2], Giering Sarah L. C.[1], Katja Klun[3], Gerhard J. Herndl[4], Lucas Cathy H.[2], Tinkara Tinta[3]

1 – National Oceanography Centre, University of Southampton Waterfront Campus, Southampton, UK

2 – Ocean and Earth Science, University of Southampton, National Oceanography Centre, University of Southampton Waterfront Campus, Southampton, UK

3 – Marine Biology Station Piran, National Institute of Biology, Piran, Slovenia

4 – Department of Functional and Evolutionary Ecology, Bio-Oceanography Unit, Faculty of Life Sciences, University of Vienna, Vienna, Austria

This chapter is in preparation for submission.

4.1 Abstract

Globally, jellyfish blooms represent large quantities of organic matter (OM; $\sim$ 290 Tg carbon) which can ultimately be degraded by microbes triggering changes to the marine ecosystem. Part of that OM is constantly released in the environment in the form of mucus. Yet, the amount of nutrients released through jellyfish mucus and the consequences for the marine ecosystem has not been clearly described. Here we characterise and quantify the nutrients (organic and inorganic) released by jellyfish through mucus production and the subsequent effect on the microbial community. Prior to microbial processing, one gram of dry jellyfish mucus in seawater releases approximately 1.7 µmol of phosphate, 3.9 µmol of dissolved inorganic nitrogen, 17.9 µmol dissolved organic nitrogen, 134.0 µmol of dissolved organic carbon and 15.1 µmol of free-dissolved amino acids. Close to half of the organic carbon released by jellyfish mucus (44 $\pm$ 14 %) is in the dissolved fraction of which 43 $\pm$ 35% is of low molecular weight: <1kDa) and is quickly utilised by microbes without clear biomass production. The prokaryotic heterotrophic production peaked at 5.0 $\pm$ 0.8 µg C L^{-1} h^{-1} before quickly decreasing likely due to the absence of phosphate. The increased consumption of phosphate caused by the degradation of nitrogen-rich mucus suggests that the release of mucus by jellyfish blooms might ultimately drive the ecosystem towards phosphorous limitation, restricting marine microbial production and thus the transfer of OM to higher trophic levels.

4.2 Introduction

Marine organic matter (OM) is a complex collection of molecules that play an important role in the functioning of marine ecosystems, influencing large-scale biogeochemical processes and ultimately affecting global climate (Lønborg et al., 2020). The dissolved fraction of marine OM (dissolved organic matter; DOM) is the largest pool of organic carbon (C) and associated elements in the ocean ($\sim$ 662 Pg C; (Carlson et al., 2015). Yet, less than 0.1% of that carbon pool is consumed by microbes within hours to days (i.e. labile; Hansell, 2013) generating one of the largest annual turnovers of carbon on the planet ($\sim$ 25 Pg C $year^{-1}$; Hansell et al., 2014). Labile DOM originates mainly from phytoplankton, heterotrophic microbes and mesoplankton (Moran et al., 2022) and is often associated with the release of particulate organic matter (POM; Hansell, 2013). Although typically classified based on size via filtration, DOM and POM form an organic matter continuum, constantly interacting with marine microbes and zooplankton (Verdugo et al., 2004). The fraction of OM that is resistant to microbial degradation may stay in the ocean interior for millennia (Jiao et al., 2010), therefore serving as an important sink for atmospheric CO_2 (Dittmar et al., 2021).

A large and often overlooked source of OM for the marine food web is the biomass of jellyfish (here referring to the cnidarian medusae; Tinta et al., 2012). As jellyfish are voracious consumers of zooplankton, a jellyfish bloom converts large amounts of carbon from primary producers to gelatinous biomass (Condon et al., 2011). Such blooms regularly exceed 100 Kg of wet weight m^{-3} over many square kilometers (Lilley et al., 2011). Currently, the mean global jellyfish biomass is estimated to be $\sim$ 290 Tg C (in the upper 200 m, cnidarian medusae only; Luo et al., 2020) with the highest densities found in productive coastal regions (Lucas et al., 2014a). Through mucus production and carcass degradation, jellyfish blooms can supply OM to the microbial pelagic community (Condon et al., 2011; Pitt et al., 2009c; Tinta et al., 2021).

In recent years, the degradation of jellyfish carcasses has received greater attention than mucus production (see review by Tinta et al., 2021). During incubation experiments, 100 mg of jellyfish carcasses released $\sim$ 51% of DOM (including DOC, dissolved nitrogen, and amino acids) and 0.6 µmol of ammonium and phosphate, which were instantly available to a microbial consortium for both respiration and production, inducing relatively high microbial growth efficiencies (65 $\pm$ 27%; Tinta et al., 2020). Specifically, the main consumers of jellyfish-derived DOM appeared to be the prokaryotes *Pseudoalteromonas*, *Alteromonas*, and *Vibrio*. These results indicate that the degradation of jellyfish OM has implications for biogeochemical cycles and pelagic food webs of coastal areas (Tinta et al., 2021).

In contrast to jellyfish carcasses, the impact of jellyfish mucus excretion and its microbial degradation is not well understood. For example, the amount of mucus excreted by jellyfish is poorly quantified with only scarce estimates available for a few species (e.g. 1.2 mg C ind^{-1} d^{-1} and 0.4 – 13.4 mg C gDW^{-1} d^{-1}; Hansson et al., 1995 and Condon et al., 2010, respectively). In addition, while it has been suggested that jellyfish mucus is rapidly respired by the pelagic microbial community without significant biomass production (Condon et al., 2011), the associated release of nutrients has not been quantified.

Though relatively little is known about the mucus released by jellyfish, the mucus released by other marine organisms provides insight into its likely properties. Marine mucus is released in the water column by most marine organisms, including fish (Reverter et al., 2018), polychaetes (Stabili et al., 2019), echinoderms (Flammang et al., 2016), tunicates (Ramesh et al., 2021) and cnidarians (Stabili et al., 2018). Overall, mucus is a complex secretion composed mainly of water ($\sim$95% of wet weight), followed by mucins ($\sim$3%) and other molecules ($\sim$2%; Bakshani et al., 2018). Mucins are very large glycoproteins (0.5–20 MDa; Bansil et al., 2006), included in the DOM high molecular weight (HMW: $\geq$1kDa) fraction and among the largest molecules in DOM (Benner et al., 1997; Guo et al., 2007). They are composed of a central protein chain with oligosaccharide sidechains (Bansil et al., 2006) and are responsible for the viscous properties of the mucus gel allowing its functions (Linden et al., 2008). The

main functions of the mucus layer are: the protection and cleaning of the underlying epithelium, the trapping of particles, the first line of defence against pathogens, and the facilitation of gaseous and nutrient exchange with the environment (Bansil and Turner, 2018 and references therein). Coral mucus is considered a valuable substrate and habitat for microbial communities due to its high nitrogen content (from 50% to 90% of OM released), thereby supporting the microbial loop and the marine food web (Fonvielle et al., 2015). Similarly to corals, jellyfish are ubiquitous in coastal waters (Lucas et al., 2014b) hence their mucus could be of global importance for marine ecosystems through its effect on nutrients and microbial communities.

This study aims to characterise the nutrients released by jellyfish mucus and their impact on the microbial community. We hypothesise that (1) the release of jellyfish mucus in seawater results in an increase of inorganic and organic nutrient concentrations, and that (2) these nutrients are quickly utilised by the surface microbial community inducing changes in its community composition. The choice of the jellyfish species (*Aurelia aurita* s.l.) and the experimental design were based on a recent study on jellyfish carcasses degradation (Tinta et al., 2020) in the Gulf of Trieste, which facilitates the comparison of results and ultimately the assessment of the comprehensive role of jellyfish blooms in coastal environments.

4.3 Material and methods

4.3.1 Sampling

Specimens of *Aurelia aurita* were collected in the proximity of the long-term sampling site oceanographic buoy Vida (45° 32.925' N, 13° 33.042' E), located in the Gulf of Trieste (northern Adriatic), during the peak and the senescent phase of their spring bloom in 2019 and 2021, respectively. Jellyfish were sampled individually from the surface water together with ambient seawater using a large plastic bucket, rinsed with ambient seawater prior to sampling. On the same day, each specimen was transported to the laboratory while kept in the dark and at *in-situ* temperature where the mucus was collected following the methods by (Hubot et al., 2022). Briefly, jellyfish were placed in a large beaker without water. The absence of water induced stress on the jellyfish which triggered mucus excretion. After 10-30 minutes, the jellyfish was removed and the mucus released in the beaker was transferred to sterile 50-mL centrifuge tubes and stored at -20°C.

The majority of the collected jellyfish mucus was freeze-dried (at - 45°C for 7 days) according to recommendations for jellyfish biomass processing (Kogovšek et al., 2014). The weight of dry-mucus was on average 4% of the frozen-mucus weight (Appendix C, Table C.1). Dry-mucus was homogenized with a sterilized pestle and agate mortar.

Subsequently, dry-mucus samples were pooled together to obtain a representative sample mix of jellyfish mucus from the study area, avoiding possible biases arising from variations in the size of different individuals within the population and from different phases of the bloom. Dry-mucus was stored in acid and Milli-Q water-rinsed and combusted glass vials at -20°C. Freeze-drying is a widespread method to preserve biomolecules (Merivaara et al., 2021) expected to maintain the biochemical properties of the fresh mucus while allowing thorough homogenisation of the material (Tinta et al., 2020). However, since this assumption had not been tested, we performed parallel experiments using jellyfish frozen-mucus (i.e. without the freeze-drying step) from the same specimen and compared the results with those from the dry-mucus. Although freezing preservation (-20°C) can injure physiological activities, morphological features and genomic DNA in various bacteria, short-term freezing (< 1 month) can preserve viable microbiomes (Takahashi et al., 2019).

4.3.2 Dialysis

A fraction of dry-mucus was dialyzed using Spectra/Por 7 Membrane tubing (Sulfur and Heavy Metal Free, Spectrum) with a molecular weight cut-off (MWCO) of 1 kDa to determine the ratio between the high- (>1 kDa) and the low- (<1 kDa) molecular weight compounds (LMW and HMW, respectively) and the C:N ratio of mucus OM (as previously described by Tinta et al., 2020). Details of the dialysis procedure are described in appendix C (section C.2). The LMW fraction of mucus OM was determined by measuring the release of dissolved organic carbon (DOC) and total dissolved nitrogen (TDN) in the dialysate (Table C.2), compared to the DOC/TDN release from the leaching experiment.

4.3.3 Leaching experiments

The concentration and composition of the particulate and dissolved organic matter (POM and DOM, respectively) and inorganic nutrients leaching from the dry-mucus were determined by dissolving 250 mg dry-mucus powder in 1 L of 0.2-μm filtered aged ($\sim$ 1 month) seawater (ASW; see subsection 4.3.5) in a glass Erlenmeyer flask (acid-rinsed, Milli-Q rinsed, and pre-combusted) on a shaker in the dark at *in-situ* temperature ($\sim$21°C; as previously described by Tinta et al., 2020). Triplicate experimental flasks were subsampled 1, 6 and 24 h after the dry-mucus additions for particulate organic carbon (POC) and particulate organic nitrogen (PON) via filtration onto combusted Whatman GF/F ($\sim$0.8 μm pore size) filters using acid-, MilliQ water rinsed and a combusted glass filtration system. The filtrate was then used to measure DOC, TDN, dissolved free amino acids (DFAA) and inorganic nutrients. Microbial

abundance (MA) samples were collected at the end of the experiment to check for contamination.

4.3.4 Mucus degradation experiment

The combined effect of mucus excretion and its biodegradation by ambient microbes on nutrient release and microbial community composition was studied via a short-term batch culture experiment including three treatments (dry-mucus, frozen-mucus and control). For each treatment, three acid-washed, Milli-Q water-rinsed and combusted 5-L borosilicate glass flasks were filled up with 0.2-μm filtered ASW and freshly collected 1.2-μm filtered coastal ambient seawater (FSW; serving as microbial inoculum) in a ratio of 9:1. Seawater for both ASW and the microbial inoculum was collected at 5 m depth in the centre of the Gulf of Trieste using 5-L Niskin bottles connected to a carousel water sampler (SBE 32, Sea-Bird Electronics). Seawater for ASW was collected in May 2020 and aged in acid-washed and Milli-Q water-rinsed 20-L Nalgene carboys for more than a month at room temperature in the dark. Seawater for the microbial inoculum was sampled and filtered on 13 July 2020, the same day as starting the experiment.

The bottles of the dry-mucus treatment received 20 mg of mucus dry-weight (DW; equivalent to a concentration of 4 mg DW L^{-1}), while the bottles of the frozen-mucus treatment received 500 mg of mucus wet-weight (WW; equivalent to a concentration of 4 mg of DW L^{-1}; based on DW= 4%WW; see Table C.1). The concentration of dried-mucus used was calculated based on a DOC release rate of 1.2 mg C ind^{-1} d^{-1} (Hansson et al., 1995) and a mucus carbon content of 1.5% DW (Hubot et al., 2022). As the mucus release rates of *A. aurita* in the Adriatic Sea were not available, we used data from the Skagerrak strait. We used the amount of mucus produced in one day by a dense bloom (>50 medusae m^{-3}) of small jellyfish (9.5 to 18 cm in diameter; Hansson et al., 1995). All bottles were incubated in the dark at *in-situ* temperature (21 °C) and mixed thoroughly prior to each subsampling. The experimental bottles were sampled at 0, 5, 10, 20, 30 and 42 h for later analysis of MA, prokaryotic heterotrophic production (PHP), POC, PON, DOC, TDN, DFAA and inorganic nutrients (analyses described below). For each sampling time, 50 mL was removed from the bottles, leaving ∼94% of the initial volume at the end of each experiment. Additionally, the MA of one replicate was directly estimated after each sampling (within 1 h) to follow the microbial growth phase. The experiment was terminated when the microbial community reached its late exponential growth phase. At the end of the experiment, 4 L of each flask was filtered to collect the microbial biomass for metagenomic analysis (see details below).

Experiments	Dialysis	Leaching		Mucus degradation		
Treatments	dry-mucus	frozen-mucus	dry-mucus	frozen-mucus	Dry-mucus	Control
Mass of added mucus	1g	6.250 g	250 mg	500 mg	20 mg	-
Replicates (per treatment)	3	3		3		
Sampling time (h)	0, 1, 4, 9, 24	0, 1, 6, 24		0, 5, 10, 20, 30, 42		
Parameters measured	DOC, TDN, DFAA and IN	POC, PON, DOC, TDN, DFAA and IN		BA, PHP, POC, PON, DOC, TDN, DFAA, IN, MA, MCP		
Medium	Milli-Q	ASW		ASW:NSW (9:1)		
Volume per replicate	25mL (tube) 500mL (beaker)	1L		5L		
Temperature (°C)	4	21		21		

TABLE 4.1: Summary of the experimental design. POC: particulate organic carbon, PON: particulate organic nitrogen, DOC: dissolved organic carbon, TDN: total dissolved nitrogen, DFAA: dissolved-free amino acids, IN: inorganic nutrients (ammonium, nitrite, nitrate, phosphate), MA: microbial abundance, PHP: prokaryotic heterotrophic production, ASW: aged seawater, NSW: natural seawater.

4.3.5 Chemical analyses

4.3.5.1 Particulate and Dissolved Organic Carbon and Nitrogen

Samples for POC and PON were filtered onto combusted Whatman GF/F filters using acid-, Milli-Q-water-rinsed and a combusted glass filtration system. GF/F filters were stored at -20°C until analysed for POC and PON by combustion at 1,150°C with an elemental analyser (Vario Micro Cube, Elementar) with a 3% accuracy. Approximately 30 mL of the GF/F filtrate was collected into acid-, Milli-Q-water-rinsed and combusted glass vials and stored at -20°C until analysis. DOC and TDN analyses were performed by a high-temperature catalytic method using a Shimadzu TOC-L analyser equipped with a total nitrogen unit (Hansell, 1993). The calibration for non-purgeable organic carbon was done with potassium phthalate and for TDN potassium nitrate was used. The results were validated with Deep-Sea Reference (DSR) water for DOC (CRM Program, Hansell Lab). The precision of the method, expressed as DSR% was $<$2%. The POC/PON data needs to be considered with caution due to the low amount of mucus additions and the small volume of water filtered (especially for the mucus experiment).

4.3.5.2 Dissolved Inorganic Nutrients

Dissolved inorganic nitrogen (NH_4^+, NO_3^-, NO_2^-) and dissolved inorganic phosphorus (PO_4^{3-}) concentrations were determined spectrophotometrically by gas-segmented continuous flow analysis (QuAAtro, Seal Analytical) following standard methods (Hydes et al., 2010). The quality control is performed annually by participating in an inter-calibration program (QUASIMEME Laboratory Performance Study).

4.3.5.3 Dissolved free Amino Acid Analysis

Samples for DFAA analyses were filtered through combusted Whatman GF/F filters using acid-, Milli-Q-water-rinsed and combusted glass filtration systems and analysed as previously described by (Tinta et al., 2020). Approximately 4 mL of the GF/F filtrate was collected in dark glass vial and stored at -20°C until analysis. 500 μL of sample was directly pipetted into acid-, Milli-Q water rinsed and combusted glass HPLC ampules and analysed by a Shimadzu Nexera X2 ultra high-performance liquid chromatograph (UHPLC) with a fluorescence detector (RF-20A XS). Pre-column derivatization was applied with ortho-phthalaldehyde according to the protocol of (Jones et al., 1981).

4.3.6 Microbial abundance

MA was determined from formaldehyde-fixed (37% formaldehyde, 2% final concentration) 1.5 mL subsamples. Samples were immediately stored at -80°C. For enumerating microbes, 1 mL of sample was filtered onto a 0.2-μm polycarbonate filter (Whatman) glass filtration system and a vacuum pump at low pressure (<200 mbar). From each sample, more than 200 microbes or at least 10 fields per filter were counted using an Olympus BX51 epifluorescence microscope. Pictures were taken using an Olympus Microscope Digital DP70 camera and analysed with computer software Olympus DP-Soft BX-51.

4.3.7 Prokaryotic Heterotrophic Production

PHP was measured by incubation of triplicate with 3H-leucine (20 nM, final concentration; Amersham) for 1 h (Kirchman et al., 1985) with samples containing trichloroacetic acid (TCA, 5% final concentration) serving as controls. The incubation was stopped by adding TCA (5% final concentration) to all samples and followed by centrifugation and washing steps (Smith et al., 1992). Radioactivity was measured using a liquid scintillation counter (Canberra Packard and TriCarb Liquid Scintillation Analyzer, model 2500 TR). PHP was calculated using the conversion factor for coast and shelf environments (1.35 kg C mol Leu^{-1}; Giering et al., 2022).

4.3.8 Microbial metagenomes

At the end of the experiment, the microbial biomass was collected onto 0.2-μm polyether sulfone membrane filters (47 mm; PALL Inc.) by filtering 4 L of each of the triplicate from the three experimental treatments (frozen-mucus, dry-mucus and control) using acid- and Milli-Q water rinsed and combusted filtration sets and applying a low (<200 mbar) pressure. Filters were immediately transferred into sterile cryotubes and stored at -80°C. DNA was extracted from the filters as described by (Angel, 2012), with slight modifications for extraction from filters (Bayer et al., 2019), as described in (Tinta et al., 2020). The DNA from each of the three treatments was pooled together and sent to Microsynth AG (Switzerland) for metagenomic DNA libraries construction (Illumina TruSeq) and sequencing (Illumina NovaSeq, 2x150bp). Raw reads were deposited at NCBI under the accession number XXX (to be deposited).

The paired reads quality was evaluated using FastQC (v0.11.9; Andrews, 2010) and trimmed with Trim-galore (v0.6.6,Krueger, 2020). Reads matching the human reference genome (GRCh38) were removed using bowtie2 (v2.5.0, Langmead et al., 2012) and samtools (v1.16.1, Li et al., 2009). Taxonomical assignment was performed using Kraken2 (v2.1.2, Wood et al., 2019) and the NCBI RefSeq database index

(k2_standard_20210517, https://benlangmead.github.io/aws-indexes/k2). Estimation of abundance was performed using Bracken (v2.8; Lu et al., 2017).

4.3.9 Statistical analysis

Statistical analysis was performed to evaluate the effect of mucus enrichment on chemical and microbiological parameters in our incubation experiments using ANOVA and assuming homoscedasticity and normality of the data. The ANOVAs were followed by post-hoc Tukey pairwise-comparison tests to identify which treatments were significantly different from each other. Results of ANOVAs and Tukey tests were confirmed using Kruskal – Wallis and pairwise Wilcoxon non-parametric tests. The statistical difference between measured parameters in triplicate of both mucus OM and the control treatments was analysed at each time point. The amino acid composition throughout the mucus degradation experiment and the microbial community composition at the end of the mucus degradation were analysed using multivariate ordination from the vegan package in R (v2.6, Oksanen et al., 2022; R Core Team, 2022). Bray-Curtis dissimilarities were calculated and visualised using non-metric multidimensional scaling (NMDS) using the metaMDS function with a stress level cut-off value $<$0.2 (Legendre et al., 1998). The differences between the amino acid composition of experimental treatments (dry-mucus, frozen-mucus and control) were tested using permutational multivariate analysis of variance (PERMANOVA; a non-parametric alternative for the multivariate analysis of variance; Anderson, 2017) using the adonis2 function. Differences in group homogeneities were tested using the function betadisper (Anderson et al., 2006) and ANOVA. The differences in species composition between the treatments were investigated with pairwise beta diversity indices using the function betadiver (Anderson et al., 2006). Results were considered significantly different at $p < 0.05$ and all statistical analyses were done using R version 4.2.2 (R Core Team, 2022).

4.4 Results

4.4.1 Release of nutrients from jellyfish mucus

The cumulative amount of organic and inorganic nutrients released from jellyfish mucus (dry-mucus and frozen-mucus) in microbe-free seawater in 24 hours was up to 3.5 higher and up to 9 times more variable for frozen-mucus than for dry-mucus (Table 4.2). The two forms of mucus showed notable differences regarding the amount of ammonium (1.3 ± 2.7 and 4.5 ± 2.9 µmol gDW^{-1} d^{-1} for dry-mucus and frozen-mucus, respectively) and nitrate (2.5 ± 0.3 and 0.3 ± 0.2 μmol gDW^{-1} d^{-1} for dry-mucus and frozen-mucus, respectively). However, the amount of DIN (3.9 ± 2.3

and 4.8 ± 2.7 µmol gDW^{-1} d^{-1} for dry-mucus and frozen-mucus, respectively) and phosphate (1.7 ± 0.1 and 2.2 ± 1.1 μmol gDW^{-1} d^{-1} for dry-mucus and frozen-mucus, respectively) released were comparable between the two forms of mucus. Overall, the relative amount of amino acids released from the dry-mucus and frozen-mucus compared to the total DFAA pool were similar (Appendix C, Table C.6), although the absolute amount was 2.6 times higher for the frozen-mucus. The most abundant amino acid was glycine, followed by taurine, representing 53.6 ± 8.3 and 8.0 ± 1.0 mol% of the DFAA pool, respectively (Appendix C, Table C.6). In the first hour following the mucus additions in ASW, mucus OM was made of 56 ± 14% of POC and 44 ± 14% of DOC for the dry-mucus while being 56 ± 3% and 44 ± 3% for POC and DOC of the frozen-mucus, respectively. The C:N ratio of the mucus-dissolved organic fractions (i.e. DOC/DON; DON=TDN-DIN) after 24 hours was 7.4 ± 0.6 and 6.0 ± 0.6 for dry-mucus and frozen-mucus, respectively. The comparison of the DOC, TDN and DON released from the dialysis of dry-mucus (1 kDa MWCO membrane) and from the addition of dry-mucus in 0.2-μm filtered ASW showed that 43 ± 35% of the DOC contained in dry-mucus is made of low molecular weight compounds (LMW <1 kDa) whereas roughly all the TDN and DON of the dry-mucus was of LMW (Appendix C, Table C.7).

	Dry-Mucus (µmol gDW^{-1} d^{-1})	**Frozen-Mucus** (µmol gDW^{-1} d^{-1})
NH_4^+	1.3 ± 2.7	4.5 ± 2.9
NO_3^-	2.5 ± 0.3	0.3 ± 0.2
NO_2^-	0.1 ± 0.01	0.04 ± 0.03
PO_4^{3-}	1.7 ± 0.01	2.2 ± 1.1
DIN	3.9 ± 2.3	4.8 ± 2.7
TDN	21.7 ± 6.3	67.6 ± 38.5
DON	17.9 ± 3.9	62.8 ± 35.8
DOC	134.0 ± 39.1	383.6 ± 248.3
DFAA	15.1 ± 2.5	35.9 ± 23.9

TABLE 4.2: Cumulative amount of dissolved nutrients (NH_4^+, NO_3^-, NO_2^-, PO_4^{3-}, DIN, TDN, DON, DOC, DFAA) leached from dry-mucus and frozen-mucus within 24 h. The values are presented as average ± standard deviation (n = 2).

4.4.2 Microbial processing of the mucus DOM pool

The microbial exponential growth phase started after 20h (Figure 4.1, A), reaching a final abundance of 1.3 ± 0.4 10^6 cell mL^{-1} in all incubators, at the end of the experiment (time = 42 hours). After 30 hours of incubation, the PHP peaked at 4.4 ± 0.7 µg C L^{-1} h^{-1} and 1.6 ± 0.2 µg C L^{-1} h^{-1} for the mucus treatments and the

controls, respectively (Figure 4.1, B), before decreasing to 0.9 ± 0.4 µg C L^{-1} h^{-1} for all treatments at the end of the experiment. The microbial growth rate and PHP were significantly different between mucus treatments and the controls at 30h ($F_{(2,6)}$ = 53.8, p<0.001 and F(2,6) = 23.6, p<0.001, respectively; Figure 4.1, A and B)). During the first 5 hours, changes in DOC concentrations differed significantly between the mucus treatments and the controls ($F_{(2,6)}$ = 5.93, p<0.05) with concentrations increasing in the mucus treatments (182.3 ± 104.5 µg C L^{-1}) and decreasing in the control treatments (-125.9 ± 144.4 µg C L^{-1}; Figure 4.1, C). All treatments (mucus and control) showed an increase in DOC concentrations at 30 hours of 8.3 ± 6.2 µg C L^{-1} h^{-1}. All treatments presented a decrease of TDN concentration of -20.1 ± 17.6 µg N L^{-1} during the first 5 hours followed by a similar increase of 21.3 ± 14.8 µg N L^{-1} during the following 5 hours (Figure 4.1, D).

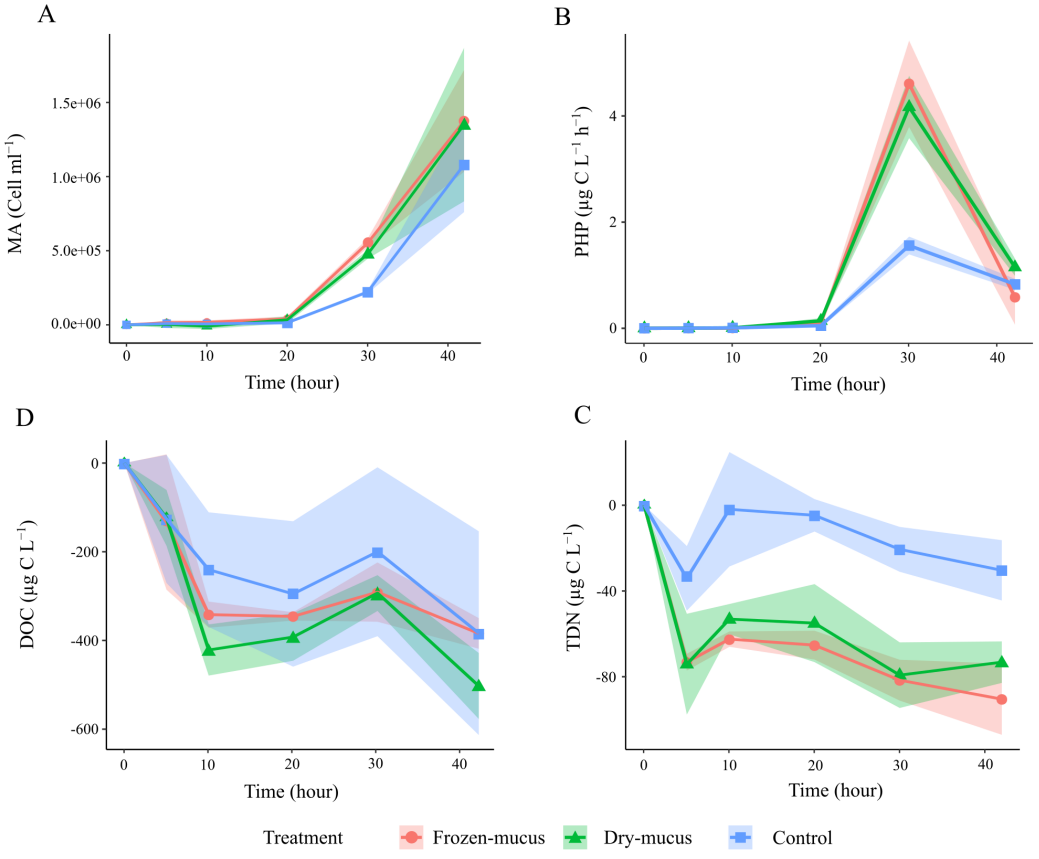

FIGURE 4.1: Change in MA (A), PHP (B), DOC (C) and TDN (D) following the addition of mucus-OM (dry-mucus and frozen-mucus) in incubators filled with ASW:FSW (9:1). Lines represent the means with the coloured area being the standard deviation.

During the experiment, ammonium and phosphate consistently decreased in all treatments (from 3.0 ± 0.2 to 1.8 ± 0.1 µM and from 0.1 to 0.0 µM, respectively; Figure 4.2) while nitrate and nitrite concentration remained overall constant (Appendix C, Figure C.4). At the beginning of the microbial exponential growth phase (between 20 and 30 hours; Figure 4.1, A), the decrease in phosphate concentration in

both mucus treatments (5.0 $\pm$ 0.6 nM h^{-1}) was highly significantly different compared to the control (2.0 $\pm$ 0.5 nM h^{-1}; $F_{(2,6)}$ = 39.7, p<0.001; Figure 4.2, B). At the same time, the decrease in ammonium concentration remained similar between all treatments (frozen-mucus, dry-mucus and control; 31.9 $\pm$ 12.2 nM h^{-1}; Figure 4.2, A).

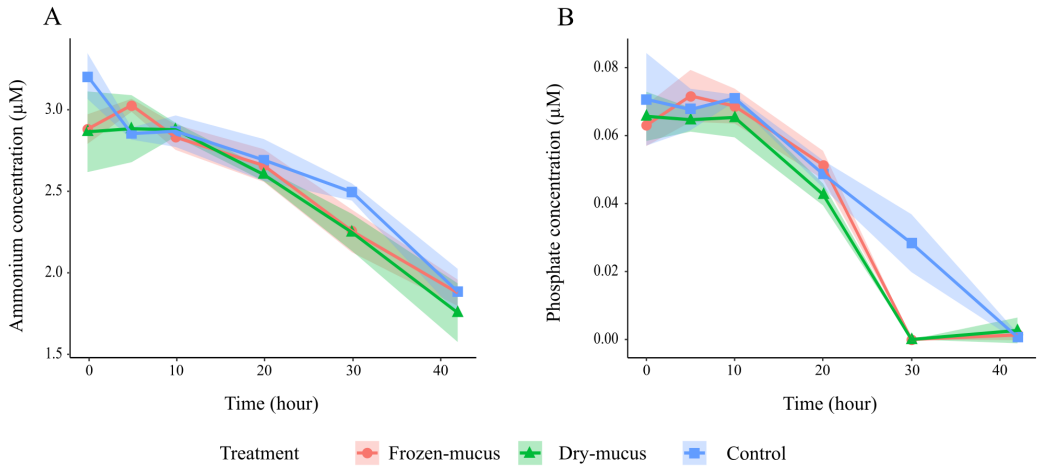

FIGURE 4.2: Ammonium (A) and phosphate (B) concentrations in treatment incubators (dry-mucus, frozen-mucus and control) in filled with ASW:FSW (9:1). Lines represent the means with the coloured area being the standard deviation.

At the beginning of the experiment, the amino acid compositions of the mucus treatments (i.e. frozen-mucus and dry-mucus) were significantly different than the control ($F_{(1,8)}$= 118.9, R^2=0.94, p<0.01), owing mainly to the differences in glycine, taurine, arginine, alanine, lysine and leucine concentrations (Figure 4.3; Appendix C, Figure C.4). The data satisfied the assumption of homogeneity of group dispersion ($F_{(1,7)}$= 0.8, p= 0.38). At the end of the experiment, the treatments presented significantly different amino acid compositions ($F_{(1,8)}$= 118.9, R^2=0.94, p<0.01) while satisfying homogeneity of group dispersion ($F_{(1,7)}$= 3.8, p= 0.09). The main changes in composition towards the end were an increase in alanine, phenylalaline and leucine for dry-mucus, an increase in histamine, glutamic acid and valine for the control, and an increase in aspartic acid for the frozen-mucus treatment (Figure 4.3; Appendix C, Figure C.4). Of all amino acids, glycine had the highest decrease in concentration, reaching zero in all incubators after 20 hours (Appendix C, Figure C.4).

The proportion of POC in the OM was higher for the dry-mucus than in the frozen-mucus (Appendix C, Table C.8). In addition, the presence of undissolved freeze-dried particles was noticed in the dry-mucus leaching incubators (personal observation). Although the use of the pestle and mortar is supposed to homogenise the freeze-dried material into a powder, it also compacted the dried material into dense particles. These "flakes" were resisting dissolution thus artificially increasing the amount of POC observed in the dry-mucus.

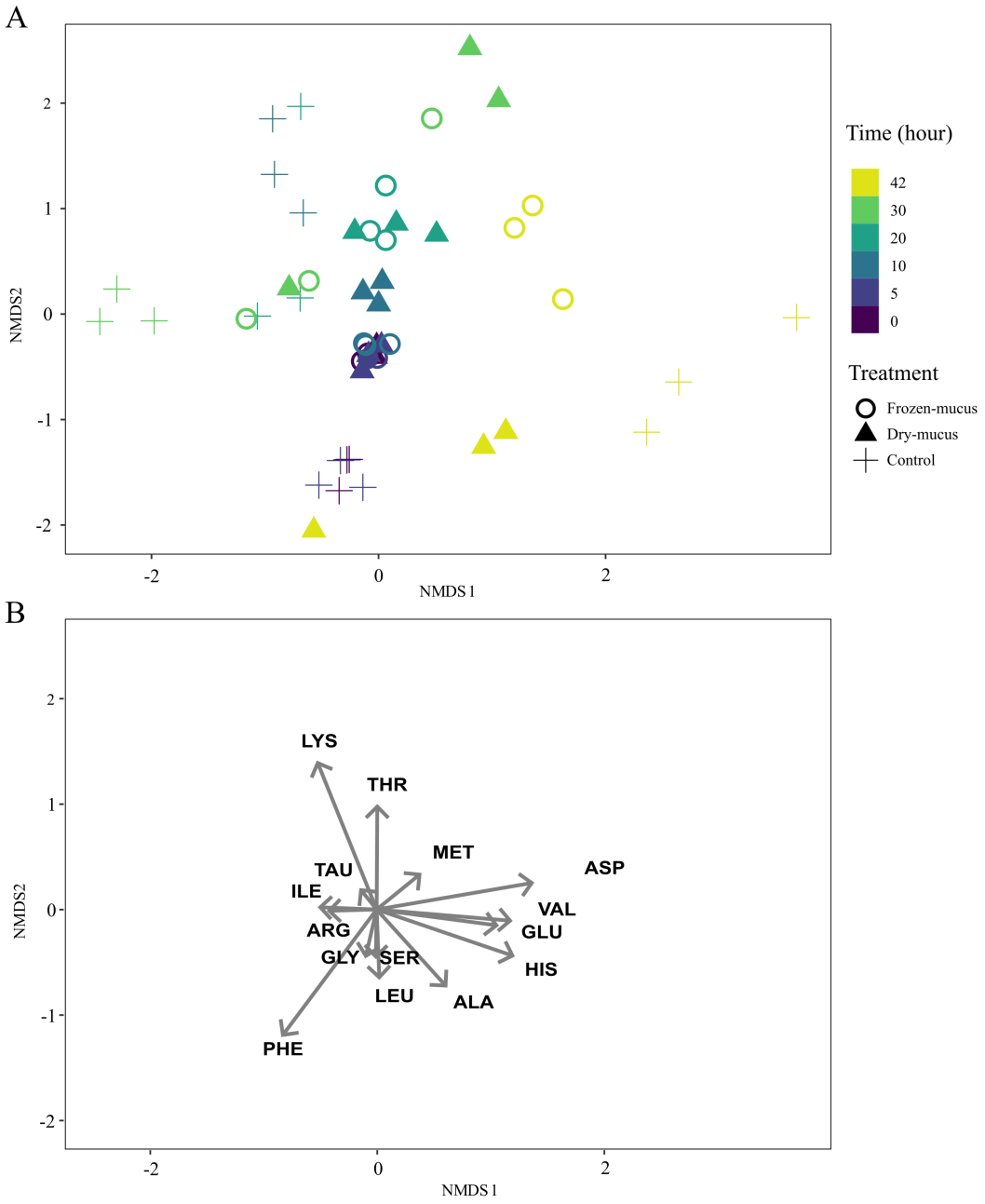

FIGURE 4.3: Results of the Nonmetric multidimensional scaling (NMDS) ordination of amino acid composition of the treatments (dry-mucus, frozen-mucus and control represented by circles, triangles and crosses, respectively) over time (0, 5, 10, 20, 30, 42h represented by the colour gradient from dark to light). The scores for dimensions 1 and 2 are shown in panel A while the contribution of amino acids for dimensions 1 and 2 are shown in panel B, with the length of the arrows indicating the importance of the respective amino acid to the dimension. GLU =glutamic acid, ASP=aspartic acid, SER=serine, HIS=histidine, GLY=glycine, THR=threonine, ARG=arginine, ALA=alanine, TAU=taurine, VAL=valine, MET=methionine, PHE=phenylalanine, ILE=isoleucine, LEU=leucine, LYS=lysine. Glutamine, asparagine and tyrosine are not shown as their contribution to the dimensions were negligible.

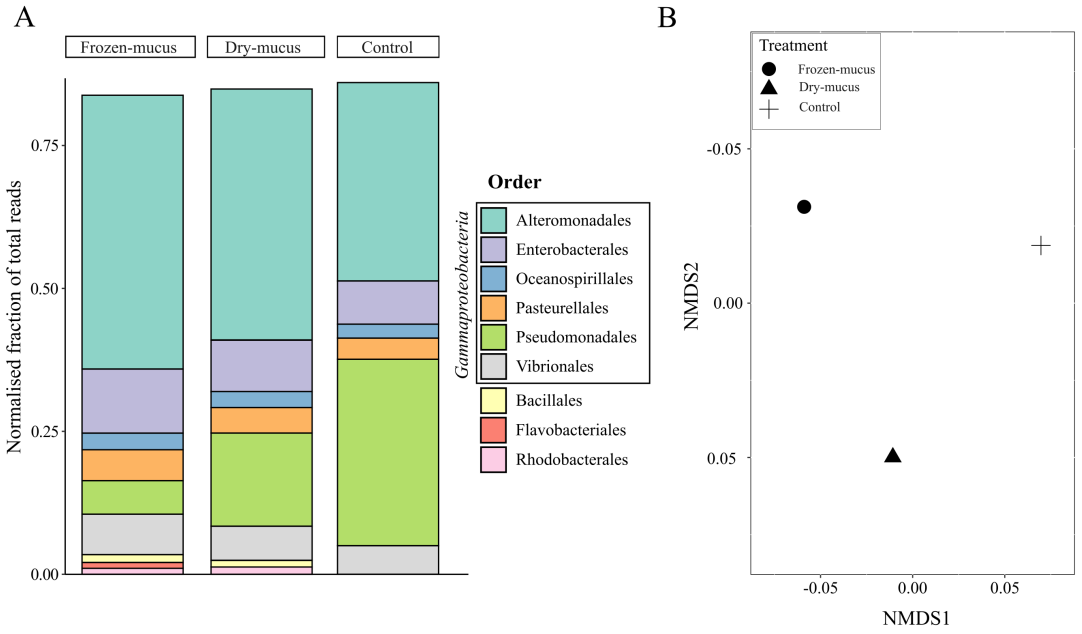

FIGURE 4.4: (A) Relative abundance of the main microbial orders (>1% of total reads abundance) and (B) nonmetric multidimensional scaling (NMDS) ordination of the normalised number of reads assigned to species for the treatments (dry-mucus, frozen-mucus and control).

4.4.3 taxonomic analysis of microbial community

The taxonomic classification of the short metagenomic reads from the three treatments (dry-mucus, frozen-mucus and control) revealed that the microbial communities present at the end of the experimental incubations were mainly composed of Gammaproteobacteria (88 $\pm$ 1%) with Alteromonadales, Pseudomonadales, Enterobacterales and Vibrionales being the dominant orders (Figure 4.4, A). Further, Alteromonadales were more dominant in the mucus treatments (48 and 44% for frozen-mucus and dry-mucus, respectively) compared to the control (34%) in opposition to Pseudomonadales, which were more abundant in the control (30%) than in the mucus treatments (5% and 14% for frozen-mucus and dry-mucus, respectively; Figure 4.4, A). The NMDS ordination (Figure 4.4, B) and the pairwise beta diversity indices (0.04 $\pm$ 0.01; Appendix C, Table C.10) show that the microbial communities of the treatments at the end of the experiment were similarly different from each other.

4.5 Discussion

Jellyfish blooms are increasingly recognized as a large source of OM for the marine ecosystem (Tinta et al., 2021), yet the consequences of the continuous release of their mucus in coastal waters are not well understood. Our series of incubation experiments (i.e., dialysis, leaching and mucus degradation) revealed that jellyfish

mucus is a source of inorganic (ammonium and phosphate) and organic (DOM and POM) nutrients that are utilised by heterotrophic prokaryotes, inducing changes in microbial community composition. Further, the results showed differences between dry- and frozen-mucus material. Combined with the results from the incubation experiments on jellyfish carcasses (Tinta et al., 2020), our results provide a better understanding of the impact of jellyfish blooms in coastal ecosystems.

4.5.1 Comparison between dry- and frozen-mucus

The nutrients released by jellyfish mucus during the leaching experiments suggested that the preservation method of mucus (dry- or frozen) affects the results, and the decision of which to use hence depends on the purpose of the study. Since frozen-mucus showed wide variations in the absolute values (standard deviation up to 9 times higher for frozen-mucus than for dry-mucus; Table 4.2), homogenised dry-mucus is recommended for biochemical applications as it allows more reproducible quantification of the material and thus facilitates replicability. The relative amount of nutrients released from the two types of mucus (dry- and frozen-mucus) was proportionately similar, yet the microbial response was different: after 42 hours the compositions of both the free amino acids and the microbial communities were distinct (Figure 4.3 and Figure 4.3, respectively). The differential microbial consumption of dry- and frozen-mucus indicated that mucus preparation changed the microbial accessibility of the mucus OM. While freezing and thawing mucus do not significantly change its structure (Macierzanka et al., 2019), freeze-drying and subsequent homogenisation of the dry material was expected to increase the surface area of the mucus (fine soluble powder) and thus its accessibility to microbes (Tinta et al., 2020). However, we observed the presence of large particles (insoluble "flakes") that formed following the pestle and mortar crushing, which by increasing the amount of insoluble material, could explain the higher proportion of POC in dry-mucus compared to frozen-mucus. Still, by changing the microbial accessibility of the mucus, the differences in surface-to-volume ratio between the dry- and frozen-mucus might have caused the observed differences in amino acid and microbial community compositions.

An alternative explanation for the different microbial responses following the mucus additions could be that the potential activity of microbes present in the mucus was affected by the preservation method. This explanation is supported by the fact that the dominant bacteria orders observed at the end of incubations (i.e. members of the gammaproteobacteria; Figure 4.4) have been reported to be abundant in the jellyfish mucus microbiome (particularly Alteromonadales and Vibrionales; Tinta et al., 2019). Short-term freezing of microbiomes ($<$ 1 month, -20°C) has been shown to preserve bacterial viability (Takahashi et al., 2019), suggesting that the microbes present in the

mucus during collection might have been viable after defrosting (though freezing can cause multiple freeze-injuries to bacteria; Ray et al., 1973). Our freeze-drying method (i.e. slow freezing via storage at -20°C without a protective agent followed by freeze-drying) followed by fast rehydration in seawater likely severely damaged the microbes in the mucus (Zhang et al., 2020b; Zhao et al., 2005). Hence, while the activity of both mucus microbiomes had likely been altered by the preservation methods, the microbiome of the frozen-mucus might have been playing a role in the microbial response to the mucus addition, which could explain the observed differences between the mucus treatments. We thus recommend the preservation of mucus via short-time freezing over freeze-drying for any usage involving mucus-derived microbes or where minimalizing disturbance to the mucus microbiome is desired.

4.5.2 Characterisation of the mucus material

Jellyfish mucus showed similarities with the carcasses (Tinta et al., 2020) in two ways: (1) the DOM (DOC and TDN) contained in mucus was rapidly released in bacteria-free seawater ($>$ 86% within the first hour) and (2) the same amino acids (glycine and taurine) were dominant in the mucus (53.6 $\pm$ 8.3 and 8.0 $\pm$ 1.0 mol% of the DFAA pool, respectively) and in the carcasses (41.9% and 37.8%, respectively). However, mucus appeared to release less nutrients per gram of DW compared to carcasses (35 $\pm$ 8% of the carcasses nutrients; Appendix C, Table C.9), which is likely due to a high salt content of dry-mucus compared to that of dry jellyfish biomass (Hubot et al., 2022). Mucus also contained a relatively higher proportion of POC than carcasses (56 $\pm$ 14% and 49 $\pm$ 8% of the OM, respectively; Tinta et al. 2020), and mucus-DOM showed a higher percentage of LMW molecules compared to the carcasses-DOM, with approximately 48% of DOC and 100% TDN being in the LMW fraction compared to 6% and 9% for the carcasses, respectively (Tinta et al., 2020). Given that labile LMW DOM can be readily assimilated by bacteria (Berggren et al., 2010), our results suggest that mucus-DOM is more readily available to the microbial community than carcasses-DOM.

The high concentration of glycine and taurine in jellyfish biomass and mucus is likely due to their specific functional roles. Glycine is the most abundant amino acid in jellyfish collagen (Cheng et al., 2017) due to its essential role in triple helix formation in secondary protein structure (Silvipriya et al., 2015). Similarly, glycine is abundant in mucin glycoproteins (Feller et al., 1990) improving the viscoelasticity of the mucus (Ganesan et al., 2020). With respect to taurine, marine invertebrates have high concentrations of this non-protein amino acid in their tissue, where it serves as an osmolyte (increasing tissue osmolarity; Welborn et al., 1995). In mucus, the presence of taurine could also increase its osmolarity allowing the mucus to maintain its level of hydration in seawater and thus its fluidity.

Furthermore, given that the mucus OM is the sum of DOM and POM, our measurements of the C:N ratios of the dry-mucus POM and DOM (3.5 ± 1.0 and 6.7 ± 1.0, respectively; prior microbial degradation) are in accordance with a recent study reporting a C:N ratio of jellyfish dry-mucus of 3.9 ± 0.4 (Hubot et al., 2022). The low C:N ratio of jellyfish dry-mucus reflects its macromolecular content dominated by proteins (80 ± 4%) followed by lipids (14 ± 4%) and carbohydrates (6 ± 3%; Hubot et al., 2022). As proteins are rich in nitrogen (∼ 16%; Jones, 1931), the low C:N ratio of the mucus-POM suggests that the large glycoproteins that mainly constitute the mucus (Bansil et al., 2006) are preferably retained in the particulate fraction. Consequently, the mucus DOM is likely poor in proteins while being enriched in lipids and carbohydrates, as suggested by its high C:N (6.7 ± 1.0) relative to the initial of the dry-mucus (3.9 ± 0.4; Hubot et al., 2022). In comparison, the mucus-DOM from *Chrysaora quinquecirrha* had a C:N = 8.1 ± 6.2 (Condon et al., 2011), supporting that mucus-DOM has a relatively higher C:N ratio compared to jellyfish dry-mucus (3.9 ± 0.4; Hubot et al. 2022). Lastly, the relatively high C:N ratio of mucus-DOM (6.7 ± 1.0) contrasts with the low C:N ratio found for jellyfish carcasses-DOM (3.4 ± 0.1; Tinta et al., 2020) and suggests that mucus-DOM contains a lower proportion of soluble proteins than carcasses-DOM.

4.5.3 Microbial utilisation of mucus

Our results showed that the addition of mucus was quickly followed by high consumption of DOC (Figure 4.1, B), which did not coincide with significant microbial biomass production (Figure 4.1, C). Given that the DOC assimilated by microbes is mainly invested into either respiration or biomass production (del Giorgio et al., 1998), my results suggest that the consumed mucus-DOC is largely channeled towards respiration instead of biomass production. These results are in accordance with previous findings on jellyfish mucus degradation (observed from a 6-h incubation; Condon et al., 2011) showing increased microbial respiration following mucus consumption. However, the low microbial production observed during the first 20 hours of our incubations (<0.3 μg C L^{-1} h^{-1}) was likely due to the microbial community adapting to the new water conditions following the dilution of the NSW (i.e. 9ASW:1NSW), whereas no dilution was performed by (Condon et al., 2011). High respiration can be caused by the maintenance of basic metabolic machinery and the production of extracellular enzymes exerting a high energy demand on microbes and resulting in low growth efficiency (del Giorgio et al., 1998). In addition, the nutrient conditions and the quality of the organic substrate feeding the community can also impact the growth efficiency (Lønborg et al., 2011). Therefore, although the experimental designs were notably different, my results agree with those from (Condon et al., 2011) indicating that mucus-DOM is mainly shunted towards microbial respiration rather than production.

The increase in DOC concentration between 20 h and 30 h of the incubation (8.3 $\pm$ 6.2 μg C L^{-1} h^{-1}) was likely caused by a transfer of carbon from the POM pool to the DOM pool. Degradation of POM is usually due to the action of extracellular enzymes hydrolysing the HMW molecules (Arnosti, 2011) thus creating a transfer of carbon from the POM to the DOM pool, which can then be used by microbes to grow. Therefore, the release of DOC from the POM pool has likely supported microbial growth. Other contributions to the DOC increase could have been from the extracellular enzymes themselves and debris from cell lysis (Carlson et al., 2015).

The highest microbial production reached during the exponential phase (5.0 $\pm$ 0.8 μg C L^{-1} h^{-1} at 30 hours) concurred with the rapid consumption of the phosphate stock during the exponential phase (Figure 4.2, B) and was followed by a drastic reduction in the microbial production rate (Figure 4.1, B), suggesting that the depletion of phosphate led to the decrease of microbial production after 30 h (1.0 $\pm$ 0.4 μg C L^{-1} h^{-1}). Prokaryotes typically have a high phosphorus content (Godwin et al., 2015) and show efficient phosphorus uptake (Vadstein et al., 2003), which accounts for around 60% of the total uptake from aquatic microbial communities (Kirchman, 1994). Therefore, the scarcity of phosphate, the readiest source of phosphorous for marine microbes (Sosa et al., 2019), can limit microbial productivity (Moore et al., 2013) mainly through constraints on RNA production rates (Loladze et al., 2011). Our results showed that the biodegradation of nitrogen-rich mucus can lead to a higher decrease in environmental phosphate concentration, which could ultimately lead to a phosphorous limitation. However, the total depletion of the phosphate stock was further caused by the low phosphate concentration at the start of the incubations ($<$0.1 μM), which was characteristic of the surface waters of the Gulf of Trieste (Lazzari et al., 2016). Therefore, the initial nutrient limitations of the surface water might influence the microbial growth efficiency of the microbes consuming jellyfish mucus. Nevertheless, given that the availability of phosphorus has major implications for the quantitative transfer of carbon in microbial food webs (Kragh et al., 2008), the increased consumption of phosphate caused by the degradation of jellyfish mucus might ultimately limit marine microbial production and thus the transfer of OM to higher trophic levels.

4.5.4 Microbial community composition

The microbial community present at the end of the experiment was dominated by Gammaproteobacteria (mainly Alteromonadales, Pseudomonadales, Enterobacterales and Vibrionales; Figure 4.4, A) which contrasted with the initial community dominated by Alphaproteobacteria as typical of the Gulf of Trieste and of coastal assemblages (Kramar et al., 2019; Tinta et al., 2012). This shift from an Alphaproteobacteria-dominated community to a Gammaproteobacteria-dominated

community confirms the results of previous studies on the degradation of mucus and jellyfish biomass about the existence of an opportunistic microbial consortium growing well on jellyfish organic matter (Tinta et al., 2020 and Condon et al., 2010, respectively). Besides being present in natural marine microbial communities, this Gammaproteobacteria consortium is also found in high proportion in the mucus (particularly Alteromonadales and Vibrionales; Tinta et al. (2019)), which suggests that the mucus microbiome could further support the microbial community shift. Generally, Gammaproteobacteria are fast-growing opportunistic bacteria adapted to eutrophic environments whereas Alphaproteobacteria are adapted to oligotrophic waters (Pinhassi et al., 2003). Within Gammaproteobacteria, Alteromonadales are particularly known for their ability to utilize labile DOC and for outcompeting other bacteria under high nutrient concentrations (Pedler et al., 2014; Sarmento et al., 2012). Therefore, the opportunistic behaviour of Alteromonadales explains their dominant presence in both mucus treatments compared to the control (Figure 4.4). In addition, Alteromonadales, Vibrionales and Rhodobacterales have been shown to outcompete other bacterial competitors and become highly dominant during the senescence of a jellyfish bloom (Kramar et al., 2018) likely due to the release of labile organic matter from the carcasses (Tinta et al., 2020). Overall, through the release of OM (via mucus and carcasses) and the inoculation of their associated microbiome, jellyfish blooms appear to favour a Gammaproteobacteria-dominated microbial community.

4.5.5 Conclusion

Jellyfish blooms can reach high densities in coastal areas (Lucas et al., 2014b) and incorporate large amounts of OM into jellyfish biomass that can ultimately become accessible to the environment and microbial degradation through two main routes, mucus and body degradation (Figure 4.5). Similarly to jellyfish carcasses, the mucus releases organic and inorganic compounds (including POC/DOC, glycine/taurine, ammonium and phosphate; Figure 4.5) that can quickly be utilised by a microbial consortium dominated by Gammaproteobacteria (mainly Alteromonadales and Vibrionales) inducing the production of microbial biomass. However, previous studies suggest that the growth efficiency of microbes utilising mucus-DOM (30%; Condon et al. (2011)) is lower than the growth efficiency of microbes utilising carcasses DOM ($65 \pm 27\%$; Tinta et al., 2020). These difference in growth suggests that carcasses-DOM is contributing more to the microbial loop than mucus-DOM. Lastly, regardless of whether the OM originates from the mucus or the carcasses, the high nitrogen content of jellyfish material might drive the ecosystem towards phosphorous limitation, preventing an efficient transfer of biomass to higher trophic levels via the microbial loop.

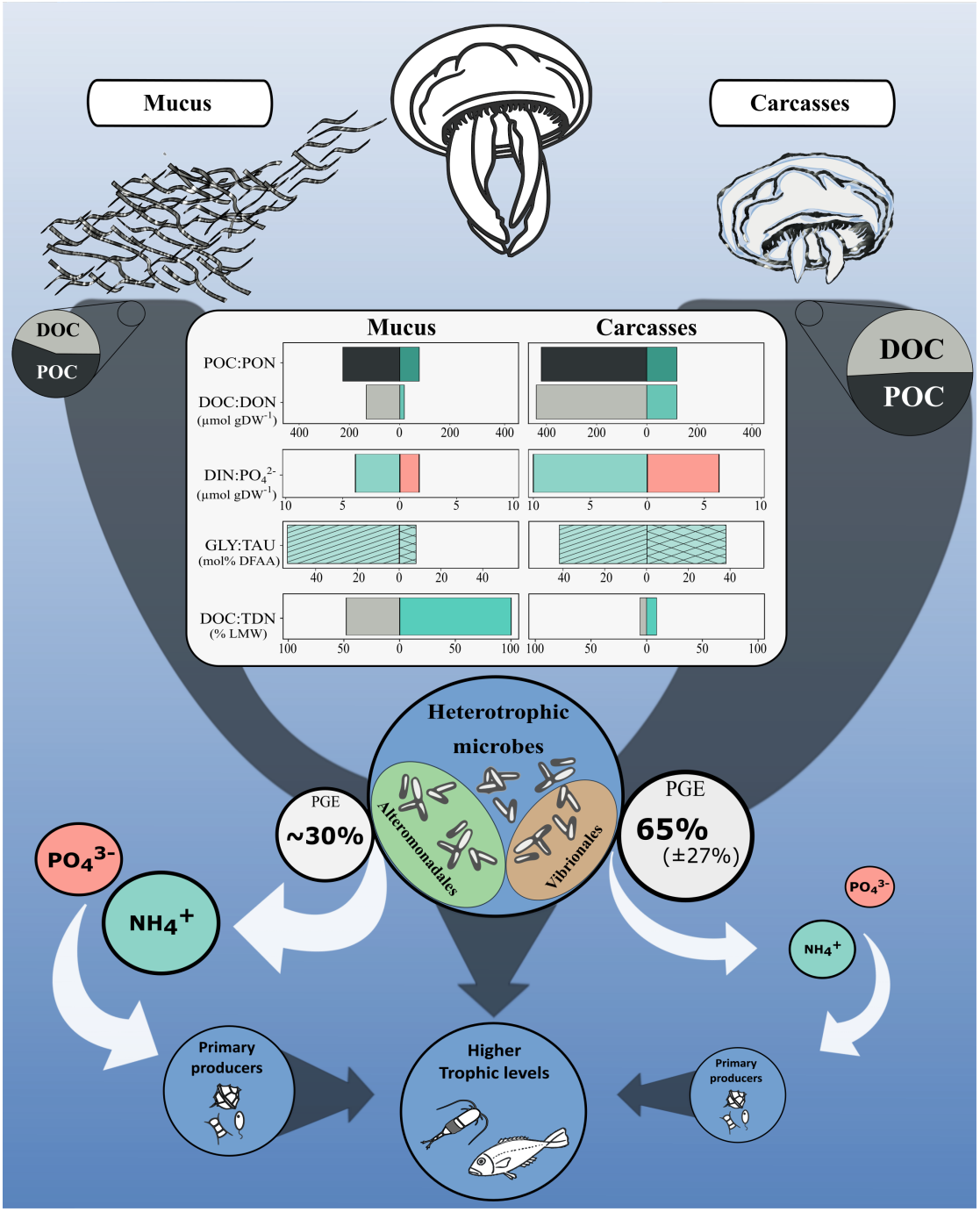

FIGURE 4.5: Conceptual diagram of the impact of jellyfish mucus and body microbial degradation on coastal marine ecosystems. The central table compares nutrients (organic and inorganic) released by a gram of dry weight (DW). POC= particulate organic carbon. PON= particulate organic nitrogen. DOC=dissolved organic carbon. DON= dissolved organic nitrogen. DIN=dissolved inorganic nitrogen. GLY= glycine. TAU=taurine. DFAA= dissolved free amino acid. TDN= total dissolved nitrogen. LMW= low molecular weight. PGE = prokaryotic growth efficiency. Jellyfish body data is from Tinta et al. (2020). Mucus PGE is from Condon et al. (2011).

Chapter 5

Discussion

I will conclude this thesis by summarising the key research findings in relation to the research aims, discussing their value and assessing the contribution they bring to the field. In this chapter, I will also review the limitations of the study and propose directions for future research.

5.1 Thesis summary

The overall objective of this thesis was to improve our understanding of the role of jellyfish in nutrient cycling and their interactions with microorganisms in order to better constrain the consequences of jellyfish blooms for marine ecosystem productivity.

The physiological flexibility and unique life history of jellyfish allow them to have complex effects on large-scale processes such as biogeochemical cycles and the marine food chain (chapter 1). Although a global increase in jellyfish abundance is still not clear, the increasing magnitude and frequency of jellyfish blooms observed in several coastal areas (e.g. Benguela ecosystem and sea of Japan; Brotz et al., 2012) is expected to impact nutrient cycling, carbon export and ecosystem productivity. To efficiently assess these impacts, a clear understanding of the effects of jellyfish blooms in a variety of ecosystems is needed. Yet, little research has focused on the fate and composition of the mucus together with the interactions between jellyfish and marine microbes. More data on the role of jellyfish in marine biogeochemical cycles will allow the construction of better ecosystem models, which can further support ecosystem-based management to better deal with jellyfish blooms and their negative impacts on human society.

The nutrients released by specimens of four jellyfish species incubated in artificial seawater (chapter 2) provided evidence that microbes living in association with

jellyfish thrive by oxidizing the readily available ammonia excreted by their host to nitrite and nitrate (i.e. up to one-third of the excreted ammonium). These results suggest that the jellyfish-associated release of nitrogen can locally provide more than 100% of the nitrogen required for primary production. I hence revealed a so far overlooked pathway when assessing pelagic nitrification rates that might be of particular relevance in nitrogen-depleted surface waters and at high jellyfish population densities.

To characterise the biochemical composition of jellyfish mucus, I analysed the macromolecular (proteins, lipids and carbohydrates) and elemental (carbon and nitrogen) composition of both mucus and body from five jellyfish species (chapter 3). My results revealed that the relative contribution of the different macromolecules and elements in the jellyfish body and mucus were similar across all studied species. This result highlighted the biochemical similarity between the jellyfish body and mucus and provided convenient and valuable ratios to support the integration of jellyfish into trophic and biogeochemical models. In the context of the observed trends of jellyfish abundance increase in many coastal areas (Brotz et al., 2012), it is increasingly important to include jellyfish in energy flux models and ecosystem studies in order to better manage the consequences of future blooms.

Finally, the incubation of jellyfish mucus in 0.2 μm-filtered aged-seawater and natural seawater revealed that mucus can be a direct source of organic and inorganic nutrients to coastal waters and be quickly utilised by microbes albeit a relatively low microbial biomass production. The changes in the taxonomical composition of the ambient microbial community were typical of organic matter utilisation, with an Alphaproteobacteria-dominated community replaced by the fast-growing opportunistic Gammaproteobacteria-dominated community. My results also pointed out that the degradation of nitrogen-rich jellyfish mucus can increase the consumption of phosphate relative to ammonium and eventually shift the ecosystem towards phosphorous limitation, which would restrict marine microbial production and ultimately the transfer of OM to higher trophic levels.

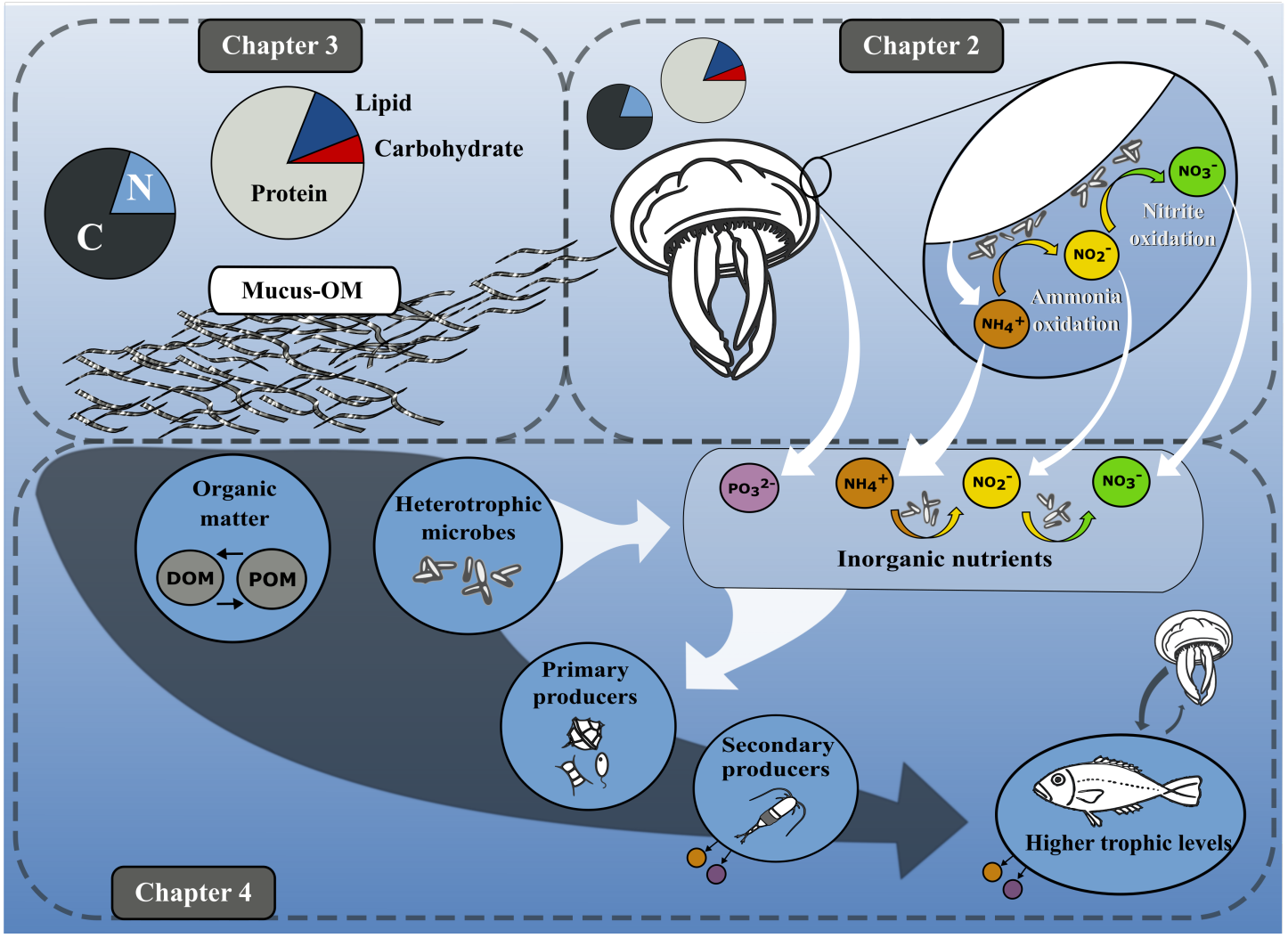

FIGURE 5.1: Conceptual schematic of the role of jellyfish and their interaction with microbes in nutrient cycles and ecosystem productivity showing: nitrification associated with pelagic jellyfish (Chapter 2), the elemental and macromolecular composition of jellyfish mucus (Chapter 3) and the microbial degradation of jellyfish mucus (Chapter 4). The flows of organic and inorganic matter are shown by grey and white arrows, respectively. Colours indicate ammonium (NH_4^+, orange), nitrite (NO_2^-, yellow), nitrate (NO_3^-, green) and phosphate (PO_4^-, purple). Coloured arrows represent ammonium-oxidation (orange-to-yellow) and nitrite-oxidation (yellow-to-green). Components linked to small coloured circles release inorganic nutrients of the same colour. The large circle zooms in on the jellyfish epithelium.

5.2 Implications

5.2.1 The marine nitrogen cycle

The marine nitrogen cycle is considered the most complex of all biogeochemical cycles in the ocean (Gruber, 2008). The study of the nitrogen cycle in combination with the complexity of jellyfish blooms (e.g. complex physiological and ecological behaviours and high spatio-temporal variability) is a challenging task that requires the use of complex mechanistic spatial-temporal models. This thesis has provided data that are particularly relevant for the investigation of the role of jellyfish blooms in the nitrogen cycle such as the allometric equations of nitrogen release, the C/N ratios of jellyfish organic matter (mucus and body) and the release and consumption of nitrogen compounds following the excretion of jellyfish mucus. Given that nitrogen is a limiting element for biological productivity, the effects of jellyfish blooms on the nitrogen cycle can exert a significant influence on other marine cycles such as the carbon cycle, thus affecting Earth's climate (Pajares et al., 2019).

The high protein content of jellyfish biomass and mucus (81 $\pm$ 4 % of macromolecules), reflected in their low C:N ratio (3.8; chapter 2; Hubot et al., 2022), shows that jellyfish blooms require large amounts of nitrogen to grow and function. Given that jellyfish feed mainly on organisms with lower C:N ratios (e.g.: 4.8 - 6.2 for crustacean zooplankton; Pitt et al., 2013), jellyfish blooms are effectively storing nitrogen into gelatinous biomass. Some of that organic nitrogen can then be transferred to higher trophic levels via predation from a large range of organisms, such as fish, birds and turtles (Hays et al., 2018), eventually supporting ecosystem productivity (see section 1.3.1, the case of the northern Benguela ecosystem). Alternatively, the organic nitrogen contained in jellyfish biomass can be released back to the environment via the excretion of both ammonium (chapter 2; Hubot et al., 2021) and mucus (chapter 3 and chapter 4; Hubot et al., 2022) and ultimately via the degradation of sinking carcasses (Tinta et al., 2020). Therefore, I propose that jellyfish blooms can be regarded as a "nitrogen buffer", storing nitrogen in their biomass when the food is abundant and releasing it back to the environment when food is scarce.

My findings show that the association of nitrifying microorganisms with jellyfish is ubiquitous in large pelagic jellyfish. Besides revealing a new pathway for pelagic nitrification in surface waters, these findings question the prevalence of these associations in marine metazoans. Previously, nitrifiers have been identified in association with benthic invertebrates such as sponges (Subina et al., 2018), corals (Hoffmann et al., 2009), zoanthids (Sun et al., 2014), bivalves (Welsh et al., 2004) and ascidians (Martínez-García et al., 2008). Frequent association between nitrifiers and pelagic invertebrates would add evidence to support that nitrification is an important component of pelagic nitrogen cycling of the sunlit ocean (Clark et al., 2022) and

would further confirm the inappropriate use of the f-ratio as a measure of the efficiency of the biological carbon pump (Yool et al., 2007). Still, the identity of the microbe(s) responsible for these nitrification rates is yet to be revealed.

5.2.2 The marine carbon cycle and carbon export

The marine carbon cycle plays a critical role in Earth's climate due to the ability of the ocean to absorb carbon dioxide from the atmosphere (Heinze, 2014). At the core of the cycle are interconversions of inorganic and organic carbon forms, which lead to major ecosystem services. Jellyfish blooms convert large amounts of organic carbon from primary producers into gelatinous biomass (Condon et al., 2011). Based on current research, the sinking of carcasses is probably the most important contribution of jellyfish blooms to ocean carbon export production. However, many aspects concerning the contribution of jellyfish mucus and carcasses to carbon export still require deeper investigations. The use of ecosystem modelling offers the most promising approach to clarify these contributions.

My results suggest that the nutrients excreted by jellyfish blooms can locally and episodically support surface primary production in coastal ecosystems via dark carbon fixation and phytoplankton production (via nitrification and photosynthesis, respectively; chapter 2; Hubot et al., 2021). Although dark carbon fixation is small compared to autotrophic phytoplankton production, it represents newly synthesized organic carbon available for the marine food web and thus needs to be included in global oceanic primary production estimates (Baltar et al., 2019). Further, by locally providing more than 100% of the nitrogen required for primary production, large jellyfish blooms can increase organic carbon production in coastal areas (chapter 2; Hubot et al., 2021). Therefore, jellyfish blooms have the potential to increase carbon export through their role in primary production. However, this hypothesis still requires investigation.

However, given the patchiness and sporadic appearance of jellyfish blooms and that primary production varies over time, the "mismatch" between the primary production and nutrient release by a jellyfish bloom can be substantial. In addition, our estimates are based on jellyfish blooms at the peak of their abundance. Thus, the comparison between our estimates of nitrogen release during jellyfish blooms and the mean daily primary production of the ecosystem aims to estimate the maximum effect that a jellyfish bloom could have in this region over a limited period of time. To estimate the overall impact on the ecosystem productivity throughout a year, high-resolution time series of jellyfish distribution and densities would be needed (see section 5.3: Limitations and future directions).

My results on the prokaryote growth efficiency of microbial communities utilising jellyfish mucus suggest little heterotrophic biomass production following the consumption of jellyfish mucus. As previously described (Condon et al., 2011), the consumption of jellyfish mucus seems to shunt organic matter toward prokaryotic respiration rather than production, significantly reducing the prokaryote growth efficiency of the ambient microbial community. On seasonal time scales, jellyfish blooms may impact coastal productivity by shunting carbon flows away from higher trophic levels via the production of mucus (Condon et al., 2011). Still, more data are needed to clarify the fate of jellyfish mucus in the environment and to assess its contribution to carbon export.

5.2.3 Marine ecosystem productivity & modelling

While jellyfish have been increasingly recognised as an important component of marine systems (Wright et al., 2021), most current marine ecosystem models still ignore or oversimplify their role in the environment (Lamb et al., 2019). A general misunderstanding of the ecological importance of jellyfish blooms in marine systems challenges their incorporation into models. My thesis has generated data that are particularly suitable for the integration of jellyfish in marine ecosystem models such as the allometric equations of inorganic nutrient release, the elemental and macromolecular ratios with the associated energy content and data on the release and consumption of nutrients linked to mucus excretion and degradation.

Recent studies have shifted the traditional view of jellyfish as trophic dead-ends by revealing their presence in a wide range of organism diets (Hays et al., 2018), therefore highlighting their role in fuelling energy towards higher trophic levels. The results of my thesis further support the importance of jellyfish in ecosystem productivity, but rather through their role in nutrient cycling and interactions with marine microbes. By supporting net marine primary productivity, jellyfish blooms indirectly support the food chain through bottom-up effects (West et al., 2009). Overall, the presence of large jellyfish blooms generates complex trophic interactions (Stoltenberg et al., 2021) which require the use of ecosystem modelling to efficiently assess their overall impact on ecosystem productivity.

Based on jellyfish density distribution, my results can be used to model flows of nutrients and energy through the ecosystem. While ecological modelling provides arguably the best approach to assess the role of jellyfish in large ecosystems (Pauly et al., 2009), the reliability of models depends on the data used to parametrise and design them (Zhu et al., 2015). To date, quantitative data on jellyfish density distribution and biology are often missing, particularly for populations in the southern hemisphere and open ocean (Lucas et al., 2014b, thus limiting the inclusion of jellyfish into models. In the context of increasing jellyfish blooms and coastal

ecosystem degradation, there is an urgent need for better management of coastal regions. By highlighting the important role of jellyfish blooms in ecosystem productivity and by providing useful data for their inclusion in ecosystem models, my thesis aims to support future ecosystem-based management decisions.

5.3 Limitations and future directions

The empirical findings and conceptual theories presented in my thesis are not free from limitations inherent to the research process. Yet, these findings and limitations can pave the way to future research paths deserving further investigation.

Based on the best data available on jellyfish blooms density distribution from acoustic surveys, I have estimated the nitrogen release associated with two large jellyfish blooms (chapter 2; Hubot et al., 2021). However, these density distributions only quantify the blooms at the specific time of the survey and therefore my nitrogen release estimates are instantaneous and do not allow the calculation of nitrogen release over a seasonal cycle. Given the high spatio-temporal variations of jellyfish blooms, my results highlight the need for increased monitoring of jellyfish blooms, particularly using high-resolution approaches such as acoustic surveys. Besides being time- and cost-effective, acoustic surveys offer a non-invasive method to acquire high-quality data on jellyfish blooms (Alvarez Colombo et al., 2009). In order to fully cover the diversity and distribution of jellyfish species, acoustic surveys should be combined with other approaches such as remote sensing (Copernicus satellites), citizen science (Jellywatch programs), molecular genetic tools (Edelist et al., 2022) and advanced video methods, including onboard/*in-situ* camera systems (Hoving et al., 2019) and drones (Hamel et al., 2021). As monitoring the abundance and distribution of jellyfish is essential to assess their contribution to ecosystem processes (Bastian et al., 2014), future efforts should aim at combining survey data with oceanographic models and advanced machine learning techniques in order to fully assess and predict the consequences of jellyfish blooms in coastal ecosystems.

Insufficient time and funding have limited the full use of the metagenomic sequencing data generated from the mucus degradation experiment (chapter 4). While using metagenomic data for species abundance estimation has the advantage of detecting less abundant taxa compared to the more traditional method of 16S rRNA gene amplicon sequencing (Durazzi et al., 2021; Kibegwa et al., 2020), more analyses can be performed on that data (e.g. functional profiling, comparative metagenomics and genome-resolved metagenomics; Scholz et al., 2012). Adding functional profiling to the analysis would have increased the implications of the study. Given that such analysis was exceeding the goals of my thesis, it was postponed until after the submission of my thesis. The analysis of the metabolic pathways and functional

differences between the mucus degradation experiment treatments will be added to Chapter 4 and will constitute a manuscript for publication.

Although I provided clear evidence of nitrification associated with large pelagic jellyfish (chapter 2; Hubot et al., 2021), no molecular data were provided to further support my results. For example, using qPCR to quantify the abundance of genes involved in the two nitrification processes such as amoA and nxrAB, would have greatly improved the robustness of my discovery. Additionally, using techniques such as 16S rRNA gene amplicon sequencing, Card-FISH and stable isotope probing could have highlighted the presence and identity of the nitrifiers associated with the jellyfish. Nevertheless, DNA samples were collected from tissue samples after the experimental incubation for further investigation using molecular tools. Surprisingly, preliminary analysis of these samples has not successfully shown the presence of the amoA gene nor any abundant known nitrifying microbes in any jellyfish microbiome. I thus hypothesised that the observed nitrification rates associated with jellyfish were due to a microorganism that had not yet been identified as a nitrifier, which calls for deeper investigation.

The enigmatic endosymbiotic Mycoplasma

A preliminary analysis of the 16S rRNA genes present on the jellyfish *Aurelia aurita* microbiome following the observation of nitrification (chapter 2; Hubot et al., 2021) has revealed that a sequence closely related to a mycoplasma bacterium largely dominates the microbial community of the jellyfish (>95% of all sequences). This observation is in agreement with a study revealing the presence of a novel mycoplasma strain associated with the medusa of *A. aurita* (Weiland-Bräuer et al., 2015). The authors suggested that the mycoplasma bacteria are endosymbiotic, thus living inside the medusa cells.

Mycoplasma are amongst the smallest bacteria known, both in terms of cell and genome size (approximatively 300- to 800-nm range and 1 Mbp; Rasmussen et al., 2021; Rideau et al., 2022). They are obligate parasites that rely on their hosts for the production of a large array of essential metabolites (Arfi et al., 2021). Still, despite their small genomes, mycoplasma displays a vast variety of phenotypic characteristics like adaptations to their host, pathogenesis, mobility (Dandekar et al., 2002) and high metabolic plasticity (Momynaliev et al., 2001). I thus hypothesise that the endosymbiotic mycoplasma could be responsible for the high nitrification rates observed in Chapter 2.

To investigate my hypothesis, I successfully participated in a NEOF pilot competition to use the PacBio long-read sequencing platform with the aim of assembling and curating the first metagenome-assembled genome of the novel mycoplasma

endosymbiotic to jellyfish and searching the jellyfish microbiome for genes homologous to the amoA and nxrAB. In addition, I received a DAAD short research grant to collaborate with the authors of the mycoplasma discovery. Further, a subset of my jellyfish microbiome sample collection was sent to Germany for 16S and 18S rRNA gene sequencing. The combined analysis of both metataxonomic and metagenomic sequencing data from my unique sample set of three species of jellyfish (i.e. *A. aurita*, *C. fulgida* and *C. pacifica*) will allow us to fully investigate the presence of the jellyfish associated mycoplasma while allowing the further exploration of the diversity of jellyfish microbiomes. In the future, the results of these analyses will be presented in a novel high-quality scientific publication.

5.4 Conclusion

Throughout my thesis, I have highlighted the key role of jellyfish in the marine nitrogen cycle. In particular, I have shown evidence of nitrification associated with large pelagic jellyfish, I have demonstrated how the high protein and nitrogen content of their body is reflected in their mucus, and I have provided detailed data on the microbial degradation of jellyfish mucus. Further, I have explored some of the consequences of jellyfish blooms on carbon export and ecosystem productivity. Finally, I have stressed the importance of using modern tools such as ecosystem modelling, acoustic surveys and molecular techniques to improve our understanding of jellyfish and lead to better management decisions. Overall, my thesis supports a more nuanced picture of the role of jellyfish in the marine ecosystem contrasting with the conventional nuisance view.

Appendix A

Supplementary Material - Chapter 2

A.1 Absolute concentrations of Jellyfish treatment

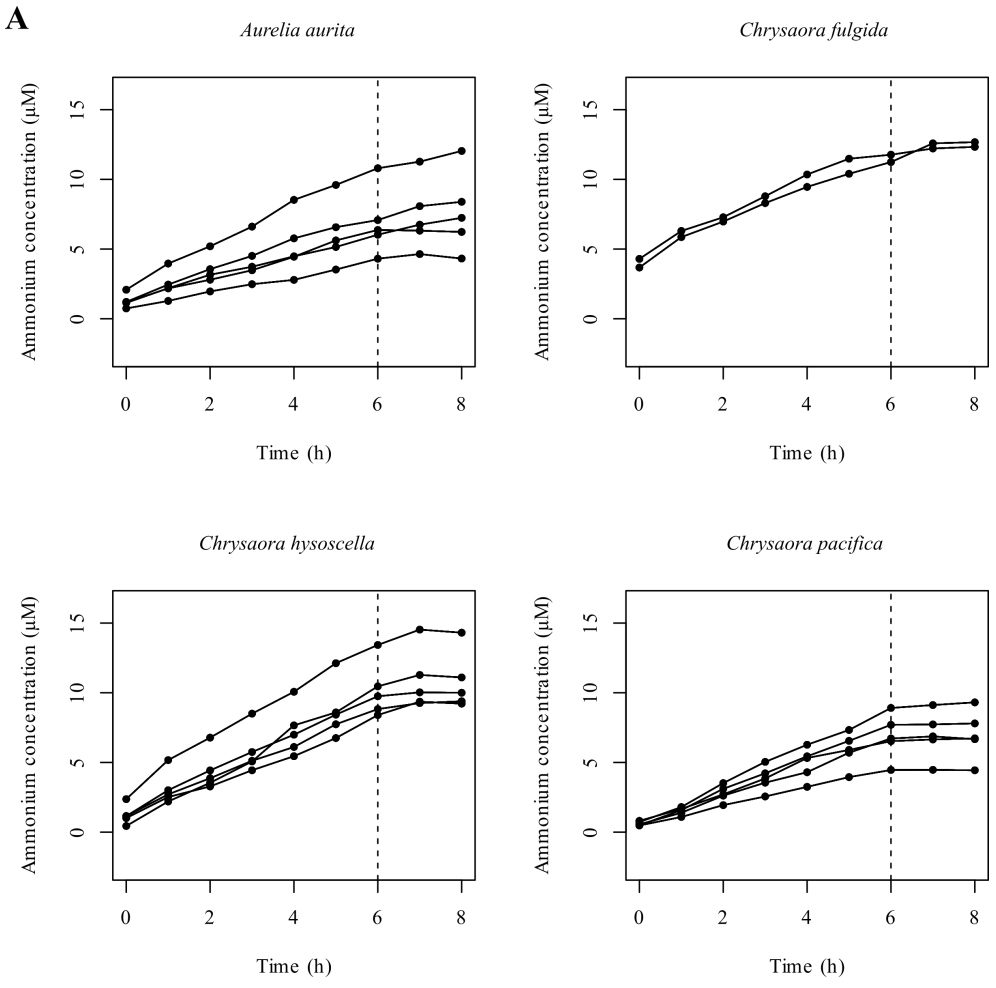

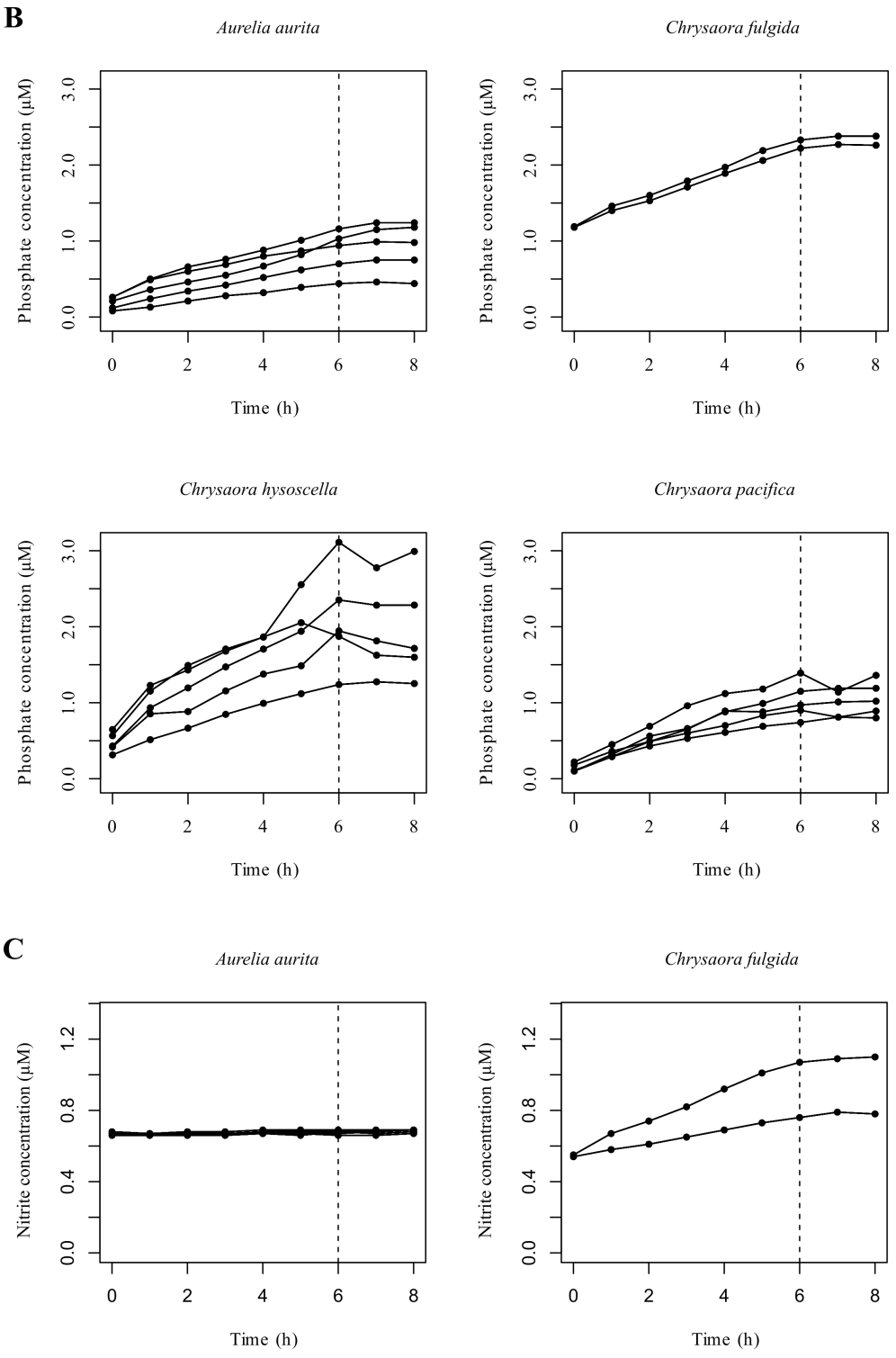
B
Aurelia aurita
Chrysaora fulgida
Chrysaora hysoscella
Chrysaora pacifica
Phosphate concentration (µM)
Time (h)
C
Aurelia aurita
Chrysaora fulgida
Nitrite concentration (µM)
Time (h)

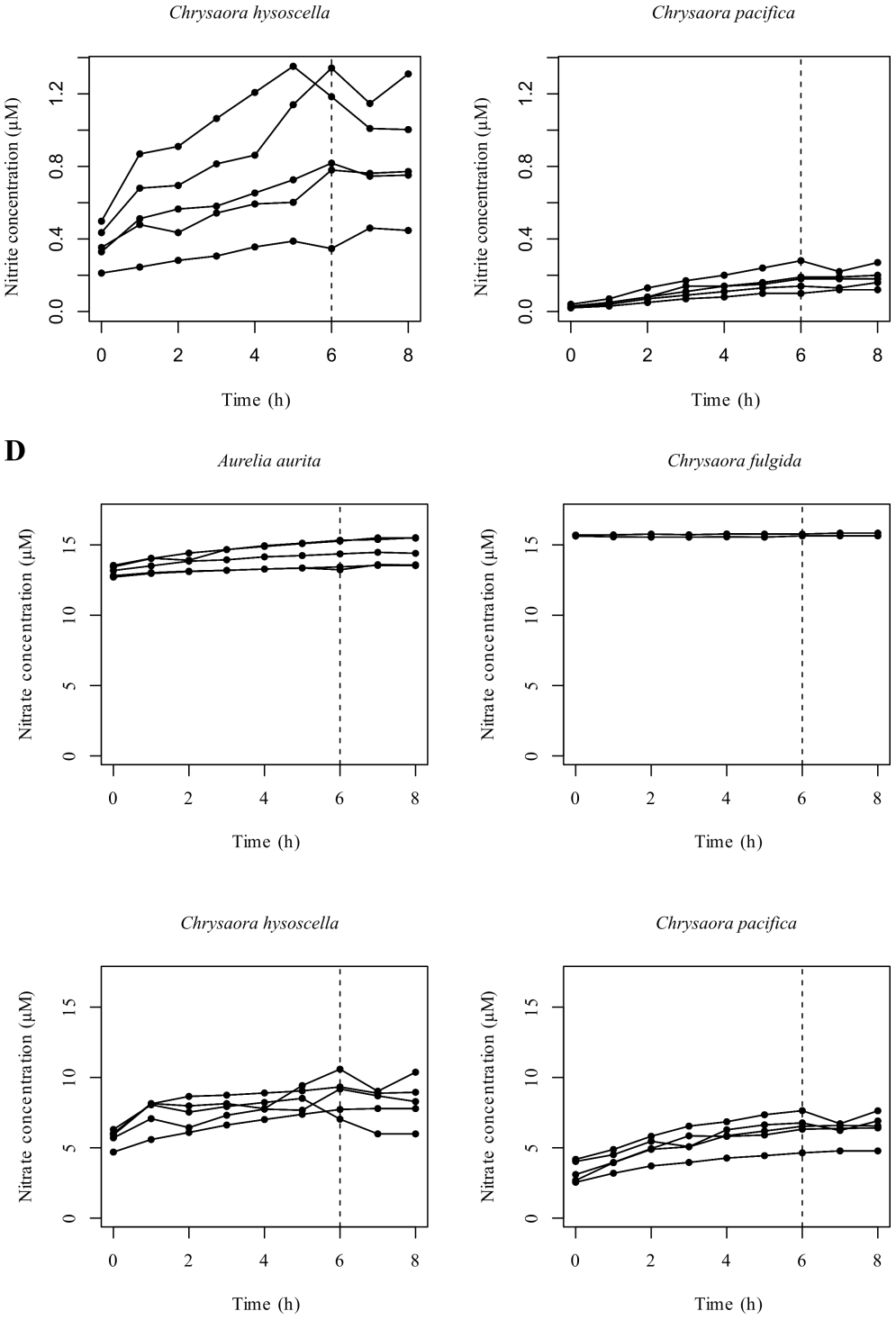

FIGURE A.1: Measured concentrations of ammonium (A), phosphate (B), nitrite (C) and nitrate (D) of the Jellyfish treatment incubators for the jellyfish species *A. aurita*, *C. fulgida*, *C. hysoscella* and *C. pacifica*. The vertical dashed line corresponds with the time when the jellyfish were removed from the incubators (6 h).

A.2 Control

A.2.1 Jellyfish-Control

In 8 cases out of 16, the nutrient concentrations of the Jellyfish treatment, which consists of artificial seawater only, showed a small but significant change in concentration with time 5 (Figure A.2 and Table A.1). An increase in concentration suggests that contamination and/or production by microorganisms occurred in the incubators. On the other hand, a decrease in concentration suggests absorption and/or consumption in the incubator. Any processes responsible for the changes in concentration in the Jellyfish-Control treatment were expected to also happen in the Jellyfish treatment incubators. Therefore, the concentrations of the Jellyfish treatment were corrected by subtracting them from the Jellyfish-Control changes in concentration. The corrections did not change the observed results.

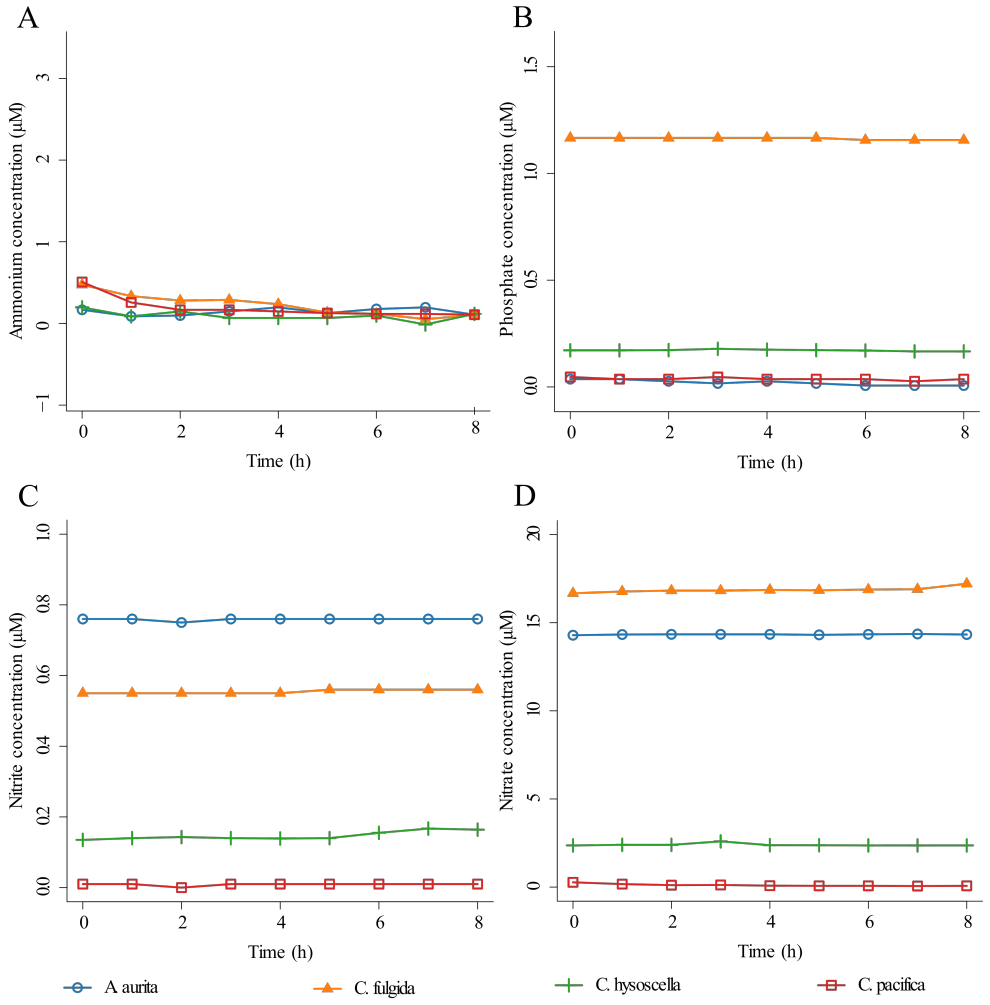

FIGURE A.2: Ammonium (A), phosphate (B), nitrite (C) and nitrate (D) concentrations of the Jellyfish-Control treatment of *A. aurita* (blue), *C. hysoscella* (green), *C. pacifica* (red) and *C. fulgida* (orange).

Ammonium

Species	Intercept	Slope	R^2	p
A. aurita	-0.02	0.00	-0.07	0.52
C. hysoscella	-0.01	-0.01	0.21	0.12
C. pacifica	0.19	-0.04	0.54	*
C. fulgida	-2.31	-0.05	0.89	**

Phosphate

Species	Intercept	Slope	R^2	p
A. aurita	-0.03	-0.0042	0.8492	***
C. hysoscella	-0.0236	-0.0013	0.2791	0.083
C. pacifica	0.1081	-0.0007	0.205	0.124
C. fulgida	1.1027	-0.0015	0.6286	*

Nitrite

Species	Intercept	Slope	R^2	p
A. aurita	0.76	0.0003	-0.06	0.48
C. hysoscella	0.13	0.0037	0.68	**
C. pacifica	0.01	0.0003	-0.06	0.48
C. fulgida	0.55	0.0017	0.71	**

Nitrate

Species	Intercept	Slope	R^2	p
A. aurita	14.32	0	0.14	0.18
C. hysoscella	2.43	-0.01	-0.08	0.54
C. pacifica	0.2	-0.02	0.67	**
C. fulgida	16.68	0.04	0.66	*

TABLE A.1: Summary table of linear regression results from the Jellyfish-Control treatment. The use of *, **, and *** denotes levels of statistical significance (p=0.05, 0.01, and 0.001 respectively).

A.2.2 Mucus-Control

The Mucus-Control treatment consisted of artificial seawater spiked every hour during the first 6 hours with different amounts of ammonium (Figure A.3, A; Table A.2). The phosphate, nitrite and nitrate concentrations did not significantly change with time, except for the phosphate and nitrite of *A. aurita* and the nitrate of *C. hysoscella* (Table A.3, B). In these 3 cases, the concentrations of the Mucus treatment

were corrected by subtracting them from the corresponding Mucus-Control changes in concentration. The corrections did not change the observed results.

Species	*A. aurita*	*C. hysoscella*	*C. fulgida*	*C. pacifica*
Ammonium spike (μL) in Mucus treatments	20	80	100	40
Ammonium spike (μL) in Mucus-control treatments	15	60	75	30
Expected increase in concentration (μM)	0.5	2	2.5	1

TABLE A.2: Volume of ammonium stock solution (100 mM) and expected increase in concentration of the Mucus and Mucus-Control treatments of *A. aurita*, *C. hysoscella*, *C. pacifica* and *C. fulgida*.

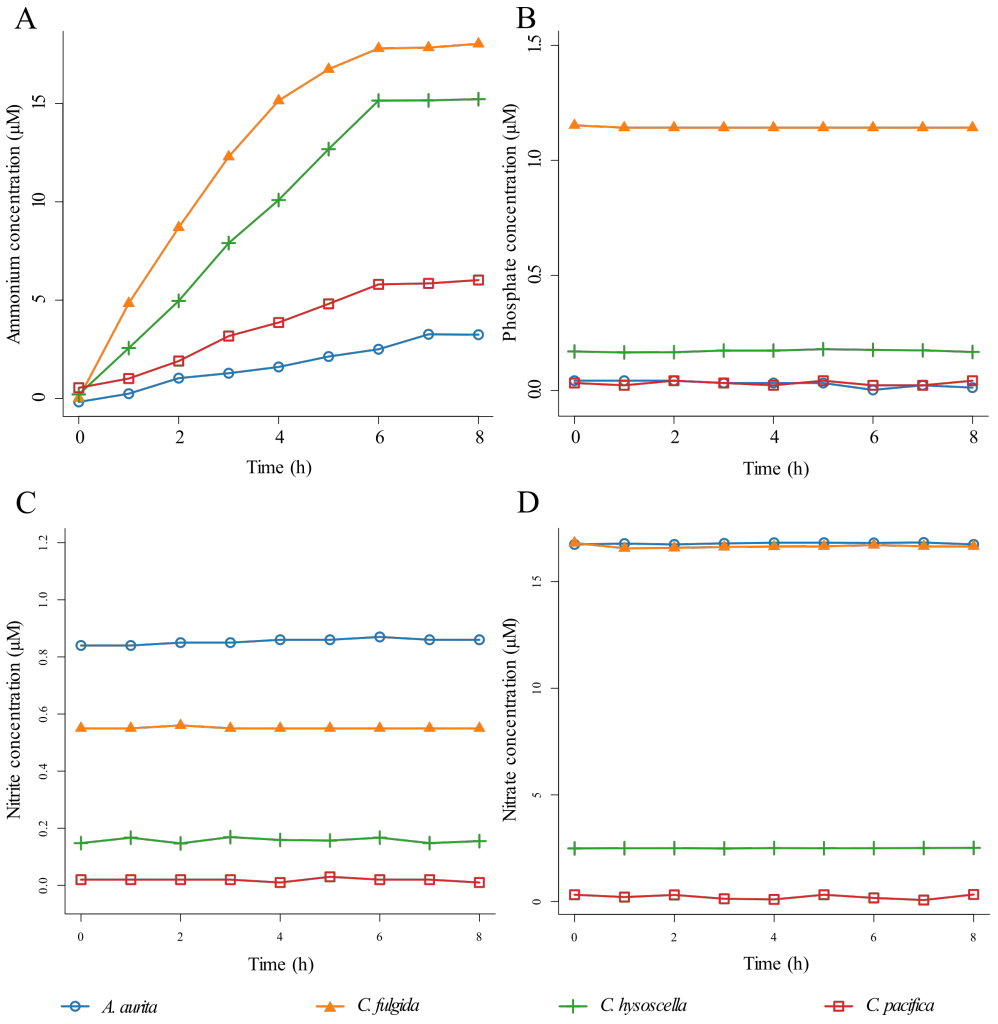

FIGURE A.3: Ammonium (A), phosphate (B), nitrite (C) and nitrate (D) concentrations of the Mucus-Control treatment of *A. aurita* (blue), *C. hysoscella* (green), *C. pacifica* (red) and *C. fulgida* (orange).

Phosphate

Species	Intercept	Slope	R^2	p
A. aurita	-0.006	-0.0043	0.6619	**
C. hysoscella	1.0938	-0.0007	0.2	0.127
C. pacifica	0.1163	0.0007	0.0645	0.253
C. fulgida	-0.0218	0.0002	-0.1401	0.9

Nitrite

Species	Intercept	Slope	R^2	p
A. aurita	0.8418	0.0032	0.6934	**
C. hysoscella	0.1575	0	-0.1428	0.989
C. pacifica	0.0209	-0.0005	-0.0835	0.555
C. fulgida	0.5524	-0.0003	-0.0571	0.476

Nitrate

Species	Intercept	Slope	R^2	p
A. aurita	16.7642	0.0053	0.0309	0.299
C. hysoscella	2.4931	0.0023	0.503	*
C. pacifica	0.2491	-0.0078	-0.0949	0.597
C. fulgida	16.6576	-0.0013	-0.14	0.899

TABLE A.3: Summary tables of linear regression results from the Mucus-Control treatment. The use of *, **, and *** denotes levels of statistical significance (p=0.05, 0.01, and 0.001 respectively).

A.3 Mucus-Treatment

The Mucus treatment consisted of artificial seawater that had previously contained jellyfish, this artificial seawater was spiked with ammonium every hour during the first 6 hours. The values of ammonium concentration measured from the Mucus treatment were subtracted from the values obtained in the Mucus-Control treatment (Figure A.3, A) in order to present the differences between the incubations (Figure A.4, A). The ammonium concentrations of the Mucus treatment - *C. hysoscella*, showed a highly significant decrease with time, while there was a significant increase of ammonium in the Mucus treatment - *C. pacifica* (Table A.3, A). Two species showed a change in nitrite (*A. aurita* & *C. pacifica*; Table A.3, B). One species showed a significant change in nitrate with time (*C. fulgida*; Table A.3, C). For nitrate and nitrite, the rates of change in concentrations were extremely low ($<$0.01 μM h^{-1}; Table A.3, B & C). The decrease in ammonium concentration in the Mucus treatment – *C. hysoscella*, suggests

the presence of microorganisms utilising ammonium. The absence of nitrite and/or nitrate increase associated with the ammonium decrease supports that the microorganisms are not nitrifiers as they do not release nitrite and nitrate. They seem to be retaining the nitrogen. The changes in nitrite concentrations were close to the detection limit ($\leq$0.02 μM) and could therefore be caused by increasing signal-to-noise ratios at low concentrations. The low rates of change for nitrite and nitrate suggest that the effect is negligible.

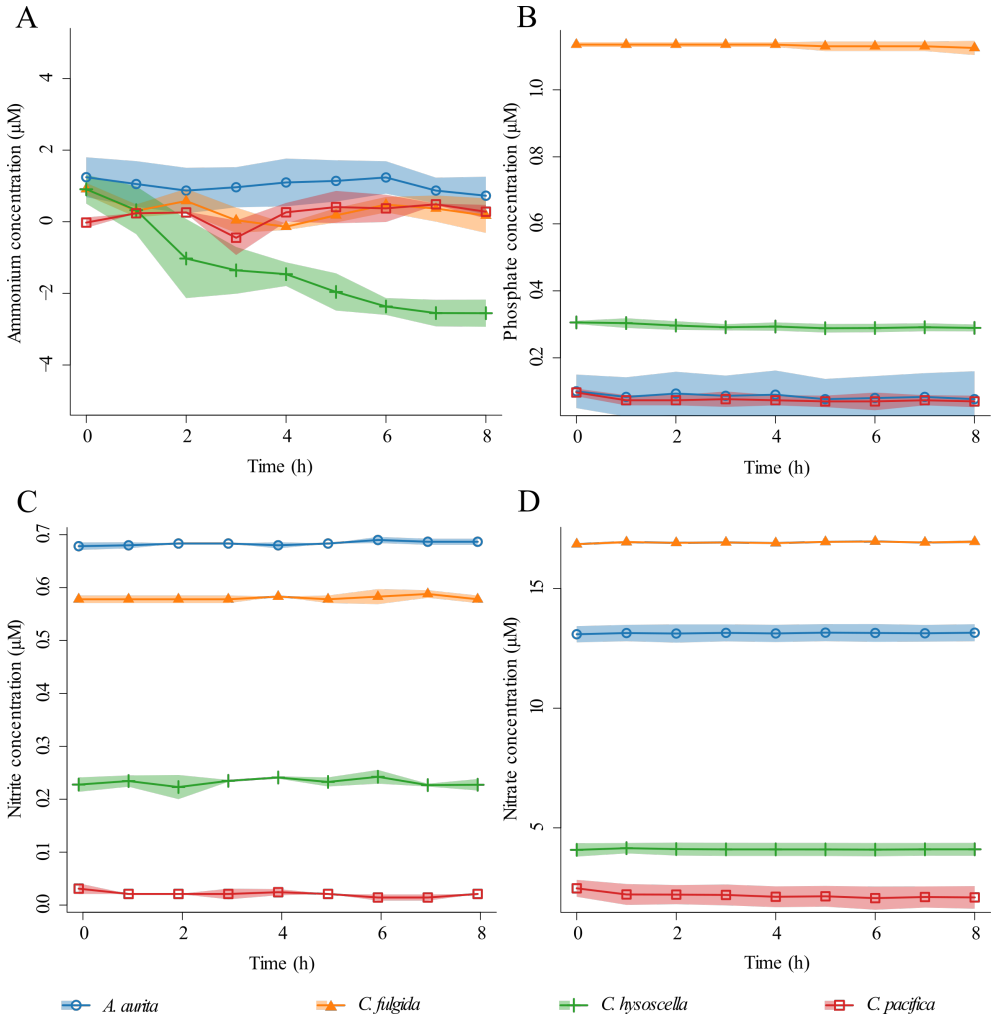

FIGURE A.4: Ammonium (A), phosphate (B), nitrite (C) and nitrate (D) blank corrected concentrations of the Mucus treatment of *A. aurita* (blue), *C. hysoscella* (green), *C. pacifica* (red) and *C. fulgida* (orange). Coloured area = standard deviation of the mean cumulative release of nutrients.

Ammonium

Species	Intercept	Slope	R^2	p
A. aurita	1.136	-0.0284	-0.0164	0.453
C. fulgida	0.511	-0.0112	-0.0547	0.735
C. hysoscella	0.3777	-0.4291	0.7644	***
C. pacifica	0.0013	0.0628	0.1659	*

Phosphate

Species	Intercept	Slope	R^2	p
A. aurita	0.0942	-0.0022	-0.0289	0.608
C. fulgida	1.1369	-0.0012	0.0523	0.183
C. hysoscella	0.3023	-0.002	0.1813	*
C. pacifica	0.0832	-0.002	0.0602	0.115

Nitrite

Species	Intercept	Slope	R^2	p
A. aurita	0.6758	0.0011	0.25	**
C. fulgida	0.5746	0.0007	0.012	0.288
C. hysoscella	0.2297	0.0002	-0.0377	0.815
C. pacifica	0.0249	-0.0012	0.193	*

Nitrate

Species	Intercept	Slope	R^2	p
A. aurita	13.115	0.0047	-0.0382	0.838
C. fulgida	16.8923	0.0082	0.2343	*
C. hysoscella	4.1106	-0.0016	-0.0396	0.923
C. pacifica	2.3264	-0.0365	0.0265	0.203

TABLE A.4: Summary tables of linear regression results from the Mucus treatment for ammonium (A), phosphate (B), nitrite (C) and nitrate (D).

A.4 ANCOVA

The regression lines were compared between species for each nutrient by analyses of covariance (ANCOVA). The data used for the analyses was lower or equal to time=6, i.e.: when the jellyfish was present in the incubator. The tables below show the p-value of the interaction between time and species. A significant interaction ($p<0.05$) means that there is a high probability that the species influence is real. In order words, the slopes of the regression lines are statistically different.

Ammonium

Species	*A. aurita*	*C. fulgida*	*C. hysoscella*	*C. pacifica*
A. aurita	NS	NS	NS	***
C. fulgida	NS	NS	*	***
C. hysoscella	NS	*	NS	***
C. pacifica	***	***	***	NS

Phosphate

Species	*A. aurita*	*C. fulgida*	*C. hysoscella*	*C. pacifica*
A. aurita	NS	NS	*	***
C. fulgida	NS	NS	NS	***
C. hysoscella	*	NS	NS	**
C. pacifica	***	***	**	NS

Nitrite

Species	*A. aurita*	*C. fulgida*	*C. hysoscella*	*C. pacifica*
A. aurita	NS	***	***	***
C. fulgida	***	NS	NS	***
C. hysoscella	***	NS	NS	NS
C. pacifica	***	***	NS	NS

Nitrate

Species	*A. aurita*	*C. fulgida*	*C. hysoscella*	*C. pacifica*
A. aurita	NS	***	***	***
C. fulgida	***	NS	NS	***
C. hysoscella	***	NS	NS	NS
C. pacifica	***	***	NS	NS

TABLE A.5: Summary tables of ANCOVA analyses in between species of the Jellyfish treatment for ammonium (A), phosphate (B), nitrite (C) and nitrate (D). The use of *, **, and *** denotes levels .05, .01, and .001 of statistical significance, respectively. NS= non-significative.

A.5 Allometric scalling

Both the inter- and intraspecies variability observed in ammonia and phosphate excretion as well as nitrification rates can be partly explained by allometric scaling of the mass-specific release rates to the wet weight of each individual (ammonium excretion: 80%, phosphate excretion: 73%, nitrification: 55%, Table V; MS, Figure 5)

Nutrient	Intercept	SD	Slope	SD	R^2	n	p
Ammonium	7.52	0.48	-0.82	0.1	0.8	17	***
Phosphate	5.91	0.63	-0.9	0.13	0.73	17	***
Nitrite	3.55	3.13	-0.88	0.67	0.05	12	0.2
Nitrate	7.95	1.29	-1.2	0.28	0.55	15	***

TABLE A.6: Summary of the linear regressions on the effect of wet-weigh on the mass-specific nutrient releases normalised to 16°C. The use of *, **, and *** denotes levels of statistical significance (p = 0.05, 0.01, and 0.001 respectively).

A.6 Lab-on-Chip analyser

An additional experiment was performed incubating a medusa of the species *A. aurita* in 4L of ASW and measuring nitrate + nitrite and nitrite concentrations using two microfluidic lab-on-chip (LoC) analysers. The LoC analysers used in this study were designed and fabricated at the National Oceanography Centre, Southampton, U.K and described in detail elsewhere (Beaton et al., 2012). Briefly, the LoC analyser is composed of a three-layer poly(methyl methacrylate) chip with precision milled microchannels, mixers and optical components consisting of light emitting diodes and photodiodes, electronics, solenoid valves and syringe pumps are mounted on the chip. Reagent preparation details can be found in Birchill et al., 2019, for nitrate + nitrite detection an off-chip cadmium column was used, for nitrite-only detection the column was removed. The standards were prepared from the same stock solutions that were used to prepare standards for gas segmented continuous flow (Seal; QuAAtro) analysis, the nitrite LoC analyser was equipped with 1.00 μM NO_2 standard and the NO_3 + NO_2 LoC analyser with a 2 μM NO_3 standard. A 0.45 μm Polyethersulfone Millipore filter was added to the end of the sample inlet tubing to prevent jellyfish mucus clogging the sensor. The incubator was fixed on a stirring table to homogenise the water.

A control and jellyfish incubation experiment were conducted. The spectrophotometric Greiss assay used on the LoC analysers measures NO_2, therefore any NO_3 present in the sample must be reduced prior to colour formation. This was achieved by the use of an off chip cadmium (Cd) column (Beaton et al. 2012). For each

experiment, the Cd column reduction efficiency on the NO_3 + NO_2 LoC analyser was determined. The NO_3 reduction efficiency of the Cd column was determined by analysing a 1.00 μM NO_2 sample with the NO_3 + NO_2 LoC analyser that was standardised with a 2.00 μM NO_3 standard (i.e. if the analyser returned a NO_3 + NO_2 $>$ 1.00 μM this would indicate ¡ 100% reduction efficiency). For the control experiment, the Cd column efficiency was 61-65% (mean 64%, n=5). For the jellyfish incubation experiment, the Cd column efficiency was 61-69% (mean 66%, n=7). Ideally the NO_3 reduction efficiency would be total (i.e. 100%), but as the NO_2 concentration was being measured simultaneously, inefficiencies in NO_3 reduction could be accounted for. All reported NO_3 + NO_2 concentrations are therefore corrected for Cd column efficiency.

The control experiment was set up in the same manner as for the jellyfish experiments but without the addition of jellyfish. Firstly, the analysers repeatedly measured the concentration of NO_2 and NO_3 + NO_2 of artificial seawater in the incubation container, which was $<$ 0.025 μM (n= 3) and 0.15 $\pm$ 0.02 μM (n= 7) respectively. Following this a 0.70 μM NO_2 spike was added to artificial seawater, therefore for target NO_2 and NO_3 + NO_2 concentration was 0.70 μM and 0.85 μM respectively. The concentration returned by the NO_2 LoC analyser was 0.70 $\pm$ 0.01 μM (n=3), whilst the NO_3 + NO_2 LoC analyser returned a lower than expected concentration of 0.72 $\pm$ 0.04 μM (n=3). A 0.50 μM NO_3 spike was then added to the same artificial seawater, therefore for target NO_2 concentration remained at 0.70 μM whilst the target NO_3 + NO_2 concentration increased to 1.35 μM. The concentration returned by the NO2 LoC analyser was 0.70 $\pm$ 0.01 μM (n=4) and the NO_3 + NO_2 was 1.33 $\pm$ 0.08 μM (n=5) respectively. In summary, the control experiments demonstrated the analytical setup worked well, with the LoC analysers responding as expected to NO_2 and NO_3 additions. The lower-than-expected concentration returned by the NO_3 + NO_2 LoC analyser after the 0.70 μM NO_2 spike may in part be due to variable Cd-column efficiencies. Future experiments should aim for total NO_3 reduction efficiency.

Prior to the addition of an *A. aurita* specimen, the concentration of NO_2 and NO_3 + NO_2 in the artificial seawater used for the jellyfish incubation experiment was $<$ 0.025 μM (n=6) and 0.06 $\pm$ 0.02 μM (n=7) respectively. Following the addition of the *A. aurita* specimen, the nitrate concentration increased linearly with a rate of 0.19 μM h^{-1} (Figure A.5, left) corresponding to the same average rate observed during the 5 replicate *A. aurita* jellyfish treatments (Figure A.5, right). The nitrite concentration remained $<$ 0.025 μM (n= 11) throughout the experiment, which is also consistent with the *A. aurita* jellyfish treatments. Eight water samples were taken to compare the value of nitrate concentration measured by the LOC sensor and with concentrations determined by gas-segmented continuous flow analysis (QuAAtro). The values are distributed around a linear regression line with a slope of 1.04 and a coefficient of determination of 0.98 (Figure A.6).

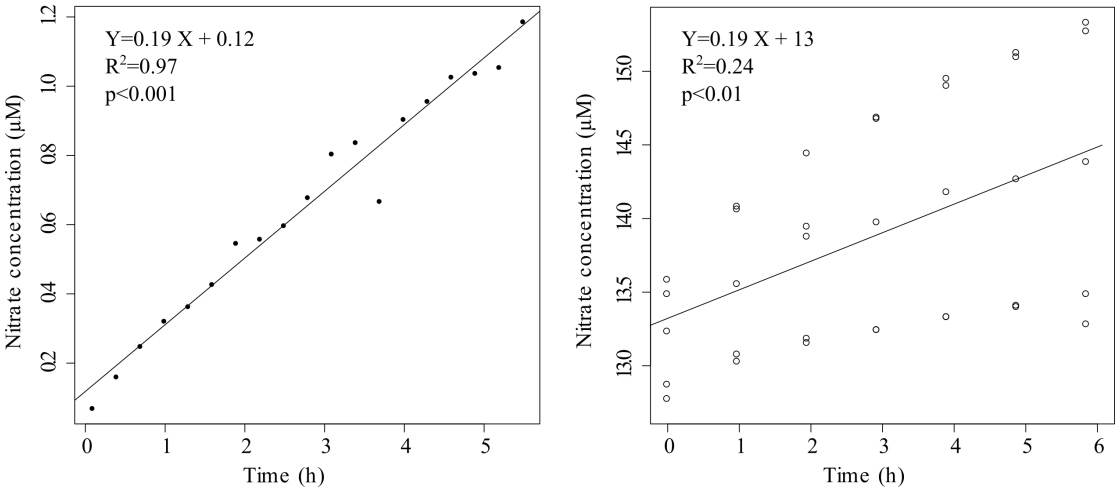

FIGURE A.5: Nitrate concentration of an incubator (Volume=4L) with a jellyfish of *A. aurita* measured by a lab-on-chip sensor (left) and nitrate concentrations of the Jellyfish treatment incubator of *A. aurita* measured by gas-segmented continuous flow (QuAAtro, right). The ASW for the Jellyfish treatment incubator was made with reverse osmosis water presenting already high concentrations of nitrate (right).

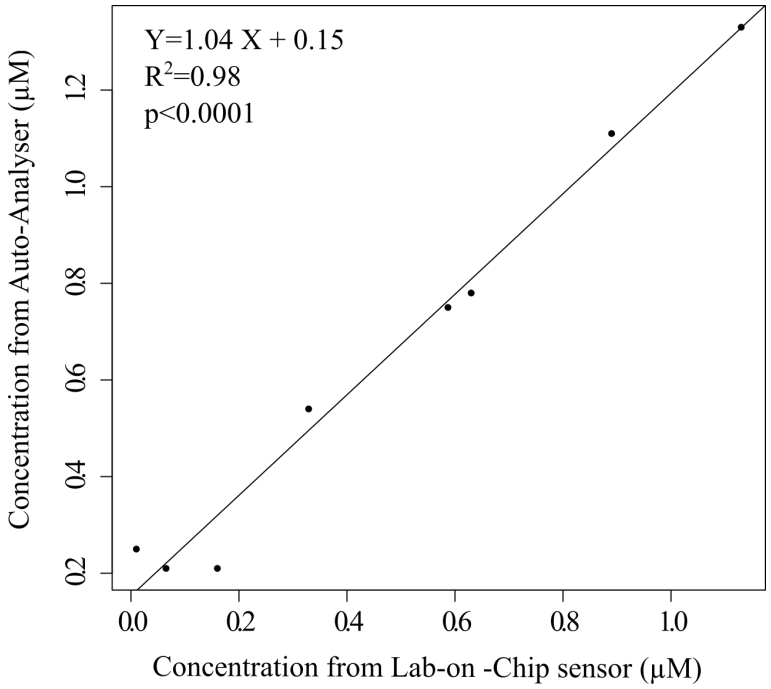

FIGURE A.6: Comparing spectrophotometric methods: Gas segmented continuous flow (QuAAtro) vs Lab-on-Chip sensor. Real-time concentrations of nitrate measured by a lab-on-chip sensor and filtered grab samples measured by gas segmented continuous flow

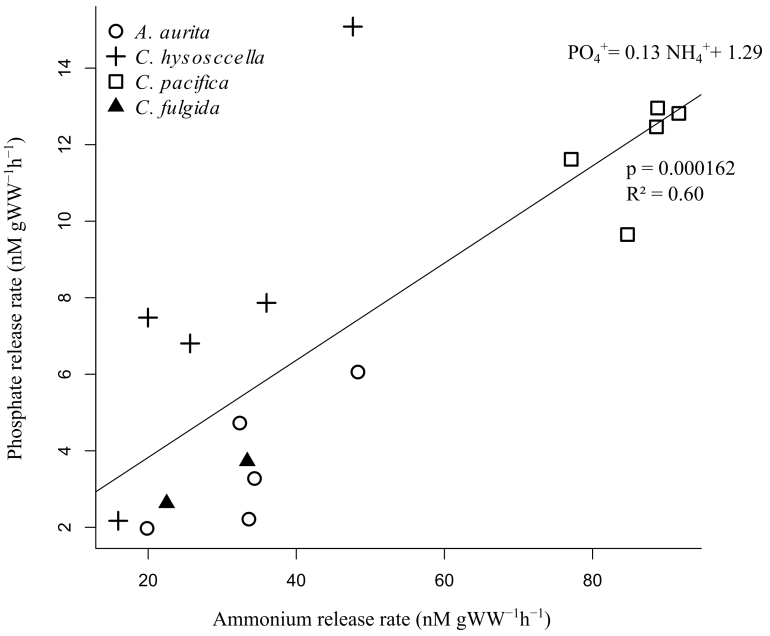

FIGURE A.7: Relationship between the weight-specific phosphate and ammonium release rates for the jellyfish *A. aurita, C. hysoscella, C. pacifica* and *C. fulgida* at 16°C. The line represents the linear regression.

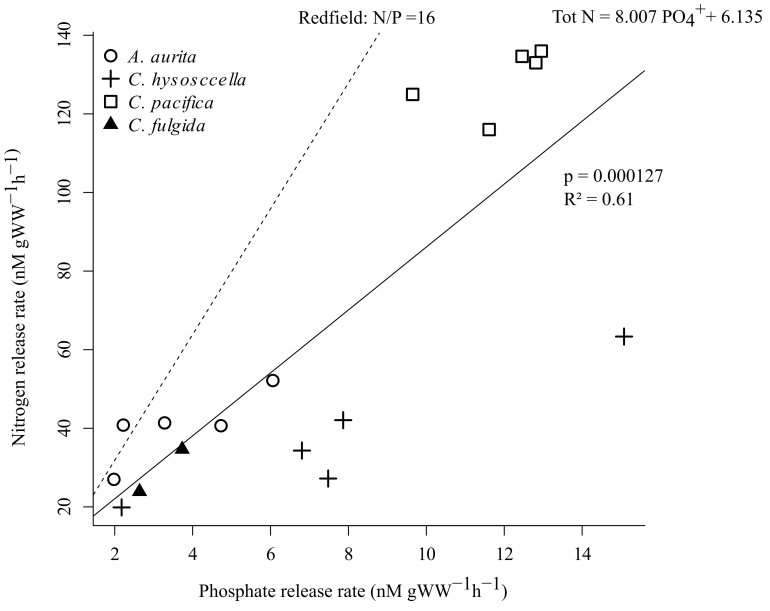

FIGURE A.8: Relationship between the weight-specific nitrogen and phosphate release rates for the jellyfish *A. aurita, C. hysoscella, C. pacifica* and *C. fulgida* at 16°C. The continuous line represents the linear regression. The dashed line indicates where N:P ratio is 16:1 (Redfield ratio).

A.7 Artificial sea water preparation

First, the containers and tools used were cleaned using 10% hydrochloric acid (overnight) and ethanol, and then rinsed 3 times with ultra-high purity (UHP) water (MilliQ $\geq$ 18.2 Mω cm^{-1}, Millipore). Two 20 L high density polyethylene containers with dispensing tap were filled with 10 L of UHP water. A pre-weighted amount of Tropic Marin PRO-REEF Sea Salt was added and the containers were shaken until total dissolution of the salt. Then, the remaining 10L of UHP water was added gradually checking the salinity to reach the experimental salinity (Table 2.1).

A.8 Calibration and limit of detection

In total, three instruments were used to measure nutrients: a Turner design Trilogy fluorometer (model 7200, US) with a UV module (7200-047), an auto-analyser (QuAAtro, Seal Analytics) and a microfluidic lab-on-chip (LoC) analyser (Beaton et al., 2012). Table A.7 presents details of the calibration and the detection limit of the instrument used.

nutrients	Instrument		*A. aurita*	*C. hysoscella*	*C. fulgida*	*C. pacifica*
Ammonium	fluorometer	Calibration points (µM)	0,1,2,3,4	0,2,4,6,8	0,2,4,6,8	0,2,4,6,8
		Coefficient (a; b for C=aA+b)	316319; 549621	307972; 667256	9045; 53464*	391522; 78287
	AA	LOD (µM)	-	0.01	-	-
		Calibration points (µM)	-	2.5, 5, 10, 15, 20	-	-
phosphate	AA	LOD (µM)	0.01	0.01	0.01	0.01
		Calibration points (µM)	0.5, 1, 1.5, 2, 2.5	0.2, 0.5, 1, 1.5, 2	0.5, 1, 1.5, 2, 2.5	0.5, 1, 1.5, 2, 2.5
nitrate	AA	LOD (µM)	0.04	0.01	0.04	0.04
		Calibration points (µM)	4.5, 9, 13.5, 18, 22.5	0.5, 1.25, 2.50, 3.7, 5	4.5, 9, 13.5, 18, 22.5	4.5, 9, 13.5, 18, 22.5
	LOC Sensor	LOD (µM)	NA	-	-	-
		Calibration points (µM)	2	-	-	-
nitrite	AA	LOD (µM)	0.01	0.02	0.01	0.01
		Calibration points (µM)	0.5, 1, 1.5, 2, 2.5	0.2, 0.5, 1, 1.5, 2	0.5, 1, 1.5, 2, 2.5	0.5, 1, 1.5, 2, 2.5

*Different Turner Trilogy fluorometer used

TABLE A.7: Calibration points and limit of detection (LOD) for the different instrument used for the analysis of samples from the experiment of the jellyfish species *A. aurita, C. hysoscella, C. fulgida* and *C. pacifica*. C= concentration (μM) and A= absorbance.

Appendix B

Supplementary Material - Chapter 3

B.1 Literature review

Species	Location	Protein (%DW)	Lipid (%DW)	Carbohydrate (%DW)	Refs
Gelatinous zooplankton					
All	Southern Ocean	7.5–17.0	1.8-4.6	0.4-1.7	[1]
Jellyfish					
Aurelia aurita	Baltic sea	5.9	2.17	2.9	[2]
Aurelia aurita	Southampton	2.1 - 28.6	1.2 - 11	0.1-1.1	[3]
Atolla wyvelli	Antartic	16.95	4.17	1.71	[1]
Rhizostoma pulmo	Mediterranean	8.6	3.5	-	[4]
Copepods					
all copepods		24 - 82	2 - 73	0.2-5.1	[5]
Pseudodiaptomus annandalei	Taiwan	57	16		[6]
Zooplankton					
All	Kerguelen Islands	21.5	8.9	3.2	[7]
Mucus		(relative %)	(relative %)	(relative %)	
Aurelia aurita	Gulf of Aqaba	73	27	5	[8]

TABLE B.1: Review of the biochemical composition (protein, lipid and carbohydrate) of members of marine zooplankton as a percentage of dry body weight, and jellyfish mucus as a relative percentage.

B.1.1 References

[1] Clarke, A., Holmes, L. J., & Gore, D. J. (1992). Proximate and elemental composition of gelatinous zooplankton from the southern ocean. *Journal of Experimental Marine Biology and Ecology*, *155*(1), 55–68. https://doi.org/10.1016/0022-0981(92)90027-8

[2] Schneider, G. (1988). Chemische Zusammensetzung und Biomasseparameter der OhrenqualleAurelia aurita. *Helgoländer Meeresuntersuchungen*, *42*(2), 319–327. https://doi.org/10.1007/BF02366048

[3] Lucas, C. H. (1994). Biochemical composition of aurelia aurita in relation to age and sexual maturity. *Journal of Experimental Marine Biology and Ecology*, *183*(2), 179–192. https://doi.org/10.1016/0022-0981(94)90086-8

[4] H.J. Ceccaldi, S. T., A. Kanazawa. (1976). Chemical composition of some mediterranean macroplanktonic organisms. *Tethys*, *8*, 295–298

[5] Båmstedt, U. (1986). Chemical composition and energy content. *The Biological Chemistry of Marine Copepods*, 1–58

[6] Rayner, T. A., Jørgensen, N. O. G., Blanda, E., Wu, C.-H., Huang, C.-C., Mortensen, J., Hwang, J.-S., & Hansen, B. W. (2015). Biochemical composition of the promising live feed tropical calanoid copepod pseudodiaptomus annandalei (sewell 1919) cultured in taiwanese outdoor aquaculture ponds. *Aquaculture*, *441*, 25–34. https://doi.org/10.1016/j.aquaculture.2015.01.034

[7] Harmelin-Vivien, M., Banaru, D., Dromard, C. R., Ourgaud, M., & Carlotti, F. (2019). Biochemical composition and energy content of size-fractionated zooplankton east of the kerguelen islands. *Polar Biology*, *42*(3), 603–617. https://doi.org/10.1007/s00300-019-02458-8

[8] Ducklow, H. W., & Mitchell, R. (1979). Composition of mucus released by coral reef coelenterates1. *Limnology and Oceanography*, *24*(4), 706–714. https://doi.org/10.4319/lo.1979.24.4.0706

B.2 Material and Methods

B.2.1 Lipid analyses

Total lipid of the samples was extracted using a single-step extraction method relying on the chloroform-methanol solvent system, following the protocol by Axelsson et al., 2014 (see protocol below). Briefly, 10 mg of freeze-dried tissue was homogenized with a 2 : 1 chloroform-methanol (v/v) mixture to a final volume of 3 mL and vortexed for 30 seconds. 1 mL of Ultra-pure water was then added to the solution, which was then vortexed briefly and centrifuged to 1000 g for 10 minutes. Subsequently, the supernatant was removed along with the cell debris and 1 mL of the lower phase was collected and transferred to a vial for nitrogen drying at 60°C. The lipid amount was measured using a charring method (Marsh et al., 1966; see protocol below) by adding 500 μL of H_2SO_4 and incubating for 15 min at 200°C. After cooling down, 3 mL of water was added and lipid concentration was determined using a UV-Vis

spectrophotometer at 375 nm. The assay was calibrated with known amounts of cholesterol (Sigma Aldrich, C8503; see table of dilutions in protocol).

Protocol:

Extraction: Single-step method (based on Axelsson et al., 2014)

1. Weight 10 mg freeze-dried tissue, add to 8 mL glass vials
2. Make standards into 8mL glass vials for a final volume of 1 mL
3. Add 2 and 3 mL of 2:1 chloroform:methanol to standards and samples, respectively.
4. Vortex for 30 sec.
5. Add 1 ml of 0.73 % w/v NaCl solution (for standards) or 1 mL of pure water (for samples)
6. Vortex briefly
7. Centrifuge to 1000 g for 10 min
8. Remove supernatant and cells debris
9. Collected 1 ml of the lower phase
10. Transfer to a small vial and dry at 60°C with nitrogen

Measurement: Charring method (based on Marsh et al., 1966)

1. Start heating the aluminium plate (320°C) and check to temperature with the laser until reaching 200°C
2. Add 500 µl of H_2SO_4 to the vials and mix gently (use face shield)
3. Place vials in the aluminium heating block for 15 min at 200°C
4. Cool the vial in water at room temperature and transfer to cold aluminium block (from fridge)
5. Add 3 ml of water, mix and let it cool down
6. Mix well before transferring 1 ml to semi-micro cuvettes and read at 375 nm

Table of dilutions:

Stock solution: 20 mg of Cholesterol to 100 ml of 2:1 chloroform:methanol = 200 mg/L

Standard	Volume of Stock (µl)	Volume 2:1 Chloro:Methanol (µl)	Final concentration (mg/l)
1	0	1000	0
2	200	800	40
3	400	600	80
4	600	400	120
5	800	200	160
6	1000	0	200

TABLE B.2: Table of cholesterol dilutions for calibration

B.2.2 Protein analyses

Total protein concentration in samples was measured using a modification of the assay by Lowry (Gerhardt et al., 1994; Lowry et al., 1951). Briefly, approximatively 20 mg freeze-dried tissue were dissolved into 2 mL of ultra-pure water (≈10 mg/mL). 100 μL of the sample solution was diluted to a final volume of 500 µL, mixed with the Lowry solution and incubated for 20 minutes in the dark at room temperature. Samples were then incubated again in the same conditions for minimum 30 minutes with 0.1 mL of Folin & Ciocalteu's phenol reagent 1N (Sigma Aldrich, F9252). Protein concentration was determined using a UV-Vis spectrophotometer at 750 nm, calibrated against bovine serum albumin (Sigma Aldrich, A3059; see table of dilution in protocol).

Protocol:

1. Weight approximatively 20 mg freeze-dried tissue, add to 8 mL glass vials with 2 ml of water (≈10 mg/mL)
2. Vortex for 30 sec.
3. Prepare a stock solution of BSA and the Lowry solution by mixing 500 µL of 1% CuSO4 and 500 µL of 2% $KNaC_4H_4O_6.4H_2O$, then add 50 mL of 2% $NaCO_3$ in NaOH

4. Transfer 100 µL of sample to a 8mL glass vial + 400 µL of water 500 µL of standard to an 8mL glass vial
5. Add 0.7 mL of Lowry Solution
6. Cap and vortex briefly at low speed
7. Incubate for 20 min in the dark at room temperature
8. After 15 min of incubation, prepare the Folin reagent dilution (1:1 Folin:water)
9. After 20 min of incubation, add 0.1 mL of diluted Folin reagent
10. Cap and vortex immediately
11. Incubate for 30 min or longer in the dark at room temperature
12. After 30 min, vortex briefly and transfer 1 mL to a semi-micro cuvette and read at 750 nm

Table of dilutions:

Stock solution: 50 mg of BSA to 250 ml of water = 200 mg/L

Standard	Volume of Stock (mL)	Volume of water (mL)	Final concentration (mg/L)
1	0	10	0
2	2	8	40
3	4	6	80
4	6	4	120
5	8	2	160
6	10	0	200

TABLE B.3: Table of BSA dilutions for calibration

B.2.3 Carbohydrate analyses

Total carbohydrate concentrations were measured using the Dubois assay (DuBois et al., 1956). 500 µL of 5% w/v phenol (ref) was mixed with 1 mL of the sample solution used for the protein assay (≈10 mg/mL). 2.5 mL of H_2SO_4 was then added to

the mixture and mix gently. After a minimum of 20 min standing, samples were vortexed and read at 490 nm against glucose.

Protocol:

1. Weight approximatively 20 mg freeze-dried tissue, add to 8 mL glass vials with 2 ml of water ($\approx$10 mg/mL)
2. Vortex for 30 sec.
3. Prepare a stock solution of glucose
4. Use 1 ml of sample + 500 μl 5% w/v phenol, mix
5. Add 2.5 ml H_2SO_4, mix gently
6. Stand $>$ 20 min
7. Vortex briefly and transfer 1 mL to a semi-micro cuvette and read at 490 nm

Table of dilutions:

Stock solution: 25 mg of glucose to 250 ml of water = 100 mg/L

Standard	Volume of Stock (mL)	Volume of water (mL)	Final concentration (mg/L)
1	0	10	0
2	2	8	20
3	4	6	40
4	6	4	60
5	8	2	80
6	10	0	100

TABLE B.4: Table of glucose dilutions for calibration

B.3 Results

B.3.1 Linear regressions

Relation	Tissue	slope	SD	Intercept	SD	n	R^2	p
Lipid ∼Protein	body	0.09	0.01	0.19	0.1	24	0.61	***
	mucus	0.13	0.02	0.05	0.04	27	0.53	***
	both	0.1	0.01	0.1	0.03	51	0.8	***
Protein:Tissue	both	-	-	-	-	-	-	0.45
Carbohydrate ∼Protein	body	0.1	0.02	-0.03	0.15	24	0.46	***
	mucus	0.06	0.01	0.01	0.02	27	0.48	***
	both	0.1	0.01	-0.04	0.05	51	0.67	***
Protein:Tissue	both	-	-	-	-	-	-	0.54
Carbohydrate ∼Lipid	body	0.7	0.21	0.04	0.17	24	0.31	**
	mucus	0.3	0.09	0.03	0.02	27	0.24	**
	both	0.78	0.1	-0.05	0.06	51	0.56	***
Lipid:Tissue	both	-	-	-	-	-	-	0.28
SM ∼AFDW	body	1	0.05	12.6	0.4	72	0.85	***
	mucus	1.21	0.07	11.09	0.15	66	0.81	***
	both	1.12	0.03	11.24	0.16	139	0.93	***
AFDW:Tissue	both	-	-	-	-	-	-	0.2
EC ∼CC	body	38.05	3.05	-0.28	0.2	24	0.87	***
	mucus	40.58	3.61	-0.09	0.06	27	0.83	***
	both	35.03	1.27	-0.05	0.06	51	0.94	***
AFDW:Tissue	both	-	-	-	-	-	-	0.78

TABLE B.5: Summary of linear regression (∼) and ANCOVA (:). SM = sum of macromolecules, AFDW = ash-free dry-wet, EC = energy content, CC = carbon content.

Appendix C

Supplementary Material - Chapter 4

C.1 Dry-mucus preparation

The jellyfish dry-mucus used in our experiments consisted of pooled freeze-dried mucus from *A. aurita* specimen collected in the Gulf of Trieste in the northern Adriatic Sea on the 18.04.2019 and on the 16.06.2021. Jellyfish were sampled individually from the surface water together with ambient seawater using a large plastic bucket, rinsed with ambient seawater prior to sampling. On the same day, each specimen was transported to the laboratory while kept in the dark and at *in-situ* temperature where the mucus was collected following the methods by Hubot et al., 2022. The collected jellyfish mucus was freeze-dried (at - 45°C for 7 days) according to recommendations for jellyfish biomass processing (Kogovšek et al., 2014). Dry-mucus was homogenized with a sterilized pestle and agate mortar. Subsequently, dry-mucus samples were pooled together to obtain a representative sample mix of jellyfish mucus from the study area, avoiding possible biases arising from variations in size of different individuals within the population and from different phases of the bloom. Dry-mucus was stored in acid and Milli-Q water-rinsed and combusted glass vials at -20°C. In addition, the percentage of dry weight (DW) in mucus wet weight (WW) was estimated by measuring the weight of eight samples of *A. aurita* mucus before and after freeze-drying (Table C.1). Mucus WW was estimated to contain 4.06 $\pm$ 0.31 % of DW. Measurements were performed using an ultra-microbalance (Mettler Toledo XPE26, readability: 1 μg).

C.2 Dialysis experiment

Dialysis of dry-mucus was performed using Spectra/Por 7 Membrane tubing (Sulphur and Heavy Metal Free Spectrum) with a molecular weight cut-off (MWCO)

Replicate	WW (g)	DW (g)	%DW
1	24.70	1.03	4.16
2	18.12	0.85	4.68
3	23.73	0.95	4.01
4	29.62	1.22	4.12
5	30.21	1.17	3.87
6	19.91	0.73	3.67
7	27.15	1.13	4.16
8	31.68	1.21	3.83

TABLE C.1: Percentage of dry weight (DW) contained in mucus wet weight (WW) from the jellyfish *A. aurita* after freeze-drying.

of 1 kDa using three replicate samples to determine the ratio between the high- (>1 kDa) and the low- (<1 kDa) molecular weight compounds (LMW and HMW, respectively). Dialysis membranes were prepared and used according to the manufacturer's instructions (Spectrum) and sealed with Spectrum™ Universal Dialysis Tubing Closures (Spectrum). For each replicate, 1 g of mucus DW was re-hydrated in 25 mL of Milli-Q water to mimic the average wet weight of the collected fresh mucus and poured into a dialysis bag. The dialysis bags were submerged in an acid-cleaned and combusted glass beaker filled with 500 mL Milli-Q water and stirred at low speed on a magnetic stirrer. Dialysis of all three replicates was performed at 4°C in the dark for 24 h by changing Milli-Q water after 2, 4, 9 and 24 h until salinity reached 0. Salinity was measured using a refractometer. At each time point the dialysate was subsampled for determining the concentrations of dissolved organic carbon (DOC), total dissolved nitrogen (TDN), dissolved free-amino-acids (DFAA) and dissolved inorganic nutrients (PO_4^- and DIN; DIN = $NH_4^+ + NO_3^- + NO_2^-$). In addition, the amount of DOC, TDN, DFAA and DIN leaching from a dialysis membrane submerged in Milli-Q water was measured and subtracted from the values of parameters measured in the dialysate. Samples for bacterial abundance were collected to check for possible bacterial contamination.

Due to bacterial contamination, the data from replicate number 2 was not included in the calculation of the final mean values (Figure C.1, Table C.2). The control data for DOC/TDN was missing (tubes broke during freezing) so the control correction (to consider DOC/TDN leached by the bag and clip) was done using the control data from Tinta et al., 2020 (same setup; DOC: 178.67 μM and TDN: 15.19 μM). Dissolved organic nutrient: DON= TDN-DIN.

	Dialysis (μmol gDW^{-1} d^{-1})	
	mean	sd
NH_4^+	2.02	0.32
NO_3^-	0.78	0.29
NO_2^-	<LOD	NA
PO_4^{3-}	1.48	0.31
DIN	2.8	0.61
TDN	21.63	3.71
DON	18.83	3.1
DOC	57.49	38.54
DFAA	9.75	0.58

TABLE C.2: Cumulative amount of dissolved nutrients (NH_4^+, NO_3^-, NO_2^-, PO_4^{3-}, DIN, TDN, DON, DOC, DFAA) that leached through a 1 kDa Molecular Weight Cut-Off (MWCO) membrane tubing within 24 h expressed in µmol per g of dry weight (DW).

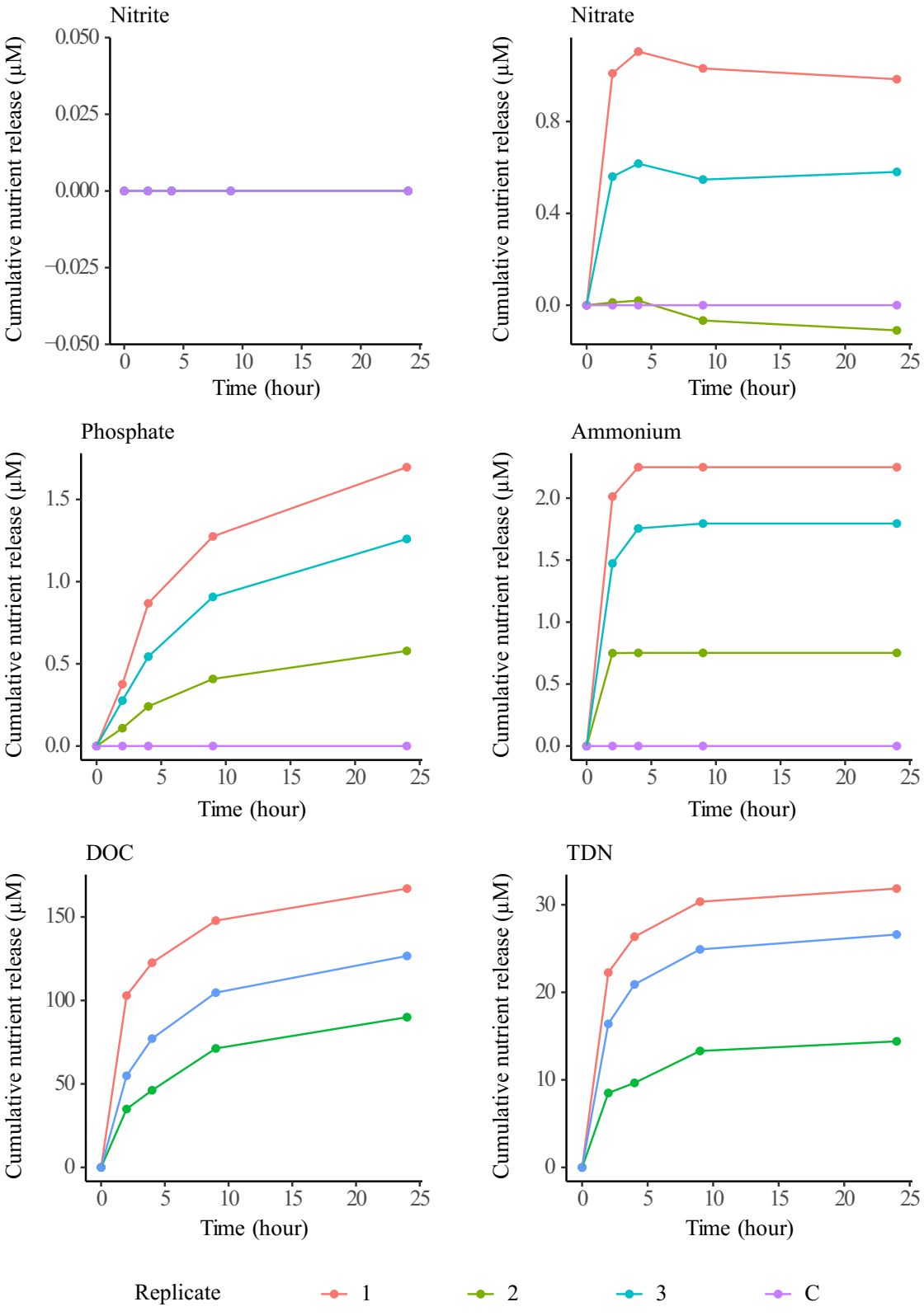
Nitrite
Nitrate
Phosphate
Ammonium
DOC
TDN
Cumulative nutrient release (µM)
Time (hour)
Replicate
1
2
3
C

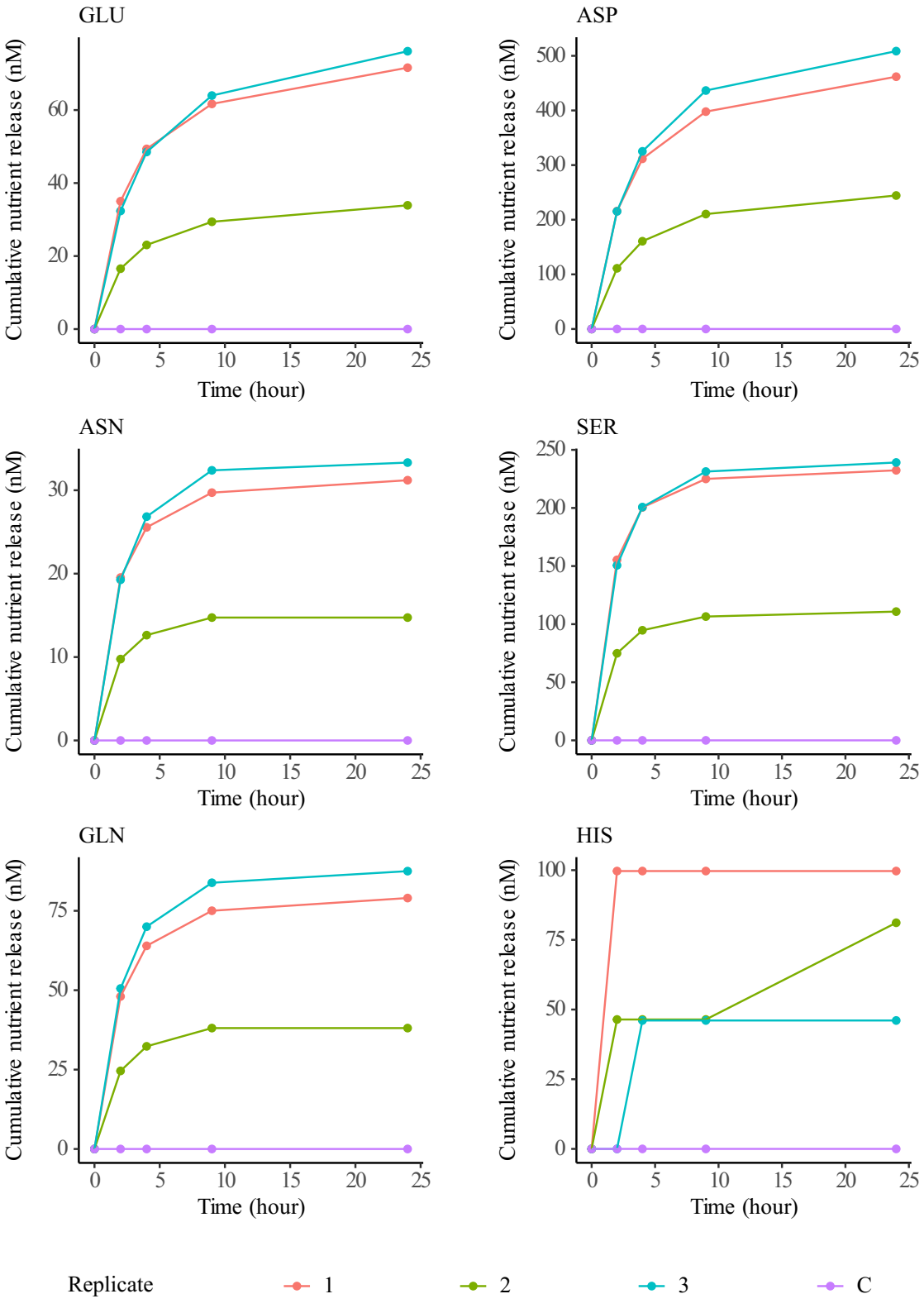
GLU
ASP
ASN
SER
GLN
HIS
Cumulative nutrient release (nM)
Time (hour)
Replicate
1
2
3
C

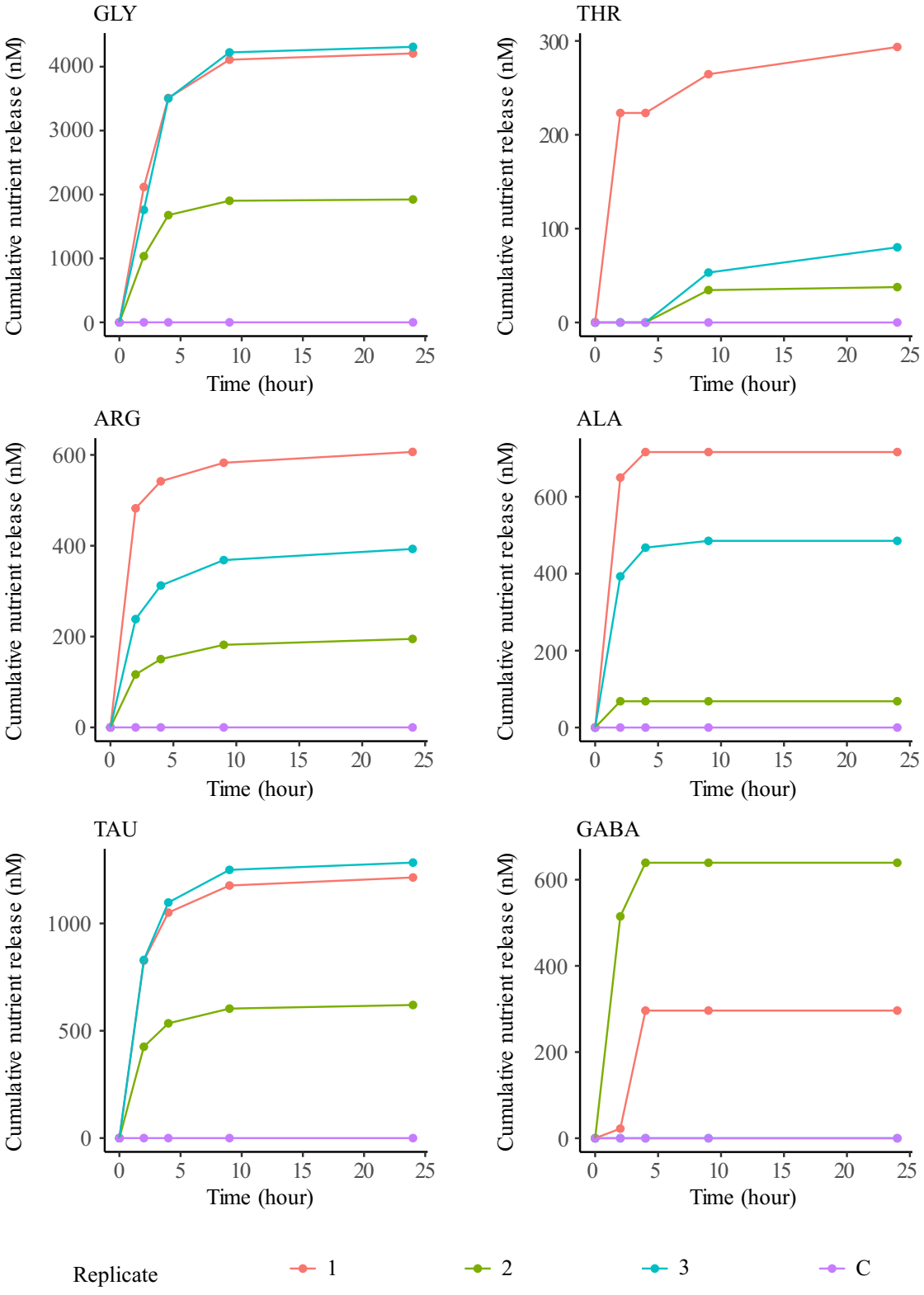
GLY
THR
ARG
ALA
TAU
GABA
Cumulative nutrient release (nM)
Time (hour)
Replicate
1
2
3
C

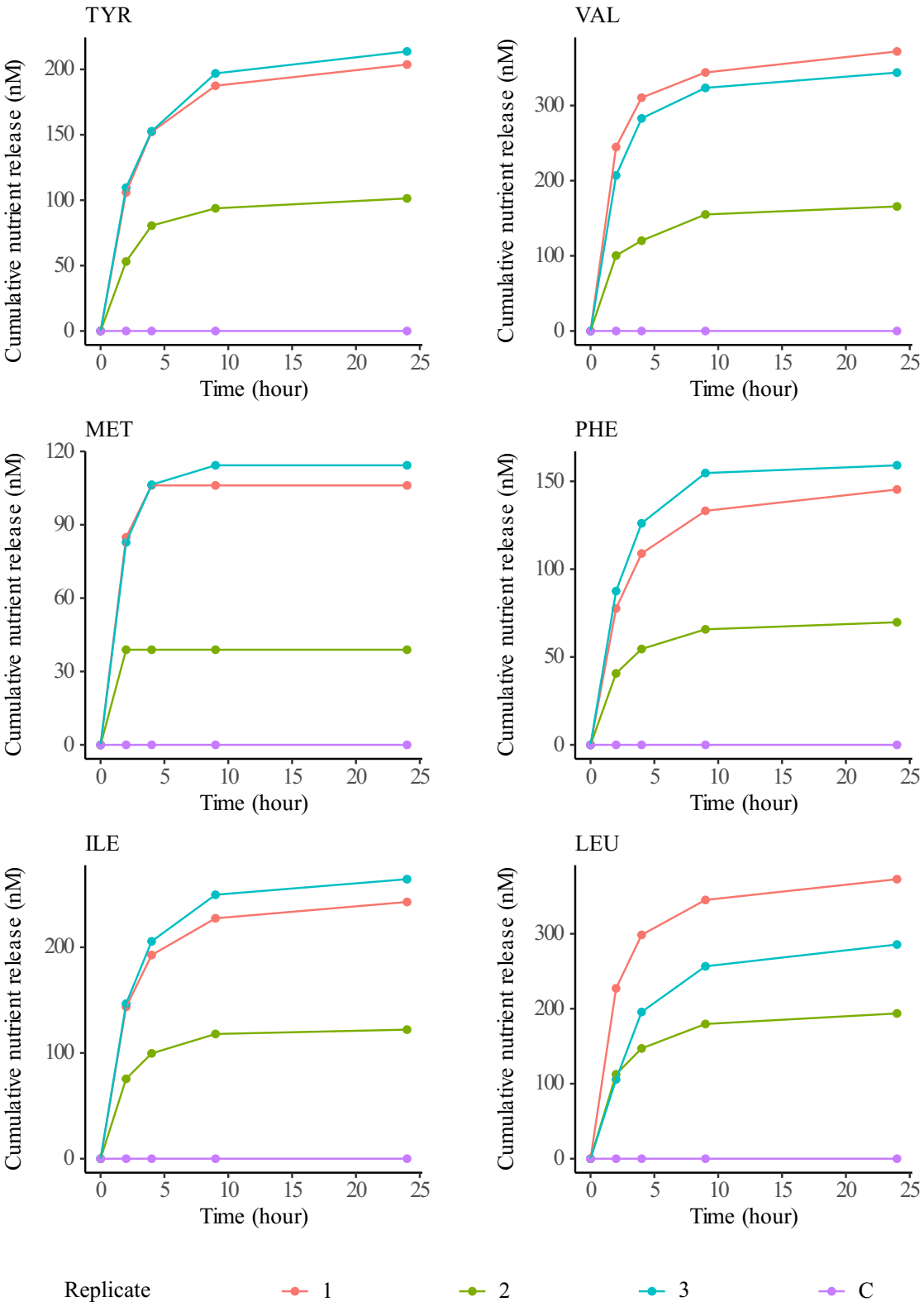
TYR
VAL
MET
PHE
ILE
LEU
Cumulative nutrient release (nM)
Time (hour)
Replicate
1
2
3
C

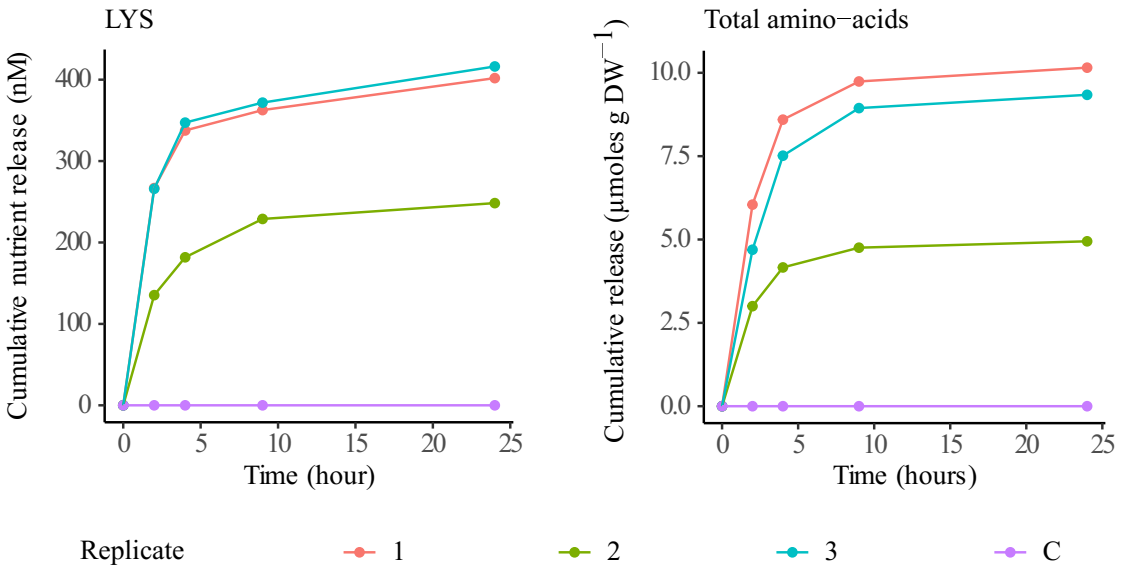

FIGURE C.1: Cumulative amount of dissolved nutrients (NH_4^+, NO_3^-, NO_2^-, PO_4^{3-}, DIN, TDN, DON, DOC, GLU =glutamic acid, ASP=aspartic acid, ASN=asparagine, SER=serine, GLN=glutamine, HIS=histidine, GLY=glycine, THR=threonine, ARG=arginine, ALA=alanine, TAU=taurine, GABA=gamma-aminobutyric acid, TYR=tyrosine, VAL=valine, MET=methionine, PHE=phenylalanine, ILE=isoleucine, LEU=leucine, LYS=lysine) that leached through a 1kDa Molecular Weight Cut-Off (MWCO) membrane tubing during 24 hours.

C.3 Leaching experiment - Dry-mucus

The concentration and composition of the particulate ($\gtrsim$0.7 μm) and dissolved ($\lesssim$0.7 μm) organic matter (POM and DOM, respectively) and inorganic nutrients leaching from dry-mucus were determined by dissolving 250 mg dry-mucus powder in 1 L of 0.2 mm filtered aged seawater (ASW) in an acid- and Milli Q water rinsed and combusted glass Erlenmeyer flask placed on a shaker in the dark at room temperature. Triplicate experimental flasks were sampled at 1, 6 and 24 h after the dry-mucus addition for later analysis of POC, PON, DOC, TDN, DFAA and inorganic nutrients. Bacterial abundance samples were collected to check for contamination.

Due to bacterial contamination, the data from replicate C was not included in the calculation of the final mean values (Figure C.2, Table C.3).

Leaching dry-mucus (μmol gDW^{-1} d^{-1})		
	mean	sd
NH_4^+	1.29	2.68
NO_3^-	2.48	0.34
NO_2^-	0.1	0.01
PO_4^{3-}	1.69	0
DIN	3.87	2.35
TDN	21.74	6.26
DON	17.87	3.91
DOC	134	39.13
DFAA	15.11	2.48

TABLE C.3: Cumulative amount of dissolved nutrients (NH_4^+, NO_3^-, NO_2^-, PO_4^{3-}, DIN, TDN, DON, DOC, DFAA) that leached from dry-mucus within 24 h expressed in µmol per g of DW.

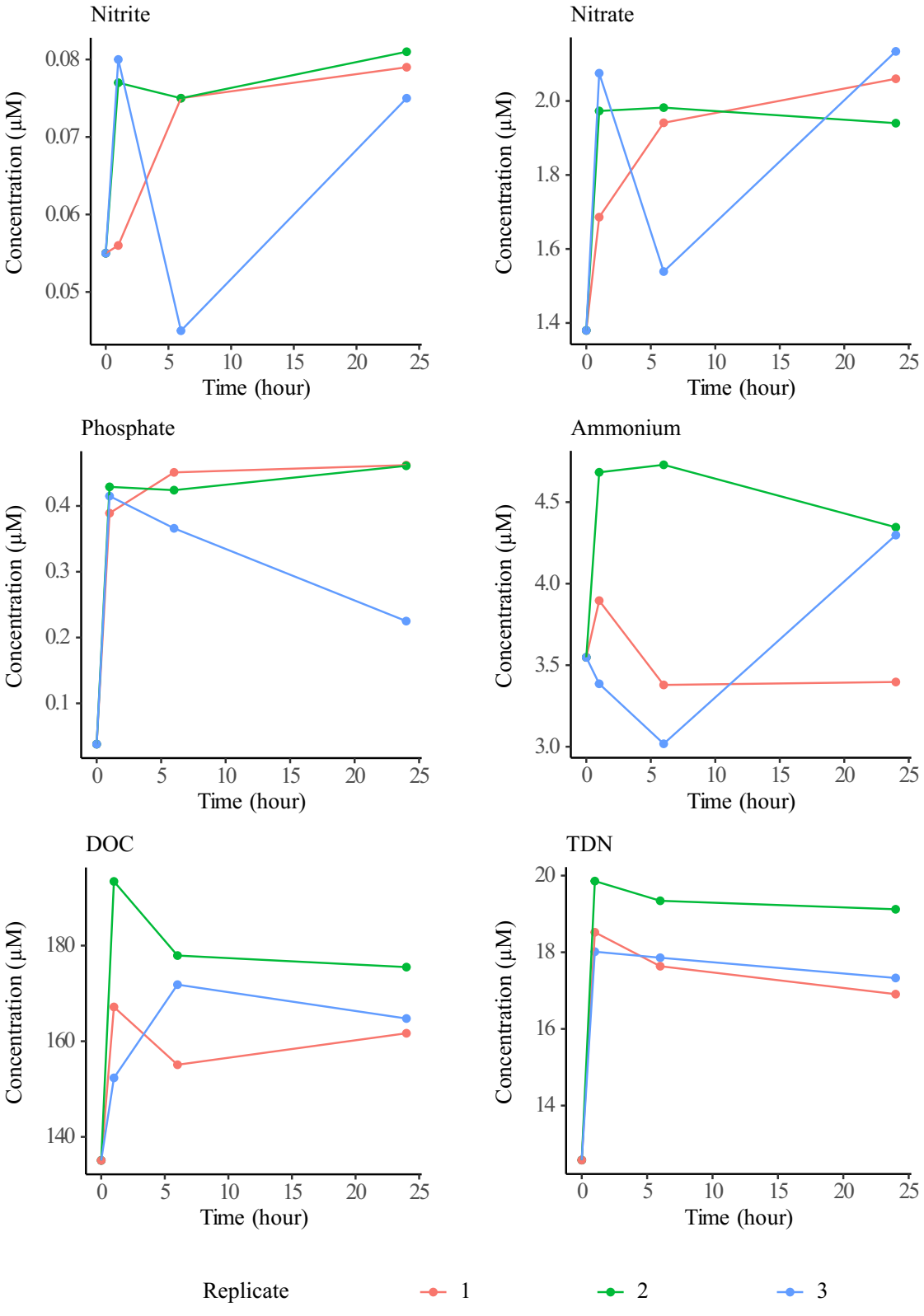
Nitrite
Concentration (µM)
0.08
0.07
0.06
0.05
0
5
10
15
20
25
Time (hour)
Nitrate
Concentration (µM)
2.0
1.8
1.6
1.4
Time (hour)
Phosphate
Concentration (µM)
0.4
0.3
0.2
0.1
Time (hour)
Ammonium
Concentration (µM)
4.5
4.0
3.5
3.0
Time (hour)
DOC
Concentration (µM)
180
160
140
Time (hour)
TDN
Concentration (µM)
20
18
16
14
Time (hour)
Replicate
1
2
3

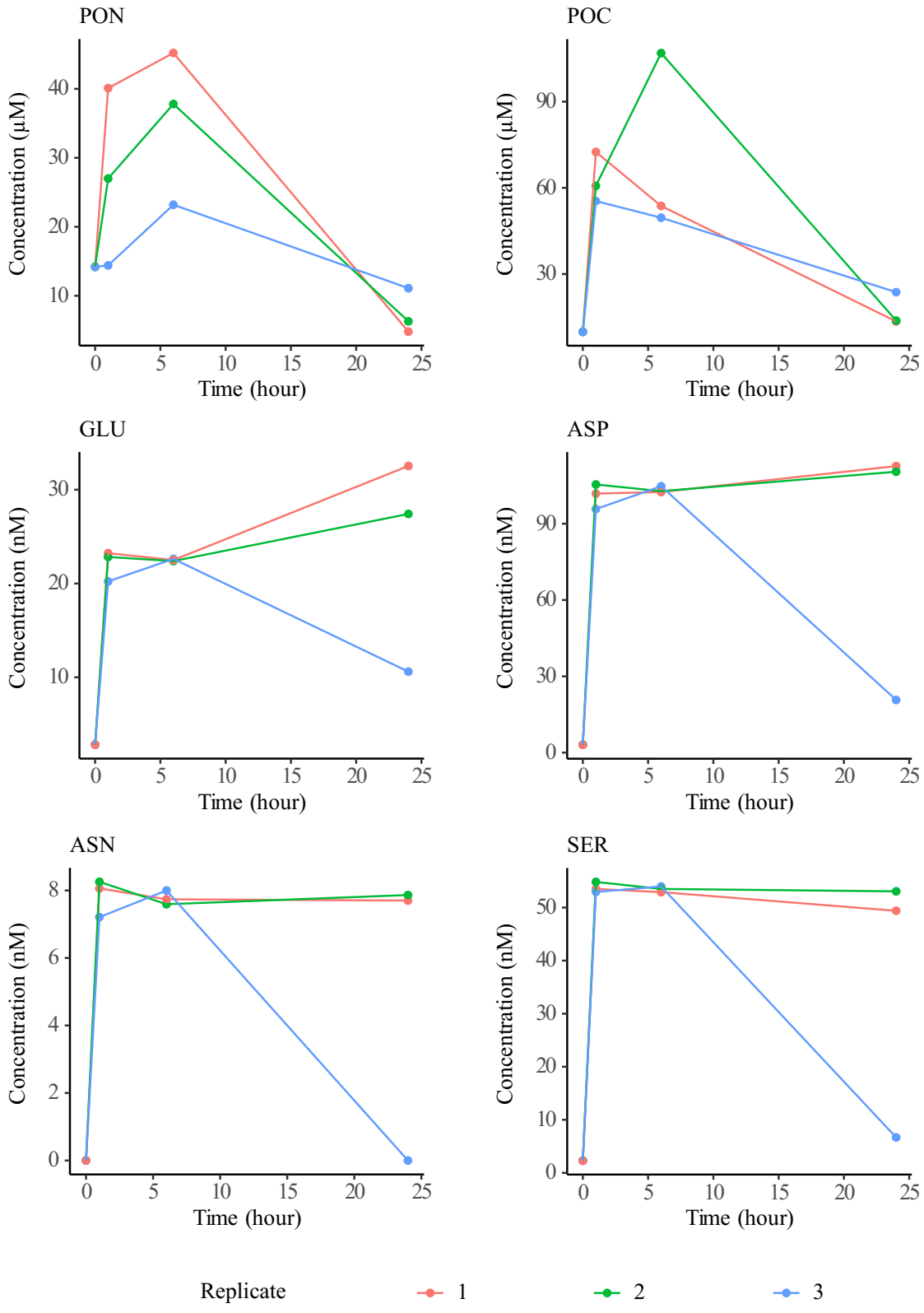
PON
POC
GLU
ASP
ASN
SER
Concentration (µM)
Concentration (nM)
Time (hour)
Replicate
1
2
3

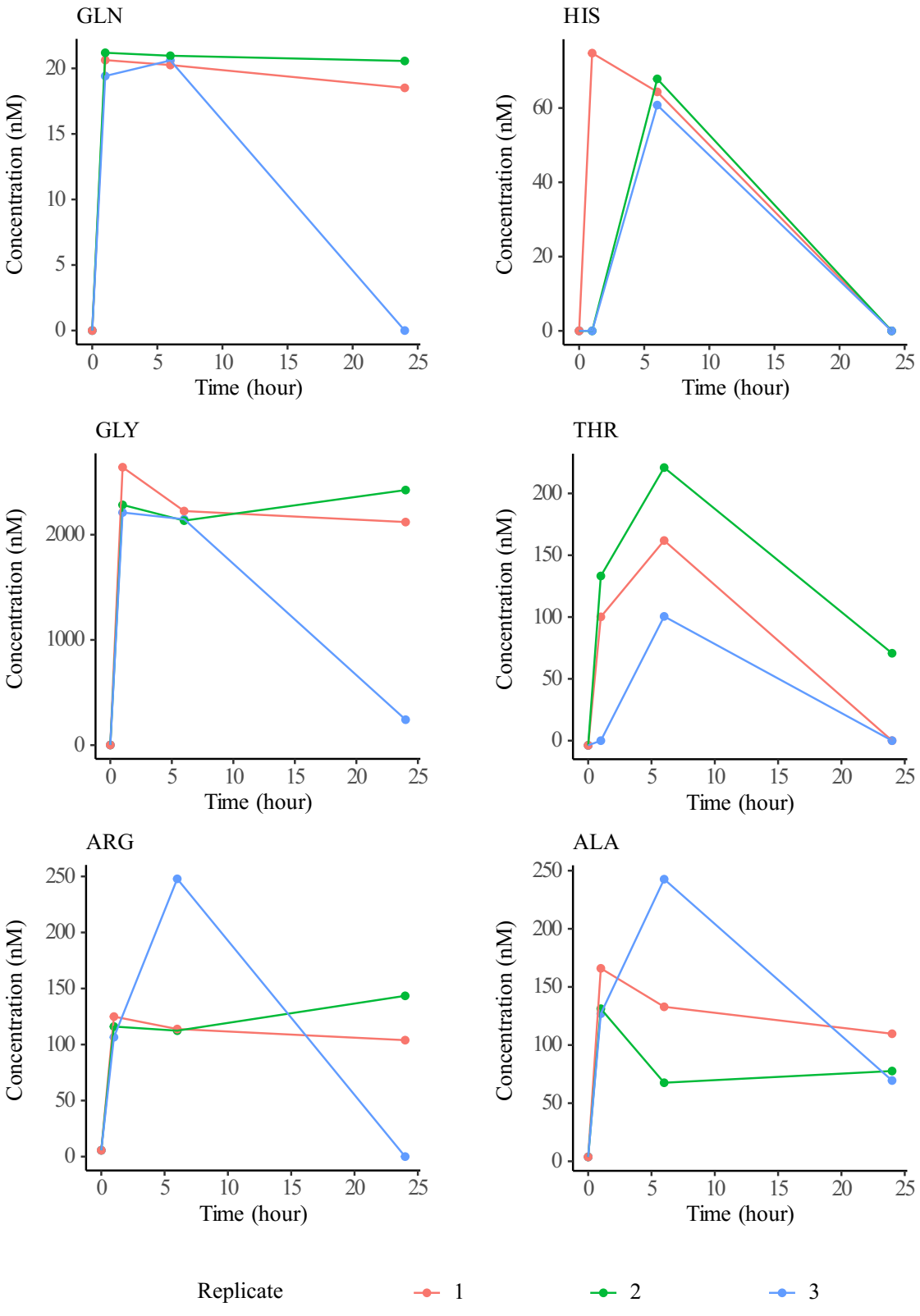
GLN
HIS
GLY
THR
ARG
ALA
Concentration (nM)
Time (hour)
Replicate
1
2
3

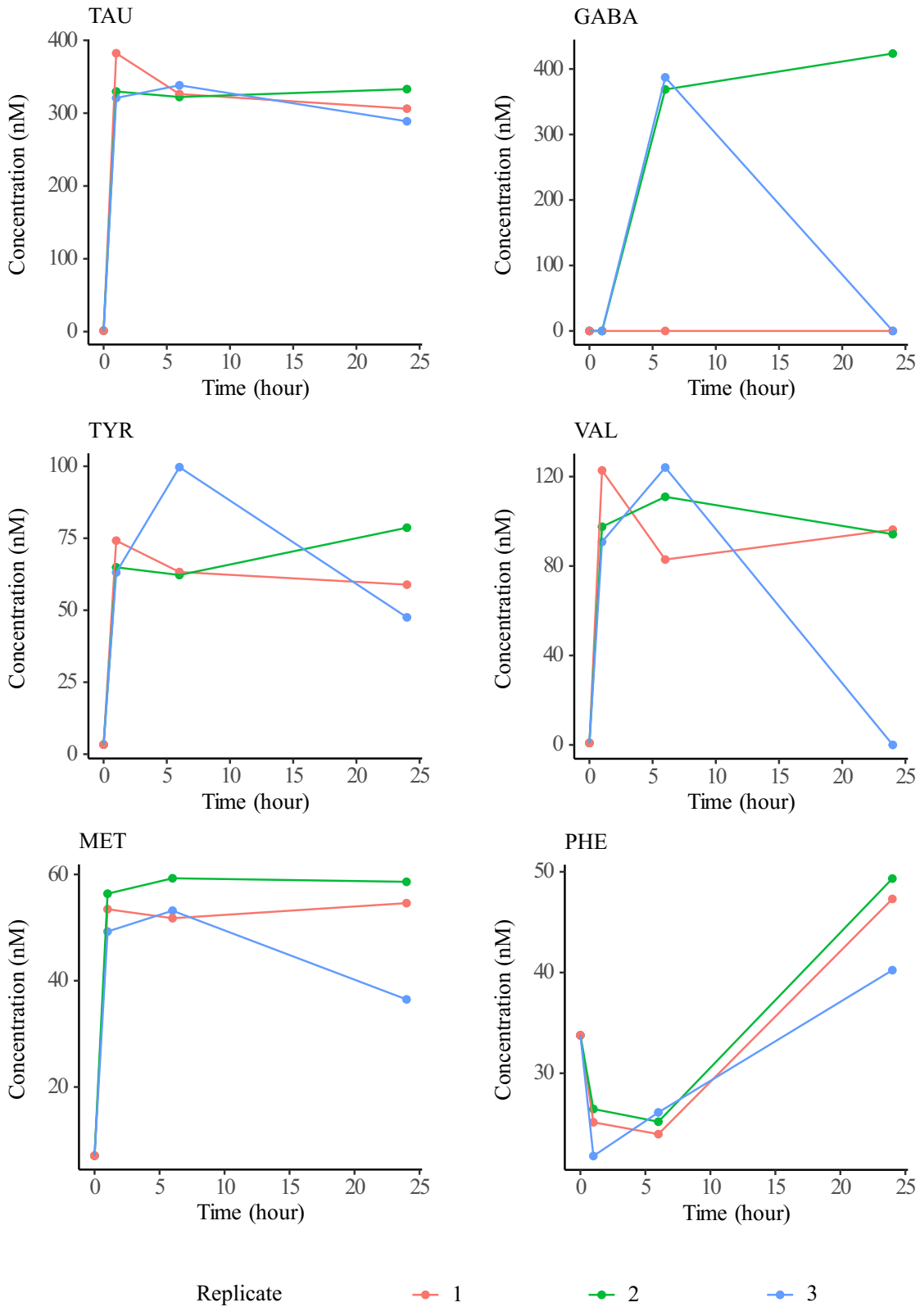
TAU
GABA
TYR
VAL
MET
PHE
Concentration (nM)
Time (hour)
Replicate
1
2
3

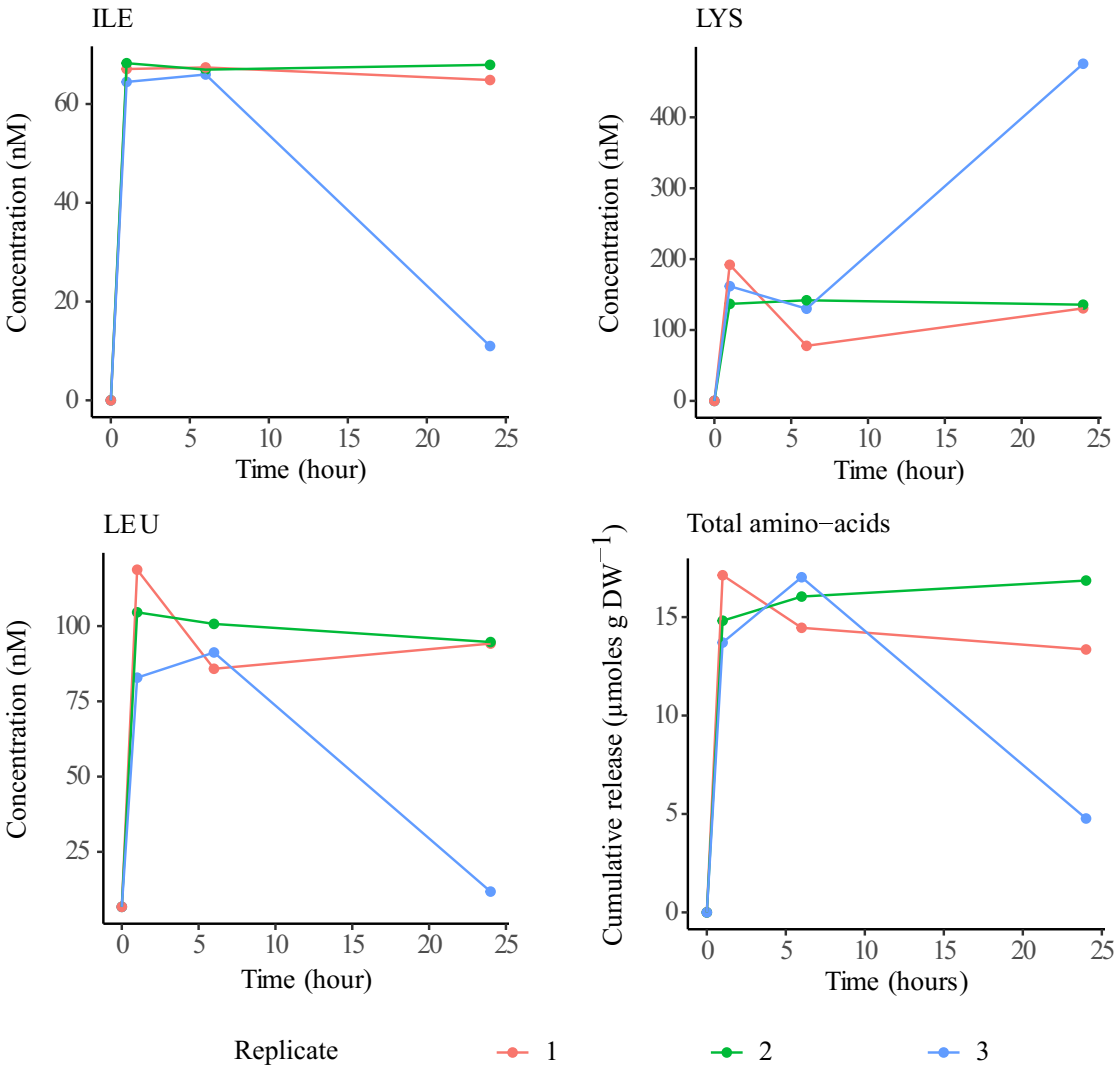

FIGURE C.2: Cumulative amount of dissolved nutrients (NH_4^+, NO_3^-, NO_2^-, PO_4^{3-}, DIN, TDN, DON, DOC, GLU =glutamic acid, ASP=aspartic acid, ASN=asparagine, SER=serine, GLN=glutamine, HIS=histidine, GLY=glycine, THR=threonine, ARG=arginine, ALA=alanine, TAU=taurine, GABA=gamma-aminobutyric acid, TYR=tyrosine, VAL=valine, MET=methionine, PHE=phenylalanine, ILE=isoleucine, LEU=leucine, LYS=lysine) that leached from dry-mucus during 24 hours expressed in µmol per g of DW.

C.4 Leaching experiment - Frozen-mucus

The concentration and composition of the POM, DOM and inorganic nutrients leaching from frozen mucus were determined by dissolving 6.250 g of frozen mucus in 1 L of 0.2 mm filtered aged seawater (ASW) in an acid- and Milli Q water rinsed and combusted glass Erlenmeyer flask placed on a shaker in the dark at room temperature. Triplicate experimental flasks were sampled at 1, 6 and 24 h after the frozen-mucus addition for later analysis of POC, PON, DOC, TDN, DFAA and inorganic nutrients. Bacterial abundance samples were collected to check for contamination.

Due to bacterial contamination, the data from replicate C was not included in the calculation of the final mean values (Figure C.3, Table C.4).

Leaching frozen-mucus (μmol gDW^{-1} d^{-1})		
	mean	sd
NH_4^+	4.48	2.88
NO_3^-	0.26	0.17
NO_2^-	0.04	0.03
PO_4^{3-}	2.22	1.07
DIN	4.78	2.67
TDN	67.60	38.47
DON	62.82	35.79
DOC	383.60	248.34
DFAA	35.89	23.92

TABLE C.4: Cumulative amount of dissolved nutrients (NH_4^+, NO_3^-, NO_2^-, PO_4^{3-}, DIN, TDN, DON, DOC, DFAA) that leached from frozen-mucus within 24 h expressed in µmol per g of DW.

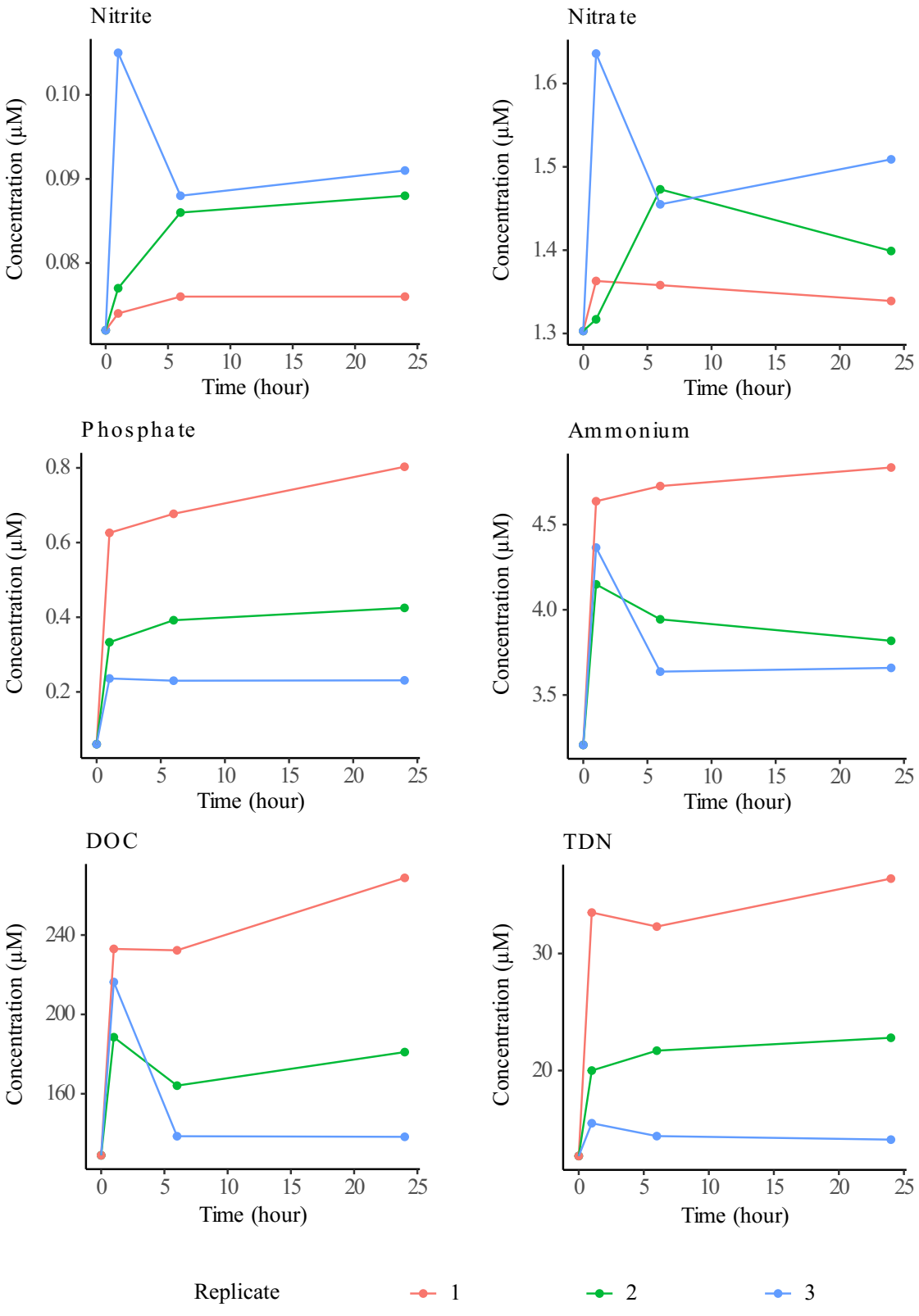
Nitrite
Concentration (µM)
0.10
0.09
0.08
0 5 10 15 20 25
Time (hour)
Nitrate
Concentration (µM)
1.6
1.5
1.4
1.3
0 5 10 15 20 25
Time (hour)
Phosphate
Concentration (µM)
0.8
0.6
0.4
0.2
0 5 10 15 20 25
Time (hour)
Ammonium
Concentration (µM)
4.5
4.0
3.5
0 5 10 15 20 25
Time (hour)
DOC
Concentration (µM)
240
200
160
0 5 10 15 20 25
Time (hour)
TDN
Concentration (µM)
30
20
0 5 10 15 20 25
Time (hour)
Replicate
1
2
3

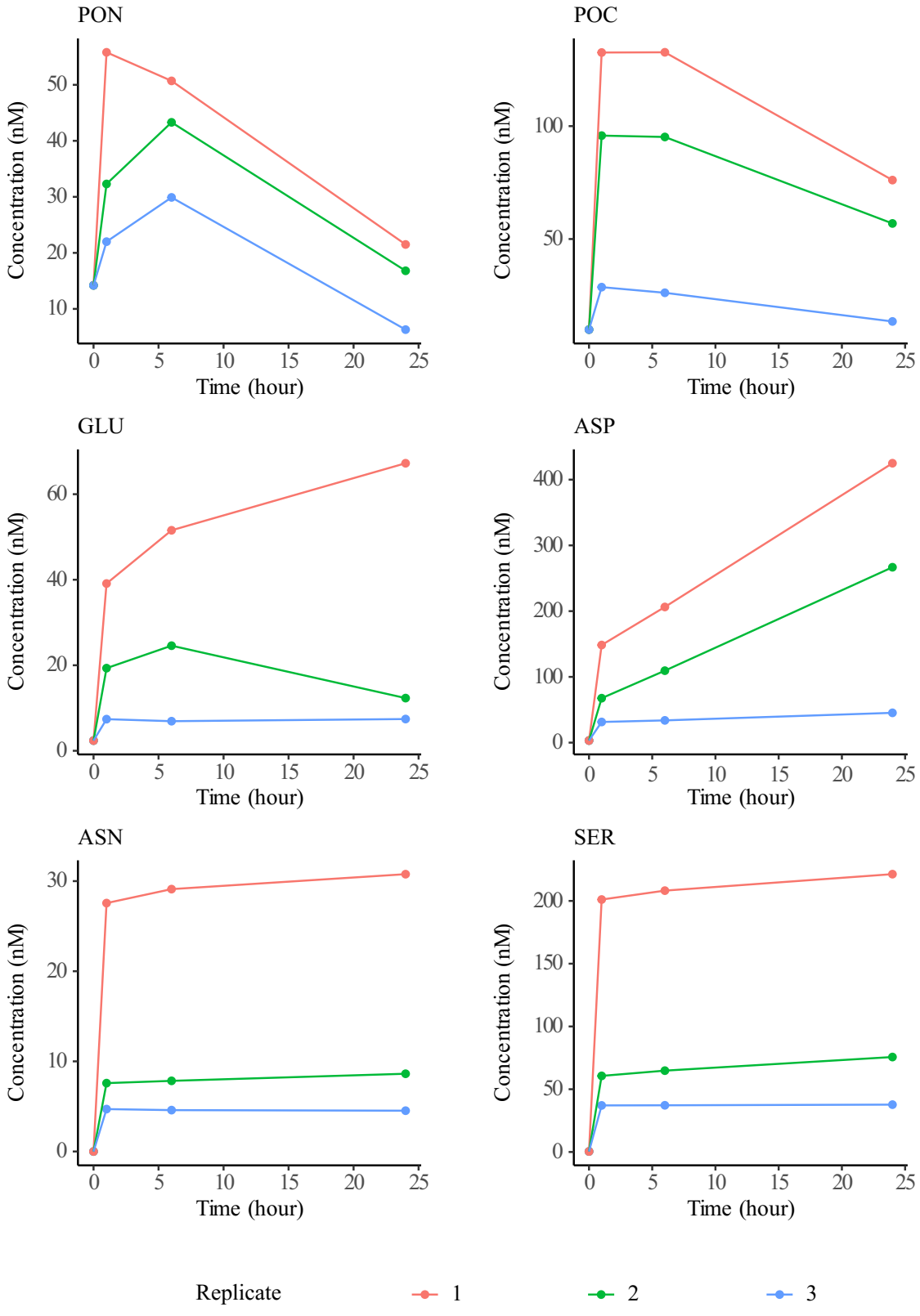
PON
POC
GLU
ASP
ASN
SER
Concentration (nM)
Time (hour)
Replicate
1
2
3

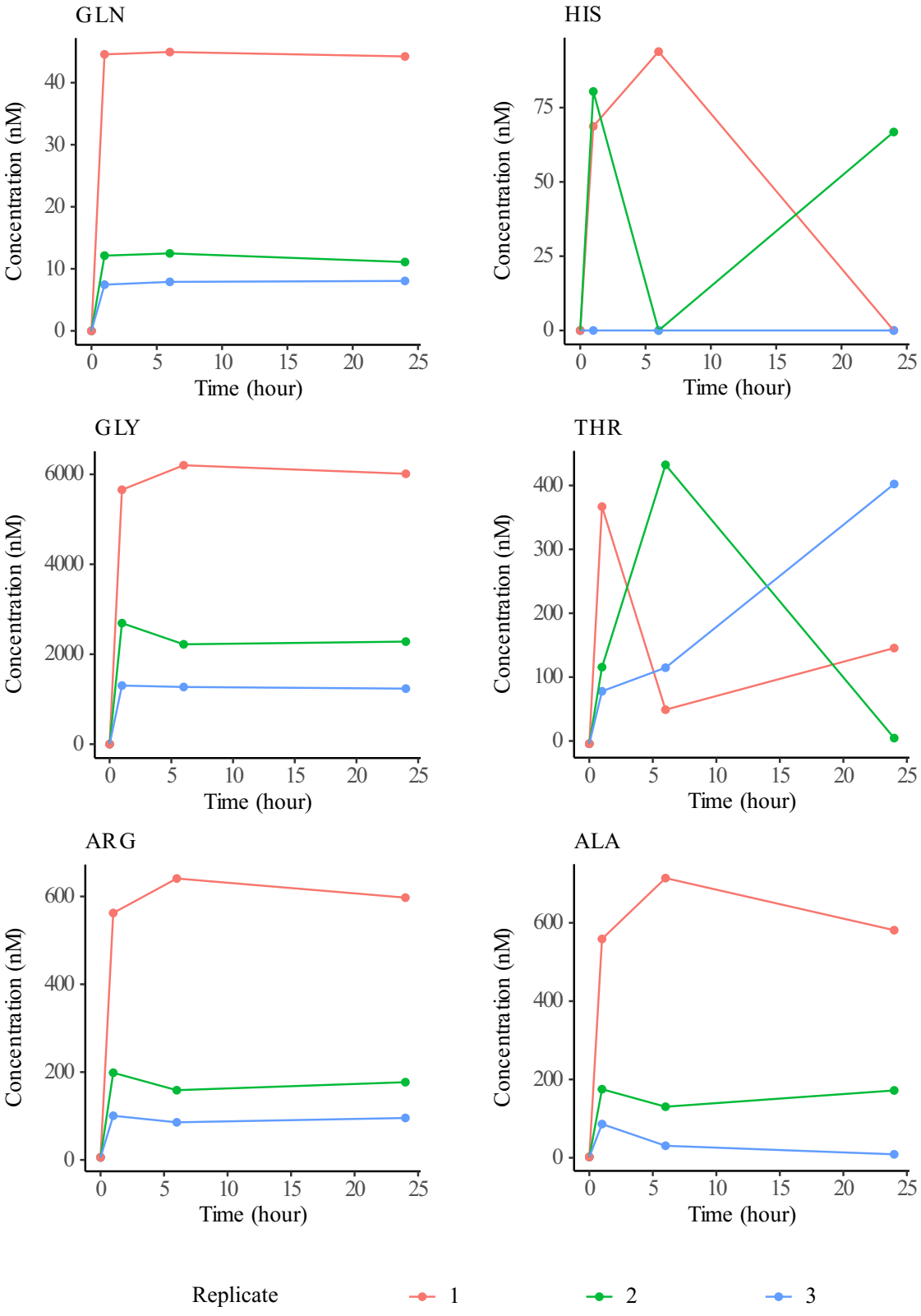
GLN
HIS
GLY
THR
ARG
ALA
Concentration (nM)
Time (hour)
Replicate
1
2
3

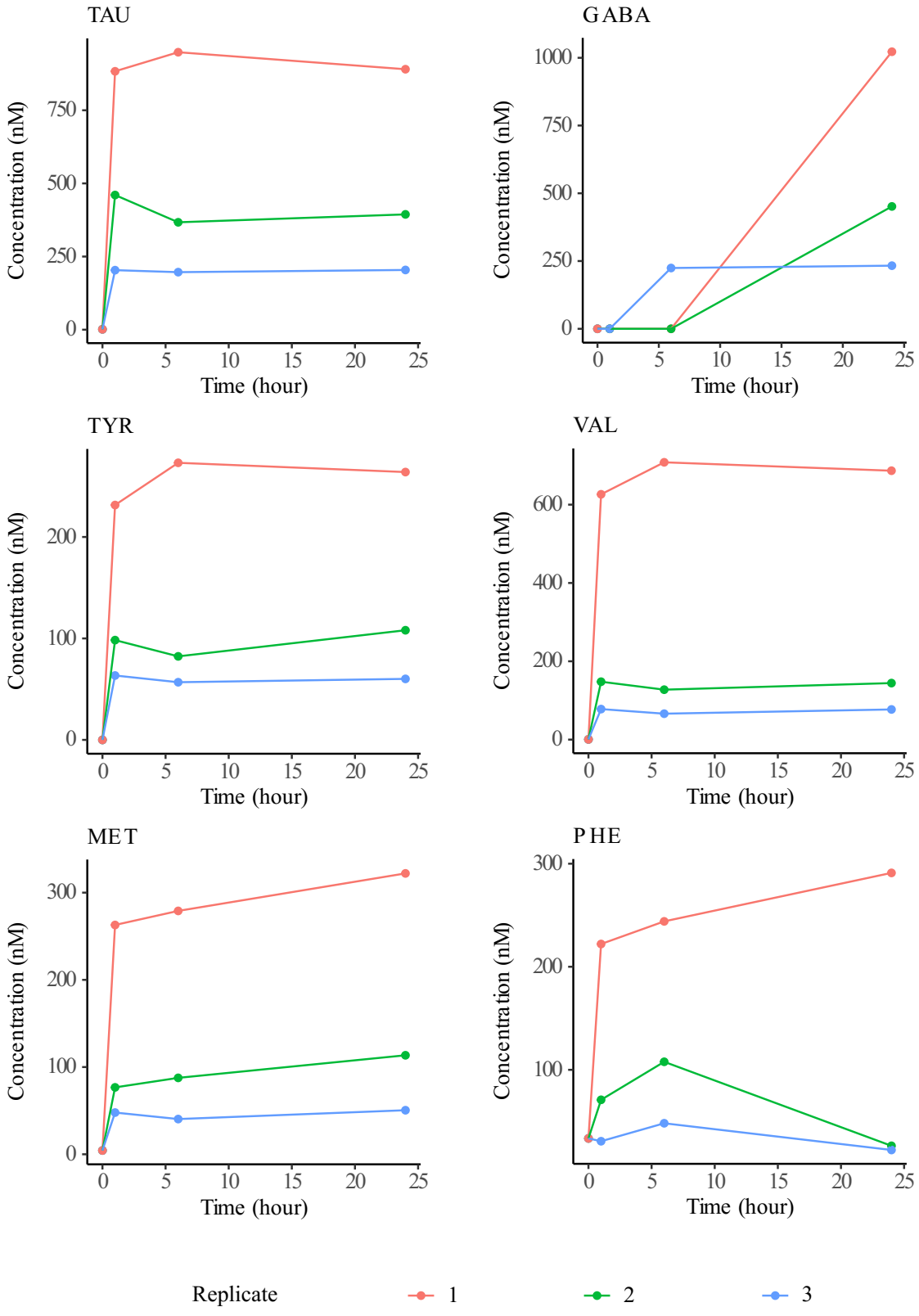
TAU
GABA
TYR
VAL
MET
PHE
Concentration (nM)
Time (hour)
Replicate
1
2
3

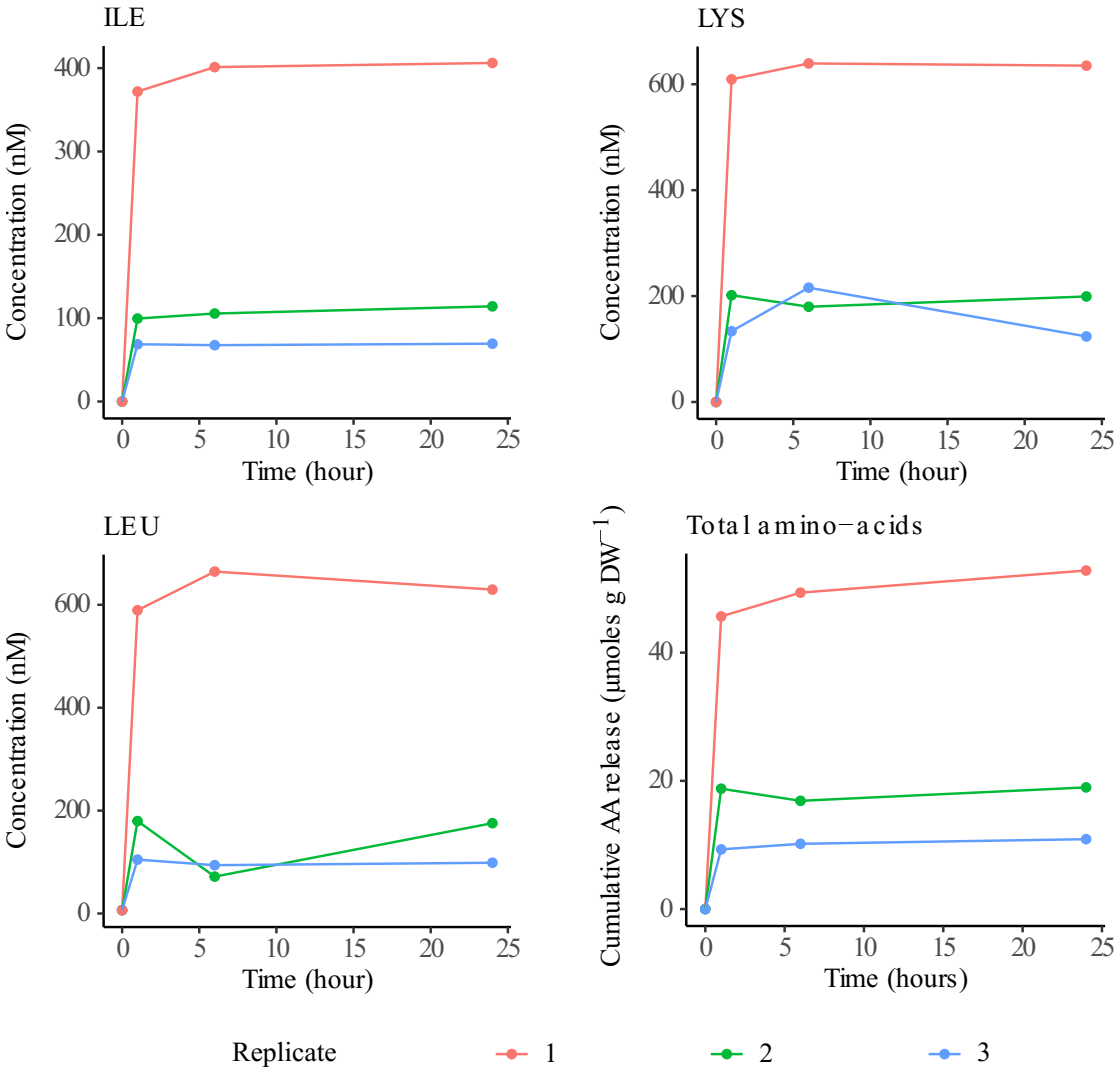

FIGURE C.3: Cumulative amount of dissolved nutrients (NH_4^+, NO_3^-, NO_2^-, PO_4^{3-}, DIN, TDN, DON, DOC, GLU =glutamic acid, ASP=aspartic acid, ASN=asparagine, SER=serine, GLN=glutamine, HIS=histidine, GLY=glycine, THR=threonine, ARG=arginine, ALA=alanine, TAU=taurine, GABA=gamma-aminobutyric acid, TYR=tyrosine, VAL=valine, MET=methionine, PHE=phenylalanine, ILE=isoleucine, LEU=leucine, LYS=lysine) that leached from frozen-mucus during 24 hours expressed in µmol per g of DW.

C.5 Summary tables

Dissolved nutrients

	Dialysis (μmol gDW^{-1} d^{-1})		Leaching dry-mucus (μmol gDW^{-1} d^{-1})		Leaching frozen-mucus (μmol gDW^{-1} d^{-1})	
	mean	sd	mean	sd	mean	sd
NH_4^+	2.02	0.32	1.29	2.68	4.48	2.88
NO_3^-	0.78	0.29	2.48	0.34	0.26	0.17
NO_2^-	<LOD	NA	0.10	0.01	0.04	0.03
PO_4^{3-}	1.48	0.31	1.69	0.00	2.22	1.07
DIN	2.80	0.61	3.87	2.35	4.78	2.67
TDN	21.63	3.71	21.74	6.26	67.60	38.47
DON	18.83	3.11	17.87	3.91	62.82	35.79
DOC	57.49	28.53	134.00	39.13	383.60	248.34
DFAA	9.75	0.58	15.11	2.48	35.89	23.92

TABLE C.5: Summary of dissolved nutrients (NH_4^+, NO_3^-, NO_2^-, PO_4^{3-}, DIN, TDN, DON, DOC, DFAA) released during the dialysis and leaching experiments (dry-mucus and frozen-mucus).

Amino acids

	Leaching dry-mucus				Leaching frozen-mucus				Mean
	Percent (%)	SD (%)	Concentration (nM)	SD (nM)	Percent (%)	SD (%)	Concentration (nM)	SD (nM)	
GLU	0.7	0.2	109.5	13.3	0.3	0.2	148.7	154.1	0.5
ASP	2.9	0.5	433.7	6.6	4.4	1.7	1370.9	447.9	3.6
ASN	0.2	0.0	31.1	0.5	0.2	0.0	78.8	62.6	0.2
SER	1.3	0.1	199.5	15.7	1.6	0.1	588.5	406.7	1.5
GLN	0.5	0.0	78.2	5.8	0.3	0.1	110.7	93.7	0.4
HIS	0.0	0.0	0.0	0.0	0.7	1.0	133.6	188.9	0.4
GLY	60.5	4.2	9084.4	862.1	46.8	1.8	16578.2	10550.9	53.6
THR	0.9	1.2	157.5	201.3	0.7	0.7	316.0	397.3	0.8
ARG	3.1	0.2	471.8	111.3	4.0	0.6	1525.7	1189.3	3.6
ALA	2.5	1.0	363.1	86.0	4.0	0.6	1494.6	1152.8	3.2
TAU	8.5	0.9	1273.0	75.7	7.5	1.1	2563.4	1403.6	8.0
GABA	5.0	7.1	847.1	1198.0	8.6	1.3	2947.7	1614.8	6.8
TYR	1.8	0.1	268.4	65.4	2.1	0.2	737.4	431.6	1.9
VAL	2.5	0.4	378.2	4.9	4.1	1.5	1659.1	1533.2	3.3
MET	1.4	0.1	203.5	19.0	2.3	0.1	848.3	582.2	1.8
PHE	0.4	0.0	58.9	6.7	0.9	1.5	500.2	748.2	0.6
ILE	1.8	0.2	265.6	8.7	2.7	0.5	1040.7	825.9	2.3
LEU	2.4	0.4	351.1	1.8	4.1	0.8	1583.7	1283.5	3.2
LYS	3.6	0.5	532.5	14.6	4.5	0.4	1668.7	1232.8	4.0

TABLE C.6: Percentages and concentrations of the amino acids (GLU =glutamic acid, ASP=aspartic acid, ASN=asparagine, SER=serine, GLN=glutamine, HIS=histidine, GLY=glycine, THR=threonine, ARG=arginine, ALA=alanine, TAU=taurine, GABA=gamma-aminobutyric acid, TYR=tyrosine, VAL=valine, MET=methionine, PHE=phenylalanine, ILE=isoleucine, LEU=leucine, LYS=lysine) released during the leaching experiment by dry-mucus and frozen-mucus. The last column is the mean of the percentage of both leaching experiments.

Low molecular weight compounds

	LMW (μmol gDW^{-1})	Dry-mucus (μmol gDW^{-1})	% of LMW in dry-mucus
DOC	57.5 ± 28.5	134.0 ± 39.1	48 ($\pm$ 35)
TDN	21.6 ± 3.7	21.7 ± 6.3	$\approx$100%
DON	18.8 ± 3.1	17.8 ± 3.9	$\approx$100%

TABLE C.7: Comparative table of the cumulative amount of DOC, TDN and DON that leached through a 1 kDa Molecular Weight Cut-Off (MWCO) membrane tubing within 24 h and that leached directly from dry-mucus in 24h. The fraction <1 kDa represents low molecular weight compounds (LMW). The amount of high molecular weight compounds (HMW, >1 kDa) is expressed as the percentage of total mucus DW per pool of compounds.

Particulate organic matter

The amount of particulate organic matter (POC and PON) released by the mucus was calculated after one hour as the concentrations decreased with time as more material gets dissolved.

	Leaching dry-mucus (μmol gDW^{-1} h^{-1})		Leaching frozen-mucus (μmol gDW^{-1} h^{-1})	
	mean	sd	mean	sd
PON	77.4	37.1	119.4	66.5
POC	226.8	33.4	417.2	104.1

TABLE C.8: Cumulative amount of particulate organic matter (POC and PON) released from dry-mucus and frozen-mucus in 1 h, expressed in µmol per g of DW of mucus per hour.

C.6 Mucus vs Carcasses

Nutrients	Dry-Mucus (µmol gDW^{-1} d^{-1})	Frozen-Mucus (µmol gDW^{-1} d^{-1})	Jelly-DM (µmol gDW^{-1} d^{-1})	Ratio Jelly-DM / dry-mucus	Ratio Jelly-DM / frozen-mucus
NH_4^+	1.3 ± 2.7	4.5 ± 2.9	6.9 ± 6.1	5.3	1.5
NO_3^-	2.5 ± 0.3	0.3 ± 0.2	3.4 ± 3	1.4	12.9
NO_2^-	0.1 ± 0.01	0.04 ± 0.03	0.58 ± 1.1	5.8	14.5
PO_4^{3-}	1.7 ± 0.01	2.2 ± 1.1	6.3 ± 0.85	3.7	2.8
DIN	3.9 ± 2.3	4.8 ± 2.7	10 ± 10	2.6	2.1
TDN	21.7 ± 6.3	67.6 ± 38.5	130 ± 10	6.0	1.9
DON	17.9 ± 3.9	62.8 ± 35.8	120 ± 10	6.7	1.9
DOC	134.0 ± 39.1	383.6 ± 248.3	440 ± 30	3.3	1.1
FDAA	15.1 ± 2.5	35.9 ± 23.9	59.95	4.0	1.7
POC	226.8 ± 33.4	417.2 ± 104.1	420 ± 70	1.9	1.0
PON	77.4 ± 37.1	119.4 ± 66.5	120 ± 10	1.6	1.0

TABLE C.9: Comparison between the nutrients (organic and inorganic) released by dry-mucus, frozen-mucus and freeze-dried jellyfish carcasses (Jelly-DM, Tinta et al. 2020) expressed in µmol gDW^{-1} d^{-1}. The two last columns present the ratio between the amount of nutrient released by Jelly-DM against the dry-mucus and frozen-mucus.

C.7 Mucus degradation experiment

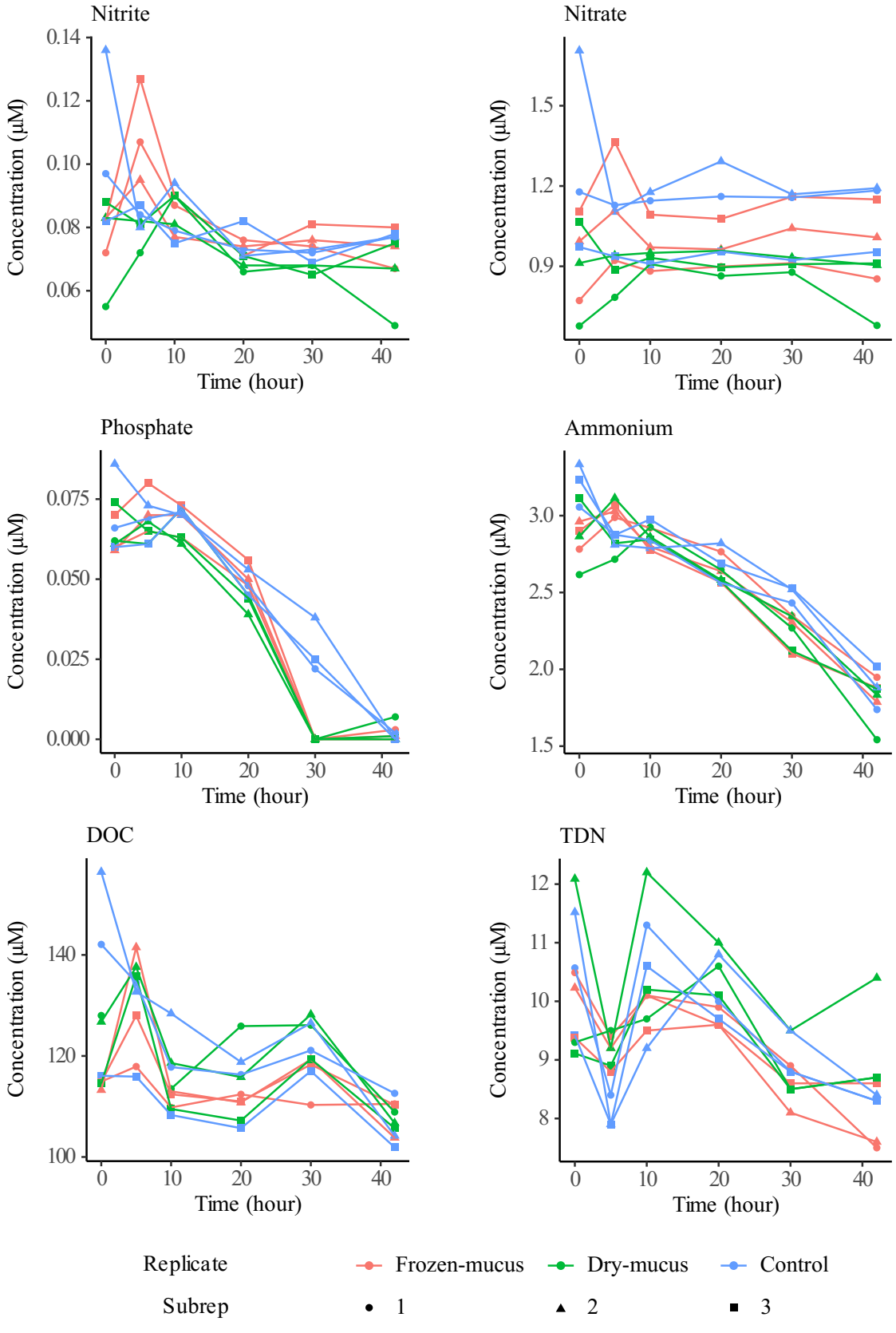

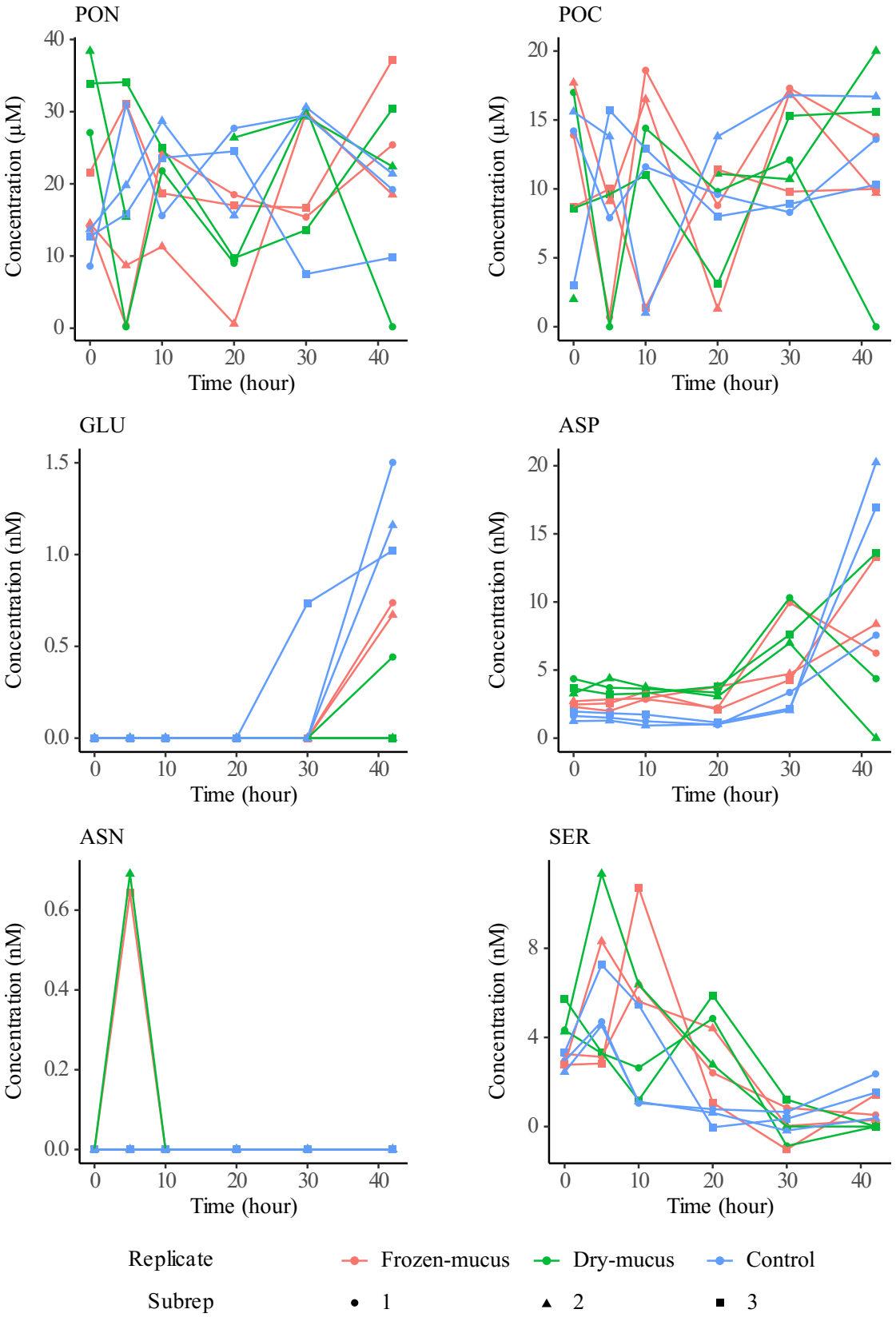
PON
POC
GLU
ASP
ASN
SER
Concentration (µM)
Concentration (nM)
Time (hour)
Replicate
Frozen-mucus
Dry-mucus
Control
Subrep
1
2
3

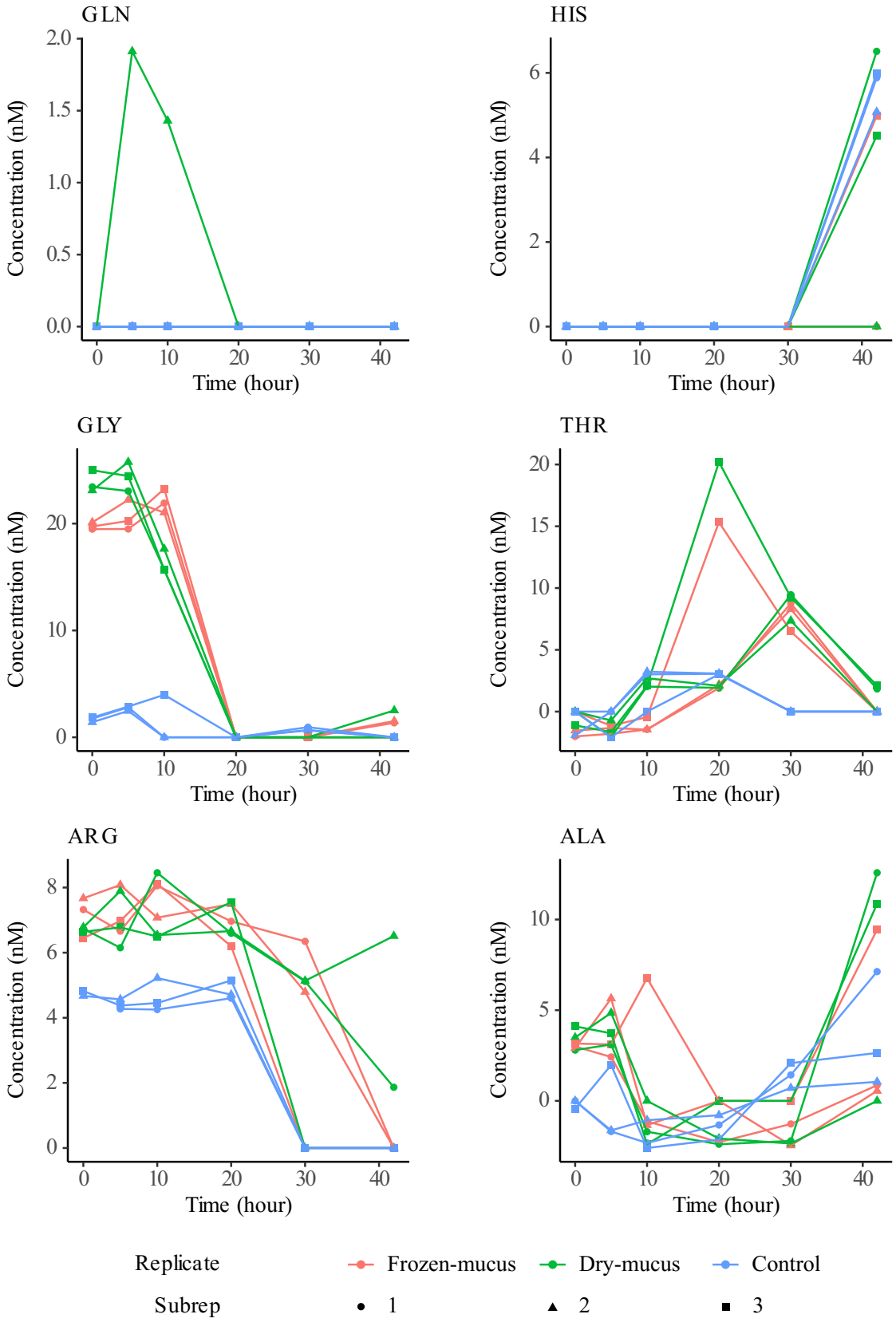
GLN
HIS
GLY
THR
ARG
ALA
Concentration (nM)
Time (hour)
Replicate
Frozen-mucus
Dry-mucus
Control
Subrep
1
2
3

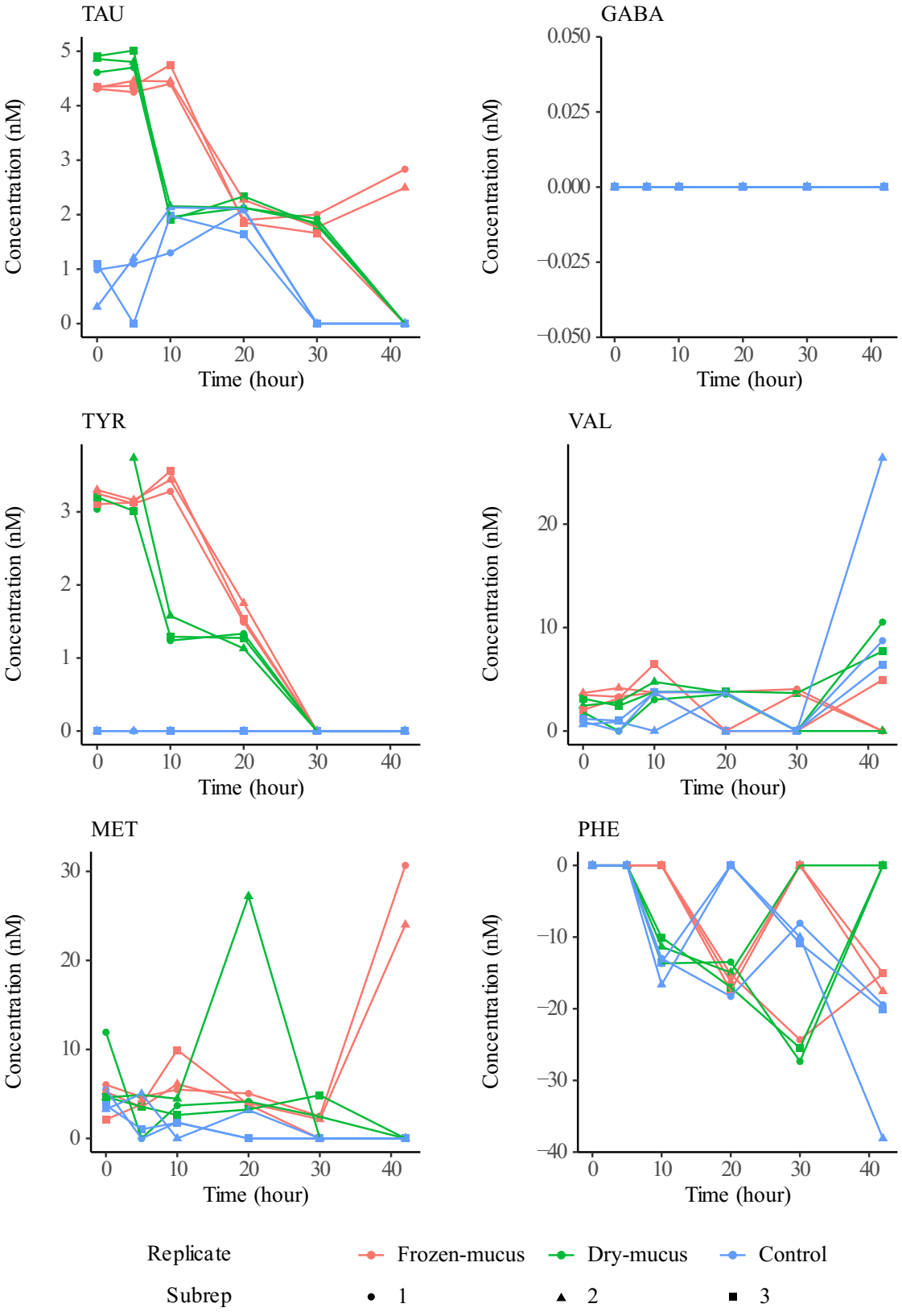
TAU
GABA
TYR
VAL
MET
PHE
Concentration (nM)
Time (hour)
Replicate
Frozen-mucus
Dry-mucus
Control
Subrep
1
2
3

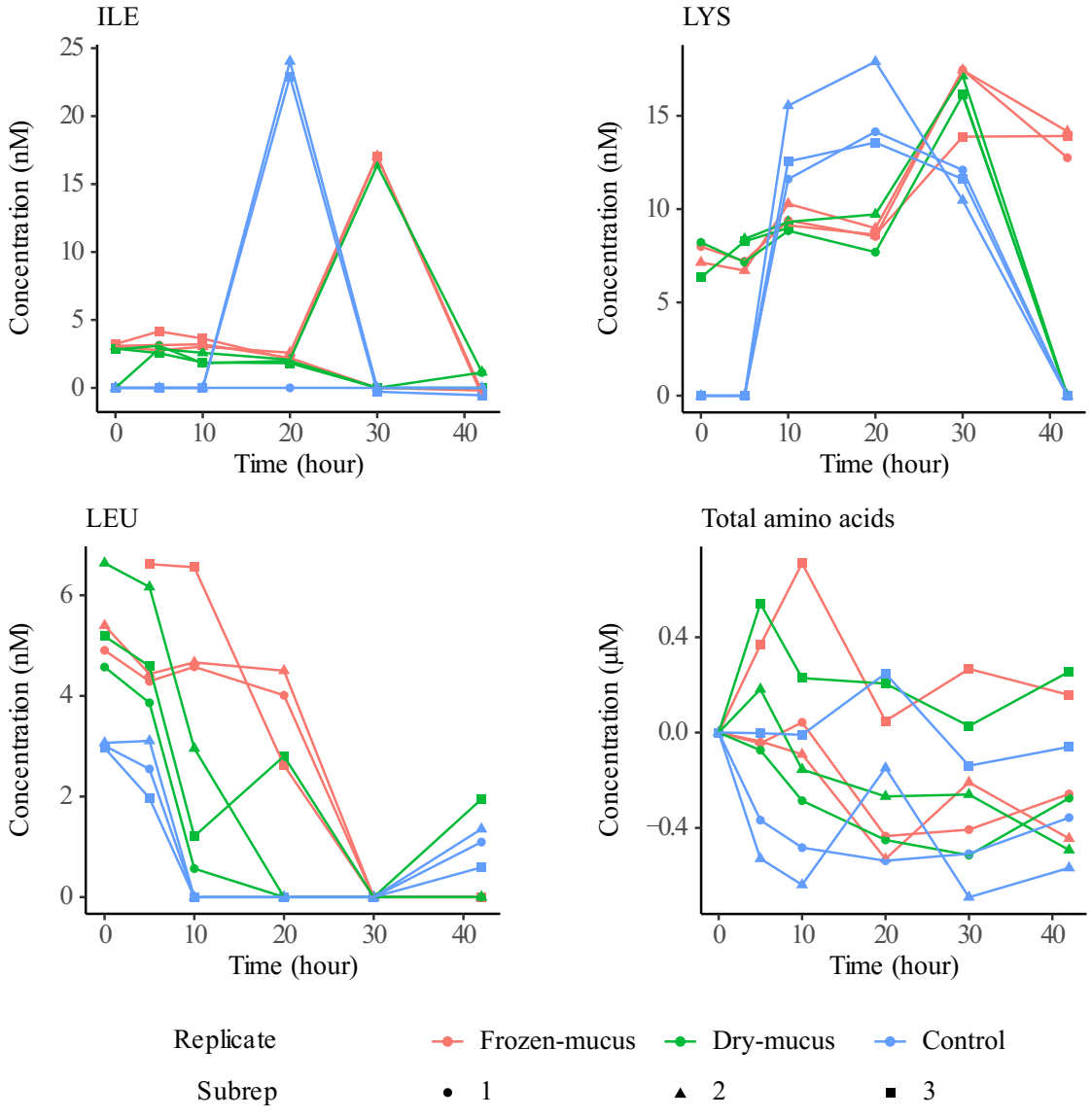

FIGURE C.4: Concentrations of dissolved nutrients (NH_4^+, NO_3^-, NO_2^-, PO_4^{3-}, DIN, TDN, DON, DOC, GLU =glutamic acid, ASP=aspartic acid, ASN=asparagine, SER=serine, GLN=glutamine, HIS=histidine, GLY=glycine, THR=threonine, ARG=arginine, ALA=alanine, TAU=taurine, GABA=gamma-aminobutyric acid, TYR=tyrosine, VAL=valine, MET=methionine, PHE=phenylalanine, ILE=isoleucine, LEU=leucine, LYS=lysine) in treatment incubators (dry-mucus, frozen-mucus and control) during 42 hours expressed in µmol per g of DW.

	Frozen-mucus	Dry-mucus
Dry-mucus	0.037	
Control	0.043	0.035

TABLE C.10: Pairwise beta diversity indices on the relative species abundances from the mucus incubation treatments (dry-mucus, frozen-mucus, control).

Bibliography

Abato, J. (2017). *Monitoring chrysaora hysoscella (cnidaria, scyphozoa) in the belgian part of the north sea using environmental DNA (eDNA).* (Master thesis). Ghent University.

Alvarez Colombo, G., Benović, A., Malej, A., Lučić, D., Makovec, T., Onofri, V., Acha, M., Madirolas, A., & Mianzan, H. (2009). Acoustic survey of a jellyfish-dominated ecosystem (mljet island, croatia). *Hydrobiologia*, *616*(1), 99–111. https://doi.org/10.1007/s10750-008-9587-6

Anderson, M. J. (2017). Permutational multivariate analysis of variance (PERMANOVA). *Wiley StatsRef: Statistics reference online* (pp. 1–15). John Wiley & Sons, Ltd. https://doi.org/10.1002/9781118445112.stat07841

Anderson, M. J., Ellingsen, K. E., & McArdle, B. H. (2006). Multivariate dispersion as a measure of beta diversity. *Ecology Letters*, *9*(6), 683–693. https://doi.org/10.1111/j.1461-0248.2006.00926.x

Andrews, S. (2010). *FastQC: A quality control tool for high throughput sequence data*. http://www.bioinformatics.babraham.ac.uk/projects/fastqc

Arai, M. N. (1996, November 30). *Functional biology of scyphozoa*. Springer.

Arai, M. N. (2009). The potential importance of podocysts to the formation of scyphozoan blooms: A review. In K. A. Pitt, J. E. Purcell, & H. J. Dumont (Eds.), *Jellyfish blooms: Causes, consequences, and recent advances* (pp. 241–246). Springer Netherlands.

Arfi, Y., Lartigue, C., Sirand-Pugnet, P., & Blanchard, A. (2021). Beware of mycoplasma anti-immunoglobulin strategies. *mBio*, *12*(6), e01974–21. https://doi.org/10.1128/mBio.01974-21

Arhonditsis, G. B., Shimoda, Y., & Kelly, N. E. (2019, January 1). Allometric theory: Extrapolations from individuals to ecosystems. In B. Fath (Ed.), *Encyclopedia of ecology (second edition)* (pp. 242–255). Elsevier. https://doi.org/10.1016/B978-0-12-409548-9.10576-7

Arnosti, C. (2011). Microbial extracellular enzymes and the marine carbon cycle. *Annual Review of Marine Science*, *3*(1), 401–425. https://doi.org/10.1146/annurev-marine-120709-142731

Axelsson, M., & Gentili, F. (2014). A single-step method for rapid extraction of total lipids from green microalgae. *PLOS ONE*, *9*(2), e89643. https://doi.org/10.1371/journal.pone.0089643

Azam, F., Fenchel, T., Field, J. G., Gray, J. S., Meyer-Reil, L. A., & Thingstad, F. (1983). The ecological role of water-column microbes in the sea. *Marine Ecology Progress Series*, *10*(3), 257–263.

Bakshani, C. R., Morales-Garcia, A. L., Althaus, M., Wilcox, M. D., Pearson, J. P., Bythell, J. C., & Burgess, J. G. (2018). Evolutionary conservation of the antimicrobial function of mucus: A first defence against infection. *npj Biofilms and Microbiomes*, *4*(1), 14. https://doi.org/10.1038/s41522-018-0057-2

Baltar, F., & Herndl, G. J. (2019). Ideas and perspectives: Is dark carbon fixation relevant for oceanic primary production estimates? [Publisher: Copernicus GmbH]. *Biogeosciences*, *16*(19), 3793–3799. https://doi.org/10.5194/bg-16-3793-2019

Båmstedt, U. (1986). Chemical composition and energy content. *The Biological Chemistry of Marine Copepods*, 1–58.

Båmstedt, U., & Martinussen, M. B. (2000). Estimating digestion rate and the problem of individual variability, exemplified by a scyphozoan jellyfish. *Journal of Experimental Marine Biology and Ecology*, *251*(1), 1–15. https://doi.org/10.1016/S0022-0981(00)00182-9

Bansil, R., & Turner, B. S. (2006). Mucin structure, aggregation, physiological functions and biomedical applications. *Current Opinion in Colloid & Interface Science*, *11*(2), 164–170. https://doi.org/10.1016/j.cocis.2005.11.001

Bansil, R., & Turner, B. S. (2018). The biology of mucus: Composition, synthesis and organization. *Advanced Drug Delivery Reviews*, *124*, 3–15. https://doi.org/10.1016/j.addr.2017.09.023

Basso, L., Rizzo, L., Marzano, M., Intranuovo, M., Fosso, B., Pesole, G., Piraino, S., & Stabili, L. (2019). Jellyfish summer outbreaks as bacterial vectors and potential hazards for marine animals and humans health? the case of rhizostoma pulmo (scyphozoa, cnidaria). *The Science of the Total Environment*, *692*, 305–318. https://doi.org/10.1016/j.scitotenv.2019.07.155

Bastian, T., Lilley, M. K. S., Beggs, S. E., Hays, G. C., & Doyle, T. K. (2014). Ecosystem relevance of variable jellyfish biomass in the irish sea between years, regions and water types. *Estuarine, Coastal and Shelf Science*, *149*, 302–312. https://doi.org/10.1016/j.ecss.2014.08.018

Basu, S., & Mackey, K. R. M. (2018). Phytoplankton as key mediators of the biological carbon pump: Their responses to a changing climate. *Sustainability*, *10*(3), 869. https://doi.org/10.3390/su10030869

Baum, J. K., & Worm, B. (2009). Cascading top-down effects of changing oceanic predator abundances. *Journal of Animal Ecology*, *78*(4), 699–714. https://doi.org/10.1111/j.1365-2656.2009.01531.x

Bayer, S., Countway, P., & Wahle, R. (2019). Developing an eDNA toolkit to quantify broadcast spawning events of the sea scallop placopecten magellanicus: Moving beyond fertilization assays. *Marine Ecology Progress Series*, *621*, 127–141. https://doi.org/10.3354/meps12991

Beaton, A. D., Cardwell, C. L., Thomas, R. S., Sieben, V. J., Legiret, F.-E., Waugh, E. M., Statham, P. J., Mowlem, M. C., & Morgan, H. (2012). Lab-on-chip measurement of nitrate and nitrite for in situ analysis of natural waters. *Environmental Science & Technology*, *46*(17), 9548–9556. https://doi.org/10.1021/es300419u

Benner, R., Biddanda, B., Black, B., & McCarthy, M. (1997). Abundance, size distribution, and stable carbon and nitrogen isotopic compositions of marine organic matter isolated by tangential-flow ultrafiltration. *Marine Chemistry*, *57*(3), 243–263. https://doi.org/10.1016/S0304-4203(97)00013-3

Berggren, M., Laudon, H., Haei, M., Ström, L., & Jansson, M. (2010). Efficient aquatic bacterial metabolism of dissolved low-molecular-weight compounds from terrestrial sources. *The ISME Journal*, *4*(3), 408–416. https://doi.org/10.1038/ismej.2009.120

Birchill, A. J., Clinton-Bailey, G., Hanz, R., Mawji, E., Cariou, T., White, C., Ussher, S. J., Worsfold, P. J., Achterberg, E. P., & Mowlem, M. (2019). Realistic measurement uncertainties for marine macronutrient measurements conducted using gas segmented flow and lab-on-chip techniques. *Talanta*, *200*, 228–235. https://doi.org/10.1016/j.talanta.2019.03.032

Blanchet, M., Pringault, O., Bouvy, M., Catala, P., Oriol, L., Caparros, J., Ortega-Retuerta, E., Intertaglia, L., West, N., Agis, M., Got, P., & Joux, F. (2015). Changes in bacterial community metabolism and composition during the degradation of dissolved organic matter from the jellyfish aurelia aurita in a mediterranean coastal lagoon. *Environmental Science and Pollution Research*, *22*(18), 13638–13653. https://doi.org/10.1007/s11356-014-3848-x

Boero, F. (2013). Review of jellyfish blooms in the mediterranean and black sea. *Studies and Reviews. General Fisheries Commission for the Mediterranean*.

Boero, F., Bouillon, J., Gravili, C., Miglietta, M. P., Parsons, T., & Piraino, S. (2008). Gelatinous plankton: Irregularities rule the world (sometimes). *Marine Ecology Progress Series*, *356*, 299–310. https://doi.org/10.3354/meps07368

Boero, F. (1994). Fluctuations and variations in coastal marine environments. *Marine Ecology*, *15*(1), 3–25. https://doi.org/https://doi.org/10.1111/j.1439-0485.1994.tb00038.x

Boyer, D. C., Boyer, H. J., Fossen, I., & Kreiner, A. (2001). Changes in abundance of the northern benguela sardine stock during the decade 1990–2000, with comments on the relative importance of fishing and the environment. *South African Journal of Marine Science*, *23*(1), 67–84. https://doi.org/10.2989/025776101784528854

Brierley, A. S., Axelsen, B. E., Buecher, E., Sparks, C. A. J., Boyer, H., & Gibbons, M. J. (2001). Acoustic observations of jellyfish in the namibian benguela. *Marine Ecology Progress Series*, *210*, 55–66. https://doi.org/10.3354/meps210055

Bristow, L. A., Mohr, W., Ahmerkamp, S., & Kuypers, M. M. M. (2017). Nutrients that limit growth in the ocean. *Current Biology*, *27*(11), R474–R478. https://doi.org/10.1016/j.cub.2017.03.030

Briz, L. D., Sánchez, F., Marí, N., & Genzano, G. (2018). Seasonal variation of gelatinous plankton consumption by fish in the south-western atlantic ocean: A question of strategy. *Marine Biology Research*, *14*(7), 739–751. https://doi.org/10.1080/17451000.2018.1508847

Brotz, L., Cheung, W. W. L., Kleisner, K., Pakhomov, E., & Pauly, D. (2012). Increasing jellyfish populations: Trends in large marine ecosystems. *Hydrobiologia*, *690*(1), 3–20. https://doi.org/10.1007/s10750-012-1039-7

Brown, J. H., Gillooly, J. F., Allen, A. P., Savage, V. M., & West, G. B. (2004). Toward a metabolic theory of ecology.

Brown, P. C., Painting, S. J., & Cochrane, K. L. (1991). Estimates of phytoplankton and bacterial biomass and production in the northern and southern benguela ecosystems. *South African Journal of Marine Science*, *11*(1), 537–564. https://doi.org/10.2989/025776191784287673

Cardona, L., Quevedo, I. Á. d., Borrell, A., & Aguilar, A. (2012). Massive consumption of gelatinous plankton by mediterranean apex predators. *PLOS ONE*, *7*(3), e31329. https://doi.org/10.1371/journal.pone.0031329

Carlson, C. A., & Hansell, D. A. (2015). Chapter 3 - DOM sources, sinks, reactivity, and budgets. *Biogeochemistry of marine dissolved organic matter (second edition)* (pp. 65–126). Academic Press. https://doi.org/10.1016/B978-0-12-405940-5.00003-0

Carr, M.-E. (2001). Estimation of potential productivity in eastern boundary currents using remote sensing. *Deep Sea Research Part II: Topical Studies in Oceanography*, *49*(1), 59–80. https://doi.org/10.1016/S0967-0645(01)00094-7

Cavan, E. L., Trimmer, M., Shelley, F., & Sanders, R. (2017). Remineralization of particulate organic carbon in an ocean oxygen minimum zone. *Nature Communications*, *8*, 14847. https://doi.org/10.1038/ncomms14847

Chen, S., Ling, J., & Blancheton, J.-P. (2006). Nitrification kinetics of biofilm as affected by water quality factors. *Aquacultural Engineering*, *34*(3), 179–197. https://doi.org/10.1016/j.aquaeng.2005.09.004

Cheng, X., Shao, Z., Li, C., Yu, L., Raja, M., & Liu, C. (2017). Isolation, characterization and evaluation of collagen from jellyfish rhopilema esculentum kishinouye for use in hemostatic applications. *PLOS ONE*, *12*, e0169731. https://doi.org/10.1371/journal.pone.0169731

Cheung, W., Ota, Y., & Cisneros-Montemayor, A. (2019, August 17). *Predicting future oceans: Sustainability of ocean and human systems amidst global environmental change*. Elsevier.

Chugoku Regional Development Bureau. (2018). Ohashi river improvement project environmental monitoring (results of monitoring in 2017). Ministry of Land, Infrastructure, Transport; Tourism.

Clark, D. R., Rees, A. P., Ferrera, C. M., Al-Moosawi, L., Somerfield, P. J., Harris, C., Quartly, G. D., Goult, S., Tarran, G., & Lessin, G. (2022). Nitrite regeneration in the oligotrophic atlantic ocean [Publisher: Copernicus GmbH]. *Biogeosciences*, *19*(5), 1355–1376. https://doi.org/10.5194/bg-19-1355-2022

Clarke, A., Holmes, L. J., & Gore, D. J. (1992). Proximate and elemental composition of gelatinous zooplankton from the southern ocean. *Journal of Experimental Marine Biology and Ecology*, *155*(1), 55–68. https://doi.org/10.1016/0022-0981(92)90027-8

Cloern, J. E., Foster, S. Q., & Kleckner, A. E. (2014). Phytoplankton primary production in the world's estuarine-coastal ecosystems. *Biogeosciences*, *11*(9), 2477–2501. https://doi.org/https://doi.org/10.5194/bg-11-2477-2014

Condon, R., K. Steinberg, D., & Bronk, D. (2010, February 1). *Production of dissolved organic matter and inorganic nutrients by gelatinous zooplankton in the york river estuary, chesapeake bay* (Vol. 32). https://doi.org/10.1093/plankt/fbp109

Condon, R. H., Graham, W. M., Duarte, C. M., Pitt, K. A., Lucas, C. H., Haddock, S. H. D., Sutherland, K. R., Robinson, K. L., Dawson, M. N., Decker, M. B., Mills, C. E., Purcell, J. E., Malej, A., Mianzan, H., Uye, S.-i., Gelcich, S., & Madin, L. P. (2012). Questioning the rise of gelatinous zooplankton in the world's oceans. *BioScience*, *62*(2), 160–169. https://doi.org/10.1525/bio.2012.62.2.9

Condon, R. H., Steinberg, D. K., Giorgio, P. A. d., Bouvier, T. C., Bronk, D. A., Graham, W. M., & Ducklow, H. W. (2011). Jellyfish blooms result in a major microbial respiratory sink of carbon in marine systems. *Proceedings of the National Academy of Sciences*, *108*(25), 10225–10230. https://doi.org/10.1073/pnas.1015782108

Conley, D. J., Paerl, H. W., Howarth, R. W., Boesch, D. F., Seitzinger, S. P., Havens, K. E., Lancelot, C., & Likens, G. E. (2009). Controlling eutrophication: Nitrogen and phosphorus. *Science*, *323*(5917), 1014–1015. https://doi.org/10.1126/science.1167755

Cortés-Lara, S., Urdiain, M., Mora-Ruiz, M., Prieto, L., & Rosselló-Móra, R. (2015). Prokaryotic microbiota in the digestive cavity of the jellyfish cotylorhiza tuberculata. *Systematic and Applied Microbiology*, *38*(7), 494–500. https://doi.org/10.1016/j.syapm.2015.07.001

Cox, P. M., Betts, R. A., Jones, C. D., Spall, S. A., & Totterdell, I. J. (2000). Acceleration of global warming due to carbon-cycle feedbacks in a coupled climate model. *Nature*, *408*(6809), 184–187. https://doi.org/10.1038/35041539

Dandekar, T., Snel, B., Schmidt, S., Lathe, W., Suyama, M., Huynen, M., & Bork, P. (2002). Comparative genome analysis of the mollicutes. In S. Razin & R. Herrmann (Eds.), *Molecular biology and pathogenicity of mycoplasmas* (pp. 255–278). Springer US. https://doi.org/10.1007/0-306-47606-1_11

Davies, J. M., & Viney, C. (1998). Water–mucin phases: Conditions for mucus liquid crystallinity1presented at TAC 97, oxford, UK, 14–15 april 1997.1. *Thermochimica Acta*, *315*(1), 39–49. https://doi.org/10.1016/S0040-6031(98)00275-5

Dawson, M. N., Gupta, A. S., & England, M. H. (2005). Coupled biophysical global ocean model and molecular genetic analyses identify multiple introductions of cryptogenic species. *Proceedings of the National Academy of Sciences of the United States of America*, *102*(34), 11968–11973. https://doi.org/10.1073/pnas.0503811102

Dawson, M. N., & Martin, L. E. (2001, February). *Geographic variation and ecological adaptation in aurelia (scyphozoa, semaeostomeae): Some implications from molecular phylogenetics*.

Dawson, M. (2003). Macro-morphological variation among cryptic species of the moon jellyfish, aurelia (cnidaria: Scyphozoa). *Marine Biology*, *143*(2), 369–379. https://doi.org/10.1007/s00227-003-1070-3

De La Rocha, C. L., & Passow, U. (2007). Factors influencing the sinking of POC and the efficiency of the biological carbon pump. *Deep Sea Research Part II: Topical Studies in Oceanography*, *54*(5), 639–658. https://doi.org/10.1016/j.dsr2.2007.01.004

del Giorgio, P. A., & Cole, J. J. (1998). Bacterial growth efficiency in natural aquatic systems. *Annual Review of Ecology and Systematics*, *29*(1), 503–541. https://doi.org/10.1146/annurev.ecolsys.29.1.503

Dittmar, T., Lennartz, S. T., Buck-Wiese, H., Hansell, D. A., Santinelli, C., Vanni, C., Blasius, B., & Hehemann, J.-H. (2021). Enigmatic persistence of dissolved organic matter in the ocean. *Nature Reviews Earth & Environment*, *2*(8), 570–583. https://doi.org/10.1038/s43017-021-00183-7

Doyle, T. K., Hays, G. C., Harrod, C., & Houghton, J. D. R. (2014). Ecological and societal benefits of jellyfish. In K. A. Pitt & C. H. Lucas (Eds.), *Jellyfish blooms* (pp. 105–127). Springer Netherlands. https://doi.org/10.1007/978-94-007-7015-7_5

Doyle, T. K., Houghton, J. D. R., McDevitt, R., Davenport, J., & Hays, G. C. (2007). The energy density of jellyfish: Estimates from bomb-calorimetry and proximate-composition. *Journal of Experimental Marine Biology and Ecology*, *343*(2), 239–252. https://doi.org/10.1016/j.jembe.2006.12.010

DuBois, M., Gilles, K. A., Hamilton, J. K., Rebers, P. A., & Smith, F. G. (1956). Colorimetric method for determination of sugars and related substances. *Analytical Chemistry*, *28*(3), 350–356. https://doi.org/10.1021/ac60111a017

Ducklow, H., Steinberg, D., & Buesseler, K. (2001). Upper ocean carbon export and the biological pump. *Oceanography*, *14*(4), 50–58. https://doi.org/10.5670/oceanog.2001.06

Ducklow, H. W., & Mitchell, R. (1979). Composition of mucus released by coral reef coelenterates1. *Limnology and Oceanography*, *24*(4), 706–714. https://doi.org/10.4319/lo.1979.24.4.0706

Dunlop, K. M., Jones, D. O. B., & Sweetman, A. K. (2017). Direct evidence of an efficient energy transfer pathway from jellyfish carcasses to a commercially important deep-water species. *Scientific Reports*, *7*(1), 17455. https://doi.org/10.1038/s41598-017-17557-x

Durazzi, F., Sala, C., Castellani, G., Manfreda, G., Remondini, D., & De Cesare, A. (2021). Comparison between 16s rRNA and shotgun sequencing data for the taxonomic characterization of the gut microbiota. *Scientific Reports*, *11*(1), 3030. https://doi.org/10.1038/s41598-021-82726-y

Edelist, D., Knutsen, Ø., Ellingsen, I., Majaneva, S., Aberle, N., Dror, H., & Angel, D. L. (2022). Tracking jellyfish swarm origins using a combined oceanographic-genetic-citizen science approach. *Frontiers in Marine Science*, *9*. Retrieved November 11, 2022, from https://www.frontiersin.org/articles/10.3389/fmars.2022.869619

Elser, J. J., & Hassett, R. P. (1994). A stoichiometric analysis of the zooplankton–phytoplankton interaction in marine and freshwater ecosystems. *Nature*, *370*(6486), 211–213. https://doi.org/10.1038/370211a0

FAO. (2015). FAO fisheries & aquaculture - fishery and aquaculture country profiles - the republic of namibia.

Feller, W. F., Henslee, J. G., Kinders, R. J., Manderino, G. L., Tomita, J. T., & Rittenhouse, H. G. (1990). Mucin glycoproteins as tumor markers. *Immunology Series*, *53*, 631–672.

Flammang, P., Demeuldre, M., Hennebert, E., & Santos, R. (2016). Adhesive secretions in echinoderms: A review. In A. M. Smith (Ed.), *Biological adhesives* (pp. 193–222). Springer International Publishing. https://doi.org/10.1007/978-3-319-46082-6_9

Flynn, B. A., Richardson, A. J., Brierley, A. S., Boyer, D. C., Axelsen, B. E., Scott, L., Moroff, N. E., Kainge, P. I., Tjizoo, B. M., & Gibbons, M. J. (2012). Temporal and spatial patterns in the abundance of jellyfish in the northern benguela upwelling ecosystem and their link to thwarted pelagic fishery recovery. *African Journal of Marine Science*, *34*(1), 131–146. https://doi.org/10.2989/1814232X.2012.675122

Fonvielle, J. A., Reynaud, S., Jacquet, S., LeBerre, B., & Ferrier-Pages, C. (2015). First evidence of an important organic matter trophic pathway between temperate corals and pelagic microbial communities. *PLOS ONE*, *10*(10), e0139175. https://doi.org/10.1371/journal.pone.0139175

Fréon, P., Arístegui, J., Bertrand, A., Crawford, R. J. M., Field, J. C., Gibbons, M. J., Tam, J., Hutchings, L., Masski, H., Mullon, C., Ramdani, M., Seret, B., & Simier, M. (2009). Functional group biodiversity in eastern boundary upwelling ecosystems questions the wasp-waist trophic structure. *Progress in Oceanography*, *83*(1), 97–106. https://doi.org/10.1016/j.pocean.2009.07.034

Füssel, J., Lücker, S., Yilmaz, P., Nowka, B., Kessel, M. A. H. J. v., Bourceau, P., Hach, P. F., Littmann, S., Berg, J., Spieck, E., Daims, H., Kuypers, M. M. M., & Lam, P. (2017). Adaptability as the key to success for the ubiquitous marine nitrite oxidizer nitrococcus. *Science Advances*, *3*(11), e1700807. https://doi.org/10.1126/sciadv.1700807

Ganesan, A. R., Mohanram, M. S. G., Balasubramanian, B., Ho Kim, I., Seedevi, P., Mohan, K., Kanagasabai, S., Valan Arasu, M., Abdullah Al-Dhabi, N., & Ignacimuthu, S. (2020). Marine invertebrates' proteins: A recent update on functional property. *Journal of King Saud University - Science*, *32*(2), 1496–1502. https://doi.org/10.1016/j.jksus.2019.12.003

Gemmell, B. J., Costello, J. H., Colin, S. P., Stewart, C. J., Dabiri, J. O., Tafti, D., & Priya, S. (2013). Passive energy recapture in jellyfish contributes to propulsive advantage over other metazoans. *Proceedings of the National Academy of Sciences*, *110*(44), 17904–17909. https://doi.org/10.1073/pnas.1306983110

Gerhardt, P., Murray, R., Krieg, N., & Wood, W. (1994). *Methods for general and molecular bacteriology*. American Society for Microbiology.

Ghermandi, A., Galil, B., Gowdy, J., & Nunes, P. A. L. D. (2015). Jellyfish outbreak impacts on recreation in the mediterranean sea: Welfare estimates from a socioeconomic pilot survey in israel. *Ecosystem Services*, *11*, 140–147. https://doi.org/10.1016/j.ecoser.2014.12.004

Gibbons, M. J., & Richardson, A. J. (2013). Beyond the jellyfish joyride and global oscillations: Advancing jellyfish research. *Journal of Plankton Research*, *35*(5), 929–938. https://doi.org/10.1093/plankt/fbt063

Giering, S. L. C., & Evans, C. (2022). Overestimation of prokaryotic production by leucine incorporation—and how to avoid it. *Limnology and Oceanography*, *67*(3), 726–738. https://doi.org/10.1002/lno.12032

Giering, S. L. C., Steigenberger, S., Achterberg, E. P., Sanders, R., & Mayor, D. J. (2012). Elevated iron to nitrogen recycling by mesozooplankton in the northeast atlantic ocean. *Geophysical Research Letters*, *39*(12). https://doi.org/10.1029/2012GL051776

Gnanadesikan, A., & Marinov, I. (2008). Export is not enough:: Nutrient cycling and carbon sequestration. *Marine Ecology Progress Series*, *364*, 289–294. https://doi.org/10.3354/meps07550

Godwin, C. M., & Cotner, J. B. (2015). Aquatic heterotrophic bacteria have highly flexible phosphorus content and biomass stoichiometry. *The ISME Journal*, *9*(10), 2324–2327. https://doi.org/10.1038/ismej.2015.34

Gordoa, A., Acuña, J. L., Farrés, R., & Bacher, K. (2013). Burst feeding of pelagia noctiluca ephyrae on atlantic bluefin tuna (thunnus thynnus) eggs. *PLOS ONE*, *8*(9), e74721. https://doi.org/10.1371/journal.pone.0074721

Graham, W. M., & Kroutil, R. M. (2001). Size-based prey selectivity and dietary shifts in the jellyfish, aurelia aurita. *Journal of Plankton Research*, *23*(1), 67–74. https://doi.org/10.1093/plankt/23.1.67

Griffin, D. C., Harrod, C., Houghton, J. D. R., & Capellini, I. (2019). Unravelling the macro-evolutionary ecology of fish–jellyfish associations: Life in the 'gingerbread house'. *Proceedings of the Royal Society B: Biological Sciences*, *286*(1899), 20182325. https://doi.org/10.1098/rspb.2018.2325

Gruber, N. (2008, January 1). Chapter 1 - the marine nitrogen cycle: Overview and challenges. In D. G. Capone, D. A. Bronk, M. R. Mulholland, & E. J. Carpenter (Eds.), *Nitrogen in the marine environment (second edition)* (pp. 1–50). Academic Press. https://doi.org/10.1016/B978-0-12-372522-6.00001-3

Guo, L., & Santschi, P. H. (2007, January 10). Ultrafiltration and its applications to sampling and characterisation of aquatic colloids. In K. J. Wilkinson & J. R. Lead (Eds.), *Environmental colloids and particles* (pp. 159–221). John Wiley & Sons, Ltd. https://doi.org/10.1002/9780470024539.ch4

Hallam, S. J., Konstantinidis, K. T., Putnam, N., Schleper, C., Watanabe, Y.-i., Sugahara, J., Preston, C., Torre, J. d. l., Richardson, P. M., & DeLong, E. F. (2006). Genomic analysis of the uncultivated marine crenarchaeote cenarchaeum symbiosum. *Proceedings of the National Academy of Sciences*, *103*(48), 18296–18301. https://doi.org/10.1073/pnas.0608549103

Hamel, H., Lhoumeau, S., Wahlberg, M., & Javidpour, J. (2021). Using drones to measure jellyfish density in shallow estuaries [Number: 6 Publisher: Multidisciplinary Digital Publishing Institute]. *Journal of Marine Science and Engineering*, *9*(6), 659. https://doi.org/10.3390/jmse9060659

Han, C.-H., Kawahara, M., & Uye, S.-i. (2009a). Seasonal variations in the trophic relationship between the scyphomedusa *Aurelia aurita* s.l. and mesozooplankton in a eutrophic brackish-water lake, japan. *Plankton and Benthos Research*, *4*(1), 14–22. https://doi.org/10.3800/pbr.4.14

Han, C.-H., & Uye, S.-I. (2009b). Quantification of the abundance and distribution of the common jellyfish aurelia aurita s.l. with a dual-frequency IDentification SONar (DIDSON). *Journal of Plankton Research*, *31*(8), 805–814. https://doi.org/10.1093/plankt/fbp029

Hansell, D., Carlson, C., Repeta, D., & Schlitzer, R. (2009). Dissolved organic matter in the ocean: A controversy stimulates new insights. *Oceanography*, *22*(4), 202–211. https://doi.org/10.5670/oceanog.2009.109

Hansell, D. A. (1993). Results and observations from the measurement of DOC and DON in seawater using a high-temperature catalytic oxidation technique. *Marine Chemistry*, *41*(1), 195–202. https://doi.org/10.1016/0304-4203(93)90119-9

Hansell, D. A. (2013). Recalcitrant dissolved organic carbon fractions. *Annual Review of Marine Science*, *5*(1), 421–445. https://doi.org/10.1146/annurev-marine-120710-100757

Hansell, D. A., & Carlson, C. A. (2014, October 2). *Biogeochemistry of marine dissolved organic matter* [Google-Books-ID: 7iKOAwAAQBAJ]. Academic Press.

Hansson, L. J., & Norrman, B. (1995). Release of dissolved organic carbon (DOC) by the scyphozoan jellyfish aurelia aurita and its potential influence on the production of planktic bacteria. *Marine Biology*, *121*(3), 527–532. https://doi.org/10.1007/BF00349462

Harmelin-Vivien, M., Banaru, D., Dromard, C. R., Ourgaud, M., & Carlotti, F. (2019). Biochemical composition and energy content of size-fractionated zooplankton east of the kerguelen islands. *Polar Biology*, *42*(3), 603–617. https://doi.org/10.1007/s00300-019-02458-8

Hays, G. C., Doyle, T. K., & Houghton, J. D. R. (2018). A paradigm shift in the trophic importance of jellyfish? *Trends in Ecology & Evolution*, *33*(11), 874–884. https://doi.org/10.1016/j.tree.2018.09.001

Healy, K., McNally, L., Ruxton, G. D., Cooper, N., & Jackson, A. L. (2013). Metabolic rate and body size are linked with perception of temporal information. *Animal Behaviour*, *86*(4), 685–696. https://doi.org/10.1016/j.anbehav.2013.06.018

Heaslip, S. G., Iverson, S. J., Bowen, W. D., & James, M. C. (2012). Jellyfish support high energy intake of leatherback sea turtles (dermochelys coriacea): Video evidence from animal-borne cameras. *PLOS ONE*, *7*(3), e33259. https://doi.org/10.1371/journal.pone.0033259

Heinze, C. (2014). The role of the ocean carbon cycle in climate change. *European Review*, *22*(1), 97–105. https://doi.org/10.1017/S1062798713000665

Hirst, A. G., Roff, J. C., & Lampitt, R. S. (2003, January 1). A synthesis of growth rates in marine epipelagic invertebrate zooplankton. In A. J. Southward, P. A. Tyler, C. M. Young, & L. A. Fuiman (Eds.), *Advances in marine biology* (pp. 1–142). Academic Press. https://doi.org/10.1016/S0065-2881(03)44002-9

H.J. Ceccaldi, S. T., A. Kanazawa. (1976). Chemical composition of some mediterranean macroplanktonic organisms. *Tethys*, *8*, 295–298.

Hoffmann, F., Radax, R., Woebken, D., Holtappels, M., Lavik, G., Rapp, H. T., Schläppy, M.-L., Schleper, C., & Kuypers, M. M. M. (2009). Complex nitrogen

cycling in the sponge geodia barretti. *Environmental Microbiology*, *11*(9), 2228–2243. https://doi.org/10.1111/j.1462-2920.2009.01944.x

Holst, S., Sötje, I., Tiemann, H., & Jarms, G. (2007). Life cycle of the rhizostome jellyfish rhizostoma octopus (l.) (scyphozoa, rhizostomeae), with studies on cnidocysts and statoliths. *Marine Biology*, *151*(5), 1695–1710. https://doi.org/10.1007/s00227-006-0594-8

Hosia, A., Falkenhaug, T., Baxter, E. J., & Pagès, F. (2017). Abundance, distribution and diversity of gelatinous predators along the northern mid-atlantic ridge: A comparison of different sampling methodologies. *PLoS ONE*, *12*(11). https://doi.org/10.1371/journal.pone.0187491

Houghton, J. D. R., Doyle, T. K., Davenport, J., Lilley, M. K. S., Wilson, R. P., & Hays, G. C. (2007). Stranding events provide indirect insights into the seasonality and persistence of jellyfish medusae (cnidaria: Scyphozoa). *Hydrobiologia*, *589*(1), 1–13. https://doi.org/10.1007/s10750-007-0572-2

Hoving, H.-J., Christiansen, S., Fabrizius, E., Hauss, H., Kiko, R., Linke, P., Neitzel, P., Piatkowski, U., & Körtzinger, A. (2019). The pelagic in situ observation system (PELAGIOS) to reveal biodiversity, behavior, and ecology of elusive oceanic fauna [Publisher: Copernicus GmbH]. *Ocean Science*, *15*(5), 1327–1340. https://doi.org/10.5194/os-15-1327-2019

Hubot, N., Giering, S. L. C., & Lucas, C. H. (2022). Similarities between the biochemical composition of jellyfish body and mucus. *Journal of Plankton Research*, *44*(2), 337–344. https://doi.org/10.1093/plankt/fbab091

Hubot, N. D., Giering, S. L. C., Füssel, J., Robidart, J., Birchill, A., Stinchcombe, M., Dumousseaud, C., & Lucas, C. H. (2021). Evidence of nitrification associated with globally distributed pelagic jellyfish. *Limnology and Oceanography*, *66*(6), 2159–2173. https://doi.org/10.1002/lno.11736

Hydes, D. J., Aoyama, M., Aminot, A., Bakker, K., Becker, S., Coverly, S., Daniel, A., Dickson, A. G., Grosso, O., Kerouel, R., van Ooijen, J., Sato, K., Tanhua, T., Woodward, E. M. S., & Zhang, J. Z. (2010). Determination of dissolved nutrients (n, p, SI) in seawater with high precision and inter-comparability using gas-segmented continuous flow analysers. [SUPERSEDED by http://dx.doi.org/10.25607/OBP-555], 87. https://doi.org/10.25607/OBP-15

Ikeda, T. (2014). Synthesis toward a global model of metabolism and chemical composition of medusae and ctenophores. *Journal of Experimental Marine Biology and Ecology*, *456*, 50–64. https://doi.org/10.1016/j.jembe.2014.03.006

Intergovernmental Panel on Climate Change (IPCC) (Ed.). (2022). Changing ocean, marine ecosystems, and dependent communities. In *The ocean and cryosphere in a changing climate: Special report of the intergovernmental panel on climate change* (pp. 447–588). Cambridge University Press. https://doi.org/10.1017/9781009157964.007

Jian-Long, G. E., Qian, M., Si-Qing, C., Liu Kun, Chang-Lin, L. I. U., Jie, T. A. N., & Bian Li. (2018). Acute and chronic toxicity of ammonia nitrogen to the polyps and ephyrae of moon jellyfish aurelia coerulea. *Oceanologia et Limnologia Sinica*, *49*(4), 809–814. https://doi.org/10.11693/hyhz20171100286

Jiao, N., Herndl, G., Hansell, D., Benner, R., Kattner, G., Wilhelm, S., Kirchman, D., Weinbauer, M., Luo, T., Chen, F., & Azam, F. (2010). Microbial production of recalcitrant dissolved organic matter: Long-term carbon storage in the global ocean. *Nature reviews. Microbiology*, *8*, 593–9. https://doi.org/10.1038/nrmicro2386

Jiao, N., Robinson, C., Azam, F., Thomas, H., Baltar, F., Dang, H., Hardman-Mountford, N., Johnson, M., Kirchman, D., Koch, B., Legendre, L., Li, C., Liu, J., Luo, T., Luo, Y.-W., Mitra, A., Romanou, A., Tang, K., Wang, X., & Zhang, R. (2014). Mechanisms of microbial carbon sequestration in the ocean – future research directions. *Biogeosciences*, *11*, 5285–5306. https://doi.org/10.5194/bg-11-5285-2014

Jones, B. N., Pääbo, S., & Stein, S. (1981). Amino acid analysis and enzymatic sequence determination of peptides by an improved o-phthaldialdehyde precolumn labeling procedure. *Journal of Liquid Chromatography*, *4*(4), 565–586. https://doi.org/10.1080/01483918108059956

Jones, D. B. (1931). *Factors for converting percentages of nitrogen in foods and feeds into percentages of proteins*. U.S. Department of Agriculture.

Junker, T., Mohrholz, V., Siegfried, L., & van der Plas, A. (2017). Seasonal to interannual variability of water mass characteristics and currents on the namibian shelf. *Journal of Marine Systems*, *165*, 36–46. https://doi.org/10.1016/j.jmarsys.2016.09.003

Karner, M. B., DeLong, E. F., & Karl, D. M. (2001). Archaeal dominance in the mesopelagic zone of the pacific ocean. *Nature*, *409*(6819), 507–510. https://doi.org/10.1038/35054051

Keister, J. E., Bonnet, D., Chiba, S., Johnson, C. L., Mackas, D. L., & Escribano, R. (2012). Zooplankton population connections, community dynamics, and climate variability. *ICES Journal of Marine Science*, *69*(3), 347–350. https://doi.org/10.1093/icesjms/fss034

Kibegwa, F. M., Bett, R. C., Gachuiri, C. K., Stomeo, F., & Mujibi, F. D. (2020). A comparison of two DNA metagenomic bioinformatic pipelines while evaluating the microbial diversity in feces of tanzanian small holder dairy cattle. *BioMed Research International*, *2020*, 2348560. https://doi.org/10.1155/2020/2348560

Kim, D.-H., Seo, J.-N., Yoon, W.-D., & Suh, Y.-S. (2012). Estimating the economic damage caused by jellyfish to fisheries in korea. *Fisheries Science*, *78*(5), 1147–1152. https://doi.org/10.1007/s12562-012-0533-1

Kirchman, D., K'nees, E., & Hodson, R. (1985). Leucine incorporation and its potential as a measure of protein synthesis by bacteria in natural aquatic systems. *Applied and Environmental Microbiology*, *49*(3), 599–607. https://doi.org/10.1128/aem.49.3.599-607.1985

Kirchman, D. L. (1994). The uptake of inorganic nutrients by heterotrophic bacteria. *Microbial Ecology*, *28*(2), 255–271. https://doi.org/10.1007/BF00166816

Kogovšek, T., Tinta, T., Klun, K., & Malej, A. (2014). Jellyfish biochemical composition: Importance of standardised sample processing. *Marine Ecology Progress Series*, *510*, 275–288. https://doi.org/10.3354/meps10959

Kopytko, N. (2015, February 19). *Spineless attacks on nuclear power plants could increase* [Bulletin of the atomic scientists].

Kowalchuk, G. A., & Stephen, J. R. (2001). Ammonia-oxidizing bacteria: A model for molecular microbial ecology. *Annual Review of Microbiology*, *55*, 485–529. https://doi.org/10.1146/annurev.micro.55.1.485

Kragh, T., Søndergaard, M., & Tranvik, L. (2008). Effect of exposure to sunlight and phosphorus-limitation on bacterial degradation of coloured dissolved organic matter (CDOM) in freshwater. *FEMS Microbiology Ecology*, *64*(2), 230–239. https://doi.org/10.1111/j.1574-6941.2008.00449.x

Kramar, M. K., Tinta, T., Lucic, D., Malej, A., & Turk, V. (2018). Bacteria associated with jellyfish during bloom and post-bloom periods. *bioRxiv*, 329524. https://doi.org/10.1101/329524

Kramar, M. K., Tinta, T., Lučić, D., Malej, A., & Turk, V. (2019). Bacteria associated with moon jellyfish during bloom and post-bloom periods in the gulf of trieste (northern adriatic). *PLOS ONE*, *14*(1), e0198056. https://doi.org/10.1371/journal.pone.0198056

Krueger, F. (2020). *Trim galore: A wrapper around cutadapt and FastQC to apply adapter and quality trimming to FastQ files* (Version 0.6.6). https://github.com/FelixKrueger/TrimGalore

Lamb, P., Hunter, E., Pinnegar, J., Creer, S., Davies, R., & Taylor, M. (2017). Jellyfish on the menu: mtDNA assay reveals scyphozoan predation in the irish sea. *Royal Society Open Science*, *4*(11), 171421. https://doi.org/10.1098/rsos.171421

Lamb, P. D., Hunter, E., Pinnegar, J. K., Doyle, T. K., Creer, S., & Taylor, M. I. (2019). Inclusion of jellyfish in 30+ years of ecopath with ecosim models. *ICES Journal of Marine Science*, *76*(7), 1941–1950. https://doi.org/10.1093/icesjms/fsz165

Langmead, B., & Salzberg, S. L. (2012). Fast gapped-read alignment with bowtie 2 [Number: 4 Publisher: Nature Publishing Group]. *Nature Methods*, *9*(4), 357–359. https://doi.org/10.1038/nmeth.1923

Larson, R. J. (1986). Water content, organic content, and carbon and nitrogen composition of medusae from the northeast pacific. *Journal of Experimental Marine Biology and Ecology*, *99*(2), 107–120. https://doi.org/10.1016/0022-0981(86)90231-5

Lazzari, P., Solidoro, C., Salon, S., & Bolzon, G. (2016). Spatial variability of phosphate and nitrate in the mediterranean sea: A modeling approach. *Deep Sea Research Part I: Oceanographic Research Papers*, *108*, 39–52. https://doi.org/10.1016/j.dsr.2015.12.006

Lebrato, M., de Jesus Mendes, P., K. Steinberg, D., Cartes, J., Jones, B., Birsa, L., Benavides, R., & Oschlies, A. (2013). Jelly biomass sinking speed reveals a fast carbon export mechanism. *Limnology and oceanography*, *58*, 1113–1122. https://doi.org/10.4319/lo.2013.58.3.1113

Lebrato, M., & Jones, D. O. B. (2011). Expanding the oceanic carbon cycle - jellyfish biomass in the biological pump. *Biochemist e-volution*, *33*, 35–39.

Lebrato, M., Pitt, K. A., Sweetman, A. K., Jones, D. O. B., Cartes, J. E., Oschlies, A., Condon, R. H., Molinero, J. C., Adler, L., Gaillard, C., Lloris, D., & Billett, D. S. M. (2012). Jelly-falls historic and recent observations: A review to drive future research directions. *Hydrobiologia*, *690*(1), 227–245. https://doi.org/10.1007/s10750-012-1046-8

Lee, M. D., Kling, J. D., Araya, R., & Ceh, J. (2018). Jellyfish life stages shape associated microbial communities, while a core microbiome is maintained across all. *Frontiers in Microbiology*, *9*. https://doi.org/10.3389/fmicb.2018.01534

Legendre, P., & Legendre, L. F. J. (1998, November 25). *Numerical ecology* [Google-Books-ID: KBoHuoNRO5MC]. Elsevier Science.

Leu, A. O., Cai, C., McIlroy, S. J., Southam, G., Orphan, V. J., Yuan, Z., Hu, S., & Tyson, G. W. (2020). Anaerobic methane oxidation coupled to manganese reduction by members of the methanoperedenaceae. *The ISME Journal*, *14*(4), 1030–1041. https://doi.org/10.1038/s41396-020-0590-x

Li, H., Handsaker, B., Wysoker, A., Fennell, T., Ruan, J., Homer, N., Marth, G., Abecasis, G., Durbin, R., & 1000 Genome Project Data Processing Subgroup. (2009). The sequence alignment/map format and SAMtools. *Bioinformatics*, *25*(16), 2078–2079. https://doi.org/10.1093/bioinformatics/btp352

Li, Y., Hao, W., Peng, S., Sun, T., Zhao, J., & Dong, Z. (2022). Composition and potential functions of bacterial communities associated with aurelia polyps. *Frontiers in Marine Science*, *9*.

Lilley, M. K. S., Beggs, S. E., Doyle, T. K., Hobson, V. J., Stromberg, K. H. P., & Hays, G. C. (2011). Global patterns of epipelagic gelatinous zooplankton biomass. *Marine biology*, *158*(11), 2429–2436. https://doi.org/10.1007/s00227-011-1744-1

Lilley, M. K. S., Elineau, A., Ferraris, M., Thiéry, A., Stemmann, L., Gorsky, G., & Lombard, F. (2014). Individual shrinking to enhance population survival: Quantifying the reproductive and metabolic expenditures of a starving jellyfish, pelagia noctiluca. *Journal of Plankton Research*, *36*(6), 1585–1597. https://doi.org/10.1093/plankt/fbu079

Linden, S. K., Sutton, P., Karlsson, N. G., Korolik, V., & McGuckin, M. A. (2008). Mucins in the mucosal barrier to infection. *Mucosal Immunology*, *1*(3), 183–197. https://doi.org/10.1038/mi.2008.5

Loladze, I., & Elser, J. J. (2011). The origins of the redfield nitrogen-to-phosphorus ratio are in a homoeostatic protein-to-rRNA ratio [_eprint: https://onlinelibrary.wiley.com/doi/pdf/10.1111/j.1461-0248.2010.01577.x]. *Ecology Letters*, *14*(3), 244–250. https://doi.org/10.1111/j.1461-0248.2010.01577.x

Lønborg, C., Carreira, C., Jickells, T., & Álvarez-Salgado, X. A. (2020). Impacts of global change on ocean dissolved organic carbon (DOC) cycling. *Frontiers in Marine Science*, *7*, 466. https://doi.org/10.3389/fmars.2020.00466

Lønborg, C., Martínez-García, S., Teira, E., & Alvarez-Salgado, X. A. (2011). Bacterial carbon demand and growth efficiency in a coastal upwelling system. *Aquatic Microbial Ecology*, *63*, 183–191. https://doi.org/10.3354/ame01495

Lőw, P., Molnár, K., & Kriska, G. (2016, May 3). *Atlas of animal anatomy and histology*. Springer.

Lowry, O. H., Rosebrough, N. J., Farr, A. L., & Randall, R. J. (1951). Protein measurement with the folin phenol reagent. *Journal of Biological Chemistry*, *193*, 265–275.

Lu, J., Breitwieser, F. P., Thielen, P., & Salzberg, S. L. (2017). Bracken: Estimating species abundance in metagenomics data [Publisher: PeerJ Inc.]. *PeerJ Computer Science*, *3*, e104. https://doi.org/10.7717/peerj-cs.104

Lucas, C. H. (1994). Biochemical composition of aurelia aurita in relation to age and sexual maturity. *Journal of Experimental Marine Biology and Ecology*, *183*(2), 179–192. https://doi.org/10.1016/0022-0981(94)90086-8

Lucas, C. H. (1996). Population dynamics of aurelia aurita (scyphozoa) from an isolated brackish lake, with particular reference to sexual reproduction. *Journal of Plankton Research*, *18*(6), 987–1007. https://doi.org/10.1093/plankt/18.6.987

Lucas, C. H. (2001). Reproduction and life history strategies of the common jellyfish, *Aurelia aurita*, in relation to its ambient environment. *Hydrobiologia*, *451*(1), 229–246. https://doi.org/10.1023/A:1011836326717

Lucas, C. H., Gelcich, S., & Uye, S.-I. (2014a). Living with jellyfish: Management and adaptation strategies. In K. A. Pitt & C. H. Lucas (Eds.), *Jellyfish blooms* (pp. 129–150). Springer Netherlands. https://doi.org/10.1007/978-94-007-7015-7_6

Lucas, C. H., Jones, D. O. B., Hollyhead, C. J., Condon, R. H., Duarte, C. M., Graham, W. M., Robinson, K. L., Pitt, K. A., Schildhauer, M., & Regetz, J. (2014b). Gelatinous zooplankton biomass in the global oceans: Geographic variation and environmental drivers. *Global Ecology and Biogeography*, *23*(7), 701–714. https://doi.org/10.1111/geb.12169

Lucas, C., Hirst, A., & Williams, J. (1997). Plankton dynamics andAurelia auritaProduction in two contrasting ecosystems: Comparisons and consequences. *Estuarine, Coastal and Shelf Science*, *45*(2), 209–219. https://doi.org/10.1006/ecss.1996.0173

Lucas Cathy H., Pitt Kylie A., Purcell Jennifer E., Lebrato Mario, & Condon Robert H. (2011). What's in a jellyfish? proximate and elemental composition and biometric relationships for use in biogeochemical studies. *Ecology*, *92*(8), 1704–1704. https://doi.org/10.1890/11-0302.1

Luo, J. Y., Condon, R. H., Stock, C. A., Duarte, C. M., Lucas, C. H., Pitt, K. A., & Cowen, R. K. (2020). Gelatinous zooplankton-mediated carbon flows in the global oceans: A data-driven modeling study. *Global Biogeochemical Cycles*, *34*(9), e2020GB006704. https://doi.org/10.1029/2020GB006704

Lynam, C. P., Gibbons, M. J., Axelsen, B. E., Sparks, C. A. J., Coetzee, J., Heywood, B. G., & Brierley, A. S. (2006). Jellyfish overtake fish in a heavily fished ecosystem. *Current Biology*, *16*(13), R492–R493. https://doi.org/10.1016/j.cub.2006.06.018

Macierzanka, A., Mackie, A. R., & Krupa, L. (2019). Permeability of the small intestinal mucus for physiologically relevant studies: Impact of mucus location and ex vivo treatment [Number: 1 Publisher: Nature Publishing Group]. *Scientific Reports*, *9*(1), 17516. https://doi.org/10.1038/s41598-019-53933-5

Makabe, R., Takeoka, H., & Uye, S.-i. (2015). Offshore dispersion of ephyrae and medusae of aurelia aurita s.l. (cnidaria: Scyphozoa) from port enclosures: Physical and biological factors. *Journal of Marine Systems*, *152*, 75–82. https://doi.org/10.1016/j.jmarsys.2015.08.002

Malej, A. (1991). Rates of metabolism of jellyfish as related to body weight, chemical composition and temperature. *In Proceedings of the II Workshop on Jellyfish in the Mediterranean*, Athens: 253–259.

Marques, R., Darnaude, A. M., Crochemore, S., Bouvier, C., & Bonnet, D. (2019). Molecular approach indicates consumption of jellyfish by commercially important fish species in a coastal mediterranean lagoon. *Marine Environmental Research*, *152*, 104787. https://doi.org/10.1016/j.marenvres.2019.104787

Marsh, J. B., & Weinstein, D. B. (1966). Simple charring method for determination of lipids. *Journal of Lipid Research*, *7*(4), 574–576.

Martínez-García, M., Stief, P., Díaz-Valdés, M., Wanner, G., Ramos-Esplá, A., Dubilier, N., & Antón, J. (2008). Ammonia-oxidizing crenarchaeota and nitrification inside the tissue of a colonial ascidian. *Environmental Microbiology*, *10*(11), 2991–3001. https://doi.org/10.1111/j.1462-2920.2008.01761.x

Martiny, A. C., Vrugt, J. A., & Lomas, M. W. (2014). Concentrations and ratios of particulate organic carbon, nitrogen, and phosphorus in the global ocean. *Scientific Data*, *1*(1), 140048. https://doi.org/10.1038/sdata.2014.48

Masuda, A., Baba, T., Dohmae, N., Yamamura, M., Wada, H., & Ushida, K. (2007). Mucin (qniumucin), a glycoprotein from jellyfish, and determination of its main chain structure. *Journal of Natural Products*, *70*(7), 1089–1092. https://doi.org/10.1021/np060341b

McInnes, J. C., Jarman, S. N., Lea, M.-A., Raymond, B., Deagle, B. E., Phillips, R. A., Catry, P., Stanworth, A., Weimerskirch, H., Kusch, A., Gras, M., Cherel, Y., Maschette, D., & Alderman, R. (2017). DNA metabarcoding as a marine conservation and management tool: A circumpolar examination of fishery discards in the diet of threatened albatrosses. *Frontiers in Marine Science*, *4*.

Mentges, A., Feenders, C., Deutsch, C., Blasius, B., & Dittmar, T. (2019). Long-term stability of marine dissolved organic carbon emerges from a neutral network of compounds and microbes. *Scientific Reports*, *9*(1), 17780. https://doi.org/10.1038/s41598-019-54290-z

Merivaara, A., Zini, J., Koivunotko, E., Valkonen, S., Korhonen, O., Fernandes, F. M., & Yliperttula, M. (2021). Preservation of biomaterials and cells by freeze-drying: Change of paradigm. *Journal of Controlled Release*, *336*, 480–498. https://doi.org/10.1016/j.jconrel.2021.06.042

Mitchell, E. G., Wallace, M. I., Smith, V. A., Wiesenthal, A. A., & Brierley, A. S. (2021). Bayesian network analysis reveals resilience of the jellyfish aurelia aurita to an irish sea regime shift. *Scientific Reports*, *11*(1), 3707. https://doi.org/10.1038/s41598-021-82825-w

Møller, L. F., & Riisgård, H. U. (2007). Respiration in the scyphozoan jellyfish aurelia aurita and two hydromedusae (sarsia tubulosa and aequorea vitrina): Effect of size, temperature and growth. *Marine Ecology Progress Series*, *330*, 149–154. https://doi.org/10.3354/meps330149

Momynaliev, K. T., & Govorun, V. M. (2001). Mechanisms of genetic instability in mollicutes (mycoplasmas). *Russian Journal of Genetics*, *37*(9), 979–992. https://doi.org/10.1023/A:1011943227915

Moore, C. M., Mills, M. M., Arrigo, K. R., Berman-Frank, I., Bopp, L., Boyd, P. W., Galbraith, E. D., Geider, R. J., Guieu, C., Jaccard, S. L., Jickells, T. D., Roche, J. L., Lenton, T. M., Mahowald, N. M., Marañón, E., Marinov, I., Moore, J. K., Nakatsuka, T., Oschlies, A., … Ulloa, O. (2013). Processes and patterns of oceanic nutrient limitation. *Nature Geoscience*, *6*(9), 701. https://doi.org/10.1038/ngeo1765

Moran, M. A., Ferrer-González, F. X., Fu, H., Nowinski, B., Olofsson, M., Powers, M. A., Schreier, J. E., Schroer, W. F., Smith, C. B., & Uchimiya, M. (2022). The ocean's labile DOC supply chain. *Limnology and Oceanography*, *67*(5), 1007–1021. https://doi.org/10.1002/lno.12053

Morandini, A. C., & Marques, A. C. (2010). Revision of the genus chrysaora péron & lesueur, 1810 (cnidaria: Scyphozoa). *Zootaxa*, *2464*(1), 1–97. https://doi.org/10.11646/zootaxa.2464.1.1

Nagata, R., Moreira, M., Pimentel, C., & Morandini, A. (2015). Food web characterization based on Δ15n and Δ13c reveals isotopic niche partitioning between fish and jellyfish in a relatively pristine ecosystem. *Marine Ecology Progress Series*, *519*, 13–27. https://doi.org/10.3354/meps11071

Nyholm, S. V., & Graf, J. (2012). Knowing your friends: Invertebrate innate immunity fosters beneficial bacterial symbioses. *Nature reviews. Microbiology*, *10*(12). https://doi.org/10.1038/nrmicro2894

Ogawa, H., Amagai, Y., Koike, I., Kaiser, K., & Benner, R. (2001). Production of refractory dissolved organic matter by bacteria. *Science*, *292*(5518), 917–920. https://doi.org/10.1126/science.1057627

Ohdera, A., Medina, M., Fitt, W., Hofmann, D. K., Attarwala, K., Henry, R., Wu, V., & Laird, H. (2022, June 25). Comparative genomic insights into bacterial induction of larval settlement and metamorphosis in the upside-down jellyfish cassiopea. https://doi.org/10.1101/2022.06.24.497576

Oksanen, J., Simpson, G. L., Blanchet, F. G., Kindt, R., Legendre, P., Minchin, P. R., O'Hara, R., Solymos, P., Stevens, M. H. H., Szoecs, E., Wagner, H., Barbour, M., Bedward, M., Bolker, B., Borcard, D., Carvalho, G., Chirico, M., De Caceres, M., Durand, S., … Weedon, J. (2022). *Vegan: Community ecology package* [R package version 2.6-2]. https://CRAN.R-project.org/package=vegan

Pachiadaki, M. G., Sintes, E., Bergauer, K., Brown, J. M., Record, N. R., Swan, B. K., Mathyer, M. E., Hallam, S. J., Lopez-Garcia, P., Takaki, Y., Nunoura, T., Woyke, T., Herndl, G. J., & Stepanauskas, R. (2017). Major role of nitrite-oxidizing bacteria in dark ocean carbon fixation. *Science (New York, N.Y.)*, *358*(6366), 1046–1051. https://doi.org/10.1126/science.aan8260

Pajares, S., & Ramos, R. (2019). Processes and microorganisms involved in the marine nitrogen cycle: Knowledge and gaps. *Frontiers in Marine Science*, *6*, 739. https://doi.org/10.3389/fmars.2019.00739

Patwa, A., Thiéry, A., Lombard, F., Lilley, M. K. S., Boisset, C., Bramard, J.-F., Bottero, J.-Y., & Barthélémy, P. (2015). Accumulation of nanoparticles in "jellyfish" mucus: A bio-inspired route to decontamination of nano-waste. *Scientific Reports*, *5*, 11387. https://doi.org/10.1038/srep11387

Pauly, D., Graham, W., Libralato, S., Morissette, L., & Palomares, M. L. D. (2009). Jellyfish in ecosystems, online databases, and ecosystem models. *Hydrobiologia*, *616*(1), 67–85. https://doi.org/10.1007/s10750-008-9583-x

Pauly, D., Watson, R., & Alder, J. (2005). Global trends in world fisheries: Impacts on marine ecosystems and food security. *Philosophical Transactions of the Royal Society of London B: Biological Sciences*, *360*(1453), 5–12. https://doi.org/10.1098/rstb.2004.1574

Pedler, B. E., Aluwihare, L. I., & Azam, F. (2014). Single bacterial strain capable of significant contribution to carbon cycling in the surface ocean [Publisher: Proceedings of the National Academy of Sciences]. *Proceedings of the National*

Academy of Sciences, *111*(20), 7202–7207. https://doi.org/10.1073/pnas.1401887111

Peng, S., Hao, W., Li, Y., Wang, L., Sun, T., Zhao, J., & Dong, Z. (2021). Bacterial communities associated with four blooming scyphozoan jellyfish: Potential species-specific consequences for marine organisms and humans health. *Frontiers in Microbiology*, *12*.

Pikesley, S. K., Godley, B. J., Ranger, S., Richardson, P. B., & Witt, M. J. (2014). Cnidaria in UK coastal waters: Description of spatio-temporal patterns and inter-annual variability. *Journal of the Marine Biological Association of the United Kingdom*, *94*(7), 1401–1408. https://doi.org/10.1017/S0025315414000137

Pinhassi, J., & Berman, T. (2003). Differential growth response of colony-forming α- and γ-proteobacteria in dilution culture and nutrient addition experiments from lake kinneret (israel), the eastern mediterranean sea, and the gulf of eilat. *Applied and Environmental Microbiology*, *69*(1), 199–211. https://doi.org/10.1128/AEM.69.1.199-211.2003

Piraino, S., De Vito, D., Schmich, J., Bouillon, J., & Boero, F. (2004). Reverse development in cnidaria. *Canadian Journal of Zoology*, *82*(11), 1748–1754. https://doi.org/10.1139/z04-174

Pitt, K. A., Connolly, R. M., & Meziane, T. (2009a). Stable isotope and fatty acid tracers in energy and nutrient studies of jellyfish: A review. *Hydrobiologia*, *616*(1), 119–132. https://doi.org/10.1007/s10750-008-9581-z

Pitt, K. A., Koop, K., & Rissik, D. (2005). Contrasting contributions to inorganic nutrient recycling by the co-occurring jellyfishes, catostylus mosaicus and phyllorhiza punctata (scyphozoa, rhizostomeae). *Journal of Experimental Marine Biology and Ecology*, *315*(1), 71–86. https://doi.org/10.1016/j.jembe.2004.09.007

Pitt, K. A., Duarte, C. M., Lucas, C. H., Sutherland, K. R., Condon, R. H., Mianzan, H., Purcell, J. E., Robinson, K. L., & Uye, S.-I. (2013). Jellyfish body plans provide allometric advantages beyond low carbon content. *PLoS ONE*, *8*(8), e72683. https://doi.org/10.1371/journal.pone.0072683

Pitt, K. A., & Purcell, J. E. (2009b, March 31). *Jellyfish blooms: Causes, consequences and recent advances*. Springer Science & Business Media.

Pitt, K. A., Welsh, D. T., & Condon, R. H. (2009c). Influence of jellyfish blooms on carbon, nitrogen and phosphorus cycling and plankton production. *Hydrobiologia*, *616*(1), 133–149. https://doi.org/10.1007/s10750-008-9584-9

Pitt, K. A., Chelsky, A., Browne, J. G., & Condon, R. H. (2014). Bloom and bust: Why do blooms of jellyfish collapse? In K. A. Pitt & C. H. Lucas (Eds.), *Jellyfish blooms* (pp. 79–103). Springer Netherlands. https://doi.org/10.1007/978-94-007-7015-7_4

Pryor, M., Blanco, B., & Galtes, J. (2009). Desalination and energy efficiency for a uranium mine in namibia, 16.

Purcell, J. E., Baxter, E. J., & Fuentes, V. L. (2013, January 1). 13 - jellyfish as products and problems of aquaculture. In G. Allan & G. Burnell (Eds.), *Advances in aquaculture hatchery technology* (pp. 404–430). Woodhead Publishing. https://doi.org/10.1533/9780857097460.2.404

Purcell, J. (1997). Pelagic cnidarians and ctenophores as predators: Selective predation, feeding rates and effects on prey populations. *Annals of the Institute of Oceaography, Paris*, *73*.

Purcell, J. E. (2009). Extension of methods for jellyfish and ctenophore trophic ecology to large-scale research. *Hydrobiologia*, *616*(1), 23–50. https://doi.org/10.1007/s10750-008-9585-8

Purcell, J. E. (2012). Jellyfish and ctenophore blooms coincide with human proliferations and environmental perturbations. *Annual review of marine science*, *4*, 209–235.

Purcell, J. E., & Arai, M. N. (2001). Interactions of pelagic cnidarians and ctenophores with fish: A review. *Hydrobiologia*, *451*(1), 27–44. https://doi.org/10.1023/A:1011883905394

Purcell, J. E., Uye, S.-i., & Lo, W.-T. (2007). Anthropogenic causes of jellyfish blooms and their direct consequences for humans: A review. *Marine Ecology Progress Series*, *350*, 153–174. https://doi.org/10.3354/meps07093

R Core Team. (2019). *R: A language and environment for statistical computing. r foundation for statistical computing*. Vienna, Austria.

R Core Team. (2021). *R: A language and environment for statistical computing. r foundation for statistical computing*. Vienna, Austria.

R Core Team. (2022). *R: A language and environment for statistical computing. r foundation for statistical computing*. Vienna, Austria.

Rädecker, N., Pogoreutz, C., Voolstra, C. R., Wiedenmann, J., & Wild, C. (2015). Nitrogen cycling in corals: The key to understanding holobiont functioning? *Trends in Microbiology*, *23*(8), 490–497. https://doi.org/10.1016/j.tim.2015.03.008

Ramesh, C., Tulasi, B. R., Raju, M., Thakur, N., & Dufossé, L. (2021). Marine natural products from tunicates and their associated microbes. *Marine Drugs*, *19*(6), 308. https://doi.org/10.3390/md19060308

Ramondenc, S., Eveillard, D., Guidi, L., Lombard, F., & Delahaye, B. (2020). Probabilistic modeling to estimate jellyfish ecophysiological properties and size distributions. *Scientific Reports*, *10*(1), 6074. https://doi.org/10.1038/s41598-020-62357-5

Rasmussen, J. A., Villumsen, K. R., Duchêne, D. A., Puetz, L. C., Delmont, T. O., Sveier, H., Jørgensen, L. v. G., Præbel, K., Martin, M. D., Bojesen, A. M., Gilbert, M. T. P., Kristiansen, K., & Limborg, M. T. (2021). Genome-resolved metagenomics suggests a mutualistic relationship between mycoplasma and

salmonid hosts. *Communications Biology*, *4*(1), 1–10. https://doi.org/10.1038/s42003-021-02105-1

Ray, B., & Speck, M. L. (1973). Freeze-injury in bacteria. *CRC Critical Reviews in Clinical Laboratory Sciences*, *4*(2), 161–213. https://doi.org/10.3109/10408367309151556

Rayner, T. A., Jørgensen, N. O. G., Blanda, E., Wu, C.-H., Huang, C.-C., Mortensen, J., Hwang, J.-S., & Hansen, B. W. (2015). Biochemical composition of the promising live feed tropical calanoid copepod pseudodiaptomus annandalei (sewell 1919) cultured in taiwanese outdoor aquaculture ponds. *Aquaculture*, *441*, 25–34. https://doi.org/10.1016/j.aquaculture.2015.01.034

Redfield, A. C. (1963). The influence of organisms on the composition of seawater. *The Sea*, *2*, 26–77.

Reverter, M., Tapissier-Bontemps, N., Lecchini, D., Banaigs, B., & Sasal, P. (2018). Biological and ecological roles of external fish mucus: A review. *Fishes*, *3*(4), 41. https://doi.org/10.3390/fishes3040041

Richardson, A. J., Bakun, A., Hays, G. C., & Gibbons, M. J. (2009). The jellyfish joyride: Causes, consequences and management responses to a more gelatinous future. *Trends in Ecology & Evolution*, *24*(6), 312–322. https://doi.org/10.1016/j.tree.2009.01.010

Rideau, F., Villa, A., Belzanne, P., Verdier, E., Hosy, E., & Arfi, Y. (2022). Imaging minimal bacteria at the nanoscale: A reliable and versatile process to perform single-molecule localization microscopy in mycoplasmas. *Microbiology Spectrum*, *10*(3), e00645–22. https://doi.org/10.1128/spectrum.00645-22

Ridgwell, A., & Arndt, S. (2015). Chapter 1 - why dissolved organics matter: DOC in ancient oceans and past climate change. In D. A. Hansell & C. A. Carlson (Eds.), *Biogeochemistry of marine dissolved organic matter (second edition)* (pp. 1–20). Academic Press. https://doi.org/10.1016/B978-0-12-405940-5.00001-7

Riisgård, H. U., Barth-Jensen, C., & Madsen, C. (2010). High abundance of the jellyfish aurelia aurita excludes the invasive ctenophore mnemiopsis leidyi to establish in a shallow cove (kertinge nor, denmark). *Aquatic Invasions*, *5*(4), 347–356. https://doi.org/10.3391/ai.2010.5.4.03

Roux, J.-P., van der Lingen, C. D., Gibbons, M. J., Moroff, N. E., Shannon, L. J., Smith, A. D. M., & Cury, P. M. (2013). Jellyfication of marine ecosystems as a likely consequence of overfishing small pelagic fishes: Lessons from the benguela. *Bulletin of Marine Science*, *89*(1), 249–284. https://doi.org/https://dx.doi.org/10.5343/bms.2011.1145

Sarmento, H., & Gasol, J. M. (2012). Use of phytoplankton-derived dissolved organic carbon by different types of bacterioplankton [_eprint: https://onlinelibrary.wiley.com/doi/pdf/10.1111/j.1462-2920.2012.02787.x]. *Environmental Microbiology*, *14*(9), 2348–2360. https://doi.org/10.1111/j.1462-2920.2012.02787.x

Schaafsma, F. L., Cherel, Y., Flores, H., van Franeker, J. A., Lea, M.-A., Raymond, B., & van de Putte, A. P. (2018). Review: The energetic value of zooplankton and nekton species of the southern ocean. *Marine Biology*, *165*(8), 129. https://doi.org/10.1007/s00227-018-3386-z

Schiariti, A., Dutto, M. S., Pereyra, D. Y., Siquier, G. F., & Morandini, A. C. (2018). Medusae (scyphozoa and cubozoa) from southwestern atlantic and subantarctic region (32-60°s, 34-70°w): Species composition, spatial distribution and life history traits [Number: 2]. *Latin American Journal of Aquatic Research*, *46*(2), 240–257. https://doi.org/10.3856/vol46-issue2-fulltext-1

Schnedler-Meyer, N. A., Kiørboe, T., & Mariani, P. (2018). Boom and bust: Life history, environmental noise, and the (un)predictability of jellyfish blooms. *Frontiers in Marine Science*, *5*. https://doi.org/10.3389/fmars.2018.00257

Schneider, G. (1989). The common jellyfish ¡emphasis type=”italic”¿aurelia aurita¡/emphasis¿: Standing stock, excretion and nutrient regeneration in the kiel bight, western baltic. *Marine Biology*, *100*(4), 507–514. https://doi.org/10.1007/BF00394827

Schneider, G. (1988). Chemische Zusammensetzung und Biomasseparameter der OhrenqualleAurelia aurita. *Helgoländer Meeresuntersuchungen*, *42*(2), 319–327. https://doi.org/10.1007/BF02366048

Scholz, M. B., Lo, C.-C., & Chain, P. S. (2012). Next generation sequencing and bioinformatic bottlenecks: The current state of metagenomic data analysis. *Current Opinion in Biotechnology*, *23*(1), 9–15. https://doi.org/10.1016/j.copbio.2011.11.013

Schuwirth, N., Borgwardt, F., Domisch, S., Friedrichs, M., Kattwinkel, M., Kneis, D., Kuemmerlen, M., Langhans, S. D., Martínez-López, J., & Vermeiren, P. (2019). How to make ecological models useful for environmental management. *Ecological Modelling*, *411*, 108784. https://doi.org/10.1016/j.ecolmodel.2019.108784

Scorrano, S., Aglieri, G., Boero, F., Dawson, M. N., & Piraino, S. (2016). Unmasking aurelia species in the mediterranean sea: An integrative morphometric and molecular approach. *Zoological Journal of the Linnean Society*, n/a–n/a. https://doi.org/10.1111/zoj.12494

Sen Gupta, A., & McNeil, B. (2012, January 1). Chapter 6 - variability and change in the ocean. In A. Henderson-Sellers & K. McGuffie (Eds.), *The future of the world's climate (second edition)* (pp. 141–165). Elsevier. https://doi.org/10.1016/B978-0-12-386917-3.00006-3

Shilova, I. N., Mills, M. M., Robidart, J. C., Turk-Kubo, K. A., Björkman, K. M., Kolber, Z., Rapp, I., Dijken, G. L. v., Church, M. J., Arrigo, K. R., Achterberg, E. P., & Zehr, J. P. (2017). Differential effects of nitrate, ammonium, and urea as n sources for microbial communities in the north pacific ocean.

Limnology and Oceanography, *62*(6), 2550–2574. https://doi.org/10.1002/lno.10590

Shimauchi, H., & Uye, S.-I. (2007). Excretion and respiration rates of the scyphomedusa ¡emphasis type=”italic”¿aurelia aurita¡/emphasis¿ from the inland sea of japan. *Journal of Oceanography*, *63*(1), 27–34. https://doi.org/10.1007/s10872-007-0003-z

Silvipriya, K., Kumar, K., Bhat, A., Kumar, B., John, A., & Lakshmanan, P. (2015). Collagen: Animal sources and biomedical application. *Journal of Applied Pharmaceutical Science*, 123–127. https://doi.org/10.7324/JAPS.2015.50322

Skrypzeck, H. (2019). *Observations on the ecology and life-history of chrysaora fulgida (reynaud 1830) (scyphozoa: Semaeostomeae) and other pelagic cnidarians in the inshore waters off central namibia*.

Smith, D. C., & Azam, F. (1992). A simple, economical method for measuring bacterial protein synthesis rates in seawater using 3h-leucine. *undefined*, 8.

Smith, N. C., Rise, M. L., & Christian, S. L. (2019). A comparison of the innate and adaptive immune systems in cartilaginous fish, ray-finned fish, and lobe-finned fish. *Frontiers in Immunology*, *10*.

Smyth, T. J., Fishwick, J. R., AL-Moosawi, L., Cummings, D. G., Harris, C., Kitidis, V., Rees, A., Martinez-Vicente, V., & Woodward, E. M. S. (2010). A broad spatio-temporal view of the western english channel observatory. *Journal of Plankton Research*, *32*(5), 585–601. https://doi.org/10.1093/plankt/fbp128

Sosa, O. A., Repeta, D. J., DeLong, E. F., Ashkezari, M. D., & Karl, D. M. (2019). Phosphate-limited ocean regions select for bacterial populations enriched in the carbon–phosphorus lyase pathway for phosphonate degradation. *Environmental Microbiology*, *21*(7), 2402–2414. https://doi.org/https://doi.org/10.1111/1462-2920.14628

Spieck, E., & Bock, E. (2015). The lithoautotrophic nitrite-oxidizing bacteria. *Bergey's manual of systematics of archaea and bacteria* (pp. 1–10). American Cancer Society. https://doi.org/10.1002/9781118960608.bm00014

Stabili, L., Licciano, M., Giangrande, A., Gerardi, C., De Pascali, S. A., & Fanizzi, F. P. (2019). First insight on the mucus of the annelid myxicola infundibulum (polychaeta, sabellidae) as a potential prospect for drug discovery. *Marine Drugs*, *17*(7), 396. https://doi.org/10.3390/md17070396

Stabili, L., Parisi, M. G., Parrinello, D., & Cammarata, M. (2018). Cnidarian interaction with microbial communities: From aid to animal's health to rejection responses. *Marine Drugs*, *16*(9), 296. https://doi.org/10.3390/md16090296

Stabili, L., Rizzo, L., Basso, L., Marzano, M., Fosso, B., Pesole, G., & Piraino, S. (2020). The microbial community associated with rhizostoma pulmo: Ecological significance and potential consequences for marine organisms and human health. *Marine Drugs*, *18*(9), 437. https://doi.org/10.3390/md18090437

Stabili, L., Schirosi, R., Parisi, M. G., Piraino, S., & Cammarata, M. (2015). The mucus of actinia equina (anthozoa, cnidaria): An unexplored resource for potential applicative purposes. *Marine Drugs*, *13*(8), 5276–5296. https://doi.org/10.3390/md13085276

Steinberg, D. K., & Saba, G. K. (2008, January 1). Chapter 26 - nitrogen consumption and metabolism in marine zooplankton. In D. G. Capone, D. A. Bronk, M. R. Mulholland, & E. J. Carpenter (Eds.), *Nitrogen in the marine environment (second edition)* (pp. 1135–1196). Academic Press. https://doi.org/10.1016/B978-0-12-372522-6.00026-8

Sterner, R. W. (1990). The ratio of nitrogen to phosphorus resupplied by herbivores: Zooplankton and the algal competitive arena. *The American Naturalist*, *136*(2), 209–229. https://doi.org/10.1086/285092

Stief, P., Poulsen, M., Nielsen, L. P., Brix, H., & Schramm, A. (2009). Nitrous oxide emission by aquatic macrofauna. *Proceedings of the National Academy of Sciences*, *106*(11), 4296–4300. https://doi.org/10.1073/pnas.0808228106

Stoecker, D. K., Michaels, A. E., & Davis, L. H. (1987). Grazing by the jellyfish, aurelia aurita , on microzooplankton. *Journal of Plankton Research*, *9*(5), 901–915. https://doi.org/10.1093/plankt/9.5.901

Stoltenberg, I., Dierking, J., Müller-Navarra, D. C., & Javidpour, J. (2021). Review of jellyfish trophic interactions in the baltic sea. *Marine Biology Research*, *17*(4), 311–326. https://doi.org/10.1080/17451000.2021.1964532

Stone, J. P., & Steinberg, D. K. (2018). Influence of top-down control in the plankton food web on vertical carbon flux: A case study in the chesapeake bay. *Journal of Experimental Marine Biology and Ecology*, *498*, 16–24. https://doi.org/10.1016/j.jembe.2017.10.008

Subina, N. S., Thorat, B. R., & Gonsalves, M.-J. (2018). Nitrification in intertidal sponge cinachyrella cavernosa. *Aquatic Ecology*, *52*(2), 155–164. https://doi.org/10.1007/s10452-018-9651-x

Sun, W., Zhang, F., He, L., & Li, Z. (2014). Pyrosequencing reveals diverse microbial community associated with the zoanthid palythoa australiae from the south china sea. *Microbial Ecology*, *67*(4), 942–950. https://doi.org/10.1007/s00248-014-0395-4

Sweetman, A., & Chapman, A. (2015). First assessment of flux rates of jellyfish carcasses (jelly-falls) to the benthos reveals the importance of gelatinous material for biological c-cycling in jellyfish-dominated ecosystems. *Frontiers in Marine Science*, *2*.

Sweetman, A. K., Smith, C. R., Dale, T., & Jones, D. O. B. (2014). Rapid scavenging of jellyfish carcasses reveals the importance of gelatinous material to deep-sea food webs. *Proceedings of the Royal Society B: Biological Sciences*, *281*(1796), 20142210. https://doi.org/10.1098/rspb.2014.2210

Takahashi, M., Ishikawa, D., Sasaki, T., Lu, Y., Kuwahara-Arai, K., Kamei, M., Shibuya, T., Osada, T., Hiramatsu, K., & Nagahara, A. (2019). Faecal freezing preservation period influences colonization ability for faecal microbiota transplantation. *Journal of Applied Microbiology*, *126*(3), 973–984. https://doi.org/10.1111/jam.14167

Takasu, H., Inomata, H., Uchino, K., Tahara, S., Mori, K., Hirano, Y., Harada, K., Yamaguchi, M., Nozoe, Y., & Akiyama, H. (2019). Spatio-temporal distribution of environmental DNA derived from japanese sea nettle jellyfish *Chrysaora pacifica* in omura bay, kyushu, japan. *Plankton and Benthos Research*, *14*(4), 320–323. https://doi.org/10.3800/pbr.14.320

Takeda, N., Deguchi, R., & Itabashi, T. (2018). Reproductive strategies in marine hydrozoan jellyfish: Sexual medusae and asexual polyps. In K. Kobayashi, T. Kitano, Y. Iwao, & M. Kondo (Eds.), *Reproductive and developmental strategies: The continuity of life* (pp. 157–174). Springer Japan. https://doi.org/10.1007/978-4-431-56609-0_8

Taylor, B. W., Keep, C. F., Hall, R. O., Koch, B. J., Tronstad, L. M., Flecker, A. S., & Ulseth, A. J. (2007). Improving the fluorometric ammonium method: Matrix effects, background fluorescence, and standard additions. *Journal of the North American Benthological Society*, *26*(2), 167–177. https://doi.org/10.1899/0887-3593(2007)26[167:ITFAMM]2.0.CO;2

Thiebot, J.-B., Arnould, J. P., Gómez-Laich, A., Ito, K., Kato, A., Mattern, T., Mitamura, H., Noda, T., Poupart, T., Quintana, F., Raclot, T., Ropert-Coudert, Y., Sala, J. E., Seddon, P. J., Sutton, G. J., Yoda, K., & Takahashi, A. (2017). Jellyfish and other gelata as food for four penguin species – insights from predator-borne videos. *Frontiers in Ecology and the Environment*, *15*(8), 437–441. https://doi.org/10.1002/fee.1529

Tinta, T., Klun, K., & Herndl, G. J. (2021). The importance of jellyfish–microbe interactions for biogeochemical cycles in the ocean. *Limnology and Oceanography*, *66*(5), 2011–2032. https://doi.org/https://doi.org/10.1002/lno.11741

Tinta, T., Kogovšek, T., Klun, K., Malej, A., Herndl, G. J., & Turk, V. (2019). Jellyfish-associated microbiome in the marine environment: Exploring its biotechnological potential. *Marine Drugs*, *17*(2), 94. https://doi.org/10.3390/md17020094

Tinta, T., Kogovšek, T., Malej, A., & Turk, V. (2012). Jellyfish modulate bacterial dynamic and community structure. *PLOS ONE*, *7*(6), e39274. https://doi.org/10.1371/journal.pone.0039274

Tinta, T., Kogovšek, T., Turk, V., Shiganova, T. A., Mikaelyan, A. S., & Malej, A. (2016). Microbial transformation of jellyfish organic matter affects the nitrogen cycle in the marine water column — a black sea case study. *Journal of Experimental*

Marine Biology and Ecology, *475*, 19–30. https://doi.org/10.1016/j.jembe.2015.10.018

Tinta, T., Zhao, Z., Escobar, A., Klun, K., Bayer, B., Amano, C., Bamonti, L., & Herndl, G. J. (2020). Microbial processing of jellyfish detritus in the ocean. *Frontiers in Microbiology*, *11*. https://doi.org/10.3389/fmicb.2020.590995

Utne-Palm, A. C., Salvanes, A. G. V., Currie, B., Kaartvedt, S., Nilsson, G. E., Braithwaite, V. A., Stecyk, J. A. W., Hundt, M., van der Bank, M., Flynn, B., Sandvik, G. K., Klevjer, T. A., Sweetman, A. K., Brüchert, V., Pittman, K., Peard, K. R., Lunde, I. G., Strandabø, R. A. U., & Gibbons, M. J. (2010). Trophic structure and community stability in an overfished ecosystem. *Science (New York, N.Y.)*, *329*(5989), 333–336. https://doi.org/10.1126/science.1190708

Uye, S., & Shimauchi, H. (2005). Population biomass, feeding, respiration and growth rates, and carbon budget of the scyphomedusa aurelia aurita in the inland sea of japan. *Journal of Plankton Research*, *27*(3), 237–248. https://doi.org/10.1093/plankt/fbh172

Vadstein, O., Olsen, L. M., Busch, A., Andersen, T., & Reinertsen, H. R. (2003). Is phosphorus limitation of planktonic heterotrophic bacteria and accumulation of degradable DOC a normal phenomenon in phosphorus-limited systems? a microcosm study. *FEMS Microbiology Ecology*, *46*(3), 307–316. https://doi.org/10.1016/S0168-6496(03)00195-8

Verdugo, P., Alldredge, A. L., Azam, F., Kirchman, D. L., Passow, U., & Santschi, P. H. (2004). The oceanic gel phase: A bridge in the DOM–POM continuum. *Marine Chemistry*, *92*(1), 67–85. https://doi.org/10.1016/j.marchem.2004.06.017

Viver, T., Orellana, L. H., Hatt, J. K., Urdiain, M., Díaz, S., Richter, M., Antón, J., Avian, M., Amann, R., Konstantinidis, K. T., & Rosselló-Móra, R. (2017). The low diverse gastric microbiome of the jellyfish cotylorhiza tuberculata is dominated by four novel taxa. *Environmental Microbiology*, *19*(8), 3039–3058. https://doi.org/10.1111/1462-2920.13763

Wagner, S., Schubotz, F., Kaiser, K., Hallmann, C., Waska, H., Rossel, P. E., Hansman, R., Elvert, M., Middelburg, J. J., Engel, A., Blattmann, T. M., Catalá, T. S., Lennartz, S. T., Gomez-Saez, G. V., Pantoja-Gutiérrez, S., Bao, R., & Galy, V. (2020). Soothsaying DOM: A current perspective on the future of oceanic dissolved organic carbon. *Frontiers in Marine Science*, *7*.

Weiland-Bräuer, N., Fischer, M. A., Pinnow, N., & Schmitz, R. A. (2019). Potential role of host-derived quorum quenching in modulating bacterial colonization in the moon jellyfish aurelia aurita. *Scientific Reports*, *9*(1), 34. https://doi.org/10.1038/s41598-018-37321-z

Weiland-Bräuer, N., Neulinger, S. C., Pinnow, N., Künzel, S., Baines, J. F., & Schmitz, R. A. (2015). Composition of bacterial communities associated with aurelia aurita changes with compartment, life stage, and population. *Appl. Environ. Microbiol.*, *81*(17), 6038–6052. https://doi.org/10.1128/AEM.01601-15

Welborn, J., & Manahan, D. (1995). Taurine metabolism in larvae of marine invertebrate molluscs (bilvalvia, gastropoda). *Journal of Experimental Biology*, *198*(8), 1791–1799. https://doi.org/10.1242/jeb.198.8.1791

Welsh, D., Castadelli, G., Bartoli, M., Poli, D., Careri, M., de Wit, R., & Viaroli, P. (2001). Denitrification in an intertidal seagrass meadow, a comparison of 15n-isotope and acetylene-block techniques: Dissimilatory nitrate reduction to ammonia as a source of n2o? *Marine Biology*, *139*(6), 1029–1036. https://doi.org/10.1007/s002270100672

Welsh, D. T., & Castadelli, G. (2004). Bacterial nitrification activity directly associated with isolated benthic marine animals. *Marine Biology*, *144*(5), 1029–1037. https://doi.org/10.1007/s00227-003-1252-z

Welsh, D. T., Dunn, R. J. K., & Meziane, T. (2009). Oxygen and nutrient dynamics of the upside down jellyfish (cassiopea sp.) and its influence on benthic nutrient exchanges and primary production. *Hydrobiologia*, *635*(1), 351–362. https://doi.org/10.1007/s10750-009-9928-0

West, E. J., Pitt, K. A., Welsh, D. T., Koop, K., & Rissik, D. (2009). Top-down and bottom-up influences of jellyfish on primary productivity and planktonic assemblages. *Limnology and Oceanography*, *54*(6), 2058–2071. https://doi.org/10.4319/lo.2009.54.6.2058

Wood, D. E., Lu, J., & Langmead, B. (2019). Improved metagenomic analysis with kraken 2. *Genome Biology*, *20*(1), 257. https://doi.org/10.1186/s13059-019-1891-0

Wright, R. M., Le Quéré, C., Buitenhuis, E., Pitois, S., & Gibbons, M. J. (2021). Role of jellyfish in the plankton ecosystem revealed using a global ocean biogeochemical model. *Biogeosciences*, *18*(4), 1291–1320. https://doi.org/https://doi.org/10.5194/bg-18-1291-2021

Wuchter, C., Abbas, B., Coolen, M. J. L., Herfort, L., Bleijswijk, J. v., Timmers, P., Strous, M., Teira, E., Herndl, G. J., Middelburg, J. J., Schouten, S., & Damsté, J. S. S. (2006). Archaeal nitrification in the ocean. *Proceedings of the National Academy of Sciences*, *103*(33), 12317–12322. https://doi.org/10.1073/pnas.0600756103

Yool, A., Martin, A. P., Fernández, C., & Clark, D. R. (2007). The significance of nitrification for oceanic new production. *Nature*, *447*(7147), 999–1002. https://doi.org/10.1038/nature05885

Zakem, E. J., Al-Haj, A., Church, M. J., van Dijken, G. L., Dutkiewicz, S., Foster, S. Q., Fulweiler, R. W., Mills, M. M., & Follows, M. J. (2018). Ecological control of nitrite in the upper ocean. *Nature Communications*, *9*(1), 1–13. https://doi.org/10.1038/s41467-018-03553-w

Zhang, Y., Qin, W., Hou, L., Zakem, E. J., Wan, X., Zhao, Z., Liu, L., Hunt, K. A., Jiao, N., Kao, S.-J., Tang, K., Xie, X., Shen, J., Li, Y., Chen, M., Dai, X., Liu, C., Deng, W., Dai, M., … Herndl, G. J. (2020a). Nitrifier adaptation to low energy

flux controls inventory of reduced nitrogen in the dark ocean. *Proceedings of the National Academy of Sciences*, *117*(9), 4823–4830. https://doi.org/10.1073/pnas.1912367117

Zhang, Z., Yu, Y.-x., Wang, Y.-g., Wei, X.-x., Liao, M.-j., Rong, X.-j., & Chen, J. (2020b). Development of a new protocol for freeze-drying preservation of pseudoalteromonas nigrifaciens and its protective effect on other marine bacteria. *Electronic Journal of Biotechnology*, *44*, 1–5. https://doi.org/10.1016/j.ejbt.2019.12.006

Zhao, G., & Zhang, G. (2005). Effect of protective agents, freezing temperature, rehydration media on viability of malolactic bacteria subjected to freeze-drying. *Journal of Applied Microbiology*, *99*(2), 333–338. https://doi.org/10.1111/j.1365-2672.2005.02587.x

Zheng, Z.-Z., Wan, X., Xu, M. N., Hsiao, S. S.-Y., Zhang, Y., Zheng, L.-W., Wu, Y., Zou, W., & Kao, S.-J. (2017). Effects of temperature and particles on nitrification in a eutrophic coastal bay in southern china. *Journal of Geophysical Research: Biogeosciences*, *122*(9), 2325–2337. https://doi.org/10.1002/2017JG003871

Zhu, Q., & Zhuang, Q. (2015). Ecosystem biogeochemistry model parameterization: Do more flux data result in a better model in predicting carbon flux? *Ecosphere*, *6*(12), 1–20. https://doi.org/10.1890/ES15-00259.1